CR-137790

26085-6001-TU00

DESIGN OF MULTI-MISSION CHEMICAL PROPULSION MODULES FOR PLANETARY ORBITERS

VOLUME II: TECHNICAL REPORT

15 AUGUST 1975

Prepared for
NASA AMES RESEARCH CENTER

under
Contract NAS2-8370

TRW
SYSTEMS GROUP

(NASA-CR-137790) DESIGN OF MULTI-MISSION CHEMICAL PROPULSION MODULES FOR PLANETARY ORBITERS. VOLUME 2: TECHNICAL REPORT (TRW Systems Group) 270 p HC $9.00 CSCL 21H

N76-14197

Unclas
G3/20 07169

26085-6001-TU00

DESIGN OF MULTI-MISSION CHEMICAL PROPULSION MODULES FOR PLANETARY ORBITERS

VOLUME II: TECHNICAL REPORT

15 AUGUST 1975

Prepared for
NASA AMES RESEARCH CENTER

under
Contract NAS2-8370

TRW
SYSTEMS GROUP

The final report of this study is presented in three volumes:

I Summary Report

II Technical Report

III Appendixes

Use of Metric and English Units in this Report

The results of this study are reported in metric and English units. The metric notation generally is quoted first. However, since in the present transition phase most of the engineering work is still being performed in terms of English units, some of the supporting calculations are reported only in these units. In other instances English units are stated first, with metric units in parentheses, e.g., in reference to a 12-foot (3.66-meter) antenna dish.

CONTENTS

CONTENTS (Continued)

CONTENTS (Continued)

CONTENTS (Continued)

CONTENTS (Continued)

CONTENTS (Continued)

CONTENTS (Continued)

ILLUSTRATIONS

ILLUSTRATIONS (Continued)

ILLUSTRATIONS (Continued)

ILLUSTRATIONS (Continued)

ILLUSTRATIONS (Continued)

TABLES

TABLES (Continued)

TABLES (Continued)

ABSTRACT

This report presents results of a conceptual design and feasibility study of chemical propulsion stages that can serve as modular propulsion units, with little or no modification, on a variety of planetary orbit missions, including orbiters of Mercury, Saturn, and Uranus. Planetary spacecraft of existing design or currently under development, viz., spacecraft of the Pioneer and Mariner families, are assumed as payload vehicles. Thus, operating requirements of spin-stabilized and 3-axis stabilized spacecraft have to be met by the respective propulsion module designs. As launch vehicle for these missions (considered for the mid-1980's or thereafter) the Shuttle orbiter and interplanetary injection stage, or Tug, plus solid-propellant kick motor was assumed. Accommodation constraints and interfaces involving the payloads and the launch vehicle are considered in the propulsion module design.

In this 12-month study TRW evaluated the applicability and performance advantages of the space-storable high-energy bipropellants (liquid fluorine/hydrazine) as alternative to earth-storable bipropellants (nitrogen tetroxide/monomethyl hydrazine). The incentive for using this advanced propulsion technology on planetary missions is the much greater performance potential when orbit insertion velocities in excess of 4 km/sec are required, as in the Mercury orbiter. Possible applications also include ballistic comet rendezvous missions. A major part of the study effort was devoted to design analyses and performance tradeoffs regarding earth-storable versus space-storable propulsion systems, and to assess cost and development schedules of multi-mission versus custom-designed propulsion modules. The report includes recommendations as to future research and development objectives in this field.

1. INTRODUCTION AND SCOPE OF STUDY

1.1 BACKGROUND

Planetary exploration by orbiting spacecraft will be achievable at reduced cost by introducing a modular system concept. This requires development of advanced chemical propulsion stages suitable for use with existing planetary spacecraft designs such as Pioneer (spin-stabilized) or Mariner (three-axis stabilized). The propulsion modules are to be used in multiple mission applications, either for outer-planet or Mercury orbit missions. This avoids the necessity of developing a different propulsion stage for each orbiter mission contemplated. However, the configurations of propulsion modules that would best accommodate spin-stabilized and three-axis stabilized payloads have not been defined, nor have technology requirements for developing such modules been identified.

In this study, the feasibility of developing multi-mission propulsion modules for these applications and their performance, weight, and cost characteristics were investigated in comparison with propulsion systems that would be custom-designed for each application. In addition, the feasibility and potential performance improvements achievable by using space-storable rather than earth-storable propellants in these propulsion modules were investigated.

Space-storable (fluorine/hydrazine) bipropellant systems with a specific impulse, I_{sp}, as large as 375 seconds offer a significant performance advantage over conventional, earth-storable (nitrogen tetroxide/monomethylhydrazine) systems having an I_{sp} of only about 290 to 300 seconds.

However, while earth-storable propulsion systems have been used extensively, for example, in the Apollo program and in the Mariner 9 Mars orbiter mission (1971), space-storable systems still require additional development before they can be considered ready for flight application. Liquid fluorine used as oxidizer also poses the design problem of storage at cryogenic temperature with no boiloff permitted

during the long trip time to the target planet. Nevertheless, the expected performance advantage of the space-storable propulsion system provides the incentive for its further development and use in missions like those considered in this study. Performance and cost comparisons between space-storable and earth-storable bipropellant systems and estimates of the time required to bring these systems to operational status were a major study objective.

A third factor of major concern in this study was the feasibility of using the Shuttle/Upper Stage as launch vehicle, since none of the missions considered would be flown before the mid-1980's. In addition to performance, accommodation of the flight spacecraft onboard the Shuttle orbiter and safety considerations regarding the handling and stowage of a propulsion system with liquid fluorine as oxidizer were matters of interest in selecting the propulsion module configuration and establishing system feasibility.

1.2 MISSION CONSTRAINTS AND PERFORMANCE REQUIREMENTS

Exploration of the outer planets beyond Jupiter by orbiting spacecraft becomes attractive and feasible only if mission times do not exceed the expected lifetimes of components and subsystems of the spacecraft that are vital to the success of the mission. The greatest part of the mission is spent in transit from earth to the planet. Reduction of flight times involves 1) larger injection energies at earth and 2) increased arrival velocities at the planet. The first requirement reduces the total mass that can be injected into the heliocentric trajectory to the planet by a given launch vehicle. The second requirement implies an increase in the mass of the retro-propulsion system used for orbit insertion at the target planet and, hence, an increase in the total injected mass for a given payload and designated orbit. The two opposing requirements are reflected in Figure 1-1 by an upward sloping curve for launch vehicle injected mass capability and a downward sloping one for spacecraft total mass versus flight time. The combination of the launch vehicle capability and the performance of the spacecraft propulsion system determines the shortest possible trip time to the target planet, as shown by the intersection of the two performance curves.

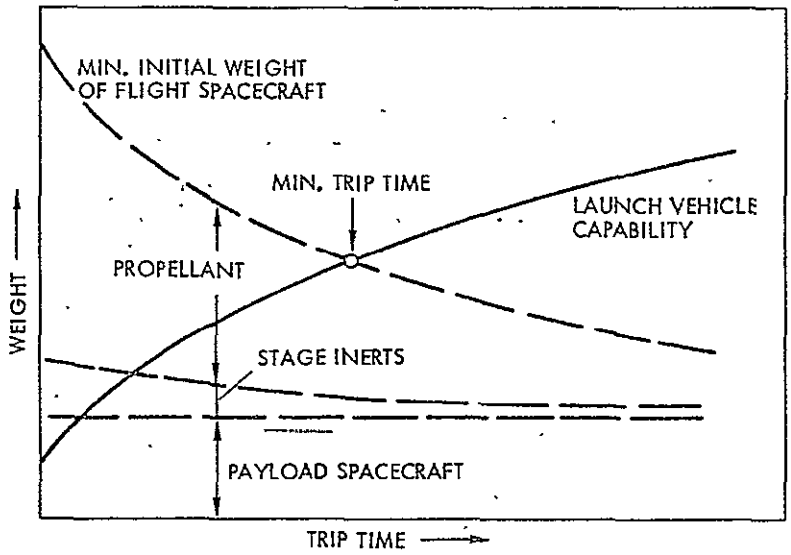

Figure 1-1. Determination of Minimum Trip Time

A propulsion system with improved performance can yield an increase in payload or a reduction of flight time, the latter particularly when the two characteristic curves have a shallow intersection, typical for the upper range of launch vehicle and retro-propulsion system capabilities. Improved retro-propulsion performance will, in fact, be essential in many cases to make an orbiter mission feasible if limited launch vehicle capability or a large required payload mass would otherwise tend to preclude it.

1.3 MISSIONS TO BE PERFORMED BY THE MULTI-MISSION PROPULSION MODULES

Missions to which the multi-mission propulsion modules are to be applied were specified by NASA to include the following:

1) 1988 Mercury orbiter mission (744- and 822-day flight times with Venus gravity assist)

2) Saturn orbiter missions for a range of flight times and payloads and for both inclined and equatorial orbits about the planet

3) Uranus orbiter missions for a range of flight times and payloads and for inclined orbits only

4) Comet rendezvous missions (Encke, Tempel 2 with two opportunities, Kopff, Faye, and Perrine-Mrkos with two opportunities).

Not all of these missions have the same priority rank, and a scientific consensus as to relative merits of these missions has not been developed. The targets were identified primarily to establish a diversity of mission profiles, environments and propulsion requirements to which the multi-mission propulsion module concept should be adaptable.

The Uranus orbiter mission is problematic because of the extremely long trip time required, ranging from 8 to 10 or more years, so that arrival velocities at Uranus remain within reasonable limits (8 to 10 km/sec). For this reason the use of Jupiter or Saturn gravity assist to reduce trip time is incompatible with orbit insertion impulse requirement.

The comet rendezvous missions listed under 4) are considered to have a low priority and are included in the study primarily to demonstrate the utility of a standardized propulsion module designed for use in multiple missions of great diversity. Impulse requirements of the comet rendezvous missions cover a wide range, the lowest being commensurate with the Saturn missions, the highest with the Mercury mission.

1.4 STUDY OBJECTIVES

The principal study objectives, as defined by NASA's contractual work statement, are the following:

1) To develop a conceptual design for each of four multi-mission chemical propulsion modules (two propellant combinations, earth-storable, space-storable, and two sizes) and to assess the capability of each in a number of missions requiring major midcourse and terminal propulsion maneuvers

2) To assess the cost, (recurring and nonrecurring) of these modules as a function of the number of missions they might serve, and to estimate total time and cost required to develop and bring the modules to operational status

3) To identify and assess the cost effectiveness of any new technologies needed and to be developed in order to meet design requirements most effectively.

Design activities and analyses conducted to meet the principal study objectives are subject to a number of study requirements and guidelines which are briefly outlined as follows:

- A common propulsion module is required that can be used practically without modification in different planetary orbiter missions specified, namely Uranus, Saturn and Mercury orbiters

- This multi-mission module must be able to withstand the environmental extremes of close solar proximity and great distances from the sun

- Propulsion module designs are required a) for spin-stabilized payload vehicles (Pioneer class) and b) for three-axis stabilized vehicles (Mariner class)

- The space-storable propulsion modules are to be compared with earth-storable systems regarding the performance of the specified missions

- The missions are to use the Shuttle orbiter and an expendable upper stage as launch vehicle. Compatibility with Shuttle launch conditions and orbital operations must be assured.

The approach to be used in meeting the multi-mission commonality requirement is to use a module size with sufficient propellant capacity for intermediate impulse requirements, e.g., as in the Saturn orbit mission. The much greater impulse requirement of the Mercury mission is met by using two propulsion modules in tandem. This not only avoids the weight penalty of overly large tank size and nearly 50 percent off-loading for the lower energy missions, with attendant propellant sloshing problems, but also yields a major performance improvement inherent in two-stage orbit insertion at Mercury

1.5 RELATION TO PREVIOUS AND CONCURRENT STUDIES

This study relates to and draws on several previous studies involving the use of space-storable (LF_2/N_2H_4) bipropellant propulsion systems. These studies were largely performed by JPL, with emphasis on application to Jupiter and Saturn orbiters (References 1, 2, 3).

A study was performed by TRW in 1972 under JPL contract to determine the thermal control methodology of using cryogenic fluorinated bipropellants as planetary orbiters (Reference 4).

Several other studies performed at JPL, NASA/Ames and TRW have defined design and performance characteristics of planetary orbiters of the Pioneer and Mariner class (References 5, 6, 7). Some of these include requirements imposed by the use of the Shuttle/upper stage as a launch vehicle for planetary missions.

A concurrent study performed by TRW under JPL contract (Reference 8) considered safety implications of carrying large quantities of liquid fluorine as propellant on Shuttle-launched payloads. Safety requirements and constraints and methods to achieve a high level of safety in handling liquid fluorine prior to and during the launch phase were developed as a result of that study. These results are directly applicable to the launch vehicle/propulsion module interface definition tasks addressed in the present design and feasibility study, and were utilized in the formulation of the propulsion module design and handling concepts.

Mission analysis, as such, was not included in the study objectives. The study did include an appreciable amount of performance evaluation including:

a) Launch performance of numerous Shuttle/upper stage combinations

b) Orbit injection performance under various maneuver modes and constraints.

In addition, the mission/system analysis effort usually associated with planetary spacecraft system design had to be expended. However, TRW's analyses were aided by results from a concurrent NASA/Ames study by D. W. Dugan (Reference 9) and by data from comprehensive Mercury orbiter mission studies performed by Martin Marietta (References 10 and 11).

1.6 ORGANIZATION OF REPORT

This report presents mission characteristics and propulsion requirements (Section 2), and gives data on performance analysis and tradeoffs for various implementations and mission modes of the multimission propulsion module (Section 3). Propulsion module design approaches and configurations for different payload vehicles, destinations and propulsion system types are covered in Section 4, while propulsion subsystem designs are defined in Section 5.

With the design concepts thus defined the next sections of the report present system evaluations in terms of environmental factors and reliability (Section 6); system performance (Section 7); development plan and

cost assessment (Section 8). Cost benefits of new technology introduced by the design concept and by the use of advanced space-storable propulsion are assessed in Section 9.

Section 10 presents highlights of the results obtained in the study, lists recommendations regarding future development of the new technology, and outlines areas recommended for further study.

Appendixes included in Volume III of this report present additional material on propulsion system technology and design; structural analysis; launch vehicle performance; and orbit insertion maneuver optimization.

2. MISSION CLASSES AND PROPULSION REQUIREMENTS

2.1 SPECIFIED MISSION SET

Primary missions to be performed by the multi-mission propulsion module, according to the work statement, are planetary orbiter missions to

Mercury	(1988)
Saturn	(1985)
Uranus	(1985).

Rendezvous missions to the comets

Tempel 2	(1983 and 1984)
Faye	(1986)
Kopff	(1991)
Perinne-Mrkos	(1990 and 1991)
Encke	(1987)

may also be within the capability of the multi-mission propulsion module, but are to be considered as a secondary objective.

These missions have in common a requirement for high impulsive energy, but have very dissimilar characteristics otherwise: they require transit times ranging from 2 to 8 years or longer, are exposed to extremely different physical environments at solar distances ranging from 0.3 to 20 AU, and vary greatly in the utilization of propulsive capabilities and thrust phase sequences.

A priority ranking for the planetary orbiter missions has not been established. However, for reasons of practical realizability the Mercury and Saturn orbit missions should probably be ranked higher than the Uranus orbit mission since the latter with transit times of 8 years or more introduces unique problems of long-life reliability.

Both Saturn and Uranus missions must use direct transfer trajectories, since the use of Jupiter gravity assist would lead to high arrival velocities and, thus, high orbit insertion velocity requirements. Transfer times are therefore quite long and, in some cases, approach the duration of a Hohmann transfer.

Comet rendezvous missions, as a class, are only being considered to increase the number of potential users of the high-performance propulsion module once developed. Thus, their ΔV requirements will not be a criterion in establishing propulsion module capabilities. In general, comet rendezvous falls in the class of "outbound" missions since transfer trajectories with aphelion distances of 3 AU or greater are usually required to achieve rendezvous with an affordable total ΔV expenditure.

2.2 SUMMARY OF MISSION PROFILES

2.2.1 Mercury Orbiter

Comprehensive mission analyses performed by Martin Marietta (References 10 and 11) have covered the spectrum of Mercury orbit missions in the late 1970's and 1980's in a search for mission opportunities with minimum velocity requirements that include single and multiple Venus swingby maneuvers. Figure 2-1 shows payload capabilities corresponding to favorable opportunities and identifies 1988 as an optimum mission year.

Two trajectory profiles were selected by NASA for consideration in this study. They both involve Venus swingby maneuvers as a means for reducing arrival velocity at Mercury, as shown by the two trajectory plots in Figure 2-2. The trajectory shown in Figure 2-2a includes a Venus swingby approximately 13 months after launch, followed by two complete revolutions around the sun for orbit phasing with Mercury, with the resultant total flight time of about 27 months. The other opportunity launched on March 22, 1988, includes two Venus encounters, with the first Venus swingby followed by two complete phasing revolutions of the spacecraft before the second Venus swingby. In addition, an extra phasing revolution is required prior to Mercury encounter. Figure 2-2 identifies earth, Venus, and Mercury positions at the encounters and summarizes mission events.

Table 2-1 lists principal trajectory characteristics of the two transfer trajectory options. The total reduction in ideal velocity requirement for the second mission mode is about 380 m/sec. The reduction

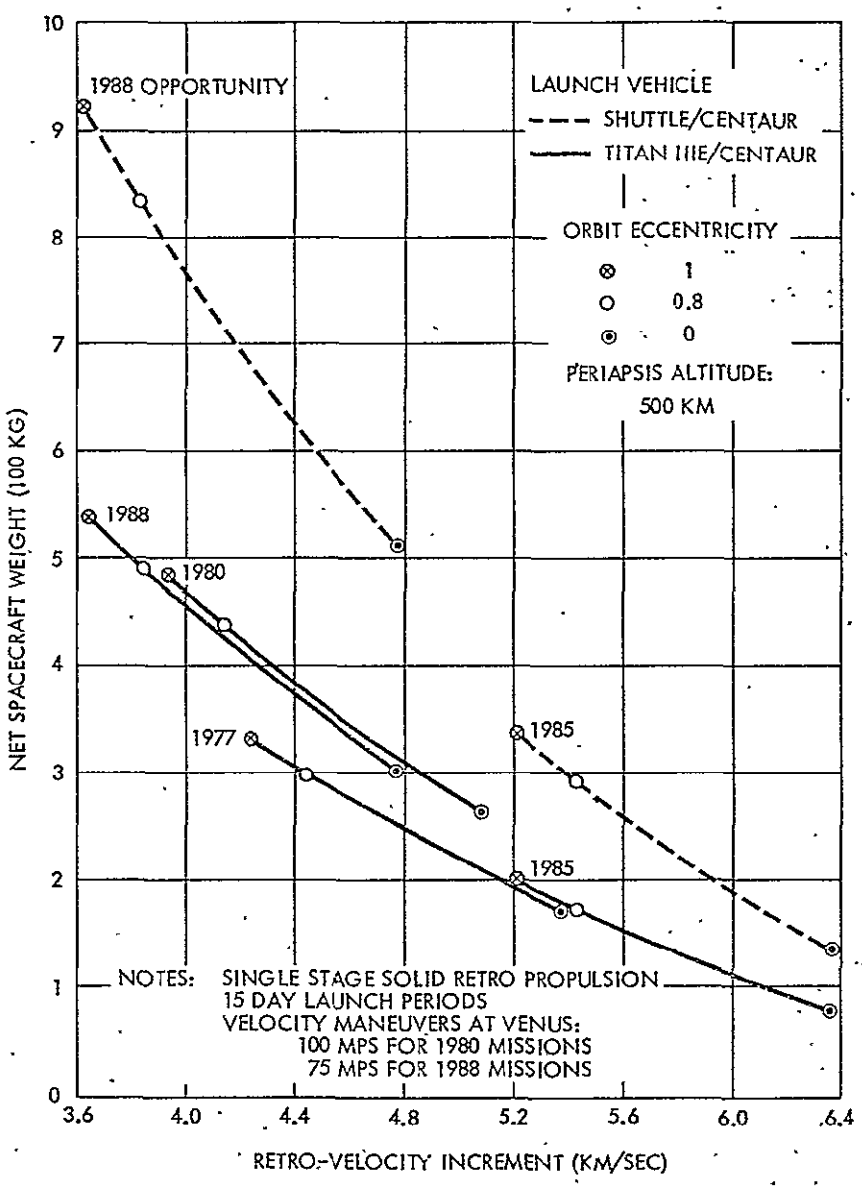

Figure 2-1. Spacecraft Weight Options for Several Mercury Orbit Mission Opportunities (from Reference 10).

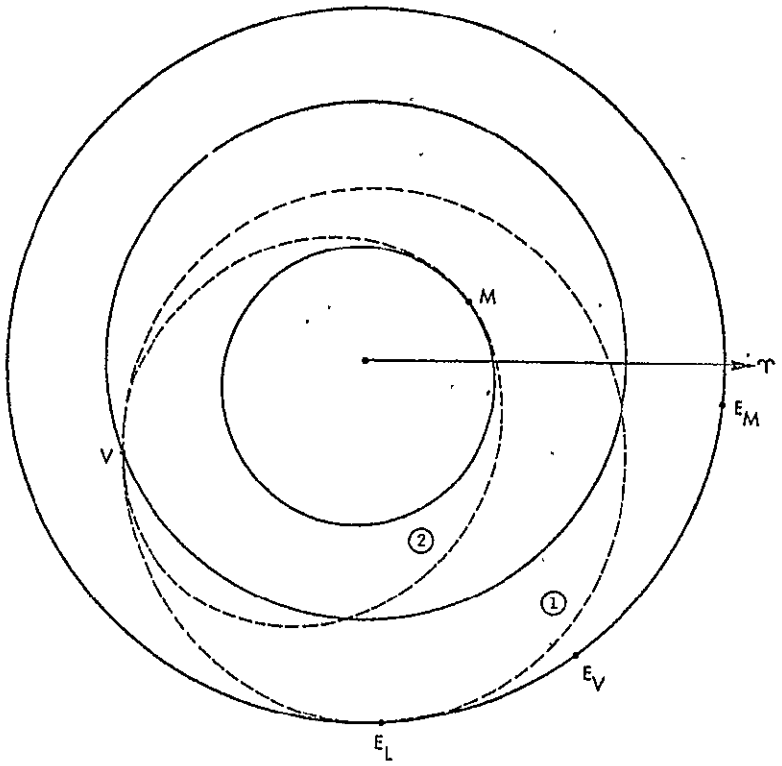

E_L: EARTH AT LAUNCH, 6-26-88
E_V: EARTH AT VENUS SWINGBY, 7-30-89
E_M: EARTH AT MERCURY ENCOUNTER 9-17-90
V: VENUS AT SWINGBY
M: MERCURY AT ENCOUNTER
① ONE COMPLETE SOLAR REVOLUTION BEFORE VENUS SWINGBY
② TWO COMPLETE SOLAR REVOLUTIONS BEFORE MERCURY ENCOUNTER

2a. Mission Option I (Single Venus Swingby)

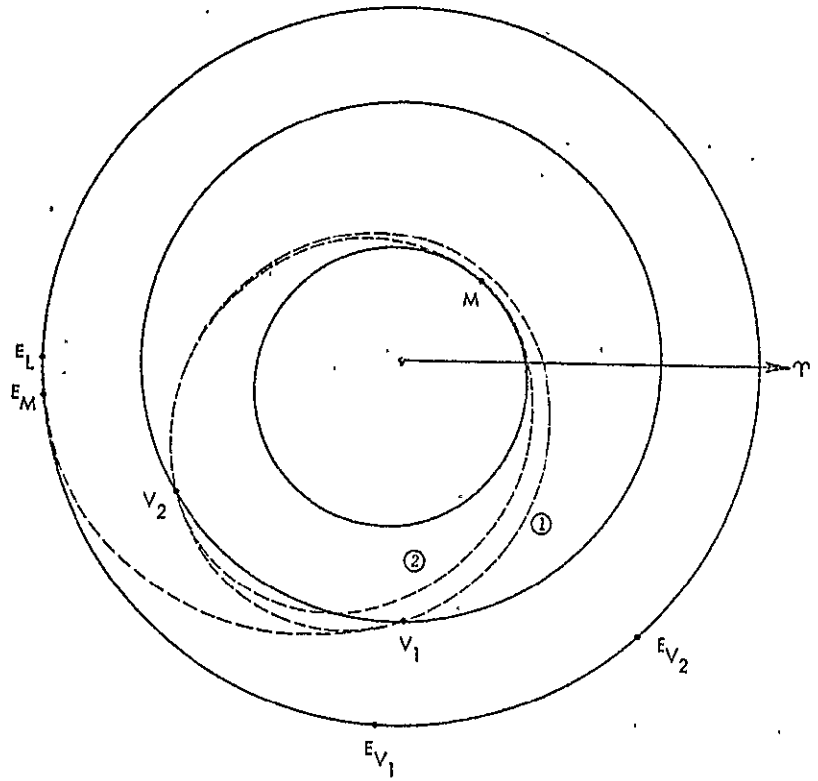

E_L: EARTH AT LAUNCH, 3-22-88
E_{V_1}: EARTH AT FIRST VENUS SWINGBY (V_1), 6-18-88
E_{V_2}: EARTH AT SECOND VENUS SWINGBY (V_2), 8-4-89
E_M: EARTH AT MERCURY ENCOUNTER (M), 3-27-90
① TWO COMPLETE SOLAR REVOLUTIONS BETWEEN FIRST AND SECOND VENUS SWINGBYS
② ONE COMPLETE SOLAR REVOLUTION BEFORE MERCURY ENCOUNTER

2b. Mission Option II (Multiple Venus Swingby)

Figure 2-2. 1988 Earth-to-Mars Transfer Trajectories via Venus (from References 10 and 11)

Table 2-1. Characteristics of Two Earth-to-Mercury Transfer Trajectories (see also Figure 2-2)

	Option 1	Option 2
Launch date	19 June 1988	12 March 1988
Flight time (days)	822	744
Launch energy, C_3 (km^2/sec^2)	36.82	25.82
Arrival velocity V_∞ (km/sec)	6.4	6.03
Ideal retro velocity (km/sec) ($r_p = 1.208\ R_M$, $e = 0.8$)	3.85	3.53
Midcourse correction and powered Venus swingby maneuver (km/sec)	0.28	0.22

of maneuver requirements is actually still greater when Mercury orbit insertion losses are taken into account. Note that in the second mission option the launch energy is only 25.8 km^2/sec^2 compared to 36.8 km^2/sec^2 in the first option, and that flight time is reduced by nearly 80 days, corresponding to about one full revolution of Mercury around the sun.

A low periapsis altitude and high orbital eccentricity are desirable to minimize the orbit insertion maneuver. Study guidelines specify a 500 km periapsis altitude of the Mercury orbit of 500 km and an eccentricity e = 0.8. A lower periapsis altitude would make approach navigation too difficult, and a higher eccentricity would adversely affect orbital stability. The maximum eccentricity commensurate with orbital stability under solar gravity perturbation is 0.9.

The duration of the orbital phase is assumed to be 1 to 2 years. This permits a thorough exploration of the physical characteristics of Mercury and its environment as well as extended observation of solar phenomena from the vantage point of Mercury's orbit. During at least three-quarters of the orbit mission life the spacecraft will be in a position to observe phenomena on the far side of the sun that cannot be observed from earth.

2.2.2 Saturn Orbiter

Representative transfer trajectory characteristics and velocity requirements for the Saturn orbiter mission are listed in Table 2-2.

Table 2-2. Saturn Orbiter Missions

Launch Date: 1/15/85

Heliocentric Distance at Departure: 0.985 AU

Trip Time (days)	a (AU)	Trajectory Data			Velocities[1]				
		e	R_{arr} (AU)	C_3[2] (km^2/sec^2)	Relative Speed at Saturn, V_∞ (km/sec)	2.5 x 61.60 R_S ΔV_1 (m/sec)	2.5 x 61.60 R_S ΔV_2 (m/sec)	2.5 x 37.8 R_S ΔV_1 (m/sec)	2.5 x 37.8 R_S ΔV_2 (m/sec)
1250	9.86	0.9002	10.07	136	9.7396	2460	541	2710	862
1400	7.55	0.8699	10.07	130	8.3100	1930	593	2180	942
1500	6.57	0.8506	10.07	126	7.2378	1600	650	1820	1010
1750	5.95	0.8349	10.06	123	6.2250	1280	690	1550	1085

[1] ΔV_1 is impulsive maneuver requirement for orbit insertion. ΔV_2 is orbit plane change to attain equatorial orbit. Actual ΔV requirements for nonimpulsive maneuvers and estimated requirements for midcourse maneuvers will be taken into account in performance calculations.

[2] Based on 20-day launch window.

Source: Planetary Flight Handbook, NASA SP-35, Vol. 7, Pt. A, B.

Trip times are assumed to range from 1250 to 1750 days (3.4 to 4.8 years), and the C_3 requirements vary from 136 to 123 km^2/sec^2, respectively. Orbit dimensions to be achieved at Saturn are 2.5 x 61.6 planet radii (R_S). This orbit has a period of 32 days, twice that of the satellite Titan and thus permits repeated Titan encounters. As an alternative, an orbit with dimensions 2.5 x 37.8 R_S and a 16-day period will also be considered. Its velocity increments are also listed in Table 2-2.

After the injection maneuver (velocity increment ΔV_1) a second velocity increment, ΔV_2, is required near the apoapsis to change the inclined initial capture orbit into an equatorial orbit. The second velocity increment increases with trip time because of the increasing minimum orbit inclinations.

In addition to the two velocity increments identified above, an apoapsis maneuver will be desirable to raise the periapsis altitude from the low value of 2.5 R_S at arrival to reduce the risk of particle impacts.

An orbital lifetime of 2 or even 3 years is being contemplated to permit extensive planetary exploration and possibly close satellite encounters. A concurrent study by JPL has shown that repeated swingby maneuvers of the satellite Titan permit significant orbit modifications with a minimum of propulsive maneuvers in addition to repeated close observations of the satellite. These maneuvers permit changing the orientation of the apsidal line and orbital inclination. It is ancitipated that additional propulsive maneuvers, totaling about 100 m/sec, are required for orbit trim and approach guidance corrections to exploit satellity gravity assist opportunities during the orbital lifetime.

2.2.3 Uranus Orbit Mission

Representative transfer trajectory characteristics and velocity requirements for the Uranus orbit mission are listed in Table 2-3. Trip times are assumed to range from 2560 to 4360 days (7 to 12 years), and C_3 requirements from 159 to 139 km^2/sec^2, respectively. Orbit dimensions at Uranus are assumed to be 1.1 x 31.2 planet radii (R_U). This orbit has a period equal to that of the satellite Titania. The orbit will be nearly polar in inclination because of the 97-degree tilt of the planet's solar

Table 2-3. Uranus Orbiter Missions

Launch Date: 2/4/85

Heliocentric Distance at Departure: 0.986 AU

Trip Time (days)	Trajectory Data				Velocities	
	a (AU)	e	R_{arr} (AU)	C_3[1] (km^2/sec^2)	Relative Speed at Uranus, V_∞ (km/sec)	1.1 x 31.2 R_U Impulsive ΔV[2] for Orbit Insertion (m/sec)
2560	269.77	0.99635	19.51	159	9.9184	2686
2860	30.88	0.96764	19.56	151	8.5780	2119
3260	17.30	0.96394	19.63	146	7.2377	1620
3660	13.69	0.92813	19.69	142	6.2548	1305
4360	11.47	0.91409	19.79	139	5.2123	986

[1] Based on 20-day launch window

[2] Actual ΔV requirements for nonimpulsive maneuvers and estimated requirements for midcourse and orbit trim maneuvers will be taken into account in performance calculations.

Source: Planetary Flight Handbook, NASA SP-35, Vol. 7, Pt. A, B.

axis which points approximately in the direction of the sun in the time period for which this mission is considered. No plane change at Uranus is contemplated.

Close encounters with Uranus' satellites are made difficult by the large inclination of their orbital plane relative to the incoming trajectory, and gravitational assists from these satellites for orbital changes is not anticipated. However, as will be discussed in Section 5, there is the possibility of modifying the initial orbit by a reasonably small apoapsis maneuver to achieve encounters with satellites such as Titania, Ariel, and Oberon.

The guidance and navigation requirements for orbit insertion at a 1.1 R_U periapsis distance may present difficulties because of the large ephemeris uncertainty of Uranus. One-sigma uncertainties in the planet's position along its orbit are estimated as about 10,000 km (0.4 R_U), based

on current ephemeris data. An onboard navigation sensor may be necessary for accurate control of the close approach to the planet indicated by the desired orbital dimensions. It is anticipated that the knowledge of Uranus' ephemeris will be greatly improved (by a projected Mariner Jupiter Uranus flyby mission with launch date in 1979 or 1980), although Uranus encounter would only take place after the launch date of the orbiter. To simplify the approach guidance problem a larger periapsis distance (1.5 R_U) may have to be considered. This would increase orbit insertion maneuver requirements by 160 to 385 m/sec for the range of approach velocities listed in Table 2-3.

An orbital lifetime of about 2 years is contemplated to permit comprehensive exploration of the planet and its physical environment. Of particular interest in this mission is the unusual configuration of Uranus' postulated magnetosphere with a magnetotail extending roughly along the polar axis. Observation of particles and fields in this environment over an extended period will provide important scientific data on the formation of planetary magnetospheres, in general, to augment the knowledge gained by magnetospheric observations at earth and Jupiter.

2.2.4 Comet Rendezvous Missions

Table 2-4 lists trajectory characteristics and ΔV requirements of the seven comet rendezvous mission opportunities defined in the study guidelines. Onboard propulsion requirements are comparable to those of Saturn and Uranus orbiters for Tempel 2, Faye, and Kopff, and to those of the Mercury orbiter for Perinne-Mrkos and Encke, and are therefore commensurate with capabilities of the planetary orbiter propulsion module. In a typical mission profile with a major midcourse maneuver, ΔV_2 will be performed in the vicinity of aphelion and a second major maneuver, ΔV_3, at destination. The midcourse maneuver is performed to adjust orbital inclination and perihelion radius and, thereby, to reduce the terminal maneuver. These maneuver requirements are the results of three-impulse trajectory studies performed by E. L. Tindle of NASA/Ames Research Center with the aid of the "TOPICS" computer program. This program is designed to determine trajectories with minimum ΔV requirements for the spacecraft propulsion system.

Table 2-4. Characteristics of Comet Mission Transfer Trajectories

Comet	Launch	Arrival	Flight Time (days)	C_3 (km^2/sec^2)	ΔV_2 [1] (km/sec)	ΔV_3 [2] (km/sec)	R_{arr} [3] (AU)
Tempel 2	19 Jul 83	1 Jun 88	1779	84.6	1.698	0.023	1.629
Tempel 2	31 Jul 84	10 Jun 88	1410	70.3	1.765	0.814	1.581
Faye	30 Oct 86	11 Aug 91	1746	67.42	2.220	1.240	1.939
Kopff	12 Jul 91	3 Jan 96	1636	72.60	1.550	0.671	1.801
Perrine-Mrkos	19 Nov 90	9 Aug 95	1724	81.42	2.104	0.678	1.358
Perrine-Mrkos	14 Nov 91	18 Aug 95	1373	71.86	2.334	1.428	1.322
Encke	13 Mar 87	22 Jul 90	1227	64.82	3.809	0.101	1.810

[1] Major midcourse maneuver

[2] Maneuver at rendezvous

[3] Radius at arrival

* Data furnished by NASA/Ames Research Center

Additional maneuvers, estimated in the 100 to 300 m/sec range, are required

a) For approach guidance correction, considering the large ephemeris uncertainty of most comets

b) for exploration of the comet's nucleus, coma and tail.

Typical relative trajectories near the comet achievable by these maneuvers are illustrated in Figure 2-3 (see also Reference 12).

Depending on the target comet, the desired dwell time in its vicinity may extend to several hundred days, to permit observation of physical changes as the comet approaches and departs from its perihelion.

2.3 SUMMARY OF MANEUVER REQUIREMENTS

The impulsive maneuver requirements identified in Section 2.2 for each mission class are summarized in Figure 2-4. Estimated ΔV requirements for midcourse corrections, orbit trim, etc., are shown in addition to the major orbit insertion and plane change maneuvers, or their equivalent in the case of comet rendezvous missions. This graph only serves to illustrate the wide range of maneuver capabilities to be

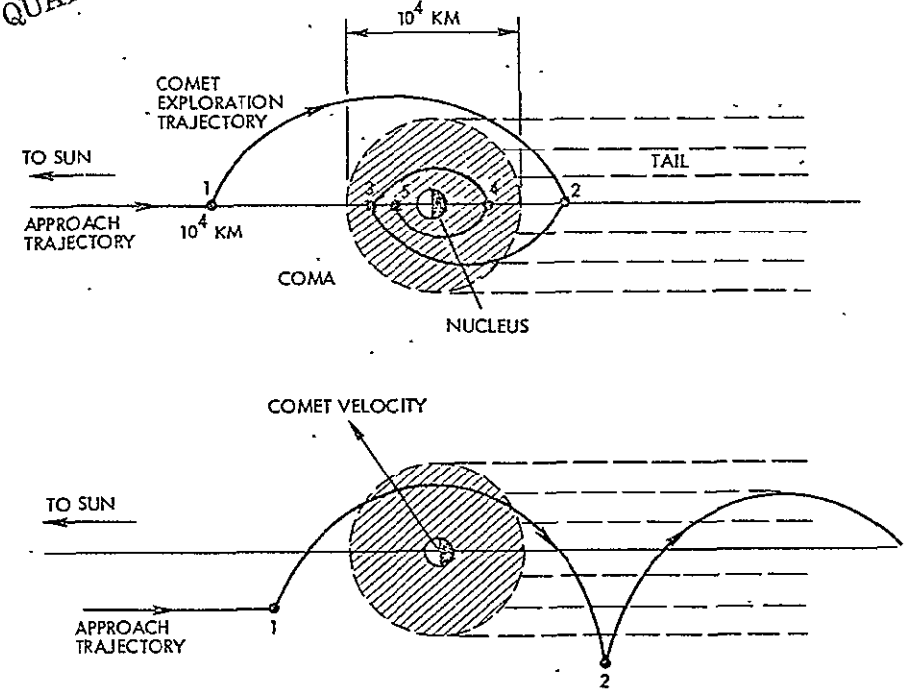

Figure 2-3. Relative Trajectory Options in Comet Vicinity (Not to Scale)

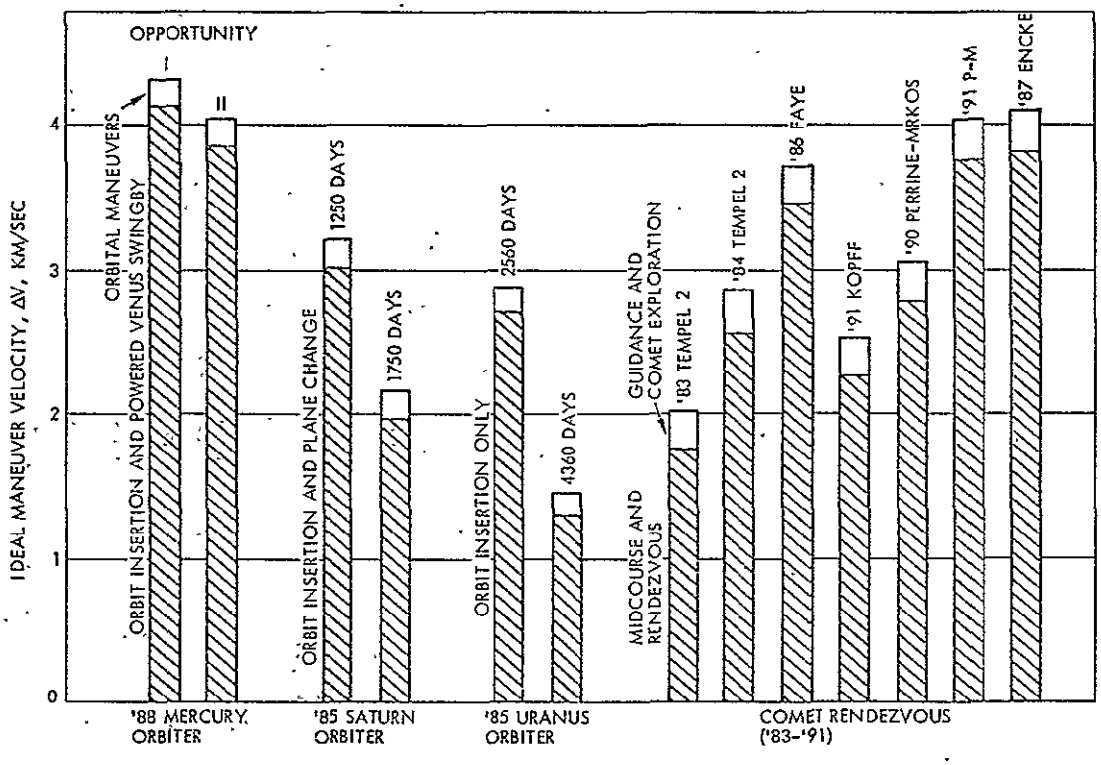

Figure 2-4. Ideal Maneuver Velocity Requirements for Specified Missions

satisfied by the multi-mission propulsion modules without taking detailed performance aspects and orbit insertion losses ("gravity losses") into account. These will be discussed in Section 3.

Figure 2-5 shows typical maneuver time histories for the various mission classes. For clearer illustration of the overall sequence of events, impulse sizes and time intervals are not drawn to scale. The graph shows the diversity of maneuver sequences and operational flexibility requirements for which each common propulsion module must be designed. In some of the missions the propulsion system may have to be operated, starting at earth departure (to augment launch vehicle performance), with long periods of dormancy between thrust periods. After the principal orbit insertion maneuver (an event which will take place only after 8 years or more of transit time in the Uranus mission), additional maneuvers are still to be performed during the orbital mission phase.

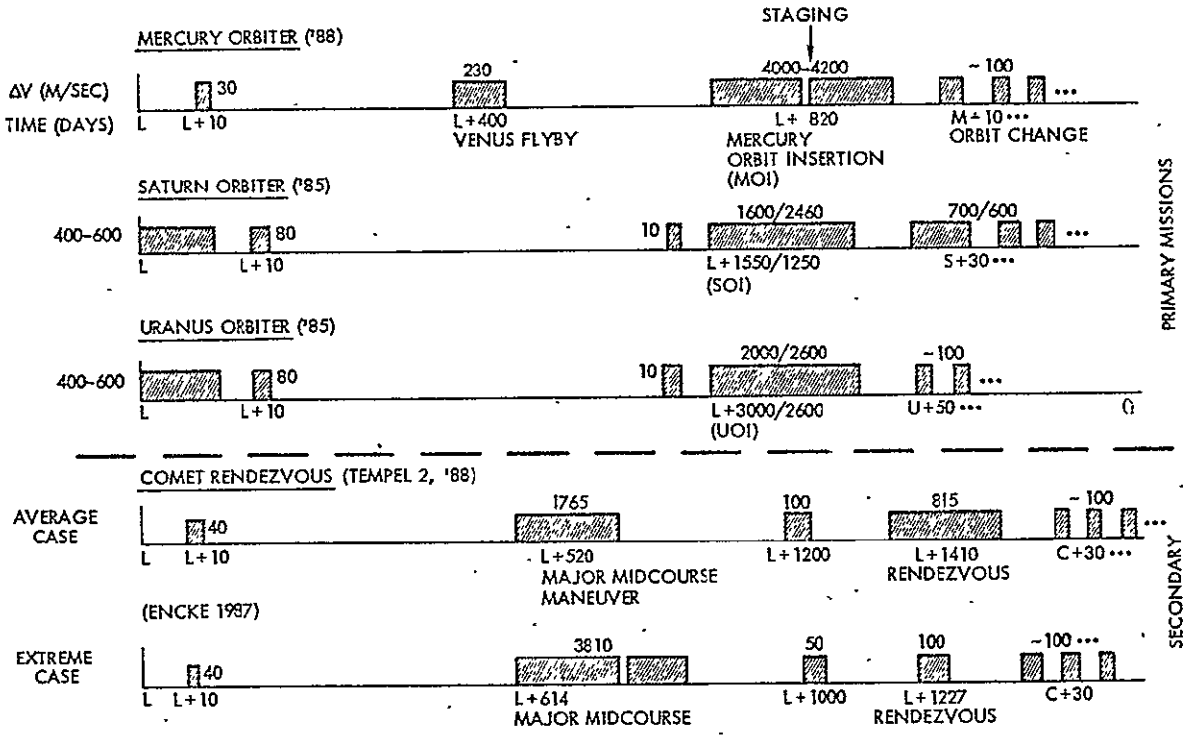

Figure 2-5. Propulsion Schedules (Preliminary); ΔV Impulses in m/sec

2.4 APPLICABILITY OF COMMON PROPULSION MODULE

Maneuver requirements of the specified mission classes, ranging from about 2500 to 4500 m/sec, can be met by a common propulsion module with fixed propellant capacity either by sizing it for the mission demanding the largest maneuver capability and using it partially loaded on the other missions; or by using two smaller modules in tandem for the most demanding mission and singly for the others.

The Mercury mission defines the tank size in either case, since even with two propulsion modules used in tandem it requires at least twice as much propellant as the other orbiter missions. Tandem use of two propulsion modules is also preferable from a performance standpoint, since two-stage orbit insertion is much more weight-effective than a single-stage maneuver, when the total velocity increment is in the 4000 to 4500 m/sec range.

Comet rendezvous missions can be flown using the propulsion module either singly or in tandem, depending on ΔV requirements.

The use of a common propulsion module in all missions of the specified set imposes inert weight penalties compared to custom-designed propulsion systems because

a) The module is oversized for some of the missions

b) The module, designed for use in tandem application, is structurally heavier than a module of the same size for single-stage application.

Performance penalties of the multi-mission concept can be partially offset by the use of available excess propellant capacity to augment launch vehicle performance and thus to reduce trip times of outer planet missions, especially in the Uranus orbiter case.

Preliminary performance comparisons, without reference to specific missions, can be made conveniently with the aid of Figure 2-6. This nomograph shows usable propellant weight versus spacecraft dry weight with parametric lines of total ΔV capability and total injected weight. Solid ΔV lines correspond to earth-storable propellants (I_{sp} = 295 sec), dashed lines to space-storable propellants (I_{sp} = 375 sec).

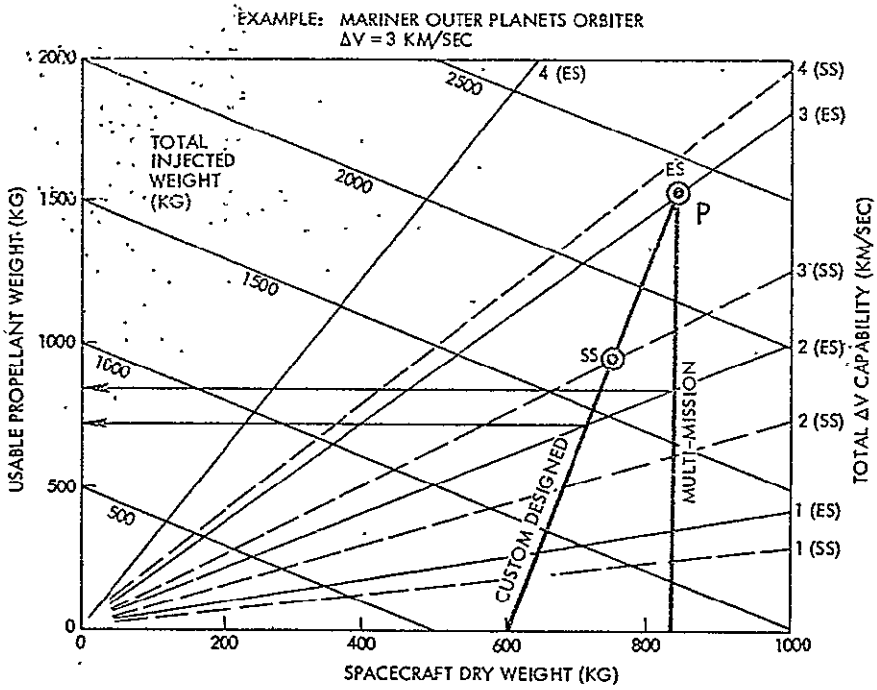

Figure 2-6. Performance of Multi-Mission and Custom-Designed Stage for Earth- and Space-Storable Propellants

Two examples are illustrated. The slanted line through points SS and ES indicates the performance of a custom-designed propulsion stage for a payload mass of 550 kg. The stage inert mass increases linearly with propellant mass, for a fixed value of 50 kg for zero propellant mass, at a rate of 16 percent of the propellant load, i.e., 16 kg for each 100 kg of propellant. The vertical line at the right indicates the corresponding characteristics for a multi-mission stage designed for the same payload and for a desired ΔV capability of 3 km/sec, assuming earth-storable propellants. The design point is indicated by the intersection (P) with the custom-stage characteristic; at ΔV = 3 km/sec. For a mission requiring a maneuver capability of only 2 km/sec the multi-mission stage uses 800 kg of propellant, and the total injected weight is 1700 kg, while the custom-designed stage uses 700 kg of propellant and requires a total injected weight of 1350 kg, i.e., a saving of 350 kg. Conversely, given an injected weight of 1700 kg the custom-designed stage achieves about 0.3 km/sec more ΔV than the multi-mission stage.

Note that the data presented by the nomograph are based on the assumption of impulsive maneuvers.

More exact performance comparisons that relate to specific mission requirements and take actual maneuver characteristics (including gravity loss, etc.) and systems weight into account will be presented in Section 7.

2.5 PAYLOAD SPACECRAFT CLASSES

Payloads specified for this study are spin-stabilized, Pioneer class, and three-axis-stabilized, Mariner class spacecraft. Depending on whether the destination is Mercury ("inbound" mission) or an outer planet or comet ("outbound" mission) the payload spacecraft of each class have different configurations, mass, and operating modes. The inbound spinner is of the Pioneer Venus type, the outbound spinner of the Pioneer 10/11 type. The inbound three-axis-stabilized vehicle is a derivative of Mariner Venus Mercury (1973), the outbound version a derivative of Mariner Jupiter Saturn (1977).

Propulsion modules to be used with Pioneer class payloads will be designated as Module A, those used with Mariner class payloads as Module B.

In the study guidelines a range of payload weights for spinning and three-axis-stabilized spacecraft is called out, namely:

340 to 408 kg (750 to 900 lb_m) for spinners

550 to 680 kg (1213 to 1500 lb_m) for nonspinners.

Since the inbound versions of each payload vehicle class, typically, have a lower mass than the outbound versions the tentative weight allocations listed in Table 2-5 are assumed here for purposes of simplified discussion. However, performance characteristics to be presented in Section 7 will take the specified range of payload weights for each payload class into account.

Figure 2-7 is a schematic illustration of the payload vehicles and their respective propulsion modules A and B, attached in tandem for inbound missions and singly for outbound missions. Missions to comets, not included in this illustration, may require tandem propulsion modules with outbound versions of the Pioneer or Mariner spacecraft.

Key payload vehicle characteristics are summarized in Table 2-6.

Table 2-5. Typical Payload Weights Assumed for Inbound and Outbound Missions, in kg (lb_m)

Payload Spacecraft Class	Propulsion Module Type	Mission Type	
		Inbound	Outbound
Pioneer	A	340 (750)	408 (900)
Mariner	B	550 (1213)	680 (1500)

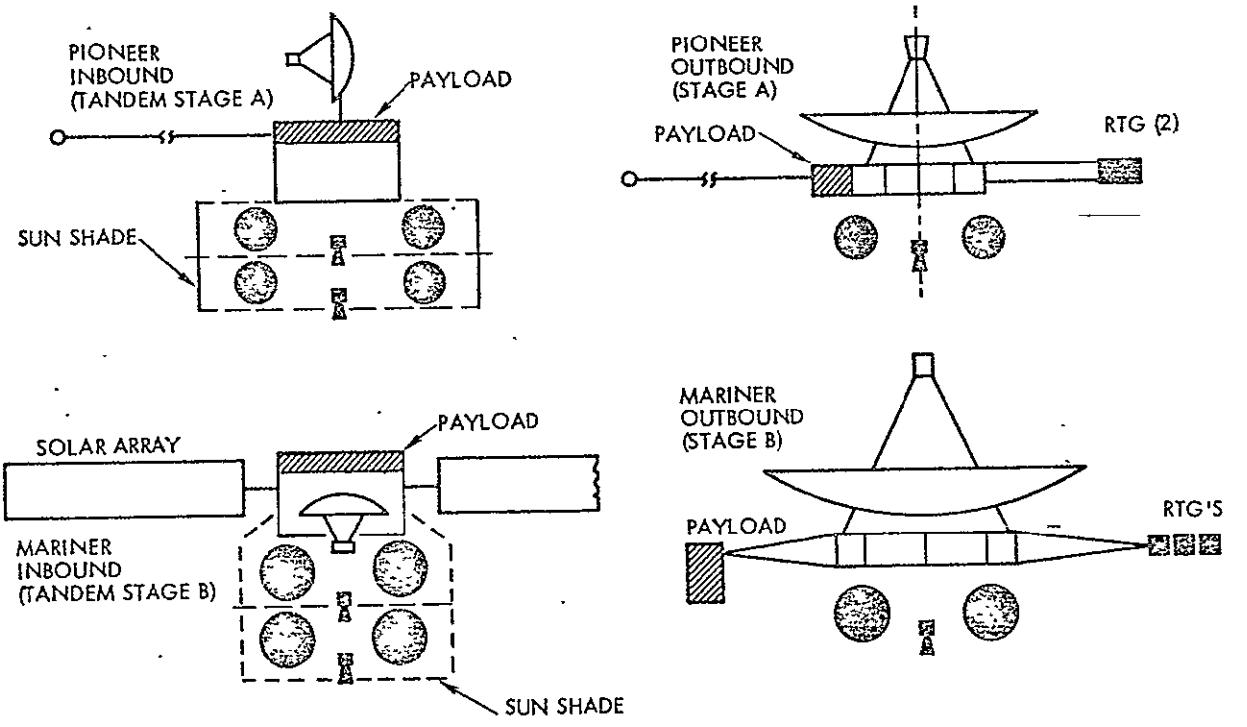

Figure 2-7. Specified Payload Spacecraft Configurations (Schematic)

Table 2-6. Principal Features of Payload Vehicles

Characteristic		Pioneer Class (Spinners)		Mariner Class (Three-Axis Stabilized)	
		Venus Orbiter	Outer Planets Spacecraft	Venus Mercury Flyby Spacecraft	Jupiter Saturn Flyby Spacecraft
Weight	kg (lb_m)	340 (750)	408 (900)	565 (1248)	680 (1500)
Maximum lateral dimension, stowed	cm (in.)	254 (100)	274 (108)	248 (98)	365 (144)
Height, deployed	cm (in.)	372 (147)	248 (98)	137 (54)	244 (96)
Center of mass location,[1] deployed	cm (in.)	99 (39)	76 (30)	60.5 (23.9)	42.5 (16.8)
Cruise orientation		Spin axis ⊥ helio-centric orbit	Spin axis points to earth	Centerline points to sun	Centerline points to earth
Interface structure					
- Form/type		Cone	Cylinder	Octagon (8 hard points)	Decagon (10 hard points)
- Dimensions/diameter	cm (in.)	114 (45)	63 (25)	152 (60)	183 (72)
Power source, type		Solar cells, body-fixed cylindrical array	2 HPG type SNAP-19 RTG's	Solar cells, 2 rotatable panels	3 MHW type RTG's
Thermal control		Bottom louvers	Bottom louvers	Front sun shade, side louvers	Side louvers
Hydrazine tank(s), diameter	cm (in.)	4 at 34 (13.5)	48 (19)	71 (28)	71 (28)
High-gain antenna					
- Arrangement		Despun, one-axis gimballed	Fixed	Two-axis gimballed	Fixed
- Size	m (ft)	1.53 (5)	2.75 (9)	1.53 (5)	3.66 (12)
Development status		In development for 1978 launch	Pioneer 10/11,[2] launched 1972-73	Mariner 10, launched 1973	In development for 1977 launch

[1] Above payload spacecraft mounting flange, empty tanks

[2] Pioneer outer planet spacecraft design is similar to Pioneer 10/11, with increased power, telemetry capability, etc.

3. PERFORMANCE ANALYSIS

3.1 LAUNCH VEHICLE PERFORMANCE

3.1.1 Diversity of Shuttle Upper Stages

A large variety of Shuttle uper stage candidates are under consideration by NASA and U.S. Air Force Agencies as part of ongoing efforts to project and definitize required launch vehicle capabilities in the Shuttle era. Upper stage performance requirements have been defined on the basis of "traffic models" for the time period of the 1980's and beyond, developed by Space Transportation System Working Groups at NASA/MSFC and elsewhere. These requirements have been published and are being updated, e.g., in Reference 13.

At the beginning of this study the principal upper stage candidates for planetary mission launches were assumed to be Centaur class vehicles (Centaur D-1S and several Centaur growth versions), used in the expendable launch mode to obtain maximum escape mission performance. Several solid propellant upper stages of the size class of Burner II (2300 lb_m) and larger were projected for planetary missions with C_3 requirements above 70 to 80 km^2/sec^2.

In the meantime, the planning for interim and ultimate Shuttle upper stages has evolved further, making a growth version of Transtage (including the dual short Transtage) a likely candidate for planetary missions with intermediate performance requirements, and the "all-up" Space Tug the projected vehicle for missions with highest performance requirements such as Mariner Saturn and Uranus orbiters (References 13 and 14).

In addition, a variety of solid propellant kick motors with capabilities greatly exceeding Burner II and TE 364-4 have entered the preliminary design/projected development stage and are to be taken into consideration. These include advanced kick stages APM-I and APM-IA with 1710 kg of solid propellant loading, with and without thrust vector control provisions, formerly termed SPM (1800),* and the 4400-lb_m solid

*In the body of this report the former term, SPM (1800), is retained.

kick stage projected for use with single or dual Transtages. Larger kick stages, such as Burner II (9000), are not weight effective for missions considered in this study and are omitted as candidates.

Toward the end of the study, the field of launch vehicle candidates identified by NASA/Ames for consideration in mission performance assessments of payload mass and flight times was broadened to include the following:

C_3 (km^2/sec^2)	Launch Vehicle
100-160	Space Tug/APM-I or APM-IA
100-160	Space Tug/BII (2300)
100-160	Space Tug/PM (2300)
100-160	Space Tug/TE 364-4
100-160	Centaur D-1S/APM-I or APM-IA
100-160	Centaur D-1S/BII (2300)
100-160	Centaur D-1S/PM (2300)
100-160	Centaur D-1S/TE 364-4
100-160	Dual Short Transtage/Solid (4400 lb_m) Kick Stage
20-90	Dual Short Transtage
20-90	Centaur D-1S
20-90	Space Tug
20-90	Titan IIIE/Centaur D-1T/BII (2300)
20-90	Titan IIIE/Centaur D-1T/TE 364-4

A parametric approach was taken in this study to evaluate mission performance of the spacecraft propulsion module with the various candidate Shuttle upper stages listed above. The method, originally suggested by D. W. Dugan of NASA, Ames Research Center, employs weight-versus-flight time characteristics of candidate launch vehicles, as illustrated in Figure 3-1. Minimum flight times for a given payload and specified planetary orbit parameters are determined by the intersections between the weight capabilities curve of each launch vehicle (solid curves) and the weight requirements curve of the payload/propulsion module combination (dashed curve), as previously discussed in Section 1.2 (see Figure 1-1).

This approach has the advantage of preserving the usefulness of data generated by this study even though projected performance characteristics of launch vehicle candidates may still change appreciably in the near future.

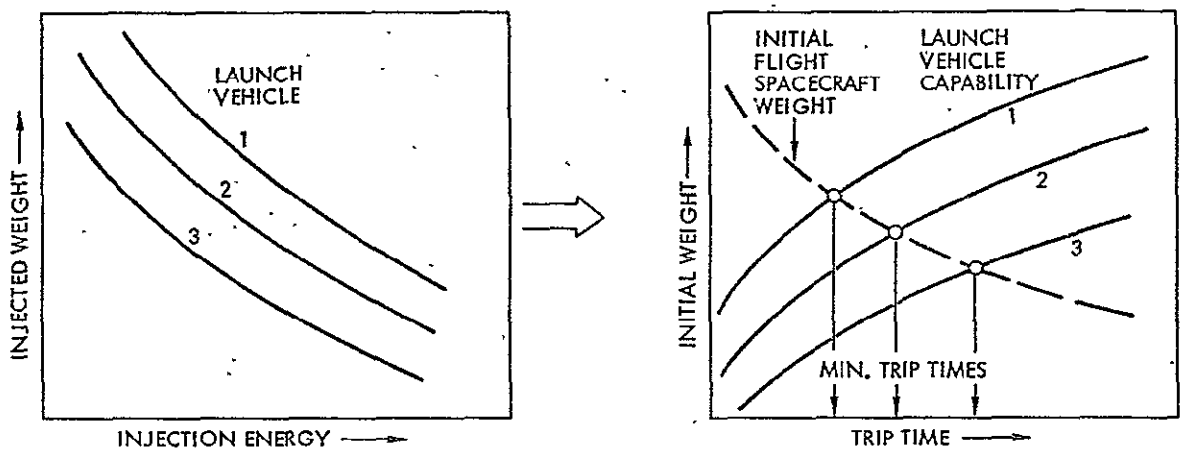

Figure 3-1. Parametric Performance Evaluation for Several Launch Vehicles

3.1.2 Performance Evaluation

Launch vehicle performance characteristics were determined by a computer program developed for detailed launch phase simulations to be described in Appendix D. Inert mass and propellant mass data and specific impulse values specified for the different upper stage candidates were used, including realistic departure phase performance penalties ("gravity losses," etc.).

The effect of nonimpulsive expendables was included in these calculations to represent finite thrust losses accurately. To take nonpropulsive expendables into account the rocket equation is modified to take the form (see also Appendix D)

$$\Delta V_{RC} = [g\, I_{sp}/(1.0 + W_{exp}/W_p)]\log_e[W_o/(W_o - W_p - W_{exp})]$$

where

ΔV_{RC} = ideal stage ΔV capability

W_{exp} = mass of nonimpulsive expendables

W_p = usable propellants

W_o = initial mass.

The performance calculations also included specified or estimated weights for inert weight elements such as interstage adapters and spin tables.

Performance data obtained by these calculations represent capabilities of the specified launch vehicles accurately, at least within tolerances warranted by the preliminary nature of the present system feasibility study, particularly in view of the on-going evolution of interim and "all-up" tug configuration concepts.

The results are in good agreement with those obtained under the same ground rules by NASA/Ames and other organizations conducting parallel launch vehicle performance studies.

3.1.3 Performance Characteristics of Launch Vehicle Candidates

Figures 3-2 and 3-3 show performance characteristics of the launch vehicle candidates for three-axis stabilized payloads with injection energies, C_3, ranging from 20 to 90 km^2/sec^2 and from 100 to 160 km^2/sec^2, respectively. Figures 3-4 and 3-5 show the corresponding characteristics for spin-stabilized payloads; the weight of the spin table, assumed as 113.4 kg (250 lb_m), was taken into account, see Appendix D. For comparison, the performance of the Titan IIIE/Centaur D-1T/TE 364-4 is shown as representative of the capability of an interim upper stage for the Shuttle.

The lower range of C_3 values is used in the Mercury orbit and comet rendezvous missions, the upper range in outer planet orbiter missions. A solid kick motor is not required for Mercury orbiters with the low C_3 requirement of 25 to 35 km^2/sec^2. (The Pioneer Mercury orbiter does not require a spin table since the spacecraft can use its own spin-up thrusters after launch vehicle separation to attain the desired spin rate.) The only missions requiring a spin table are Pioneer outer planet orbiters, and possibly some comet rendezvous missions where a solid kick motor must be used.

More complete data on launch vehicle performance evaluated in this study, the assumed mass and I_{sp} values are given, and data sources listed, in Appendix D.

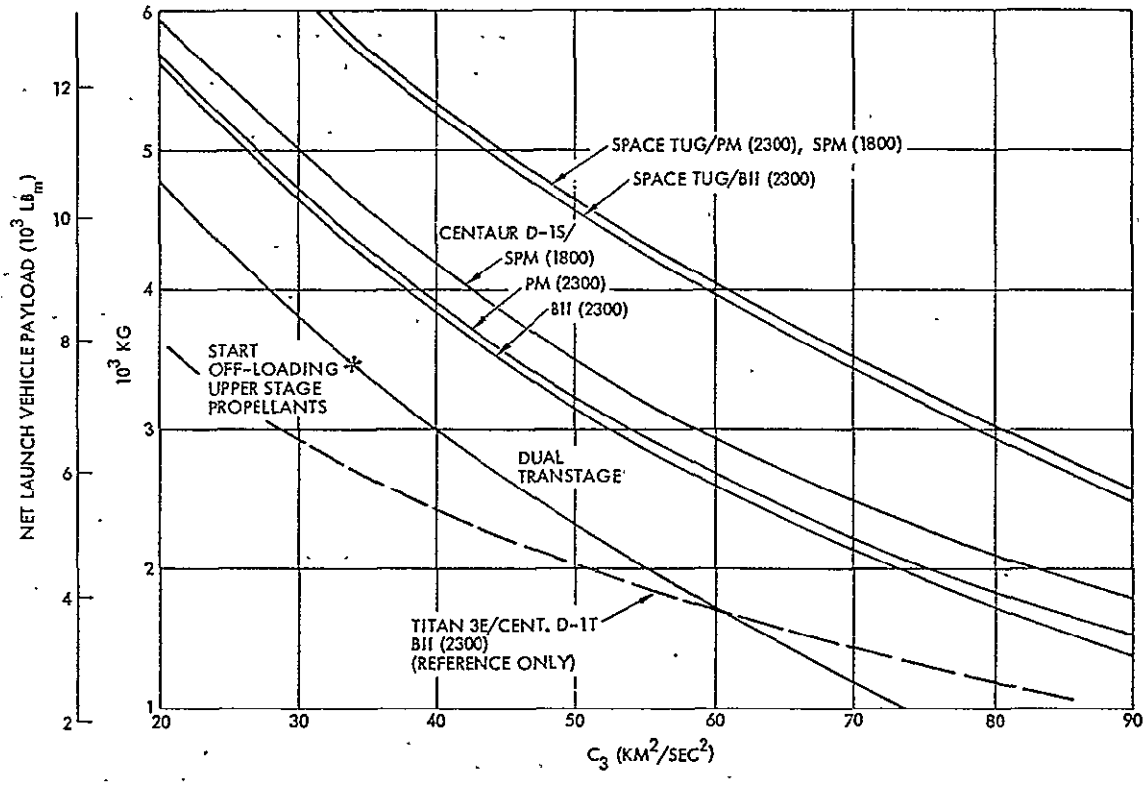

Figure 3-2. Performance of Shuttle Plus Upper Stages (Nonspinning Payloads) — Low C_3 Range

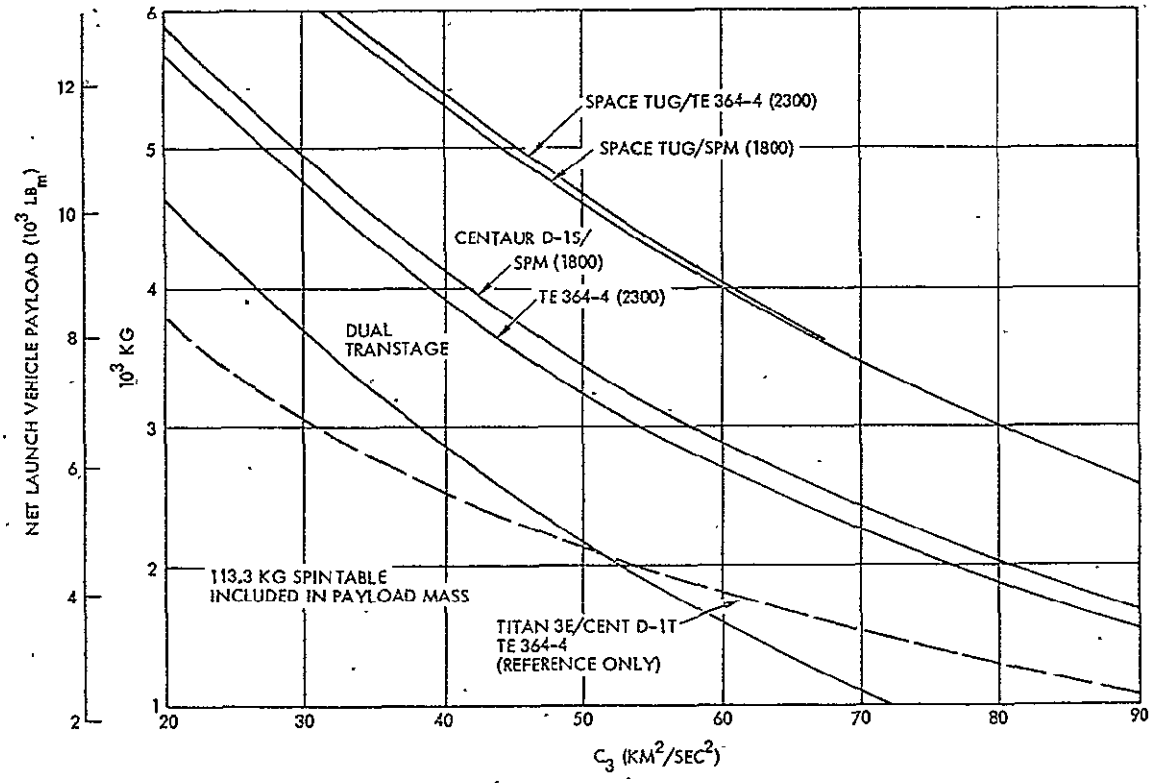

Figure 3-3. Performance of Shuttle Plus Upper Stages (Spinning Payloads) — Low C_3 Range

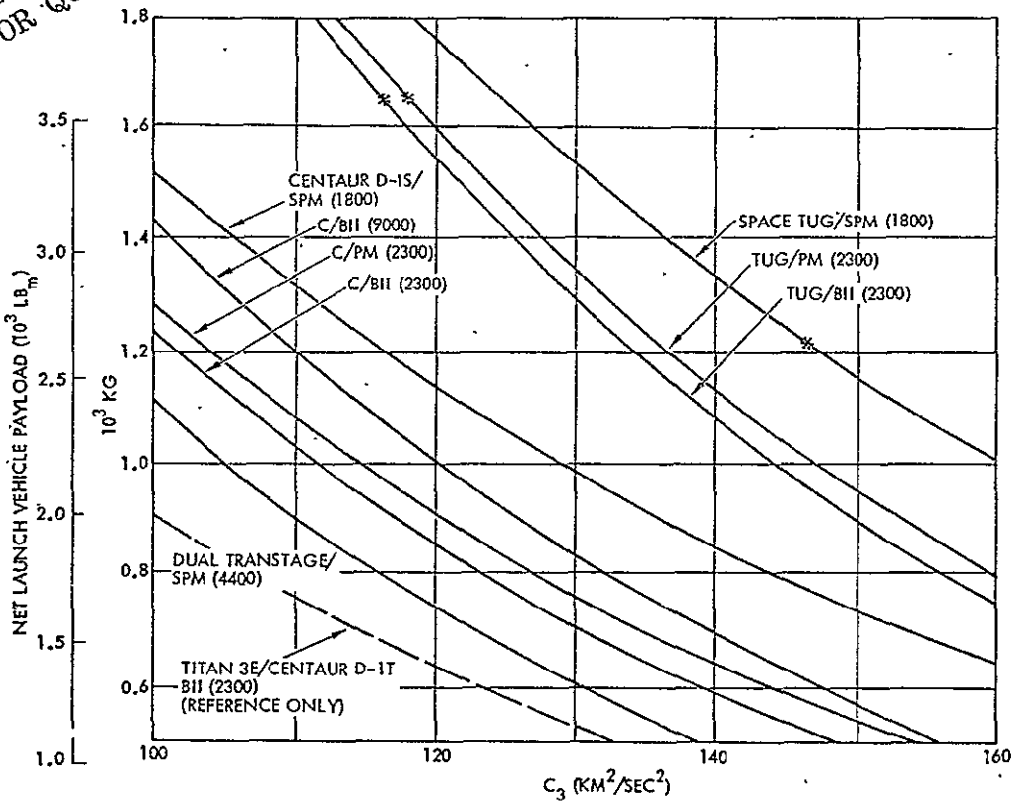

Figure 3-4. Performance of Shuttle Plus Upper Stages (Nonspinning Payloads) – High C_3 Range

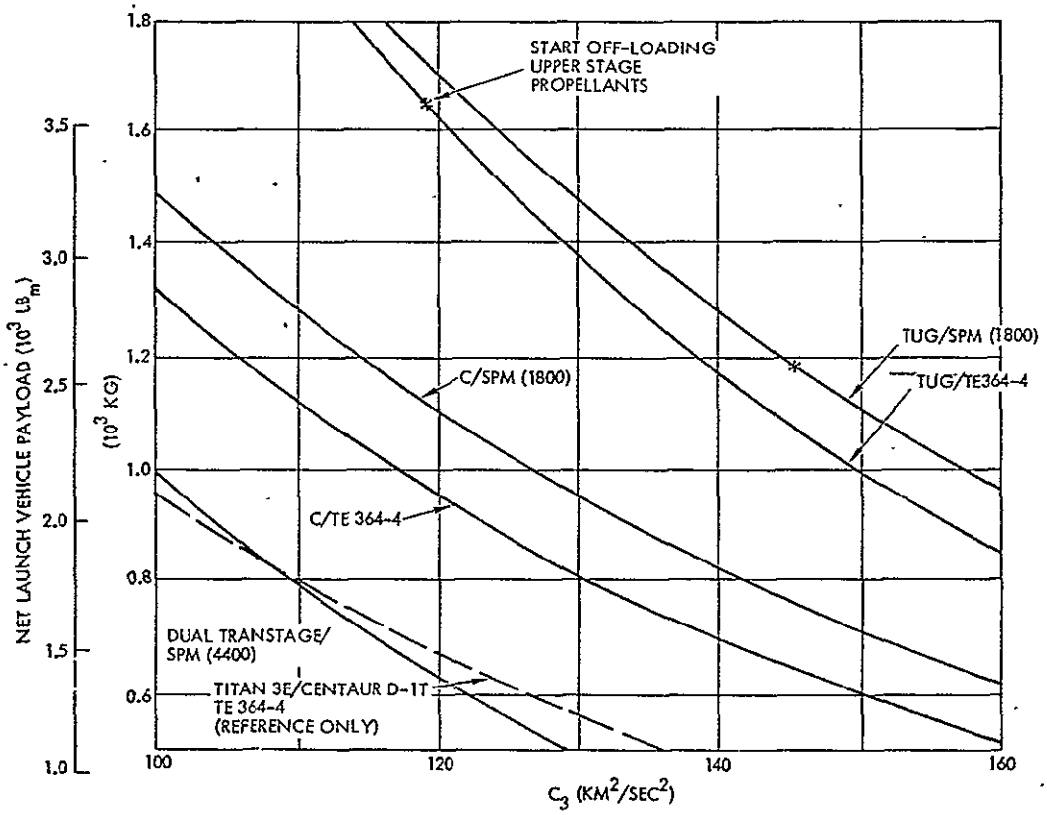

Figure 3-5. Performance of Shuttle Plus Upper Stages (Spinning Payloads) – High C_3 Range

3.2 APPROACH TO PROPULSION MODULE SIZING

Size determination of the propulsion module was based on propellant requirements for the Mercury orbiter, with two identical modules used in tandem, as discussed in Section 2.

The analysis required initial estimates on propulsion module inert weight as function of propellant mass, and selection of efficient maneuver modes during Mercury orbit insertion that would lead to minimum, or nearly minimum, propellant requirements. Restricting the size (and hence the inert weight) of the multi-mission propulsion module by selecting a near-optimum thrust mode at Mercury is essential to limiting weight penalties due to oversize in the outer planet missions.

Figure 3-6 shows a flow diagram illustrating the principal inputs and steps involved in propulsion module sizing. They include the following:

Item 1 Maneuver requirements, defined by trajectory characteristics (arrival conditions) and thrust orientation mode

Item 2 Specified weight of payload spacecraft

Item 3 Scaling relation between propulsion module inert weight and propellant weight based on empirical values and subject to updating by design iteration

Item 4 Assumed thrust level, selected by a tradeoff between maneuver efficiency (reduction of orbit insertion loss) and structural load tolerance of the deployed flight spacecraft

Item 5 Total flight spacecraft (payload and propulsion module) dry weight, based on Items 2 and 3

Item 6 Propellant weight used to perform required maneuvers with selected thrust level, thrust orientation mode and total spacecraft dry weight. Feedback to Item 3 establishes stage inert weight.

Item 7 Propulsion module sizing and design, based on input from Item 6

Item 8 Structural and weight analysis of selected design; output to be compared to initial propulsion module inert weight assumptions (Item 3). Procedure generally requires iteration.

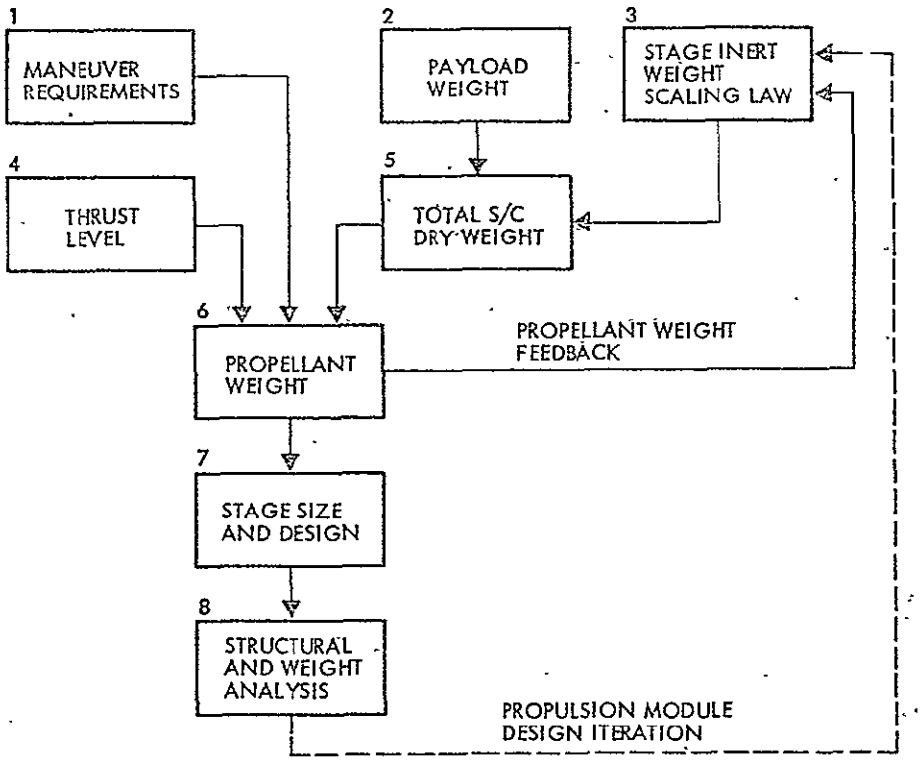

Figure 3-6. Propulsion Module Sizing Flow Diagram

This section only presents analysis of the initial part of the procedure, Items 1 through 6. Items 7 and 8 will be discussed under system design (Sections 4 and 5). Updated performance characteristics, involving Items 3, 5 and 6 will be presented in Section 7.

3.3 INITIAL SCALING RELATIONS FOR PROPULSION MODULE INERT WEIGHT

A linear scaling law was assumed relating the propulsion module inert weight W_i to propellant weight W_p

$$W_i = C_1 W_p + C_2$$

where C_1 and C_2 are empirical values based on previous design experience and assumed range of propellant weights.

For the initial propulsion module sizing task the following coefficients were assumed:

C_1 = 0.15 to 0.25 for earth-storable and space-storable propellants

$$C_2 = \begin{cases} 27.2 \text{ kg } (60 \text{ lb}_m) \text{ for earth-storable propellants} \\ 36.3 \text{ kg } (80 \text{ lb}_m) \text{ for space-storable propellants} \end{cases}$$

These coefficients relate to other, nondimensional, parameters usually considered in propulsion stage performance studies, such as propellant mass fraction p (usable propellant mass/total stage mass) and stage structure ratio σ (structure mass/total stage mass) as follows:

$$p = \frac{1}{1 + C_1 + C_2/W_p}$$

$$\sigma = 1 - p$$

Figure 3-7 shows the mass fraction p versus total stage mass parametrically for three values of the coefficient C_1. The dashed line corresponds to empirical data used in concurrent NASA/Ames studies and is shown here for comparison.

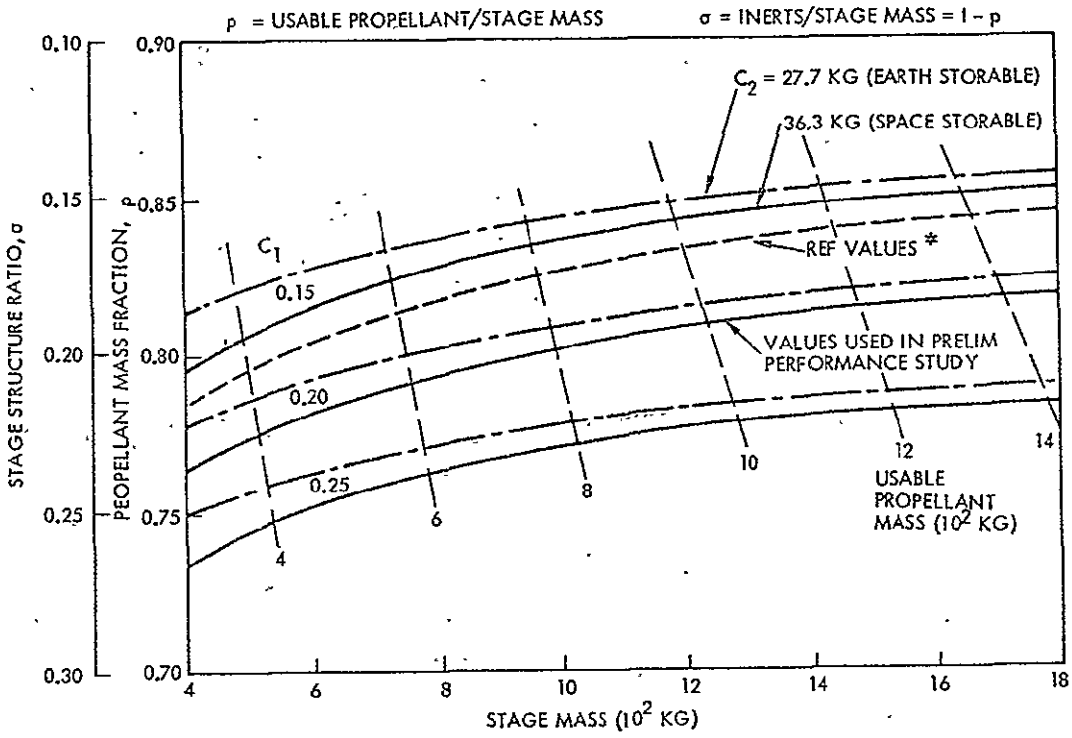

*DATA FOR SPACE STORABLE STAGE ASSUMED BY D.W. DUGAN (NASA/ARC).

Figure 3-7. Propellant Mass Fraction Versus Stage Mass

Based on past design experience, propellant mass fractions are generally in the range of 0.80 to 0.83 for values of stage mass typical for this application. It was therefore felt that a C_1 value of 0.25 was too conservative and C_1 = 0.15 too optimistic for initial design estimates.

Propellant Mass Dependence on C_1 and C_2

Analytical results relating the above scaling law to propellant mass requirements are of interest in assessing the influence of the coefficients C_1 and C_2. The analysis shows that for single stage operation, the propellant mass is

$$W_p = \frac{W_{pl} + C_2}{\frac{1}{r-1} - C_1}$$

where W_{pl} = payload mass

$r = e^{\Delta V / I_{sp} g}$ = the mass ratio of initial mass to burnout mass

ΔV = total velocity increment, including orbit insertion losses.

Figure 3-8 shows the propellant ratio q as function of ΔV and r with C_1 as parameter for both earth-storable and space-storable propellants. Figure 3-9 shows the relative change of propellant ratio, in percent, by changing C_1 from 0.15 to 0.20 and 0.25, respectively. It is apparent that the value of C_1 has a large influence on propellant requirements for large ΔV or r values. The critical value of r is that for which the denominator in the above equation is reduced to zero:

$$r_{crit} = 1 + \frac{1}{C_1}$$

Thus a change of C_1 from 0.15 to 0.25 reduces the critical mass ratio from 7.67 to 5.0 and the critical ΔV value from 5.92 to 4.67 km/sec.

These factors explain the strong dependence of W_p on the coefficient C_1. The relations characterize a regenerative weight growth: an increase in propellant requirements increases the inert mass, which in

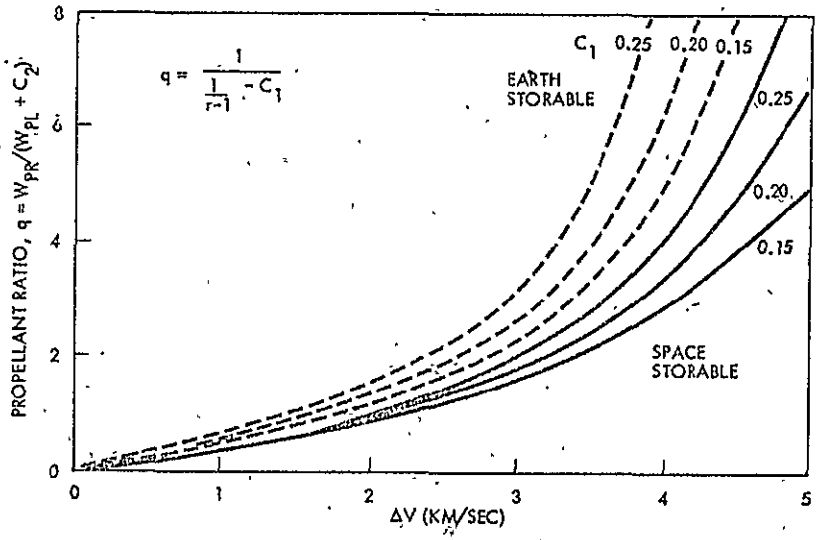

Figure 3-8. Influence of C_1 on Propellant Ratio (q)

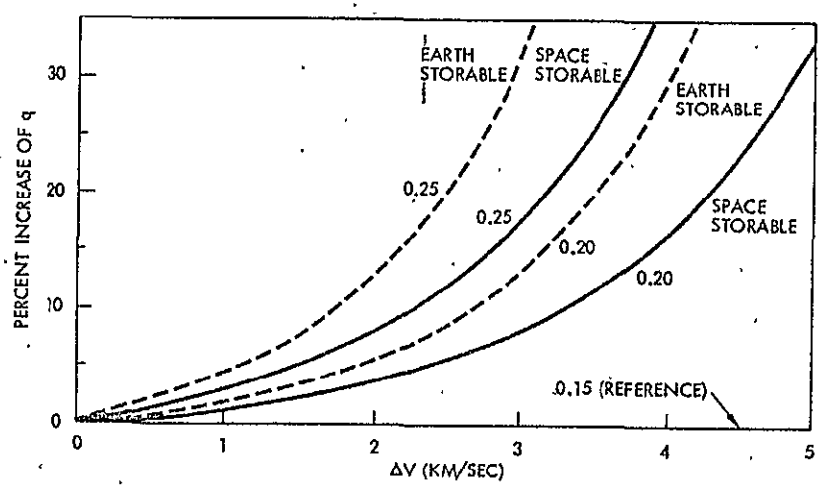

Figure 3-9. Percent Increase of Propellant Ratio with C_1

turn increases the propellant requirements, and so forth (see also the feedback path between blocks 3, 5 and 6 in Figure 3-6).

Similar results are obtained for the influence of coefficients C_1 and C_2 in the case of tandem stage operation with equal stage size. The mass ratios of the first and second propulsion stages (and the corresponding ΔV values) have critical values

$$r_{1_{crit}} = 1 + \frac{1}{2\,C_1 + 1}$$

$$r_{2_{crit}} = 1 + \frac{1}{C_1}$$

at which the propellant mass would theoretically increase to infinity. These values are analogous to the critical mass ratio for single stage operation. Figure 3-10 shows the influence of C_1 on propellant mass in the tandem stage application.

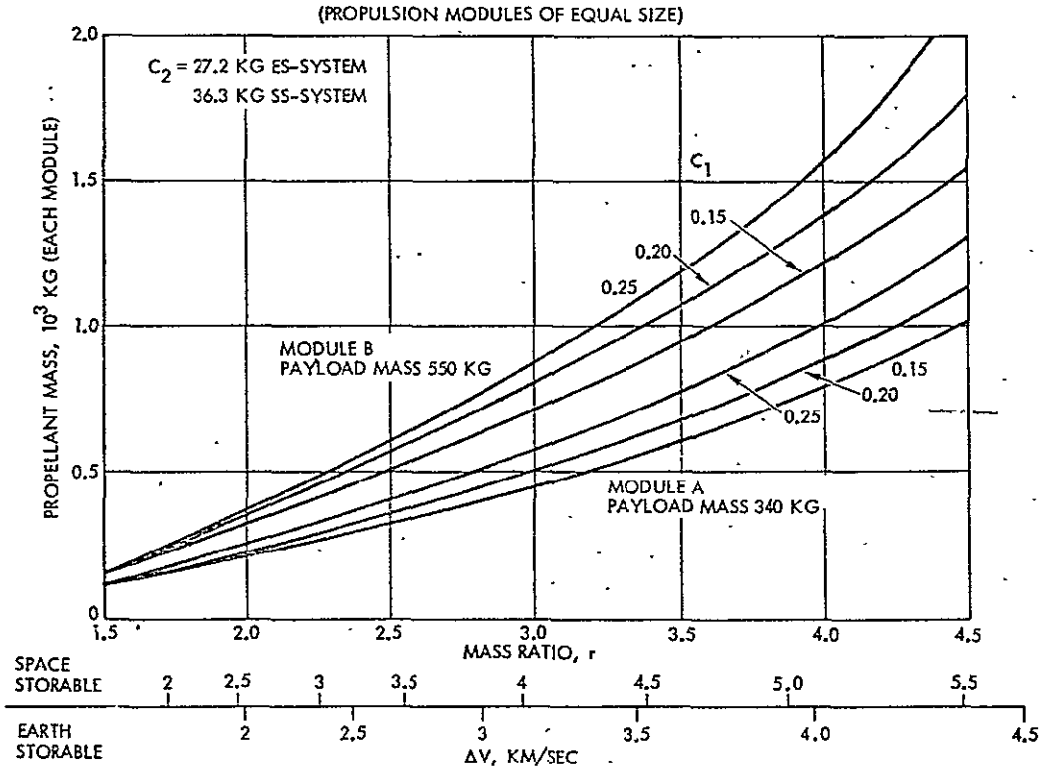

Figure 3-10. Propellant Mass for Two-Stage Mercury Orbit Mission

These results show the importance of keeping the proportionality factor C_1 as low as possible. The fixed-weight parameter C_2 is much less critical, adding only to the proportional increase of propellant mass with payload mass. Mission-peculiar weight elements such as the sun shade required only for the Mercury orbiter are reflected in the parameter C_2 rather than C_1.

3.4 ORBIT INSERTION PERFORMANCE AT MERCURY

3.4.1 Thrust Orientation Mode

Optimum and near-optimum orbit insertion modes at Mercury were determined by a systematic performance optimization technique (see Appendix E) for given arrival conditions and a specified periapsis altitude (500 km), periapsis location and eccentricity of the capture orbit. Principal results of this investigation are these (see also Appendix F):

1) Optimum time for thrust initiation is well in advance of closest approach, such that roughly half of the retro-thrust maneuver occurs before and and half of the maneuver after closest approach.

2) Fixed thrust orientation with optimal pointing of the thrust vector introduces only a small performance penalty (about 1 to 2 percent) compared to a more nearly optimal variable thrust-pointing maneuver with the thrust vector pointing opposite to the velocity vector.

3) The optimum fixed thrust orientation is parallel (and opposite) to the velocity vector at periapsis, i.e., at an orientation normal to the intended apsidal line orientation. Departures of more than 5 degrees from this orientation cause a rapid increase in maneuver propellant. For example, for a 10-degree departure from the optimum propellant requirements increase by 10 percent for space-storable propellants and by 15 to 20 percent for earth-storable propellants (assuming Pioneer class payloads spacecraft and a thrust force of 600 lb_f, or 2730 N).

Mariner class spacecraft can implement a variable thrust pointing maneuver quite readily, using a stored program of orientation commands and an attitude gyro. Pioneer class spacecraft preferably maintain a fixed attitude during the maneuver. The performance data obtained show that the greater simplicity of a fixed maneuver attitude in the case of Pioneer class payload outweighs the performance gain obtainable by introducing the more sophisticated maneuver mode.

3.4.2 Effect of Thrust Level (Preliminary)

Figure 3-11 shows the dependence of the minimum initial mass and the propellant mass on thrust level and compares the results to impulsive thrust performance. A thrust level increase by 200 lb_f from 600 to 800 lb_f (2730 to 3630 N) increases the initial mass by 35 kg (77 lb_m) corresponding to a propellant mass increase per module by 15 kg (33 lb_m). No account is taken here of any penalties in weight because of larger thrust. A more complete treatment is used to select thrust levels in Sections 4 and 5.

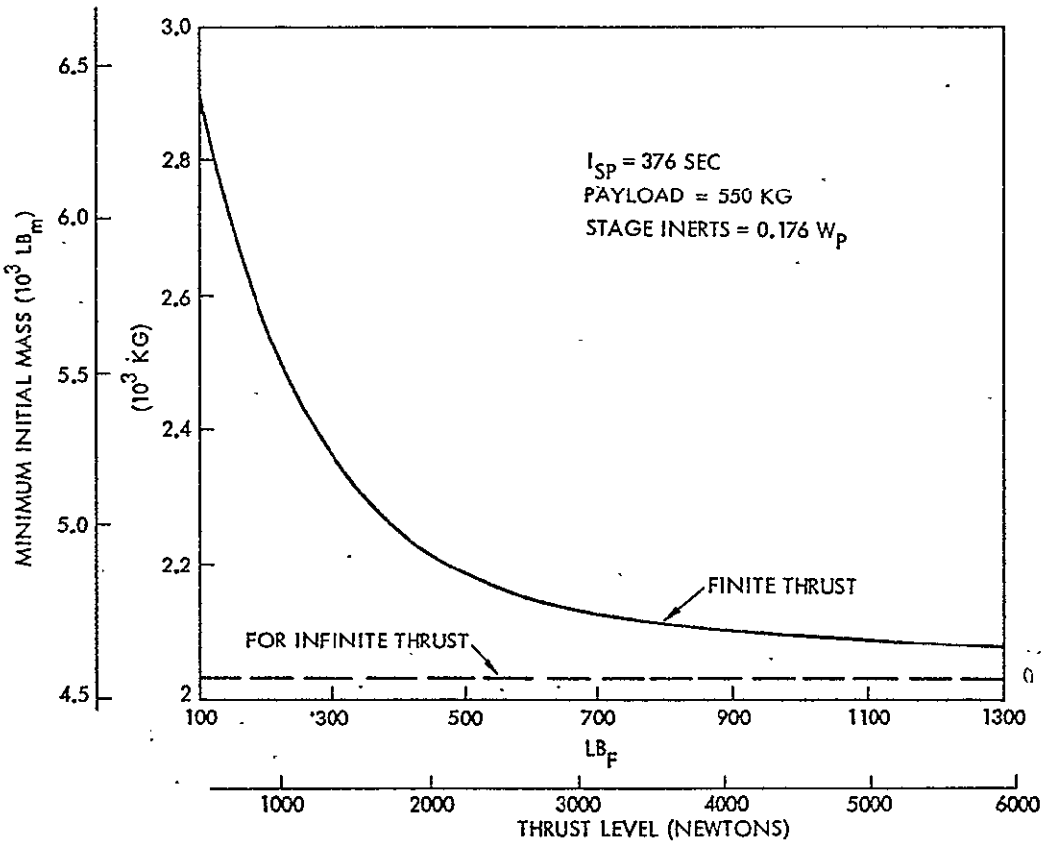

Figure 3-11. Minimum Initial Mass Versus Thrust Level for Mercury Orbiter (Tandem Stages)

The peak acceleration occurring toward the end of second-stage operation with an 800 lb_f thrust level (0.7 g with Pioneer class and 0.5 g with Mariner class payloads) will cause high structural loads in deployed appendages (see Section 4). The possibility of using a lower thrust level in the second propulsion module in the interest of reducing

these loads was investigated and the resulting loss in orbit insertion efficiency was evaluated. Results presented in Figure 3-12 show that such thrust level reductions can lead to unacceptably large performance penalties. With the second-stage thrust level reduced by 50 percent to 400 lb_f (1815 N) the performance penalty would be almost as large as if the same lower thrust level were used in both stages. Therefore the concept was not given any further consideration.

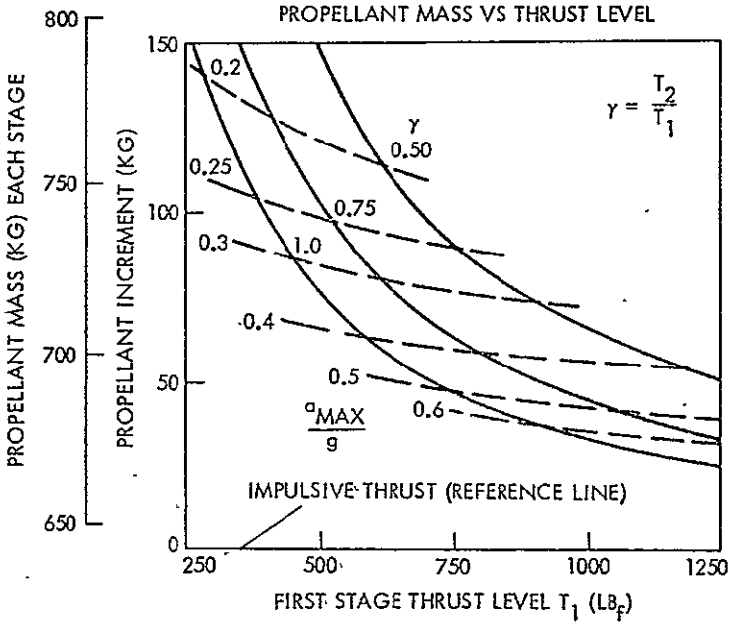

Figure 3-12. Effect of First and Second Stage Thrust Level on Propellant Mass for Mercury Orbit Insertion (Space-Storable System, Module B)

3.5 USE OF PROPULSION MODULE FOR LAUNCH-ENERGY AUGMENTATION (PRELIMINARY)

The multi-mission propulsion module, sized for Mercury orbit insertion requirements, has a large excess propellant tank capacity in some of the outer planet orbiter cases and comet rendezvous missions considered above. This extra propellant capacity can be utilized in a post-launch maneuver to increase payload capacity or reduce trip time. An analysis of launch-vehicle performance augmentation by the spacecraft propulsion module was conducted and is discussed in this section.

In order to perform this maneuver most effectively little or no time must be allowed to elapse between launch-vehicle upper-stage burnout and ignition of the onboard propulsion module. The performance loss caused by delaying the maneuver is due primarily to the decrease in spacecraft velocity with increasing distance from earth. Figure 3-13 shows the loss of maneuver effectiveness with increasing (nondimensional) earth distance, r/r_E, in terms of the ratio $\Delta V_\infty/\Delta V_i$ and with V_∞ as parameter where ΔV_i is the magnitude of the augmentation maneuver. For example, for V_∞ = 12 km/sec, typical for a slow trip to Uranus, the effectiveness ratio decreases from 1.37 at r/r_E = 1 to 1.08 at r/r_E = 5 and 1.04 at r/r_e = 10.

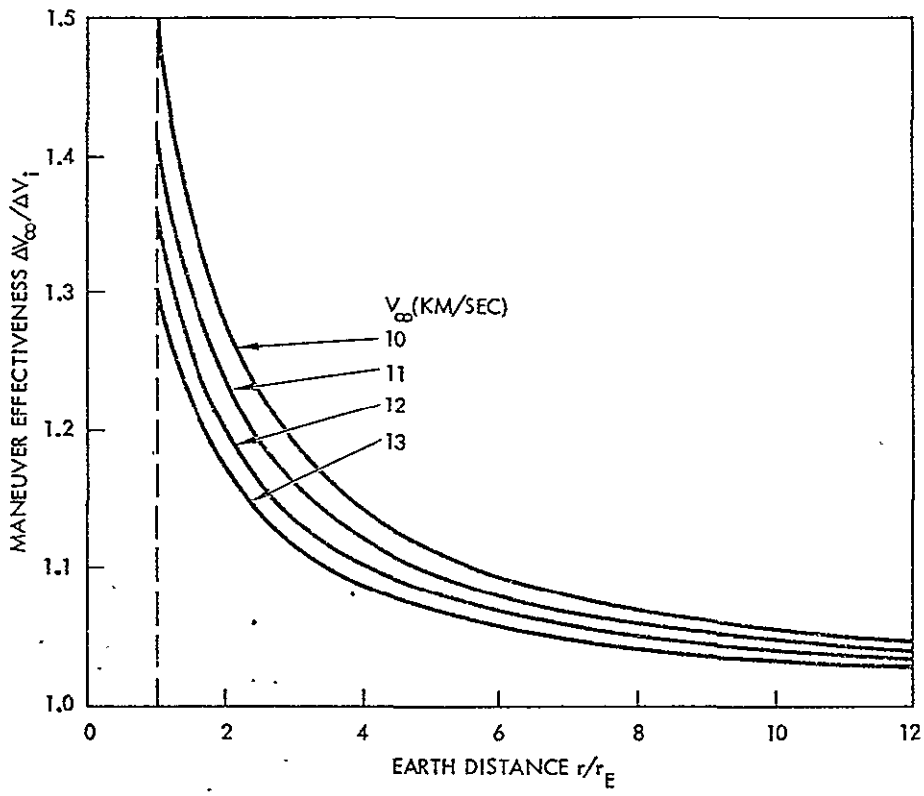

Figure 3-13. Maneuver Effectiveness Versus Earth Distance

At injection energies C_3 ranging from 120 to 160 km^2/sec^2, typical for the outer planet missions being considered, the spacecraft reaches distances of 5 earth radii 37 to 42 minutes after injection at 160 km orbital altitude and 10 earth radii in 78 to 87 minutes. Even a few

minutes of thrust initiation delay will cause a significant reduction in maneuver effectiveness already penalized by the low thrust level used in the outer-planet orbiter version of the propulsion module.

Examples of C_3 augmentation by expenditure of spare propellant are given in Figures 3-14 and 3-15. A thrust of 900 N (200 lb_f) is assumed for outer-planet propulsion modules. Gravity losses are included in the integration. The first of these figures shows ΔC_3 for two gross spacecraft weights (1000 and 1500 kg) as function of propellant expenditure ΔW_p with Centaur D-1S/SPM (1800) used as launch vehicle upper stage. The upper two graphs represent space-storable, the lower two earth-storable propellants. The second figure shows the corresponding results with the Space Tug/SPM (1800) used as upper stage. The effect of elapsed time between upper stage burnout and propulsion module ignition is shown parametrically for 0, 3 and 6 minutes of coast. Even a delay of only 6 minutes can reduce the achievable ΔC_3 increment by 20 to 50 percent.

The maneuver is much less effective for earth-storable than for space-storable propellants. This reflects the tradeoff between onboard propulsion-module versus launch-vehicle upper-stage performance. The tradeoff is favorable in the case of space-storable propellants (I_{sp} = 376 seconds) versus the solid propellant kick motor (I_{sp} = 290 seconds), but unfavorable in the case of earth-storable propellants with approximately the same I_{sp} as the solid motor.

Figure 3-16 shows augmentation of the Centaur D-1S/SPM (1800) and Space Tug/SPM (1800) launch capability by expenditure of 100, 300 and 500 kg of space-storable propellants. Zero coast time is assumed. An injected payload mass increase of more than 100 kg and a ΔC_3 of 5 to 10 km^2/sec^2 achievable by this technique in the C_3 range of interest can significantly improve the Saturn and Uranus missions (see Section 7). However, use of the technique with earth-storable propellants appears hardly worthwhile.

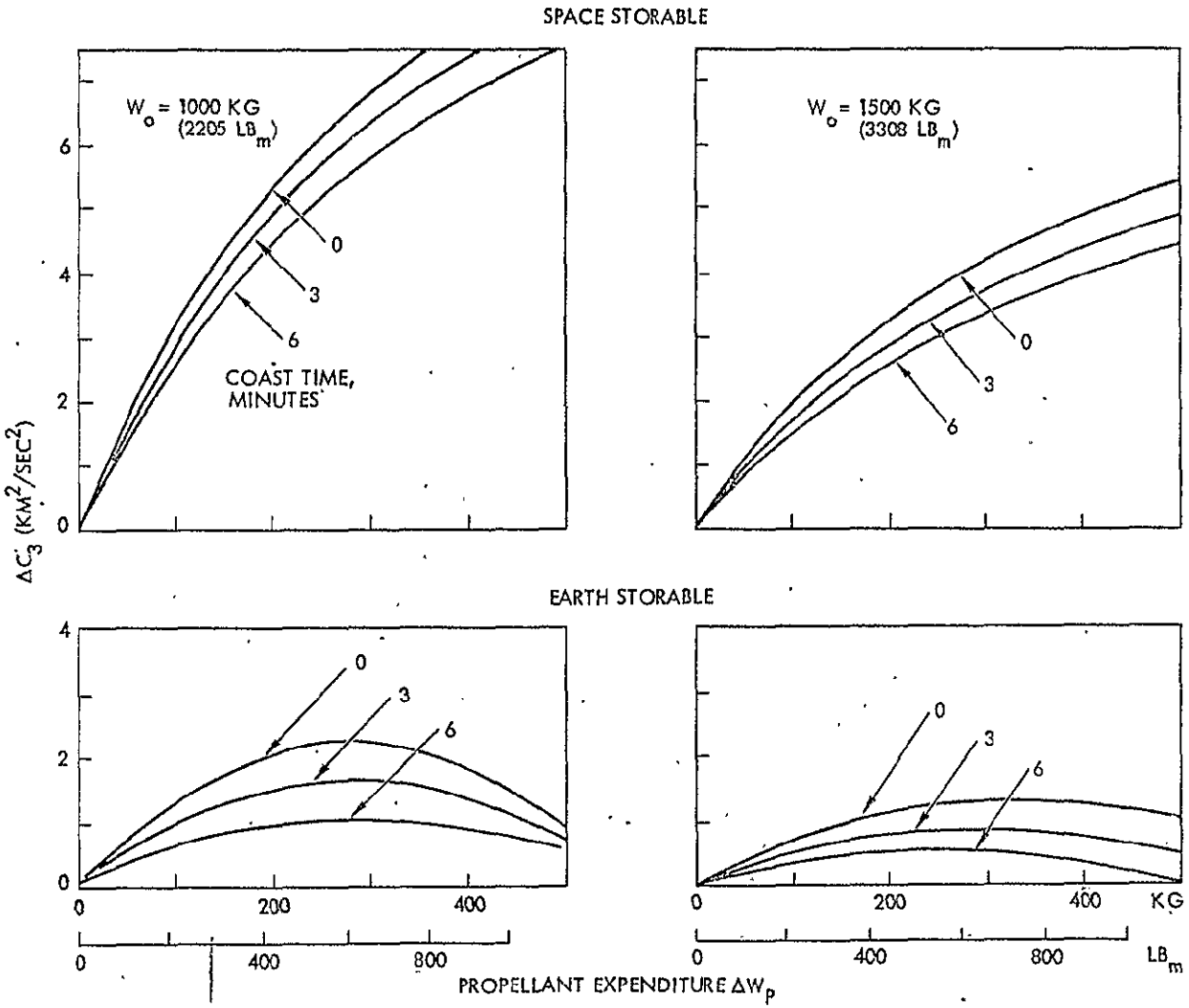

Figure 3-14. C_3 Augmentation by Propulsion Module Versus ΔW_p (for Centaur/SPM (1800) Upper Stages

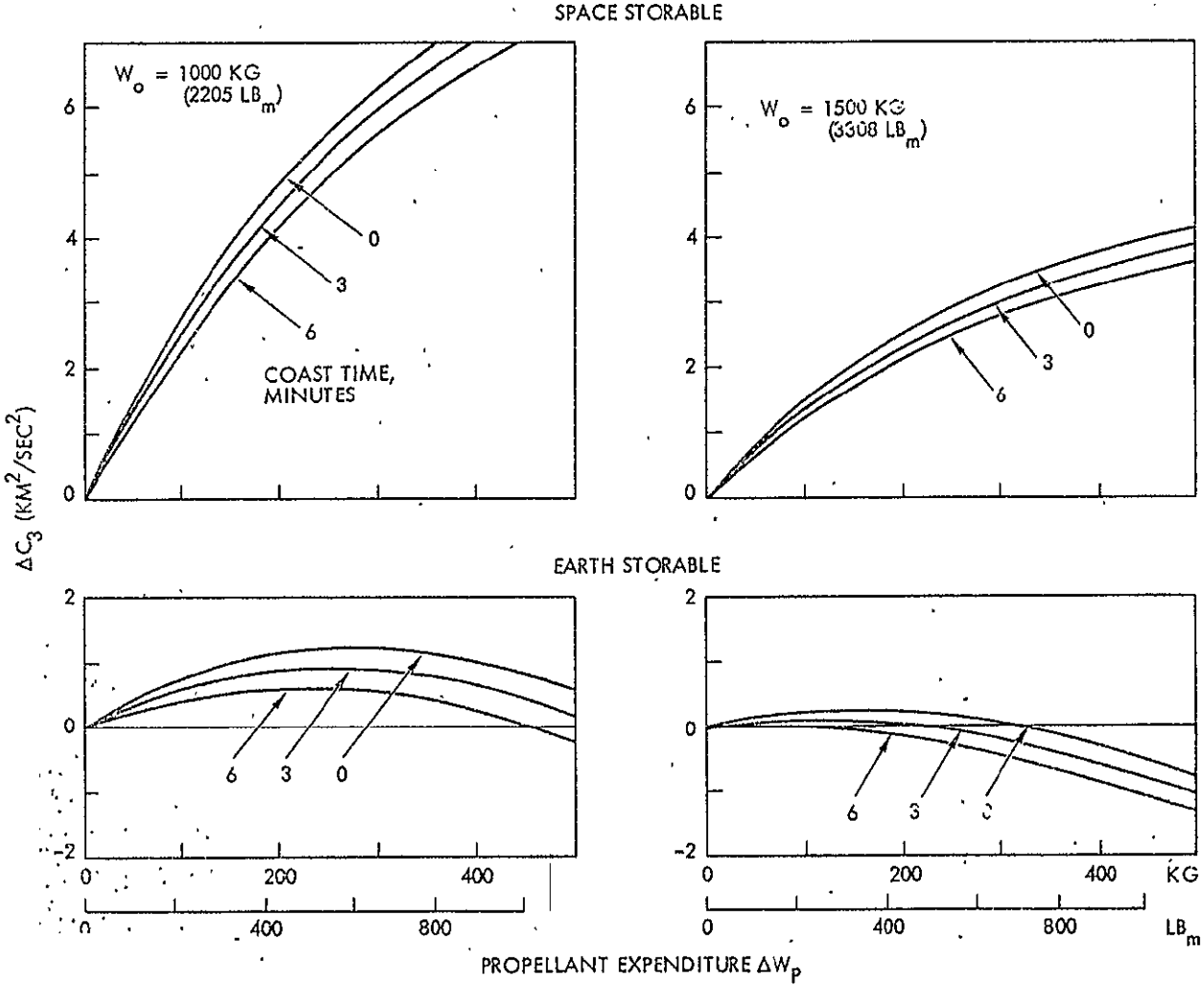

Figure 3-15. C_3 Augmentation by Propulsion Module Versus ΔW_p (for Space Tug/SPM (1800) Upper Stages)

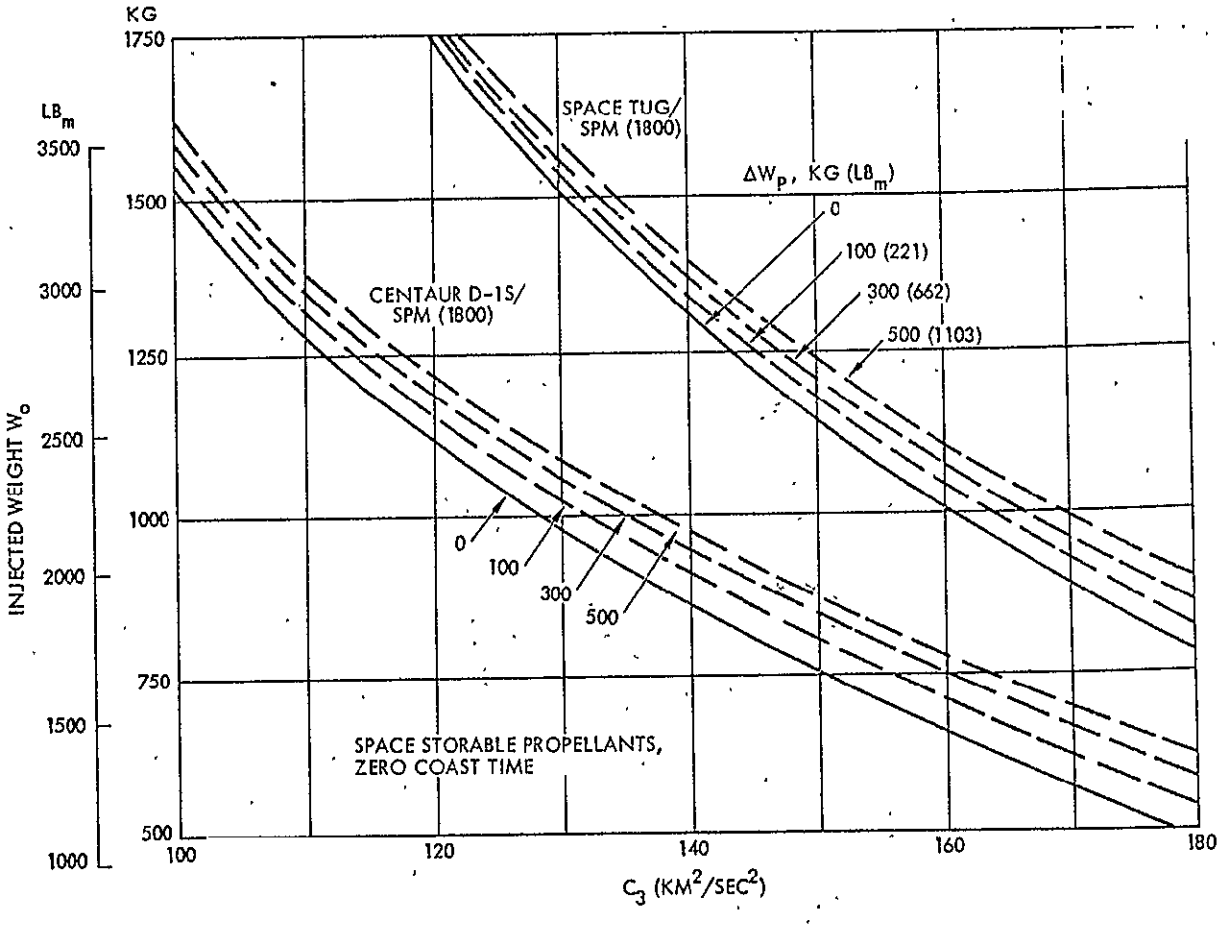

Figure 3-16. C_3 Augmentation by Propulsion Module

4. PROPULSION MODULE CONFIGURATION

This section discusses propulsion module design approaches and alternate configuration concepts considered during the study and describes the preferred design adopted for use with Pioneer and Mariner class payload spacecraft. It also discusses propulsion-module interfaces with these payloads and with the Shuttle/upper stage launch vehicle, and summarizes payload design modifications made necessary by propulsion module accommodation.

Design characteristics of the propulsion subsystem, as part of the propulsion module, will be described separately in Section 5.

4.1 CONFIGURATION GUIDELINES AND CONSTRAINTS

Principal configuration constraints are imposed by the requirements of multi-mission applicability, conformance with the specified payload vehicle designs (i.e., Pioneer class and Mariner class), and accommodation onboard the Shuttle orbiter during launch. The use of space-storable bipropellants, fluorine and hydrazine, also imposes design constraints different from and more stringent than those for earth-storable bipropellants, nitrogen tetroxide and monomethyl hydrazine, especially in the areas of thermal control and safety provisions.

These considerations lead to design requirements which are summarized as follows.

Multi-Mission Applicability

- Compatibility with both inner-planet (Mercury) and outer-planet versions of the same spacecraft class
- Adaptability to the physical environment of the inbound and outbound missions, especially thermal control characteristics
- Applicability in single or tandem configurations: singly for the outer planet missions, in tandem for the Mercury mission (and some of the comet missions) with appropriate structural and interface design features
- Conformance with mass distribution requirements of either the spinning or three-axis controlled payload spacecraft

class in single and tandem stage arrangements, during all phases of deployment, operation and propellant depletion

- Conformance with maneuver modes and operational sequences of the inbound and outbound versions of each class of payload vehicle, during the transit phase and at destination

- Compatibility with requirements of engineering subsystem and scientific instrument operation of the inbound and outbound versions of each payload spacecraft, e.g., avoidance of unduly severe field-of-view obstruction of onboard sensors, high-gain antennas, etc.

Launch from the Shuttle Orbiter

- Compatibility with payload accommodation constraints of the Shuttle orbiter, including those of size and weight, center-of-mass location, and structural dynamic loads occurring during launch and abort.

- Compatibility with thermal environment and interface criteria of the Shuttle

- Convenient integration with the Shuttle upper stage and installation in the Shuttle cargo bay during the time-limited Shuttle turn-around and prelaunch preparation phase

- Compatibility with Shuttle safety requirements in ground handling, loading, storage, launch and orbital operations, abort and emergency landing

- Capability of performing a rapid propellant dump during the orbital phase, while stowed in the Shuttle cargo bay, in the event of a leak or other hazards involving the propulsion module, or in preparation to Shuttle abort for other reasons.

In addition, several general design guidelines and criteria related to cost effectiveness and reliability are to be observed. These include:

- Minimum or no changes in configuration of the multipurpose propulsion module developed for each payload class when applied to different missions

- Flexibility of adaptation to different mission requirements

- Flexibility of operating modes, permitting change from nominal maneuver sequences under unexpected conditions

- Maximum use of existing technology
- Simplicity of design and operation
- Ease of payload integration with minimum impact on the payload spacecraft in terms of design modifications and special interface requirements
- Ease of handling and integration with the Shuttle orbiter and its upper stages, and avoidance of special interface requirements if possible
- Moderate requirements by the propulsion module on mission control support during all mission phases
- Compatibility with long mission life by provision of high-reliability design features, or by including redundancy of critical components.

4.2 DESIGN APPROACH

The design approach followed in this study was aimed at satisfying the different propulsive energy requirements of the various missions by a single baseline propulsion module design. An important consideration, while meeting the design criteria and constraints listed above, was to avoid imposing excessive weight penalties and functional complexities on one mission class as a result of conforming with the special requirements of another. For example, the Mercury mission requires a sun shade for thermal protection, but such a device is designed so that it can be readily removed when using the propulsion module in outer-planet missions where it is not needed.

The baseline propulsion module was designed to conform with different sizes and shapes of a) the inbound and outbound versions of each class of payload vehicle, and b) of the various Shuttle upper stages by appropriate design of interstage adapters.

Among the more difficult problems in design commonality that have to be addressed are those of propellant-tank sizing, mass properties control, thrust-level selection, and thermal control implementation. The following paragraphs will discuss the approaches used to resolve these questions.

4.2.1 Propulsion Module Sizing

As previously discussed, the propellant-mass requirement of the Mercury orbiter is more than twice that of the outer-planet orbiters. To use a baseline propulsion module with a common tank size for single-stage orbit injection at all planets appeared impractical and weight-ineffective. The preferred approach is to use two propulsion modules of equal size for the Mercury orbiter for two-stage orbit insertion. The advantages are:

1) More weight-effective orbit insertion at Mercury

2) Reduced inert weight of the individual propulsion module, giving improved performance of the outer-planet orbiter missions

3) Reduced ullage due to propellant offloading in the outer-planet orbiters and, hence, reduced propellant sloshing during launch.

Propulsion tank sizes determined from the preliminary performance calculations discussed in Section 3 are presented in Table 4-1 for Mercury orbiters using Module A or B, with earth-storable or space-storable propellants. These data were used to proceed with preliminary propulsion module designs, subject to subsequent weight and size iterations as explained in connection with Figure 3-6.

4.2.2 Mass Properties Control

Center-of-mass locations and moments of inertia of the payload spacecraft are fundamentally changed by the addition of the large propulsion module in single or tandem stage arrangement.

This is of concern primarily in the case of the (spin-stabilized) Module A application. The combined configuration tends to have an unfavorable moment-of-inertia ratio. Long-term spin stability requires that the spin moment of inertia (I_z) be at least 1.1 times greater than the maximum transverse moment of inertia (I_x or I_y).

The design approach taken in the study was to keep the height of the propulsion module as low as possible while placing the spherical propellant tanks at a radial distance large enough to achieve a moment-of-inertia ratio of 1.1 or larger, starting with separation from the launch

Table 4-1. Mercury Orbiter Propellant Requirements for Preliminary Stage Sizing; Weights in kg (lb_m)

Module Type	Usable Propellant, Each Stage	Stage Inert Weight, Each Stage	Spacecraft		Stage Total Tank Volume m^3 ($in.^3$)	Tank Diameter cm (in.)
			Initial Weight	Dry Weight		
A, earth-storable	1159 (2556)	259 (571)	3176 (7003)	599 (1321)	1.33 (81,000)	85 (33.5)
space-storable	612 (1349)	160 (353)	1884 (4155)	500 (1103)	0.79 (42,700)	69 (27.2)
B, earth-storable	1961 (4324)	420 (926)	5312 (11713)	970 (2139)	2.11 (129,000)	100 (39.4)
space-storable	991 (2185)	234 (516)	3000 (6615)	784 (1729)	1.15 (90,000)	82 (32.3)

Assumptions:

- Four spherical tanks, 15 percent volume margin
- Thrust force 600 lb_f (2730 N)
- Revised scaling law $W_i = 0.20\ W_p + 27.2$ kg (60 lb_m) for earth-storable, or +36.3 kg (80 lb_m) for space-storable propellants
- Mission No. 1 (launch date 19 June 1988)
- Module A uses fixed thrust, Module B variable thrust pointing
- Maneuver requirements include 500 m/sec for Earth-Mercury transit phase (~300 m/sec) and Mercury orbit phase (~200 m/sec).

vehicle upper stage. This lateral separation of propellant tanks is beneficial also from a thermal isolation standpoint for the fluorine/hydrazine combination, by suppressing conductive heat transfer through the support truss.

The use of at least four tanks is essential in the spinning configuration for proper mass balance of the dissimilar oxidizer and fuel weights, which differ by a ratio of about 1.5:1. Previous design studies (References 19 and 20) have shown that transverse center-of-mass shifts occurring in a two-tank configuration due to propellant depletion is difficult or impractical to compensate. This shift tends to produce an angular tilt of the principal axis of inertia which causes the geometrical center line of the spacecraft and, hence, the axis of the high-gain antenna beam, to describe a conical motion around the instantaneous spin axis. The resulting degradation of the spacecraft-to-earth communication link would be unacceptable.

In the four-tank configuration the unequal oxidizer and fuel masses are located on diametrically opposite sides of the propulsion module. This assures a continuously balanced mass distribution even if the propellant depletion is not uniform which would be the case if a portion of the hydrazine fuel is expended as monopropellant.

Toroidal tanks were also being considered for the spinner as a possible design option having the advantage of providing symmetrical propellant distribution around the spin axis at all stages of propellant depletion. However, this alternative was subsequently discarded primarily since tanks of an extremely low tube cross-section (tube diameter/mean toroid diameter ratio of about 1:5) would be required to satisfy the spin stability requirement with a minimum moment of inertia ratio of 1.1 in the tandem and single stage configuration of Module A. This and other reasons for discarding the toroidal-tank design concept will be discussed in greater detail in Section 4.3.

Small residual center-of-mass deviations from the geometrical center line and small thrust axis misalignments (of the order of 0.25 cm) are acceptable if the resulting spacecraft nutation during thrust phases is limited to less than about 1 degree in the outer-planet missions and 2 degrees in the Mercury mission. This can be achieved by increasing the spacecraft's angular momentum by a spin-up maneuver prior to each thrust phase. Typically, the spin rate will be increased from the nominal value of 10 rpm in the cruise mode to 30 rpm in the case of the Mercury orbiter and from 5 rpm in cruise to 15 rpm in the outer-planets orbiter. The increased spin rate also provides greater structural stiffness of deployed appendages against relatively large axial acceleration due to thrust. The maximum thrust acceleration is about 0.7 g in the Mercury-orbiter case, but only about 0.15 g for the outer-planets orbiter with the propellant tanks nearly empty and the thrust levels of 800 and 200 pounds (3580 and 900 Newtons) adopted for these missions, respectively.

Mass properties, spin dynamics and thrust level selection will be discussed below in greater detail. (See also Appendix G.)

In the case of the (nonspinning) Module B design, mass properties control is not as critical as with Module A, since changes of center-of-mass location can be met within reasonable limits by thrust-vector

gimballing. Nevertheless, a four-tank configuration has the advantage of more precise mass balance at all stages of propellant depletion compared with a two-tank configuration, especially with space-storable (F_2/N_2H_4) propellants, since in this case it is desirable to use a significant portion of the hydrazine fuel in the monopropellant-thrust mode for small ΔV maneuvers and for attitude control. The design of the propulsion module tends to place the combined center-of-mass rather close to the main engine gimbal joint such that even a few inches of lateral c.m. displacement from the center line would require an undesirably large steady-state gimbal deflection.

4.2.3 Thrust-Level Considerations

Thrust-level selection involves a trade between performance gains attainable by high thrust acceleration (because of a resulting reduction of orbit-insertion loss) and weight penalties accruing from the increased structural load on deployed spacecraft appendages and from larger engine and other inert weights. This tradeoff is quite sensitive since orbit insertion performance at Mercury depends strongly on thrust-phase duration which in turn is inversely proportional to thrust level. Figure 4-1 illustrates this fact by the large increase in the orbiter's gross initial mass as the thrust level is reduced. The data shown are typical, representing results of orbit-insertion performance analysis for a Mercury arrival velocity of 6.4 km/sec, with payload spacecraft mass shown as parameter, and with the inert-mass coefficient (C_1, change of inert mass per unit change of propellant mass) assumed as 0.2. Figure 4-2 shows principal mass-element changes with a thrust level change from 600 to 800 pounds as function of the payload mass.

Weight penalties accruing from increased thrust level include increases due to the size of the thruster and associated propulsion system hardware and the required structural strengthening of weak appendages such as solar panels, sun shades, experiment booms in the case of the Mercury orbiter, and RTG deployment arms and experiment booms of the outer planet orbiters. Assessment of these weight penalties depends on design details to be considered later.

In addition to the weight factor, per se, there are also considerations of the cost elements involved in redesigning the payload vehicle to

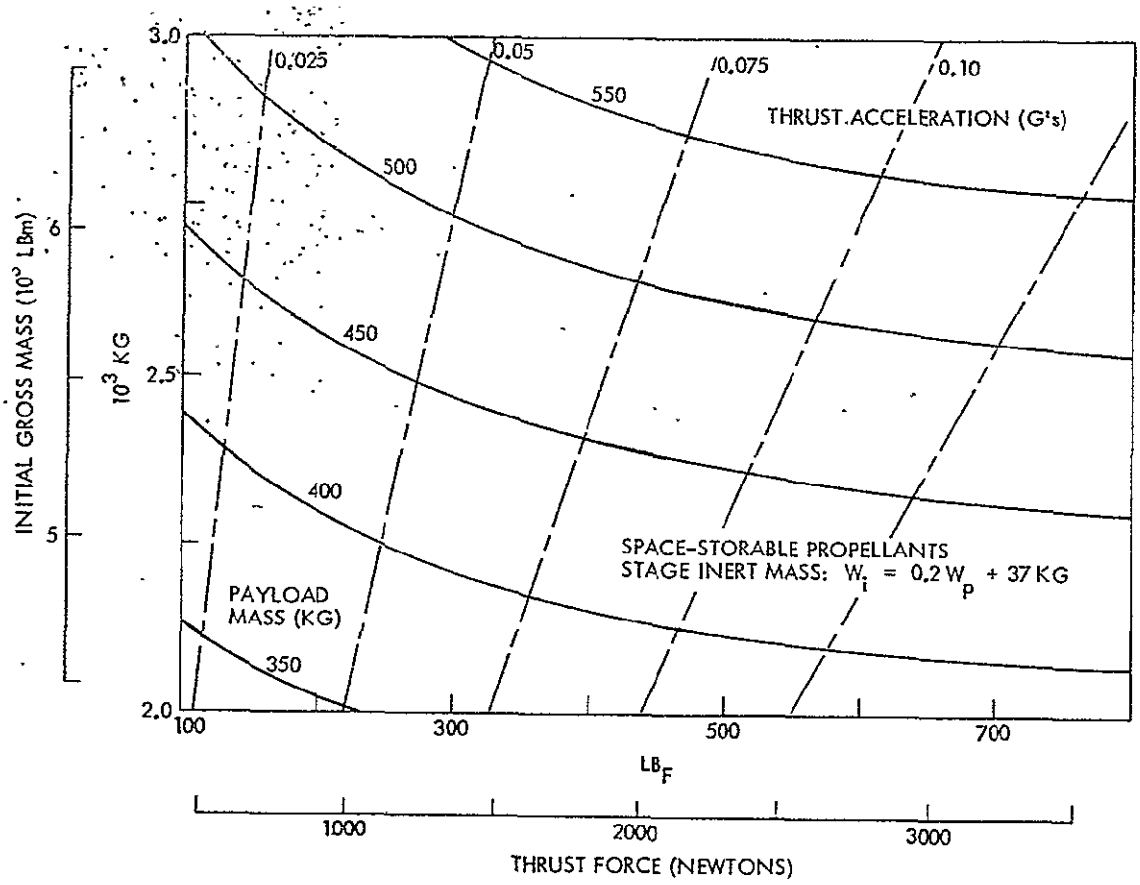

Figure 4-1. Influence of Thrust Level on Initial Gross Mass for Mercury Orbit Insertion

strengthen deployed appendages. Optimization of the propulsion system performance must not ignore effects on the payload spacecraft design. However, a full evaluation of the entire design impact tends to be outside the scope of this study.

It is interesting to note that the deployed solar panels of Mariner Venus Mercury as originally designed cannot withstand axial accelerations exceeding 0.01 g. The use of any reasonable thrust level of at least 10 times that figure requires a redesign, possibly the use of guy wire support of the deployed panels, since retraction of the panels prior to each main thrust application as an approach to resolve the problem would be impractical.

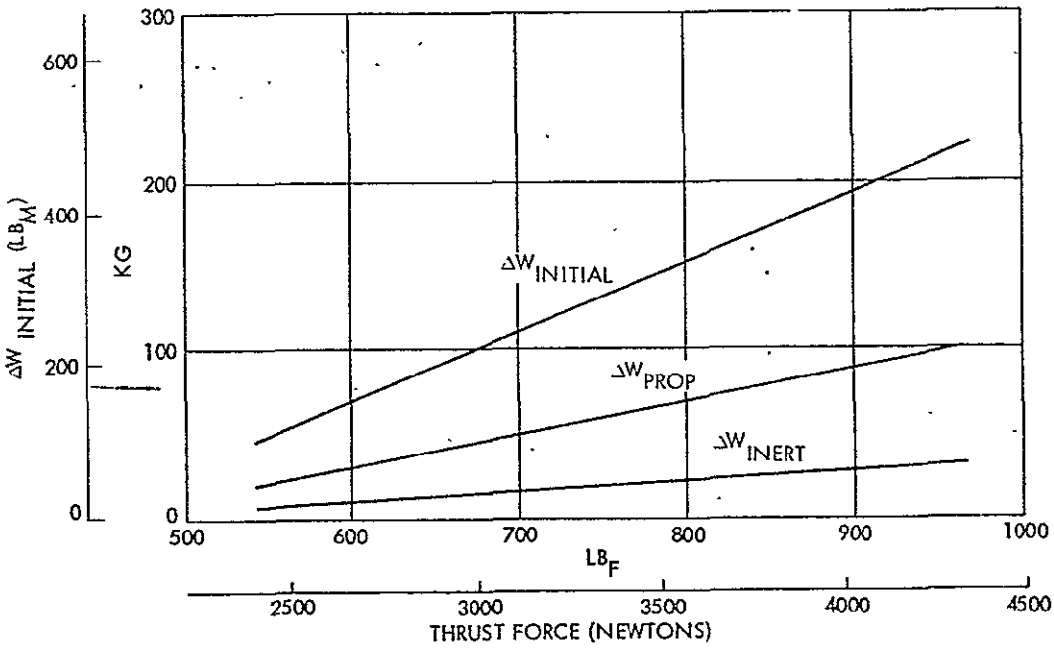

Figure 4-2. Effect of Thrust-Level Increase from 600 to 800 lb_f on Weight Elements for Mercury Orbiter (Space-Storable-Propellants; Preliminary Inert-Weight Scaling).

Further analysis shows that the thrust-level requirements of the Mercury mission are not really compatible with those of the outer-planet orbit missions. This is best explained by comparing the design characteristics of the payload-spacecraft classes that are to accommodate the multi-mission propulsion modules. The matrix shown in Table 4-2 summarizes key thrust-level selection constraints for the spinning and non-spinning payload vehicles in inbound and outbound missions.

In the multi-mission propulsion system design any major performance penalty incurred in the Mercury orbiter due to low thrust level greatly increases the required propellant tank capacity and hence module size and inert weight. This in turn can penalize the performance of the outer-planet missions severely.

As an acceptable compromise it is preferred to allow a modification of the thrust level by exchanging the engine selected for the Mercury orbit module for a smaller engine in missions to the outer planets. The design

Table 4-2. Principal Thrust Level Selection Constraints

Mission Constraints	Module A Payload (Spinning)	Module B Payload (Nonspinning)
Mercury Orbiter:	• Pioneer Venus orbiter class	• Mariner Venus/Mercury flyby class
Incurs major performance penalty for low thrust level	• Designed to withstand up to 8 g thrust acceleration (solid motor) in Venus orbit mission	• Deployed solar panels designed for accelerations ≤0.01 g
	• Can readily accommodate desired large thrust level (600 to 800 pounds)	• Solar panel support must be redesigned in any case to accommodate orbit insertion thrust
Outer Planet Orbiters:	• Pioneer 10 and 11 Jupiter flyby class	• Mariner Jupiter/Saturn flyby class
Can accept low thrust level with small performance loss	• Designed to withstand only up to 0.1 g thrust acceleration	• Instrument and RTG support arms can tolerate up to 0.2 g
	• Retraction of RTG and experiment booms prior to thrust initiation impractical	• Long experiment booms can be retracted prior to thrust initiation
	• Minor redesign can accommodate up to 0.2 g. Acceleration level >0.4 g requires more significant design changes	

impact of this approach on the multi-mission propulsion system can be minimized if the propellant feed system is designed to accommodate the larger propellant flow rate to be used with the full size (Mercury orbiter version) engine, and the system uses common elements such as valves, injector assemblies, and combustion chambers of equal diameter in the full-size and reduced-size engine applications. The accruing small weight and cost penalty is felt to be acceptable in exchange for the significant performance improvement of the common system to be gained by this approach.

4.2.4 Thermal Control Design Approach

Thermal design approaches for the earth-storable and space-storable propulsion systems are fundamentally different. In the earth-storable system both oxidizer and fuel tanks are to be maintained within a temperature range of 70 to 120°F. Conventional techniques of thermal insulation against undesirable external heating and against heat losses to cold space can be applied. The storage tanks as well as the propellant lines and externally mounted thruster control valves require the use of

electrical and/or radioisotope heating elements to prevent freezing of the propellants, a technique used successfully on Pioneer 10 and 11. Thermal interface problems with the payload spacecraft must be addressed to permit adequate payload waste-heat dissipation in those cases where the attachment of the propulsion module(s) obstructs the view of cold space by heat rejection surfaces provided in the original payload spacecraft design. The question of thermal protection against the intense solar heat flux in the Mercury orbit mission as well as against the potentially significant reradiated heat flux from the dayside of the planet itself will be discussed below.

In the space-storable system the cryogenic oxidizer (LF_2) tank must be maintained between about -306 and -230°F to avoid excessive thermal expansion and vapor pressure, while the warm fuel (N_2H_4) tank is to be held in the temperature range of 70 to 120°F. Thermal control of the cold LF_2 tanks requires the following approach which was defined in a previous TRW design study (Reference 4):

- Minimize heat leaks into the tank since at the specified low storage temperature the tanks can radiate excess heat only at a very low rate.
- Provide an adequately large solid angle (view factor) for radiation of heat from the cold tank to cold space to assure thermal balance at the specified low storage temperature. This requirement affects the relative location of the cold tanks and the sun shade required in the Mercury orbit mission.
- Omit thermal insulation of the cold tank to facilitate its heat rejection to cold space.
- Provide thermal coatings of appropriately high emissivity and low absorptance.
- Protect the tank against sources of significant thermal irradiation within the propulsion module and from the payload by appropriate shielding. Warm tanks that can be seen by the cold tanks must be effectively insulated.
- Prevent conductive heat transfer to the cold tanks, e.g., from the warm tanks or other warm system components by using sufficiently long and thin-walled support struts.

In the case of the Mercury orbiter the payload spacecraft as well as the attached propulsion modules require thermal protection by a sun

shade in order to survive the solar flux which at Mercury's perihelion distance (0.307 AU) increases to a value 10.6 times greater than at earth. Exposure to the IR flux from Mercury's hot surface during day-side traverses must be kept to an acceptable level. This can be accomplished by appropriate control of the closest approach distance to the subsolar region of the planet, e.g., selection of the orbital mission profile and by an orbit change maneuver to raise the periapsis distance in advance of the onset of seasonal subsolar region overflights.

These requirements and other factors involving thermal protection of the Mercury orbiter will be discussed more fully in Section 6.

Short exposures to direct solar illumination during the launch phase and during midcourse maneuvers (e.g., near Venus) can be accepted without causing a prohibitive cold-tank temperature increase.

In the outbound missions the propulsion module is generally protected against prolonged solar illumination by the large high-gain antenna dish acting as a sun shade (outer-planet Mariner payload) or by added sun-shade extensions to augment the smaller antenna dish size in the case of the outer-planet Pioneer payload. Prolonged side-sun illumination that would occur during the first two months of the outbound cruise with the high-gain antenna pointed at earth can be avoided by using medium- and low-gain antenna coverage instead since high data rate telemetry will not be required during this mission phase.

4.2.5 Structural Design Approach

The major loads to be supported by the propulsion module structure are the module's own propellant tanks and the mass of the vehicle (or vehicles) located above the module. The structure transfers the combined load to the launch vehicle upper stage adapter. Load characteristics vary greatly depending on the mission to be flown.

The worst-case condition for which the structure must be designed is presented by the Mercury orbiter mission. In this case the external load to be carried consists of the payload spacecraft plus the fully loaded upper propulsion module, mounted in tandem. Since both modules to be

used in this configuration are to be of identical design, a heavier structure is required than if the modules were designed individually. The resulting weight penalty affects not only the Mercury mission performance but also those of the outer-planet orbiters which will make use of the same structural design. It is essential that this weight penalty be minimized by using an efficient structural design approach.

Dynamic loading conditions occurring during Shuttle launch and abort phases are listed in Table 4-3 (from the current issue of "Space Shuttle System Payload Accommodations," Reference 21).

Table 4-3. Shuttle Payload Maximum Design Accelerations (g's)

Condition	Upper Stage Loading	a_x	a_y	a_z
Lift-Off	Full	-2.9	±1.0	±1.5
High Q boost	Full	-2.0	±0.5	±0.6
Booster end burn	Full	-3.3	±0.2	-0.75
Orbital operation	Full	-0.2	±0.1	±0.1
Entry and descent	Empty	0.75	±1.25	1.0
Landing	Empty	+1.0	±0.5	2.8
Crash (ultimate load)	Empty	9.0	±1.5	-4.5

Sign convention:
+x forward
+y left
+z upward

Shuttle safety requirements demand that the total payload consisting of the propulsion module (or modules) and the payload spacecraft remain structurally intact under conditions of a survivable crash landing, with an ultimate longitudinal acceleration of 9 g. However, as a factor that alleviates this condition it is reasonable to assume that all propulsion-module propellants will be dumped as a safety measure prior to the abort and entry phase (see Section 4.8.3 and Appendix B). In consequence, the critical load conditions occur during liftoff and boost with the fully loaded tandem stack of propulsion modules.

In the case of outer-planet orbiters the peak load occurs at burnout of the solid kick motor. The thrust force is about 15,000 lb_f (68,100 Newtons). With a maximum acceleration of about 5 g (for a total mass of 3000 lb_m (1360 kg)) the resulting compressive and buckling stresses are more severe than those occurring during the Shuttle ascent phase (3.3 g).

A detailed analysis of load characteristics and structural designs adopted for the multi-mission propulsion module is presented in Appendix C.

Several structural design concepts were investigated during the study that use different approaches to tankage support, principal load transfer and load path separation. The alternatives included shells and trusses as main structural elements. The structural concept which appears to offer the most efficient load-carrying capability under the existing configuration constraints is illustrated in Figure 4-3. It is a hybrid structure comprising a cylindrical shell in the center and support trusses for each of the four peripherally arranged spherical propellant tanks. Its principal design advantages include the following:

- The central cylinder is an efficient load transfer structure considering the fact that more than 70 percent of the total load to be transferred is the axial load from the upper module and the payload vehicle.
- The cylindrical shell is better suited than a truss in applications involving distributed loads above the interface (Pioneer inbound and outbound configurations transfer the load through a shell structure) or below the interface (cylindrical interstage adapter to the solid kick motor).
- A cylindrical shell conforms better with a V-band (Marman clamp) separation joint than a truss structure. V-band separation joints require fewer explosive separation devices to assure failure-free operation than trusswork separation joints.
- Individual trusses used to support the propellant tanks are readily integrated with the central cylinder by attachment at the separation interface rings, at the top and bottom of the module.
- The central cylinder permits convenient attachment of the conical main engine support structure. The cone is

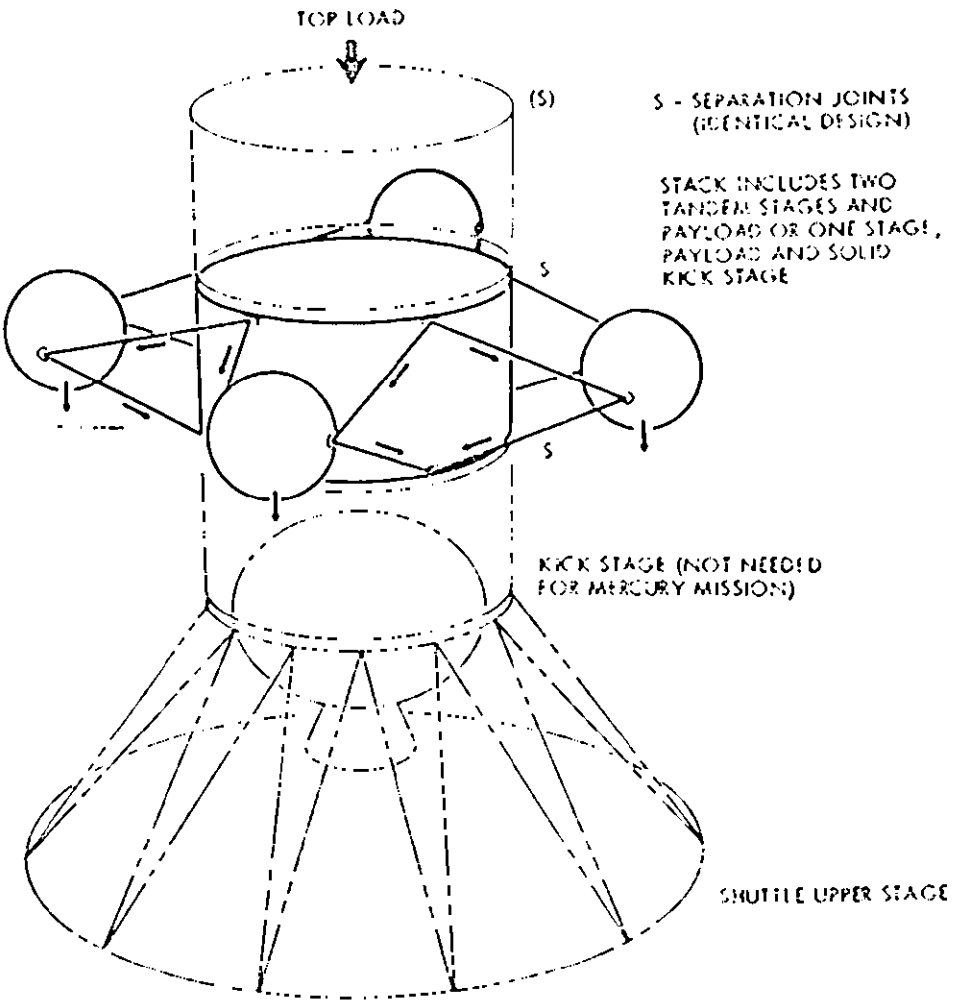

Figure 4-3. Payload/Propulsion Module/Kick Stage Structure Concept

attached to a reinforcement ring located at the middle of the support cylinder.

- Heat transfer between the engine radiation shield, the central support structure, and the propellant tanks can be minimized by insulating the truss attachment points and by appropriate choice of strut length, wall thickness and thermal coating. (Load path separation provided by the hybrid structure favors thermal separation in the case of space-storable propellants.)

- The peripheral location of propellant tanks (especially the wide separation of tanks required for dynamic stability in the case of Module A) is readily accommodated by the hybrid design concept.

Alternate design approaches will be discussed and evaluated in Section 4.3. The selected structural designs for Modules A and B will be shown in greater detail in Sections 4.4 and 4.5.

4.2.6 Retention of Propulsion Module at Destination

The question of whether to retain or to jettison the propulsion module after completing orbit insertion at the target planet (or in comet missions, after completing the rendezvous maneuver) is of appreciable importance in the definition of the module design, functional capabilities and operational sequences. System implications of retaining the propulsion module for the duration of the planetary orbit phase (or in comet missions, the time interval of close proximity to the comet) were investigated, and relative advantages versus disadvantages were assessed in qualitative terms as follows:

1) Retention of Propulsion Module

Advantages	Disadvantages
• Increased flexibility of orbital phase	• Exposure of propulsion module to increased meteoroid impact hazard
• Ability to make significant orbit trims late in the mission (desirable from scientific standpoint)	• Extended electrical power requirement for propulsion module heating
• Ability to use main propellant supply for auxiliary propulsion (performance gain)	
• Propulsion module shields spacecraft rear side against meteoroids	

2) Staging of Propulsion Module

Advantages	Disadvantages
• Reduced mass and moments of inertia improve auxiliary propulsion performance	• Possible malfunction of pyrotechnic separation devices after long transit time introduces failure mode

- Elimination of some science instrument and antenna field-of-view obstructions
- Required increase in payload spacecraft propulsion capability in lieu of using spare propellant capacity of the propulsion module could be potentially costly (tank size)

The tradeoff between performance advantages of using the main propulsion-system propellant supply to handle auxiliary propulsion functions (if the propulsion module is retained) versus performance advantages gained by staging does not provide a decisive argument for or against propulsion module retention in terms of weight differences only. However, it appears that the advantage of providing a more flexible mission strategy in unknown environments (safety, scientific mission yield) by utilizing the spare propellant capacity will justify retention of the module.

In the Saturn orbiter mission the major plane-change maneuver required after orbit insertion to achieve a low-inclination orbit should be performed as late as possible to permit extension of exploration at higher latitude and to minimize exposure to ring-particle impacts. The planetary environment can be explored more effectively with the aid of swingby maneuvers of the satellite Titan. These options are the subject of a concurrent study by JPL* which shows the wide range of mission options, including plane changes and apsidal rotations, available in a largely nonpropulsive mission sequence. An ample propellant margin provided by the multi-mission propulsion module will add flexibility and corrective maneuver capability. Orbital lifetimes of up to 3 years are being contemplated.

This philosophy implies a multiple restart capability for an increased number (10 to 15) of successive thrust events. The expected increase in propulsion system development and test cost to meet this requirement is offset by the greater scientific mission potential.

*A report is currently in preparation by Dr. Phil Roberts (personal communication), Reference 30.

At Uranus the use of extra propellant will significantly enhance the scientific exploration scope by permitting periapsis altitude and apsidal orientation changes. Close encounters of the inner satellites Miranda and Ariel or the outer satellites Titania and Oberon will thus become feasible. The unusual pole-on magnetospheric configuration resulting from Uranus' polar axis tilt offers interesting scientific exploration possibilities that can be fully exploited only by extended orbital life and maneuver capabilities.

At Mercury, an extension of orbital life to several (earth) years would permit observation of changes in Mercury's geophysical environment due to changes in solar weather during and after the peak of solar activity which will occur in 1990. This again implies increased orbit control maneuver requirements. As a side benefit of an extended Mercury orbiter mission the spacecraft remains at a most favorable vantage point for close-distance solar observations. During three-fourths of its orbital phase it can view far-side solar activity unobservable from earth. During the prolonged eclipse seasons that will occur in 40-45 day intervals it can make use of Mercury as occultation disk for observation of the solar corona. These observations can be performed twice per orbit in relatively rapid succession.

Similarly, in comet rendezvous missions, an adequate maneuver propellant margin (100 to 200 m/sec) for in-situ coma and tail exploration is essential for a maximum scientific data yield.

Performance considerations which favor retention of the propulsion module are felt to outweigh the two principal disadvantages associated with retention, namely longer exposure of propellant tanks to possible micrometeoroid penetration, and extended use of electrical heater power for propellant tanks and feed lines during the orbital mission phase.

The micrometeoroid impact protection problem will be addressed in Section 6. Granted that the micrometeoroid flux rate tends to be greater in the vicinity of the target (e.g., Saturn and Mercury) than during the transit phase, the risk of losing the mission because of a penetrating impact on one of four propellant tanks is reasonably small. If such an impact should occur it would affect only a small amount of

residual propellant, not the entire remaining propulsion capability. Means to prevent loss of either all remaining propellant or oxidizer through a single penetration leak must be provided in any case to safeguard against loss of the mission before reaching destination. The use of four rather than two propellant tanks in the case of Module B (where both options are acceptable) provides some degree of functional redundancy if the necessary isolation valves in the pressurization and feed system are added.

The second concern, i.e., extended use of power for propulsion system thermal control and for propellant management valves at a time when power reserves are continually diminishing, is a matter for detailed spacecraft system design tradeoffs exceeding the scope of this study. To alleviate the power drain due to retention of the propulsion module a design approach was taken that relies to a large extent on radioisotope heating, as in the Pioneer 10 and 11 spacecraft and the Pioneer Jupiter orbiter design (Reference 6).

4.2.7 Auxiliary Propulsion Functions

If the propulsion module is retained in the orbital mission phase it can be used to perform auxiliary propulsion functions (orbit corrections and attitude control maneuvers) in addition to the primary high-thrust maneuvers. The following configuration and performance aspects favor this design option:

1) A common propellant supply can be used for auxiliary and primary propulsion. This simplifies the design, avoids propulsion hardware duplication and reduces unusable (residual) propellant mass.

2) A performance advantage can be gained, particularly, if the auxiliary propulsion system can utilize the same bipropellant as the main engine rather than monopropellant hydrazine.

3) If the auxiliary system uses monopropellant hydrazine from the common propellant supply (in the case of space-storable propulsion) it will operate on regulated pressure rather than in the blowdown mode, with higher average specific impulse.

4) If the auxiliary system uses hydrazine only which is drawn from the common propellant supply (in the space-storable case) the mixture ratio of the bipropellant main engine is thereby improved if equal-volume tanks for fuel and oxidizer are used, as will be discussed in Section 5.

5) The hydrazine storage tank(s) of the payload spacecraft would require enlargement to meet increased auxiliary propulsion requirements of the heavier flight spacecraft and the longer mission life. Generally this would require some change of the payload's central equipment compartment layout. This is avoided by using the propulsion module tanks as a common propellant source. The weight thus saved partly offsets the weight increases due to strengthening deployed appendages against greater accelerations or other modifications.

   It should be noted that an auxiliary thruster rearrangement on the payload spacecraft would be required, in any case, because of the addition of the propulsion module(s) at the aft end.

6) Integration of all propulsion functions into the propulsion module implies simpler assembly and test operations and hence lower program cost compared to a system where both the payload and the propulsion module carry propulsion system elements.

7) Placement of auxiliary thrusters on the propulsion module, in many instances, helps to reduce or avoid unwanted inter-axis coupling torques caused by the large center-of-mass offsets along the spacecraft centerline. This reflects in propellant savings and simpler maneuver sequences.

A notable exception to the use of common propellants by the auxiliary propulsion system and advantages that might be derived from that option occurs in the case of Module B with earth-storable propellants. The three-axis stabilized flight spacecraft requires much smaller minimum impulse bits in the limit cycle attitude control mode than those achievable, in general, with bipropellant (N_2O_4/MMH) auxiliary thrusters.

Propellant requirements to maintain a spacecraft of given design and moments of inertia within a specified limit cycle deadband are proportional to the square of the minimum impulse bit. The Mariner outer-planets spacecraft uses monopropellant thrusters of 0.2 lb_f (0.89 Newton) thrust force operating at minimum pulse lengths of 30 msec. Even with the larger moments of inertia of the Mariner orbiter configuration the

thrust force should not exceed 0.5 lb_f (2.2 Newtons). The available technology of auxiliary bipropellant thrusters does not permit efficient or precisely controlled operation at these small thrust levels and short pulse lengths. Minimum impulse bits are at least one order of magnitude too large. In consequence, for Mariner orbiters that use propulsion Module B with earth-storable bipropellants, a separate monopropellant supply is needed and can be provided by the hydrazine tank (or tanks) carried by the payload spacecraft, but appropriately enlarged for this application. Relocation of the auxiliary thrusters into the propulsion module is still the preferred design option, mainly for reasons explained under items 6) and 7) of the above list.

Table 4-4 summarizes the preferred design approach used to implement auxiliary propulsion functions with the different payload spacecraft and propulsion technologies under consideration.

In addition to the small auxiliary thrusters used by the flight spacecraft, a set of larger thrusters is required during the launch phase of outer planet orbiters to provide thrust vector control for the 15,000-lb_f (67,000-Newton) solid-propellant kick motor. The system design retains the arrangement used in Mariner Jupiter Saturn with four 115-lb_f (512-Newton) main TVC engines and four smaller (5-lb_f, 22.2-Newton) roll control thrusters, supplied either by the hydrazine or bipropellant tanks of the liquid propulsion module. After solid motor separation the control circuits in the payload spacecraft are reconfigured as in the case of Mariner Jupiter Saturn to meet the different attitude control requirements of the flight spacecraft.

4.3 PROPULSION MODULE DESIGN EVOLUTION AND SELECTION RATIONALE

Numerous propulsion module design alternatives were investigated and compared in the process of selecting preferred configurations (which will be described in Sections 4.4 and 4.5). Some of the alternatives will be discussed in this section to outline the design evolution and the selection rationale. The alternatives considered included primarily the shape, number and arrangement of propellant tanks and various support structure concepts.

Table 4-4. Auxiliary Propulsion Implementation

Propulsion Module Type	Propellants for Main Engine	Force lb_f (Newton)	Type	Minimum Thrust Pulse (sec)	Pressure (psi)	I_{sp} (sec)	Remarks
A	N_2O_4/MMH	2 to 5 (9.1 to 22.3)	Bipropellant N_2O_4/MMH	0.5	300 (regulated)	260-280	• Bipropellant thrusters most efficient; within state of technology
	F_2/N_2H_4	1 to 2 (4.5 to 9.1)	Monopropellant N_2H_4	0.03	300 (regulated)	180-220	• Uses spare fuel tank capacity (provided to improve main engine mixture ratio)
B	N_2O_4/MMH	0.3 to 0.5 (1.4 to 2.3)	Monopropellant N_2H_4	0.03	150-300 (blowdown)	170-220	• Requires separate hydrazine tank(s) on payload spacecraft (bipropellant thrusters would have larger than acceptable minimum impulse bit)
	F_2/N_2H_4	0.3 to 0.5 (1.4 to 2.3)	Monopropellant N_2H_4	0.03	300 (regulated)	180-220	• Uses spare fuel tank capacity

Notes:

- All but Module B (earth storable) use auxiliary propellant from own propellant supply
- Auxiliary thrusters on propulsion module in all cases
- Optimum mixture ratio (1.5:1) in space-storable case implies extra fuel tank capacity if equal volume tanks are used

4.3.1 Propellant Tank Configurations

The alternatives included spherical, cylindrical and toroidal propellant tanks.

Four rather than two spherical or cylindrical tanks per module appear preferable because of the balanced (symmetrical) mass distribution and lower propulsion module height, as previously discussed. In the case of spin-stabilized spacecraft a balanced mass distribution is a requirement.

Cylindrical tanks are a viable alternative to spherical tanks to conserve propulsion module height since they can be mounted with their long dimension perpendicular to the spacecraft centerline.

Spherical tanks with a conical extension on one side, also known as "teardrop" tanks, are preferred in the spin-stabilized configuration since this shape facilitates passive propellant acquisition without the aid of capillary devices (see below).

Toroidal tanks, in principle, provide a favorable mass balance in spin-stabilized spacecraft. Design studies and model tests were performed by Martin Marietta Corporation (References 22 and 23) to determine weight and cost data; materials requirements; ease of fabrication; passive propellant acquisition characteristics using capillary devices; and dynamic characteristics, including spin stability and slosh damping. These studies indicated favorable characteristics on all counts, but projected development costs as slightly higher than those of spherical tanks.

Figure 4-4 illustrates lateral tank spreading requirements for attaining moment-of-inertia ratios sufficient for long-term dynamic spin stability. As previously stated, the ratio of spin moment of inertia to the transverse moments of inertia, I_S/I_T, should not be less than 1.1. The diagrams indicate inner boundaries, corresponding to $I_S/I_T = 1.1$, on the placement of tanks in single or tandem arrangement. The boundaries are nearly conical (actually they are hyperboloids of revolution) with half-cone angles depending on the ratio μ of stage mass to payload mass.

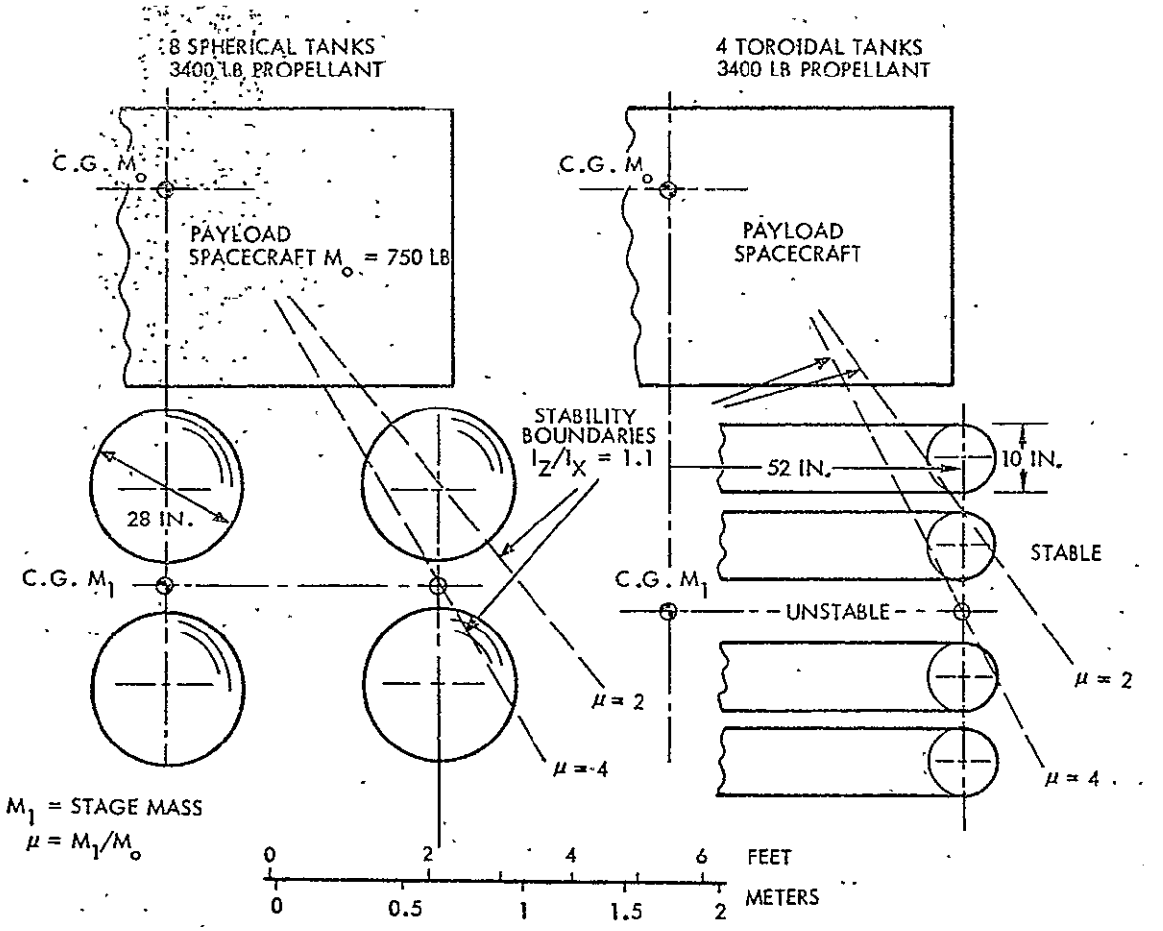

Figure 4-4. Dynamic-Stability Constraints on Tankage for Tandem Stage Configuration (Pioneer Mercury Orbiter)

Mass centers of the cross-sections of stacked toroidal tanks (at the right in Figure 4-4) must be placed farther away from the centerline than those of spherical tanks (left side) to satisfy the dynamic stability criterion $I_S/I_T \geq 1.1$. The boundaries shown correspond to mass ratios $\mu = 4$ for two fully-loaded tandem modules, and $\mu = 2$ for a fully-loaded single module. (They correspond to a simplifying assumption of the stage mass being approximately equal to the propellant mass.) The diagram indicates that the toroids would be so slim (aspect ratios of less than 1:5) as to make passive propellant acquisition somewhat doubtful.

Arrangement of two toroids concentrically in each propulsion module has been considered as an alternative to overcome the aspect ratio problem. It has the disadvantage of requiring development of two toroids of different dimensions.

In addition to the problem of small tube diameters some questions regarding toroidal tank mounting, support, and the thermal isolation of alternately mounted warm and cold tanks remain unsolved.

For nonspinning spacecraft toroidal tanks pose problems of propellant sloshing and attitude-control stability that would need more detailed analysis. Figure 4-5 illustrates the basic destabilization problem due to thrust application and propellant sloshing in a nonspinning toroidal tank. Assume in a partially empty tank the propellant mass center is located to the left of the centerline. The combined mass center is then also on the left. If the thrust vector is initially aligned with the centerline the vehicle will start rotating counterclockwise driving the propellant farther to the left (acceleration a_-). If the thrust vector is aligned with the vehicle mass center to null the torque then the propellant will be accelerated to the right (acceleration a_+). The destabilizing effect increases with the magnitude of the thrust acceleration. However, it can be reduced by addition of slosh-suppression baffles. Three-dimensional effects, not included in the above simplified model, tend to aggravate the problem since a strong coupling of the two transverse motions is unavoidable. The problem is analagous to balancing a steel ball in the center of a convex plate.

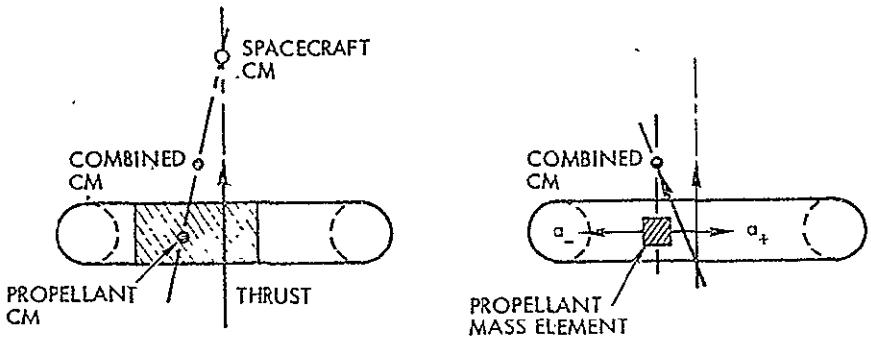

Figure 4-5. Propellant Sloshing in Nonspinning Toroidal Tanks

Another factor of concern is the relatively short separation, typical for the configurations being contemplated, between engine gimbal and vehicle center-of-mass locations. This means that relatively large transient thrust vector deflections are required to counteract perturbations to restore equilibrium.

4.3.2 Structural Concepts Alternatives

Figure 4-6 illustrates some of the alternate structural design concepts considered in the study.

Figure 4-6a shows a trusswork of eight upright main support struts and diagonal stabilizers. The four propellant tanks are supported between main strut pairs. The configuration is intended primarily for non-spinning spacecraft (Module B) with tanks located relatively close to the centerline. Tank pressurization and expansion tends to cause a bending force on the main struts. Load paths for upper vehicle support and tank support combine in the main struts. The structure is held together by relatively heavy rings that form the separation joints. Separation is effected by a large number of explosive bolts.

Figure 4-6b shows a basket truss arrangement as main support structure. The main truss is outside of the propellant tank locations. The design is primarily for nonspinning applications because of tank placement constraints imposed by the outer truss. Upper and lower support rings are provided to facilitate stacking of modules and stage separation. Again, as in the preceding case, a large number of explosive separation bolts is required. The diameters of the outer truss and ring structures are relatively large, and structural weight is comparatively heavy. Additional trusswork is required inside the basket truss to support the propellant and pressurant tanks and the center-mounted engine.

Figure 4-6c shows a reversal of the preceding structural concept with slanted main support trusses partly inboard of the tank locations. Auxiliary trusses are used to support the outriggered tanks individually. The concept is primarily intended for spinners. End support rings are of comparatively small diameter, compatible with the use of Vee-band separation joints, provided they are made strong enough to limit deformation due to discrete kick loads. This structure is relatively compact and weight-effective. Load path separation is similar to that of the hybrid structure (see Figure 4-3) in which the main support truss is replaced by a cylindrical shell but outriggered tank support trusses are retained. The shell structure provides a more efficient transfer of the

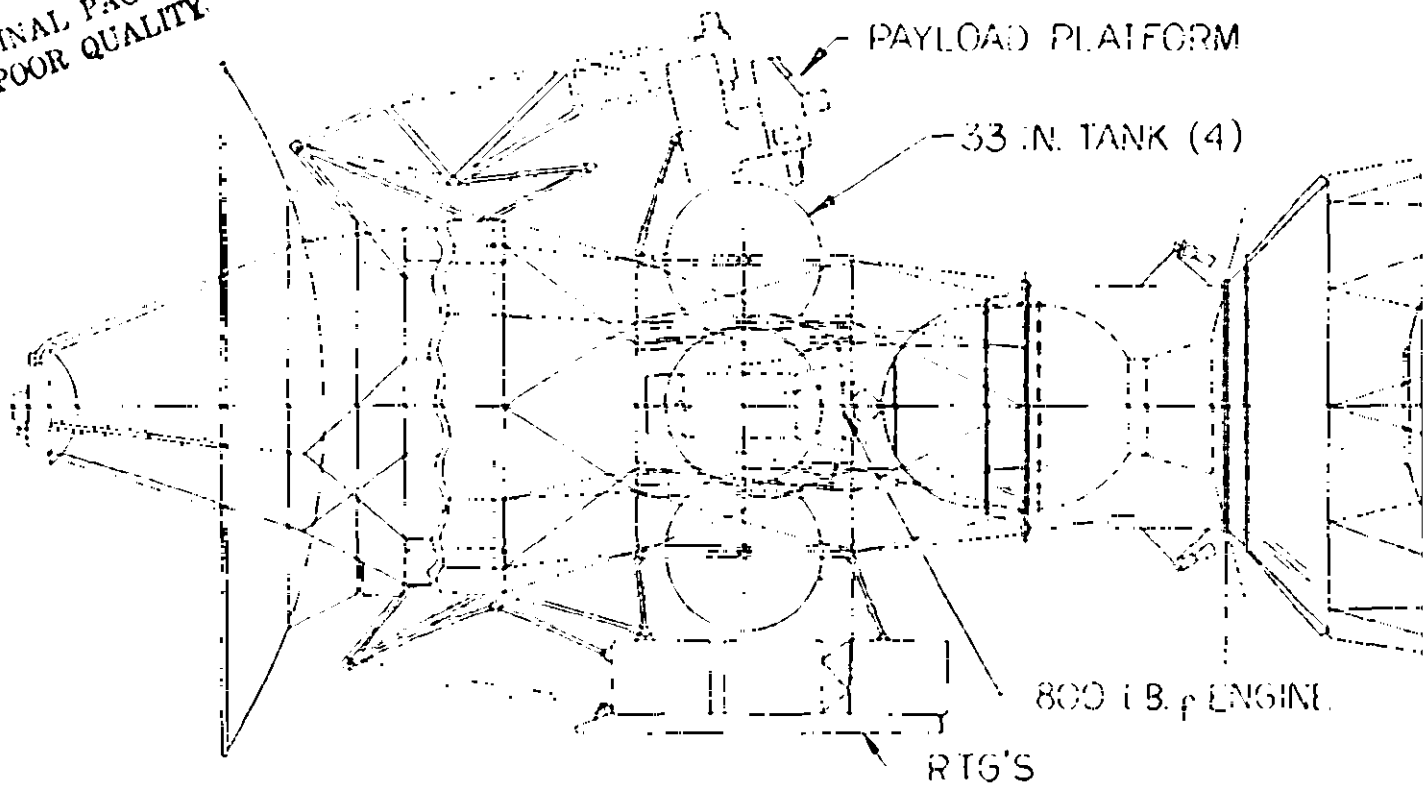

A. UPRIGHT MAIN SUPPORT STRUTS AND DIAGONAL STABILIZERS (MARINER PA

FOLDOUT FRAME

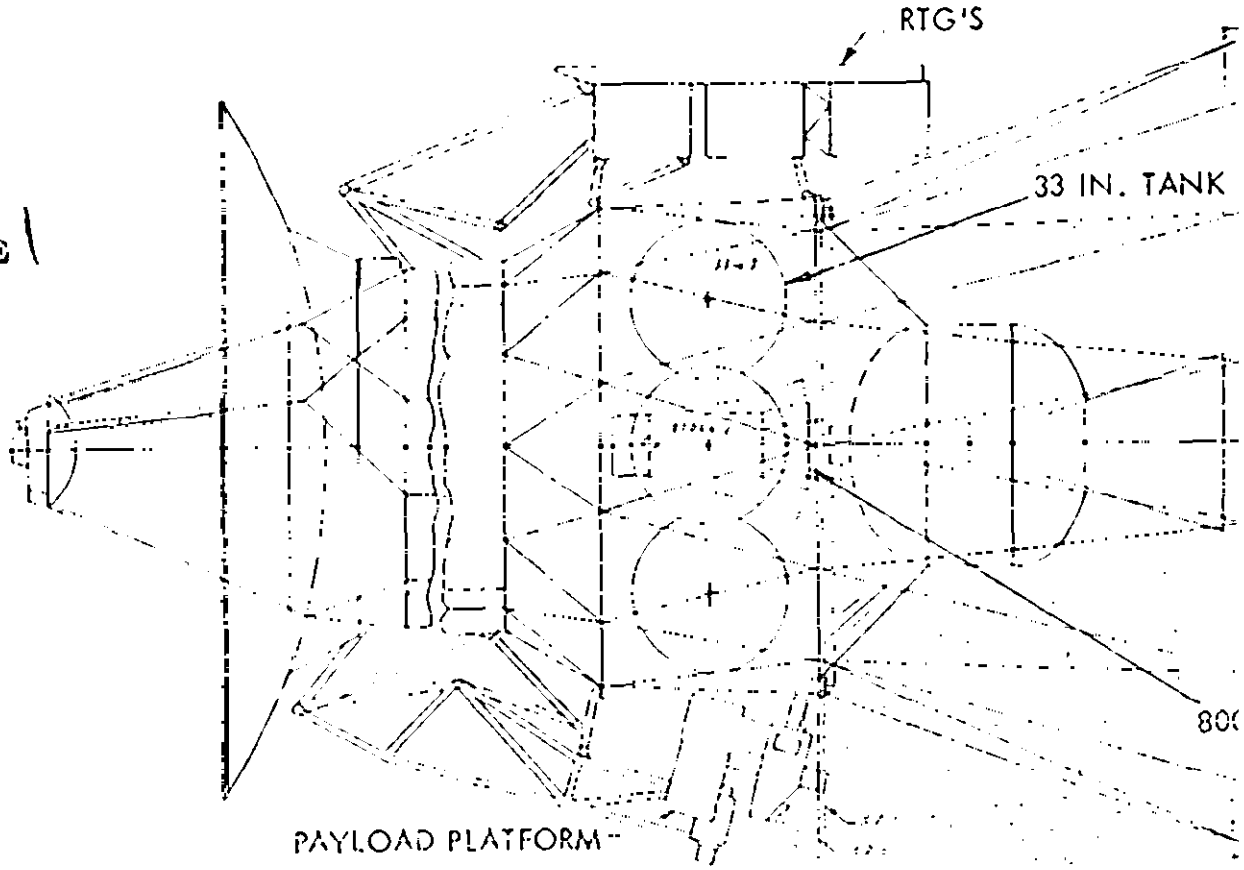

B. BASKET TRUSS CONCEPT OUTSIDE PROPELLANT TANKS (MARINER PA

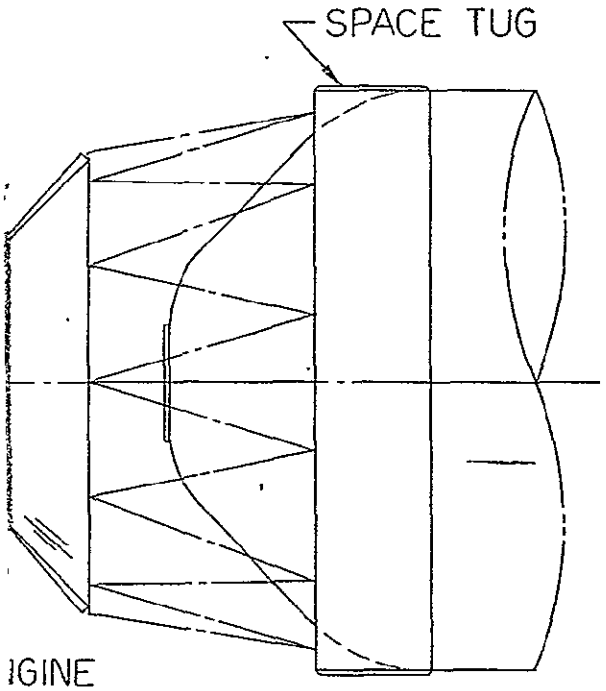

MARINER PAYLOAD)

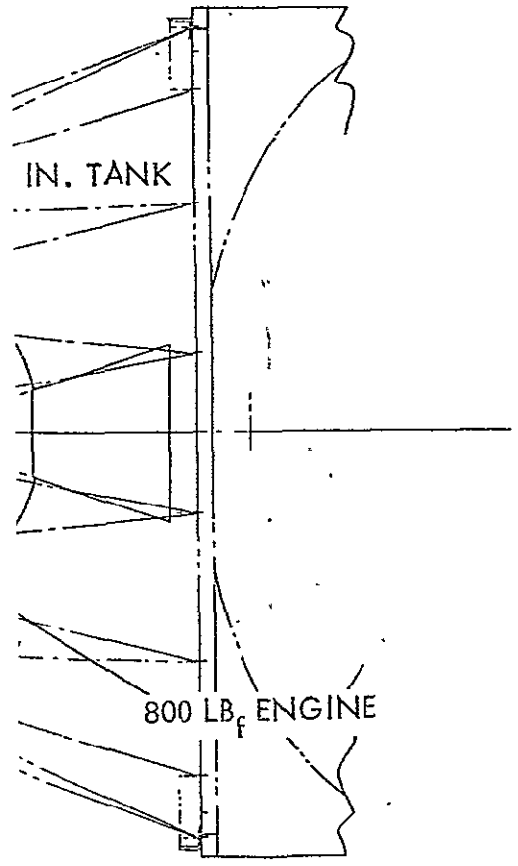

MARINER PAYLOAD)

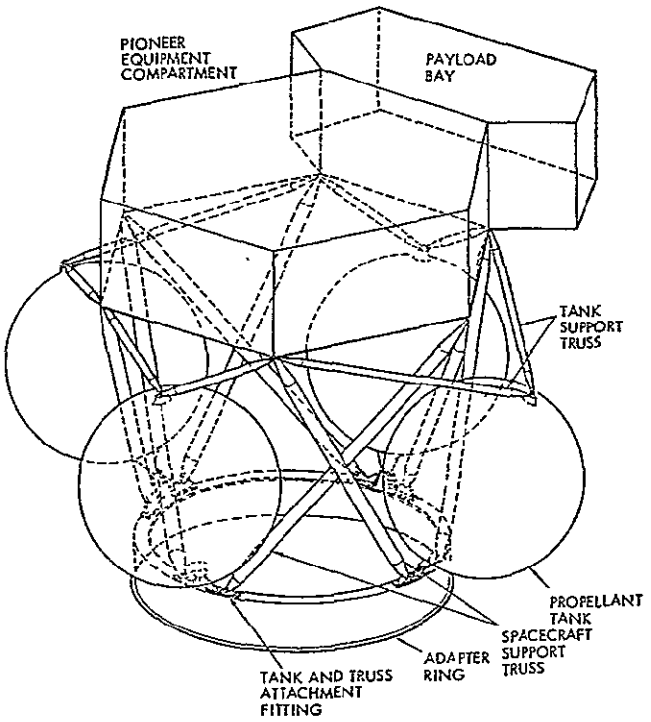

C. INTERNAL MAIN SUPPORT STRUTS AND OUTRIGGERED TANKS (PIONEER PAYLOAD)

FOLDOUT FRAME 2

Figure 4-6. Alternate Structural Design Concepts

distributed loads from Pioneer spacecraft adapter rings above and into the second propulsion module or the solid kick-stage support structure below.

Other alternatives (not shown here) were considered that include shell structures for equatorial propellant tank support and truss structures holding a tank support pallet of four rings on which the tanks also are mounted equatorially. These concepts did not promise a weight-effective structural design and presented difficulties as to effective isolation between warm and cold tanks against conductive heat transfer. Note that the truss configurations shown in Figure 4-6 all lend themselves to effective thermal separation of tanks.

4.3.3 Kick Stage Support Structure

Several design alternatives for supporting the solid kick motor were investigated. To prevent the heavy spacecraft/propulsion module combination from transferring structural loads into the kick stage motor case (with the design characteristics of the future SPM (1800) kick stage still quite undefined), a preferred design approach is one that isolates the kick stage altogether from the principal load path between the payload/propulsion module combination and the Shuttle/Tug. The kick stage is suspended by the structure that connects it to the payload/propulsion module stack. Separation is effected by a Vee-band separation joint. A cylindrical shell supports the payload/propulsion module combination and connects it to the Shuttle/Tug adapter truss. Care is exercised to provide a sufficiently large fly-out angle (about 15 degrees is desirable) for the kick motor during separation from the Shuttle upper stage.

4.3.4 Summary of Preferred Design Rationale

Figure 4-7 summarizes the steps involved in selecting the preferred design concept for propulsion Module A. The principal design alternatives are listed and the rationale for the selected design is briefly indicated at each step of the selection process.

Figure 4-8 is a similar block diagram summarizing the selection rationale for propulsion Module B.

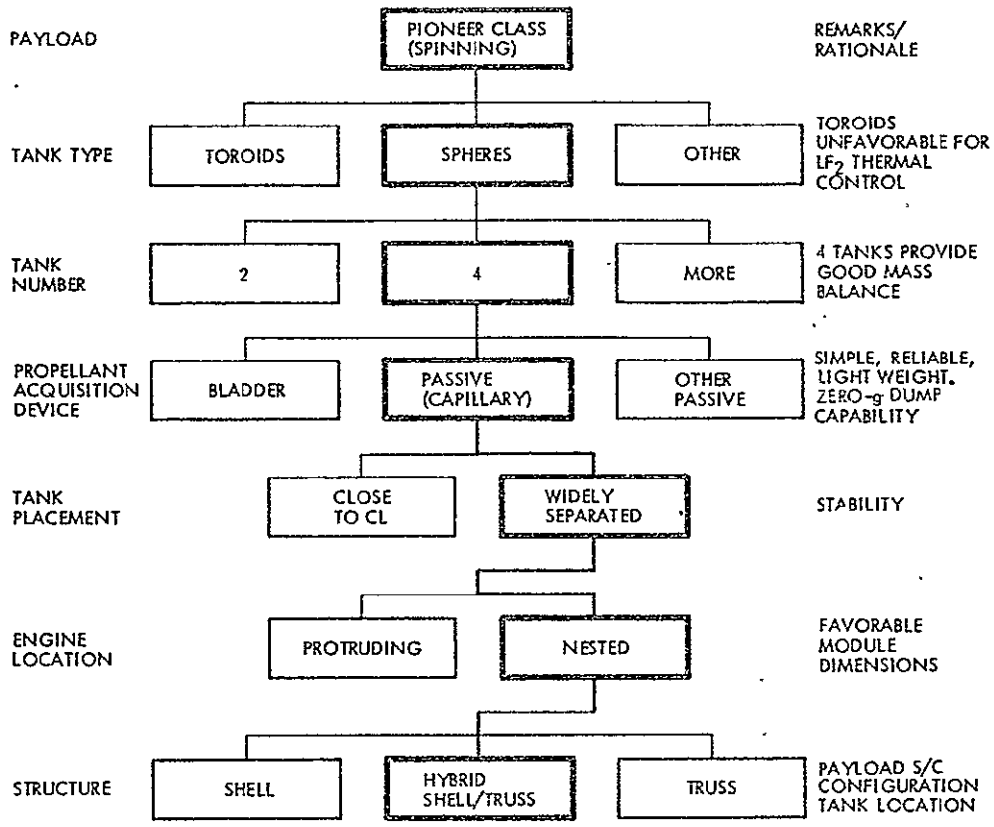

Figure 4-7. Preferred Design Options for Propulsion Module A

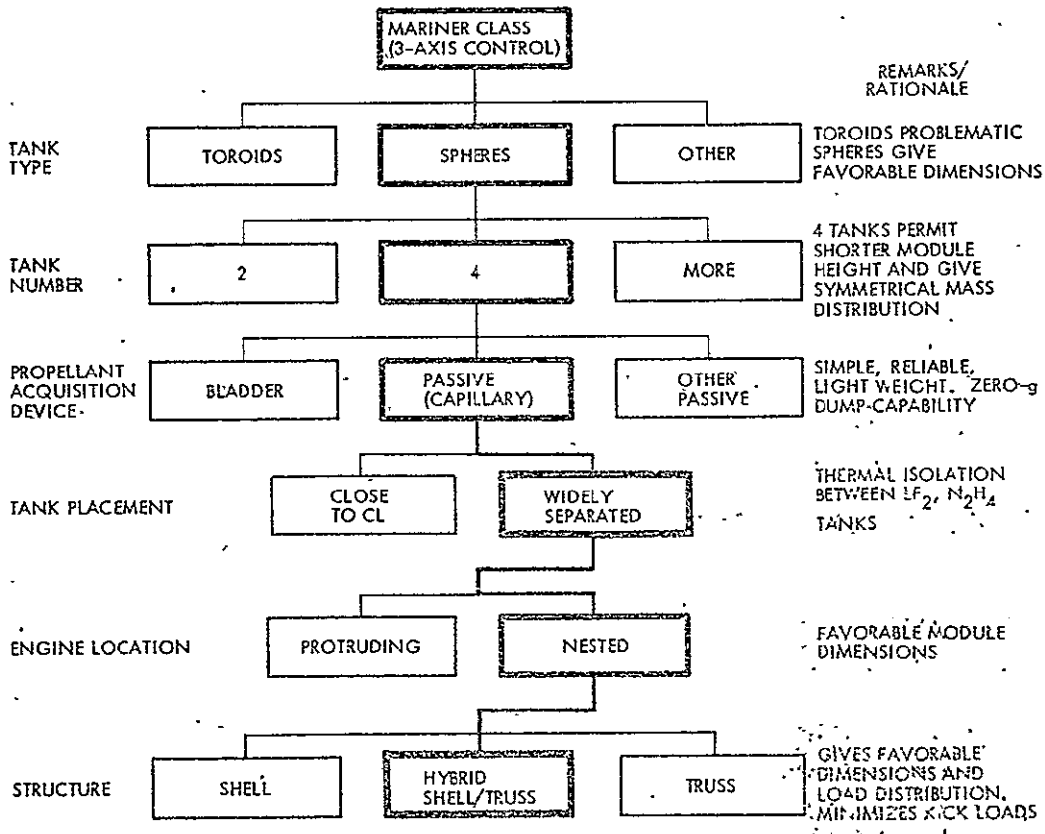

Figure 4-8. Preferred Design Options for Propulsion Module B

4.4 SELECTED DESIGN FOR MODULE A (SPIN-STABILIZED PAYLOAD)

4.4.1 Configuration for Mercury Orbiter

Figure 4-9 shows the selected propulsion module design for spin-stabilized payloads (Module A), arranged in tandem configuration for the Mercury orbiter mission. The side view shows the stowed configuration in the Shuttle cargo bay, with the vehicle attached to a Centaur-class upper stage. A solid kick motor is not needed for this mission. The rear view is shown on the right. This version of Module A is designed for space-storable propellants.

The payload is a modified version of the Pioneer Venus orbiter, with the cylindrical solar array replaced by a conical array having a half angle of 30 degrees. This solar array configuration is comparable to that of the Helios (1974) spacecraft, designed for solar distances as close as Mercury's perihelion (0.31 AU).

In the cruise mode the vehicle's spin axis is oriented perpendicular to the plane of motion and, hence, the sun line. In this orientation the despun antenna can always be pointed at the earth with only small elevation angle changes from the nominal 90-degree position.

Departures from the cruise attitude are necessary during the Mercury orbit insertion and other maneuvers and are permissible as long as the side-sun orientation is maintained to assure continuous protection of the propulsion module by the deployed sun shade.

The propulsion module consists of four outriggered teardrop-shaped propellant tanks and four pressurant tanks, a central cylindrical support shell, and four identical truss structures that tie the propellant tanks to the central cylinder. The 800-lb_f (3560-Newton) main engine is mounted inside the cylinder, enclosed by a radiation shield and supported by a 32-degree thrust cone. The large 800-lb_f engine is the one selected for the Mercury mission; a smaller engine is used in the outer-planets orbiters.

The support truss for each propellant tank is attached to the tank at two mounting bosses. The attach point locations on the tank sides are

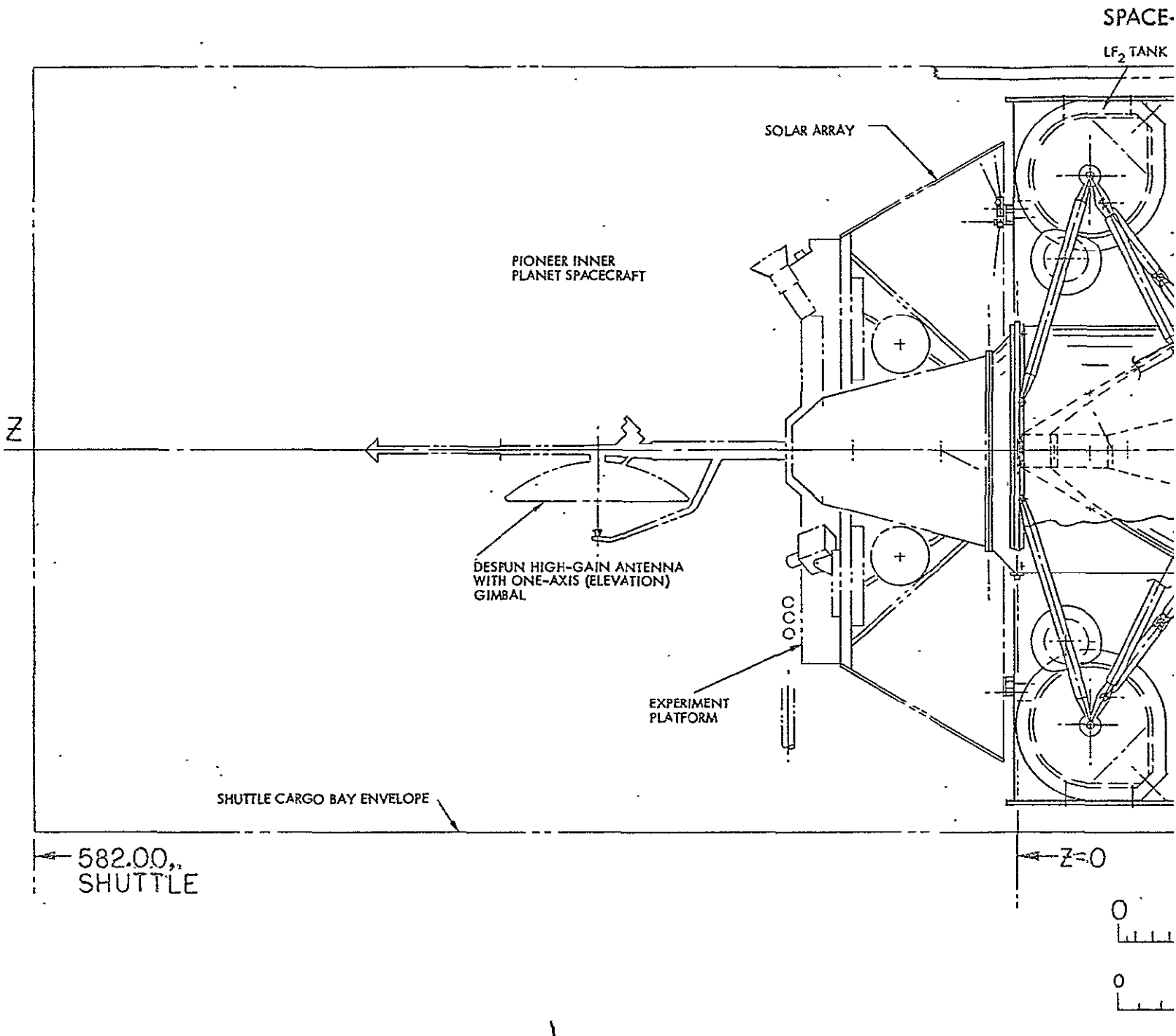

SPACE-STORABLE PROPELLANTS

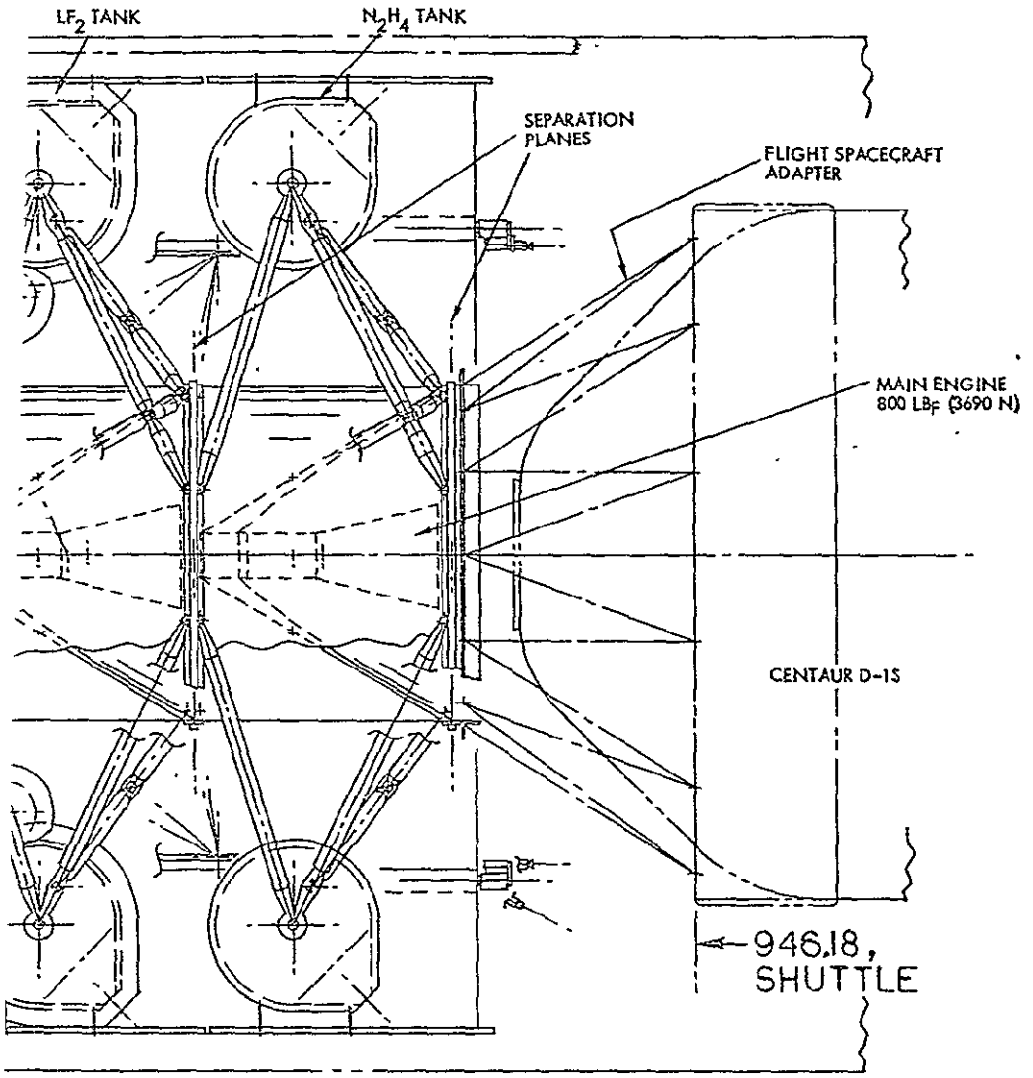

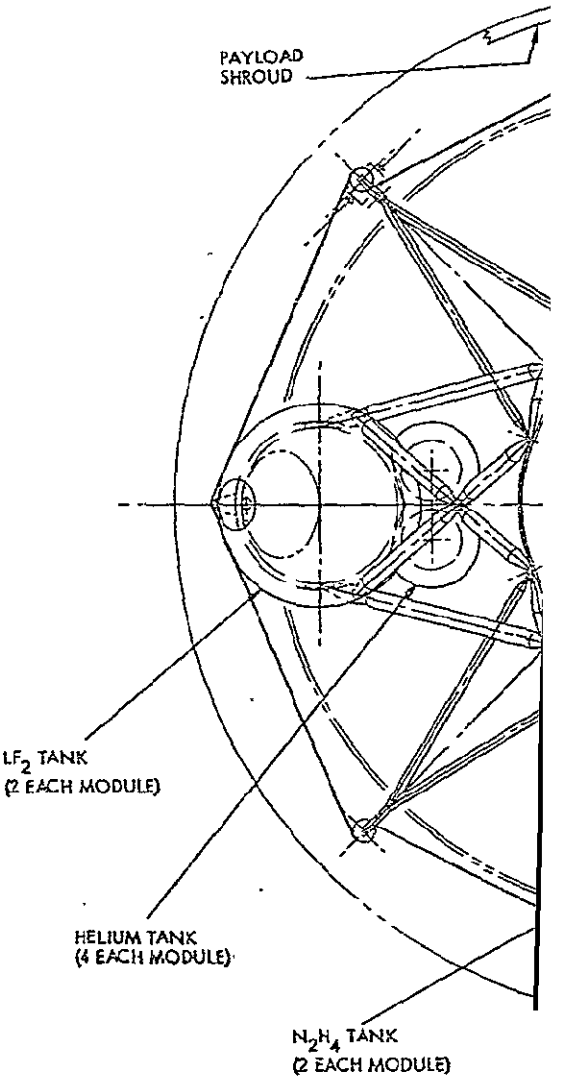

Z=0

0 1000 2000 3000
MILLIMETERS
0 50 100
INCHES

FOLDOUT FRAME 2

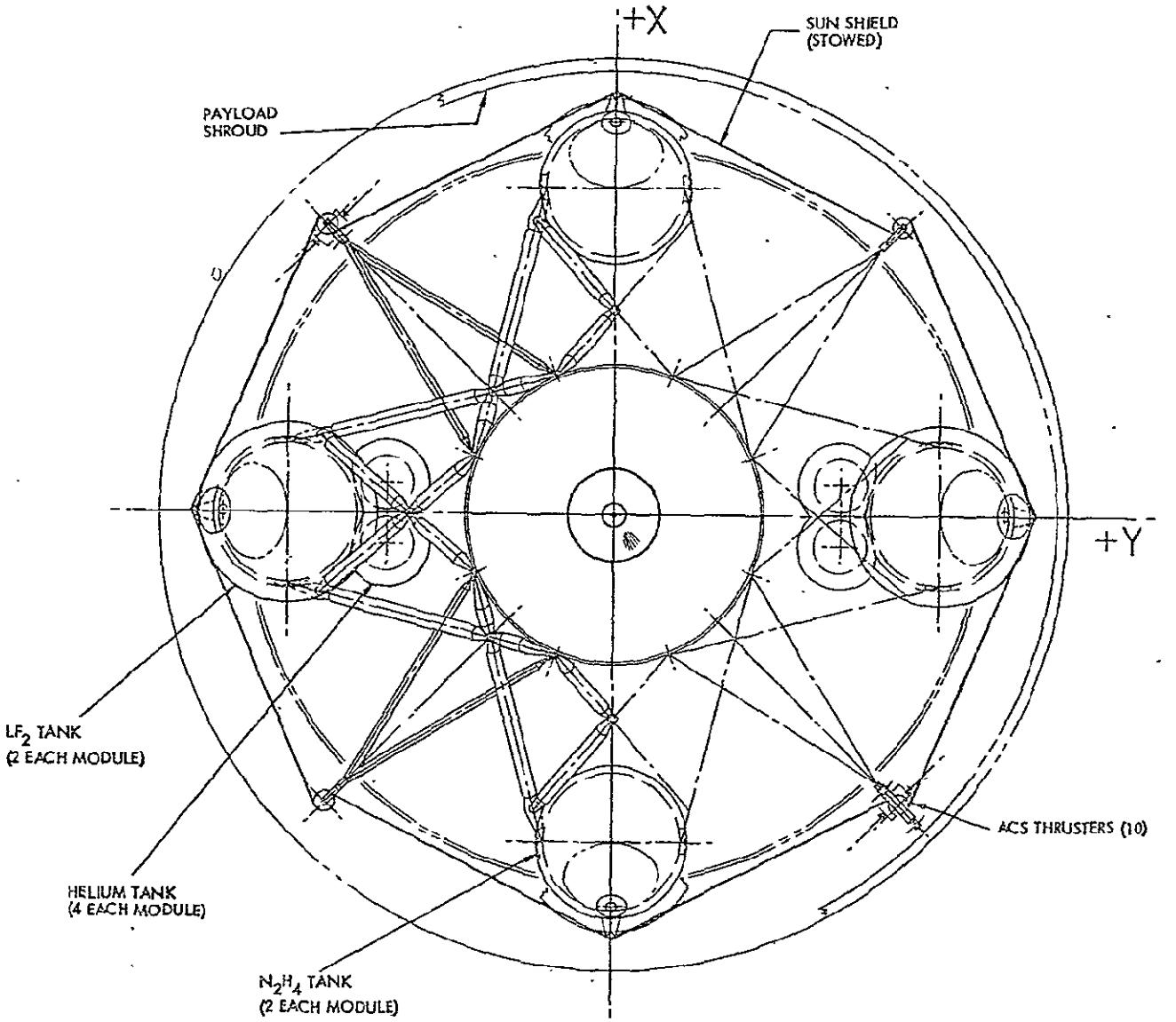

FOLDOUT FRAME 3

Figure 4-9. Propulsion-Module Configuration for Pioneer Mercury Orbiter (Tandem Configuration)

3-inch (7.6 cm) closed-cell foam layer is used to enclose the cold oxidizer and pressurant tanks to prevent frost from forming on these tanks prior to launch.

All tanks are enclosed by secondary tank walls at about 1-inch (2.54 cm) interwall spacing. The outer container serves

a) As a safety measure against spillage of propellants (especially fluorine) into the Shuttle cargo bay, or at the launch site, in the event of a leak and

b) —To provide additional shielding against meteoroid impact.

This will be more fully discussed in Section 5. Neither the foam layer nor the secondary wall have an appreciable effect on the radiation characteristics of the cryogenic tank to cold space.

Another safety provision (not shown in the design drawing) is the addition of propellant dump lines to permit rapid disposal of propellants either in the event of a leak while the vehicle is being carried by the Shuttle orbiter, or in preparation of a Shuttle abort due to other reasons.

The teardrop shape of the propellant tanks was adopted as a design feature that provides passive, bladder-free propellant acquisition. This saves weight and increases system reliability. As a result of centrifugal action the propellant is always located in a tank region that is adjacent to and includes the conical outlet, regardless of the state of propellant depletion, with or without axial thrust (Figure 4-10). Thus, the teardrop tank design assures gas-free propellant acquisition in any mission phase. It also facilitates complete propellant drainage if required while on the launch stand.

In addition, the teardrop tank tends to reduce propellant sloshing and increases wobble damping in the fully deployed spacecraft configuration.

4.4.3 Sun Shade Design and Operation

The Mercury orbiter must always be oriented with its spin axis perpendicular to the sun line as required by the payload spacecraft design. The concept of a spin-deployed cylindrical sun shade for the propulsion module featured in the selected configuration of Module A is

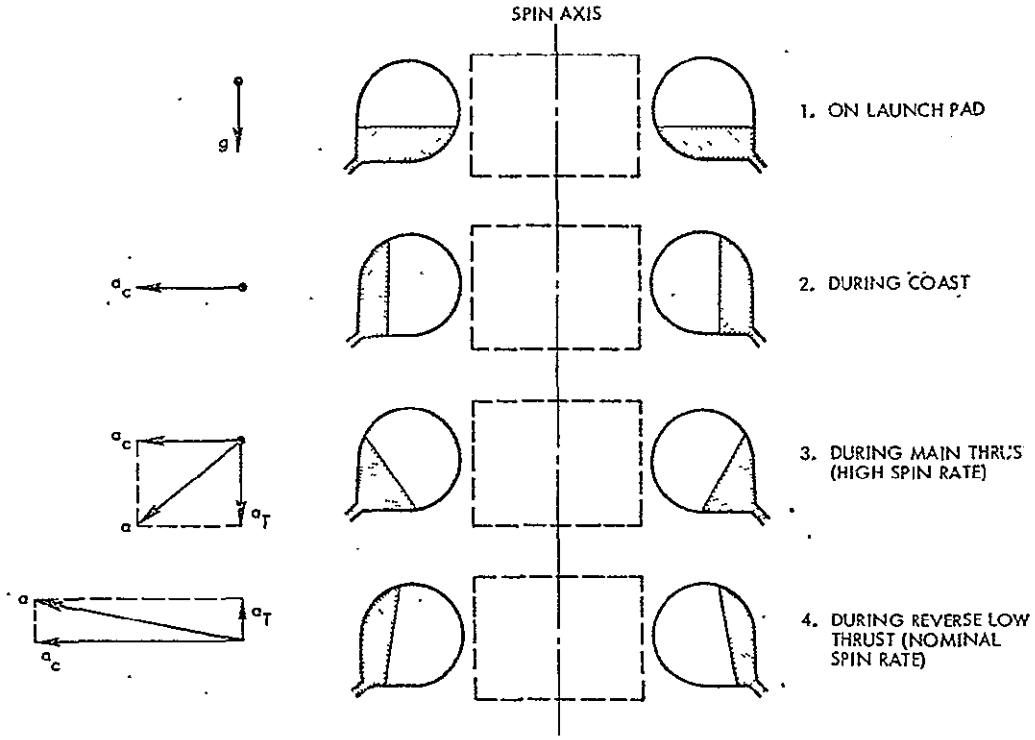

Figure 4-10. Passive Propellant Expulsion with Teardrop Tanks, Module A

illustrated in Figure 4-11. The sun shade consists of a thin sheet of Beta cloth dispensed in window-shade fashion from four roll-up mandrels. Initially, i.e., in the stowed configuration, the shade is

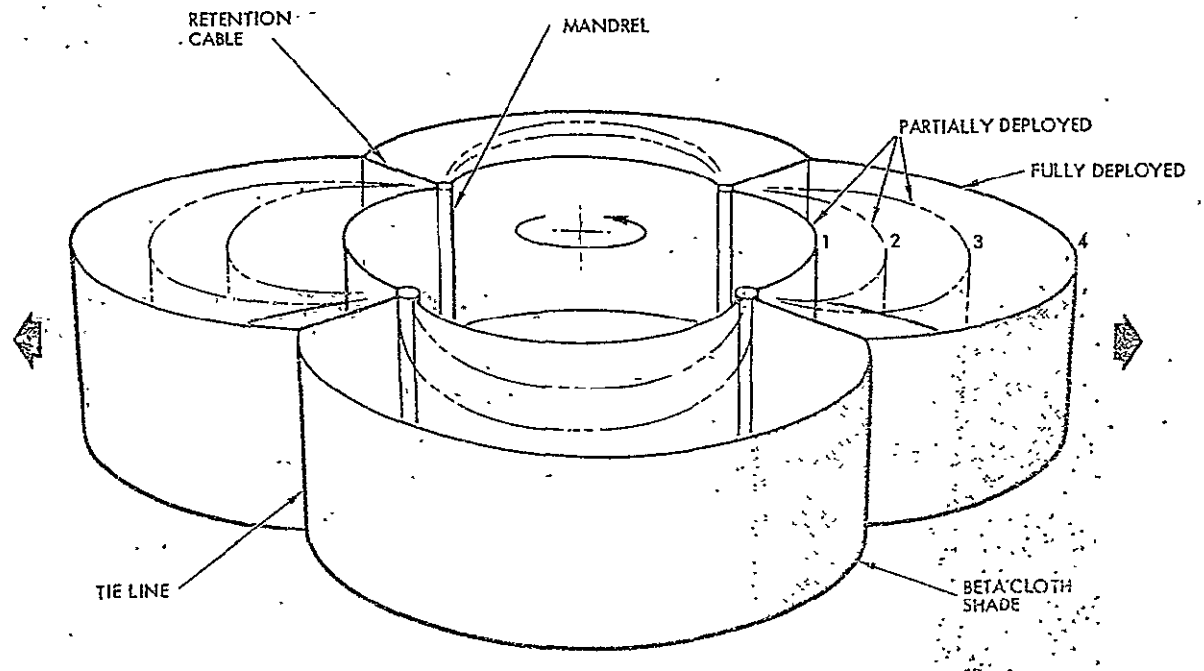

Figure 4-11. Deployment Sequence of Cylindrical Sun Shade

tightly wrapped around the tandem-mounted two propulsion modules, supported by the roll-up mandrels and the propellant tanks. Deployment in radial direction takes place under centrifugal action as soon as the motor-driven roll-up mandrels begin to release the stowed sheet. When fully deployed the sheet assumes a nearly circular cylindrical configuration, held in at four locations by the support arms and a web of lanyards, or cables, extending radially from the roll-up mandrels. This is shown in the design drawing (Figure 4-12) in side and end views.

The deployed sun shade, in addition to shielding the propulsion module fully against solar illumination also provides at least partial protection of the cold tanks against the infrared heat flux from Mercury during passes over the day side. Appreciable temperature increases of the LF_2 tanks due to unshielded residual heat flux can be avoided by appropriate choice of orbit orientation and closest approach distances in view of the very short exposure time during each Mercury dayside passage (see Section 6).

The large deployed sun shade shown in the drawing with maximum dimensions of 34 feet (10.4 m), is based on the thermal radiation requirement of the upper propulsion module's cold tanks. Since the cylindrical height of the shade is 95 inches (242 cm) to assure full side-sun protection the presence of the shade accounts for a major part of the radiation field-of-view blockage, hence the large diameter. Even this size allows only a 25 to 30 percent viewing factor for the cold tanks, the lowest values consistent with thermal balance at the upper limit of the specified cryogenic temperature range (-250°F) for liquid fluorine.

A more attractive, smaller deployed diameter of about 25 feet (7.6 m) could probably be achieved by reducing the propulsion module height, e.g., by shortening the engine assembly as will be discussed in Section 5. A shorter stack height reduces the height of the sun shade, which in turn permits shade diameter reduction in about the same proportion. To improve the design this and other possibilities of size reduction will be further investigated below.

The design drawing (Figure 5-12) also shows the much smaller deployed sun shade appropriate for the earth-storable propellant version of Module A. The maximum diameter is only 21.6 feet (6.6 m) in this

case since thermal radiation blockage from the propellant tanks is of no concern. Sun shade deployment is simplified by eliminating the web of retention cables and two of the roll-up mandrels. The sheet is held by four radial supports, as in the case of the space-storable version of Module A, but two of these are fixed attachment booms in the earth-storable system.

In both the space-storable and earth-storable versions of Module A the sun shade must be retracted to the stowed position before executing main thrust maneuvers, since the deployed sheet would not be rigid enough to withstand the axial thrust acceleration, even at increased spin rate. Therefore high reliability of the repeated deployment and retraction sequences required with each main thrust application is absolutely essential for mission success. This is a potential weakness of the design.

Low-thrust ΔV maneuvers and precession maneuvers can be executed with the sun shade remaining in the deployed configuration. The precession maneuvers must be performed at a sufficiently slow rate to avoid excessive sun shade deformation, especially with the large diameter configuration used in the case of space-storable propellants.

The dynamics of the sun shade deployment, stability and attitude control characteristics will be further discussed in Appendix G.

A promising design alternative in which heat pipes are used for thermal control of the cryogenic tanks was conceived toward the end of this study (see Section 6). With this design approach a much smaller sun shade diameter would be adequate for thermal protection of the module, and deployment and operation would become much simpler. Further study of this concept is recommended.

4.4.4 Module A Configuration for Outer Planet Orbiters

Figure 4-13 shows the outer-planet orbiter application of Module A with space-storable propellants. The payload is the Pioneer 10/11 class outer-planets spacecraft. The Shuttle/upper stage combination assumed here for a Saturn orbiter mission is the Centaur D-1S/SPM (1800). SPM (1800) is the designation of a currently proposed new kick motor with 1800 kg (3969 pounds) of solid propellant mass and motor case.

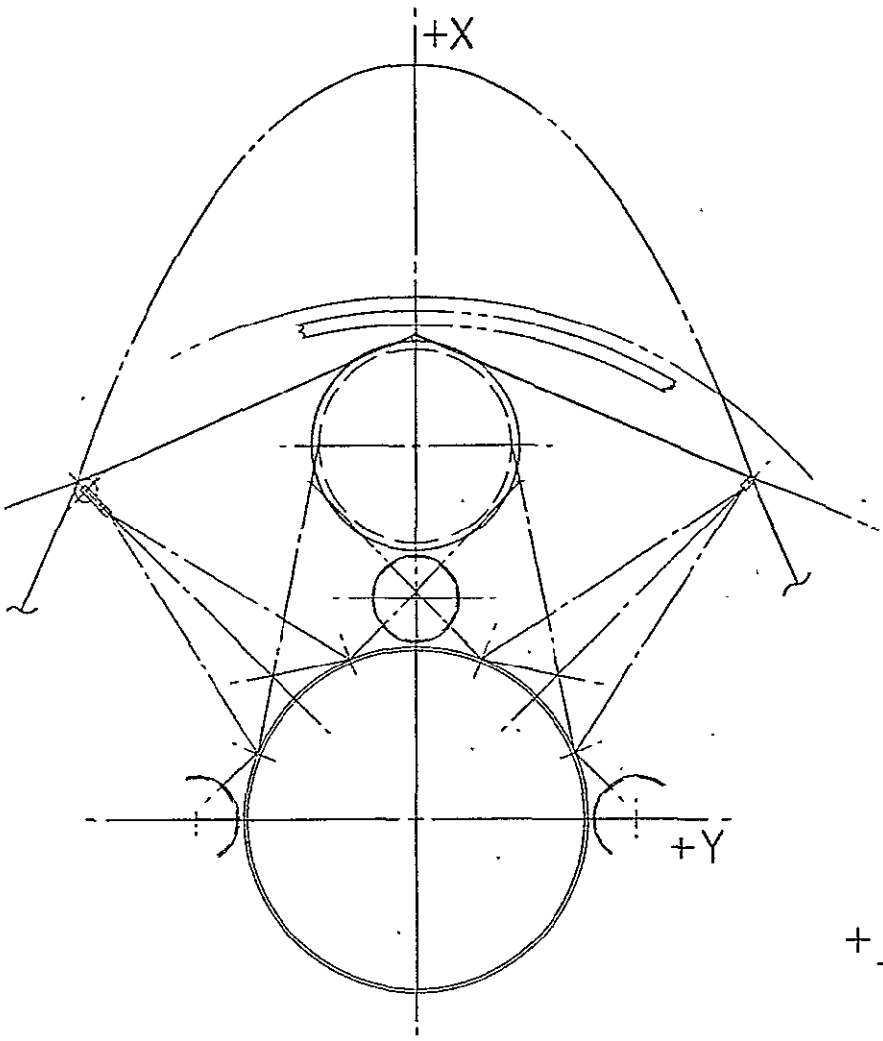

LOOKING AFT

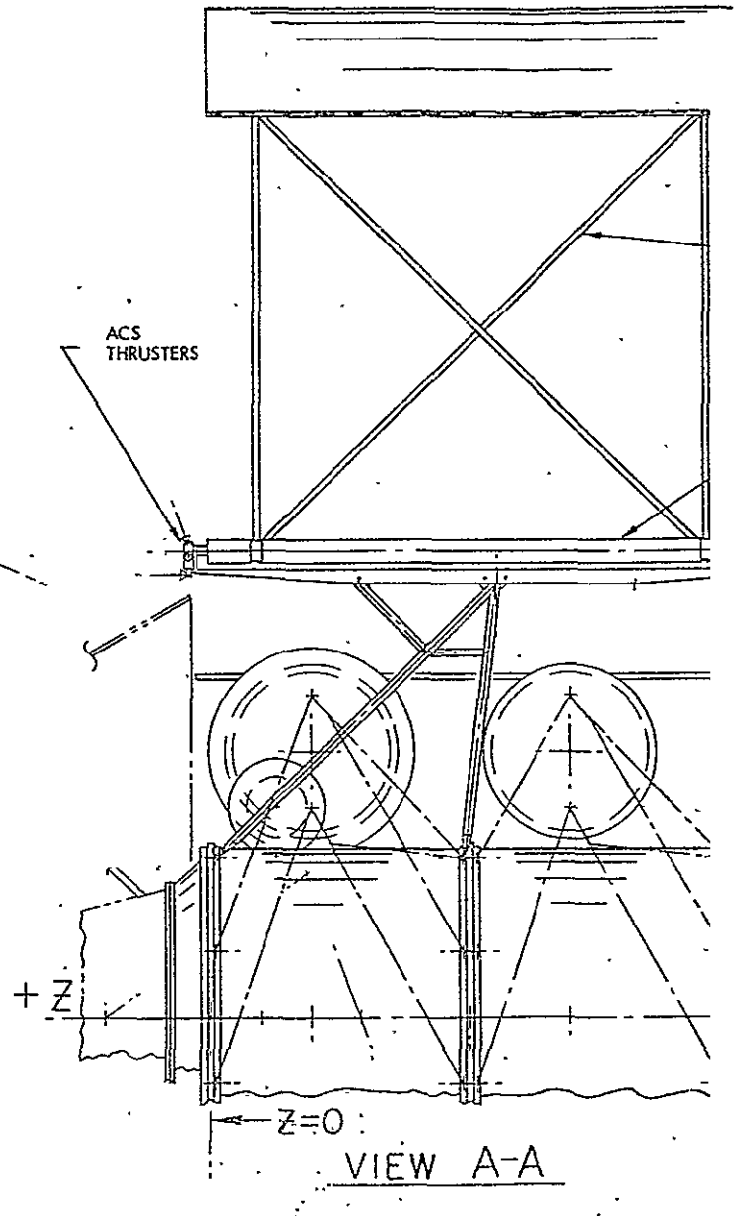

VIEW A-A

EARTH-STORABLE PROPELLANT CONFIGURATION

FOLDOUT FRAME

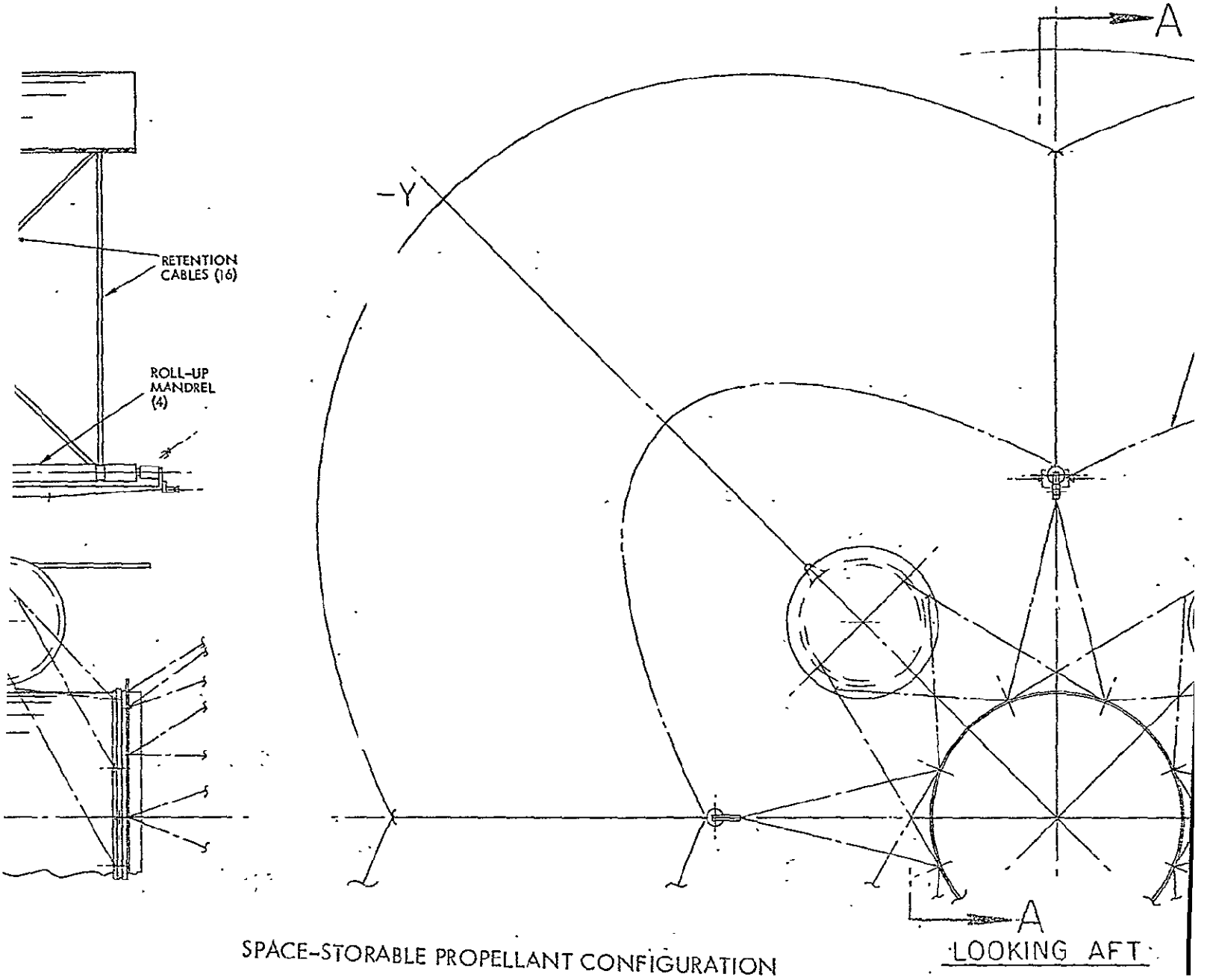

SPACE-STORABLE PROPELLANT CONFIGURATION

LOOKING AFT

FOLDOUT FRAME 2

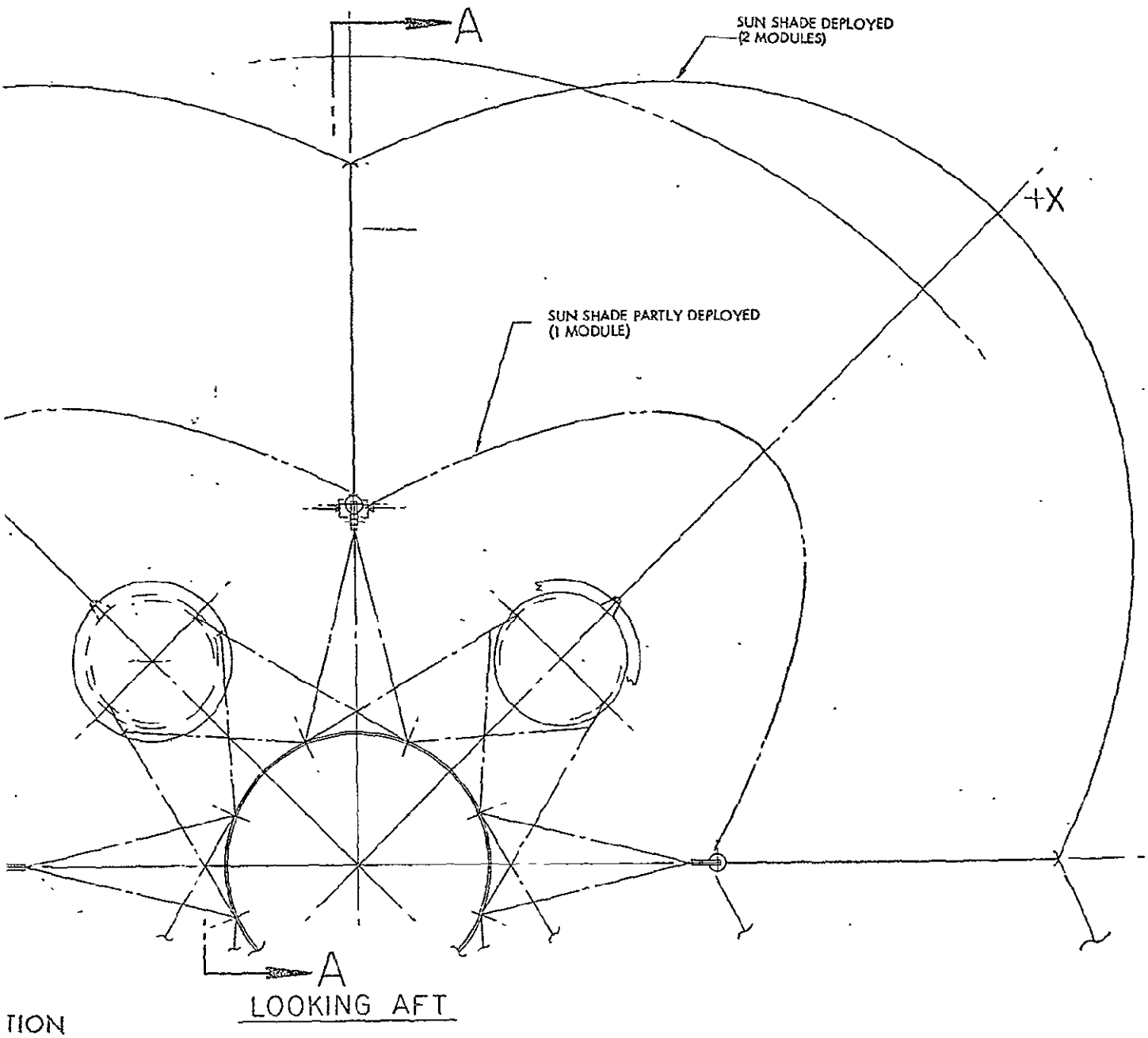

TION

Figure 4-12. Pioneer Mercury Orbiter, Deployed Sun Shade

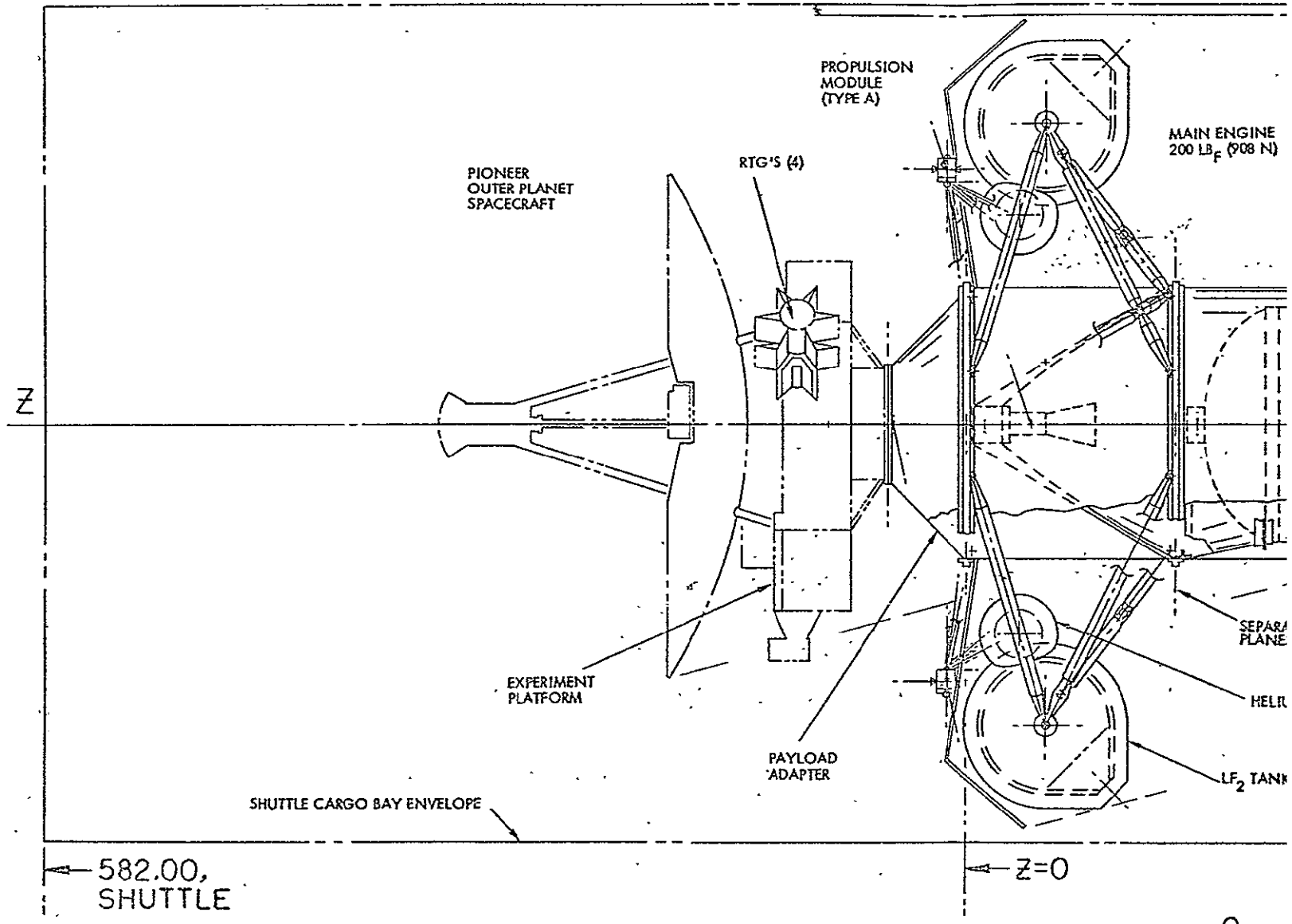

Figure 4-13. Propulsion Module A Configuration for Pioneer Outer Planet Orbiter

FOLDOUT FRAME 4

FOLDOUT FRAME 5

PROPELLANTS

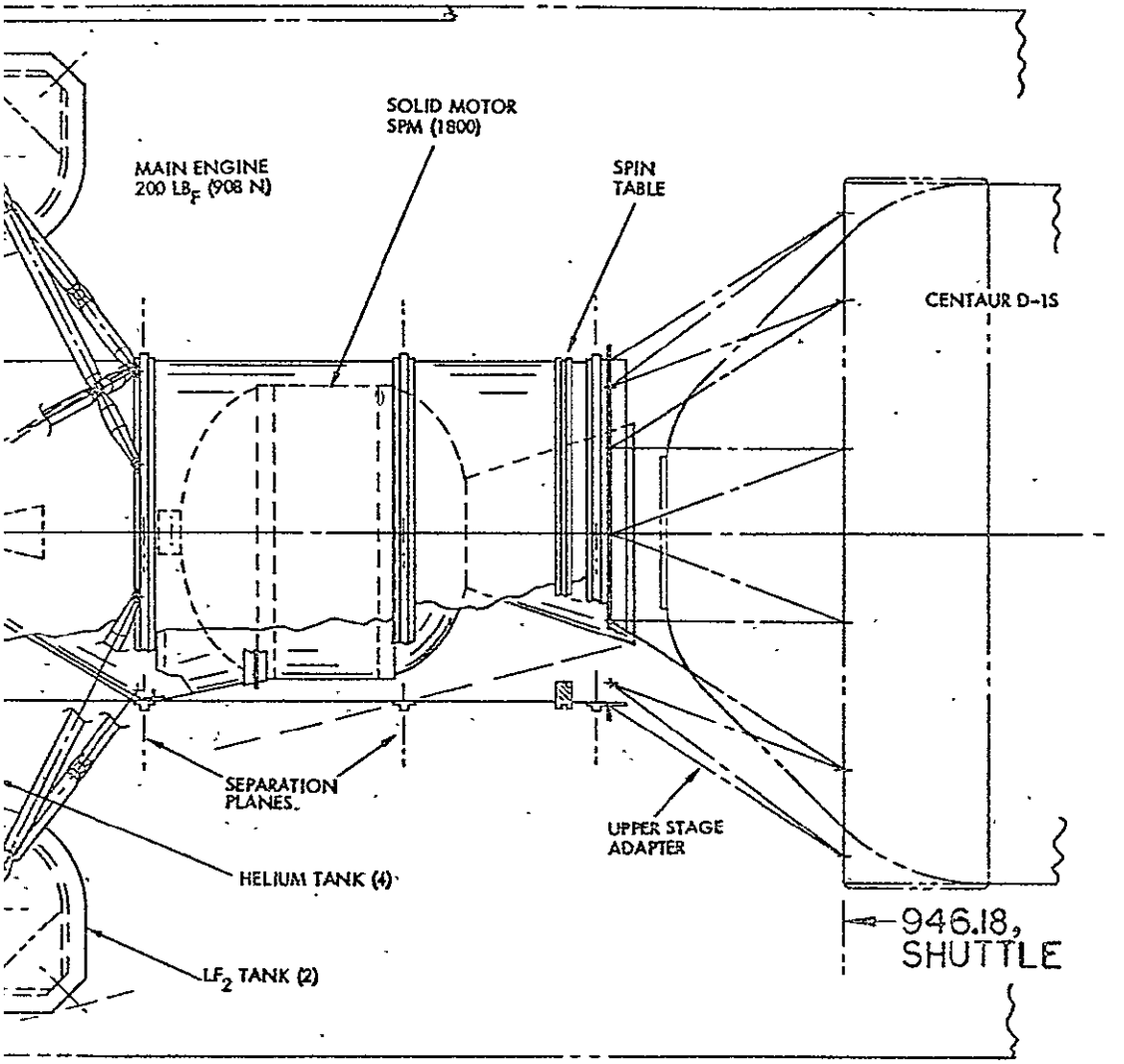

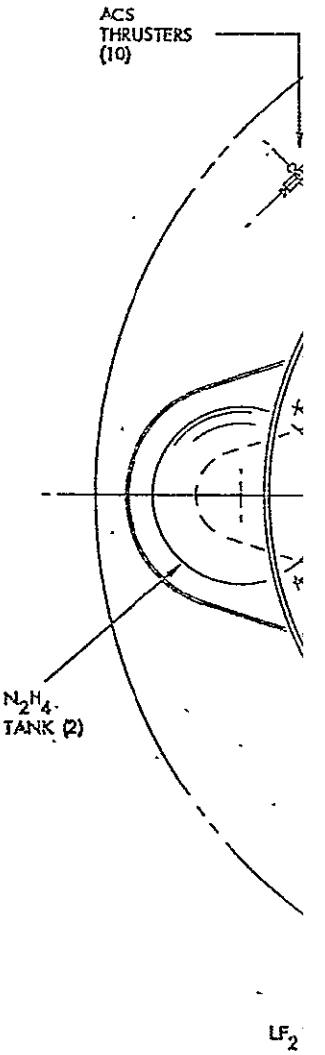

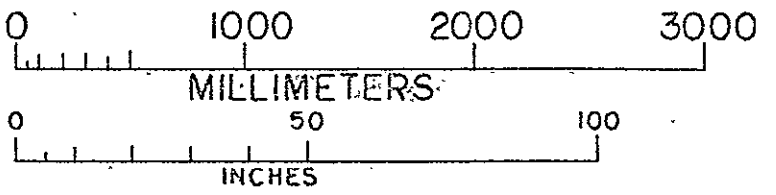

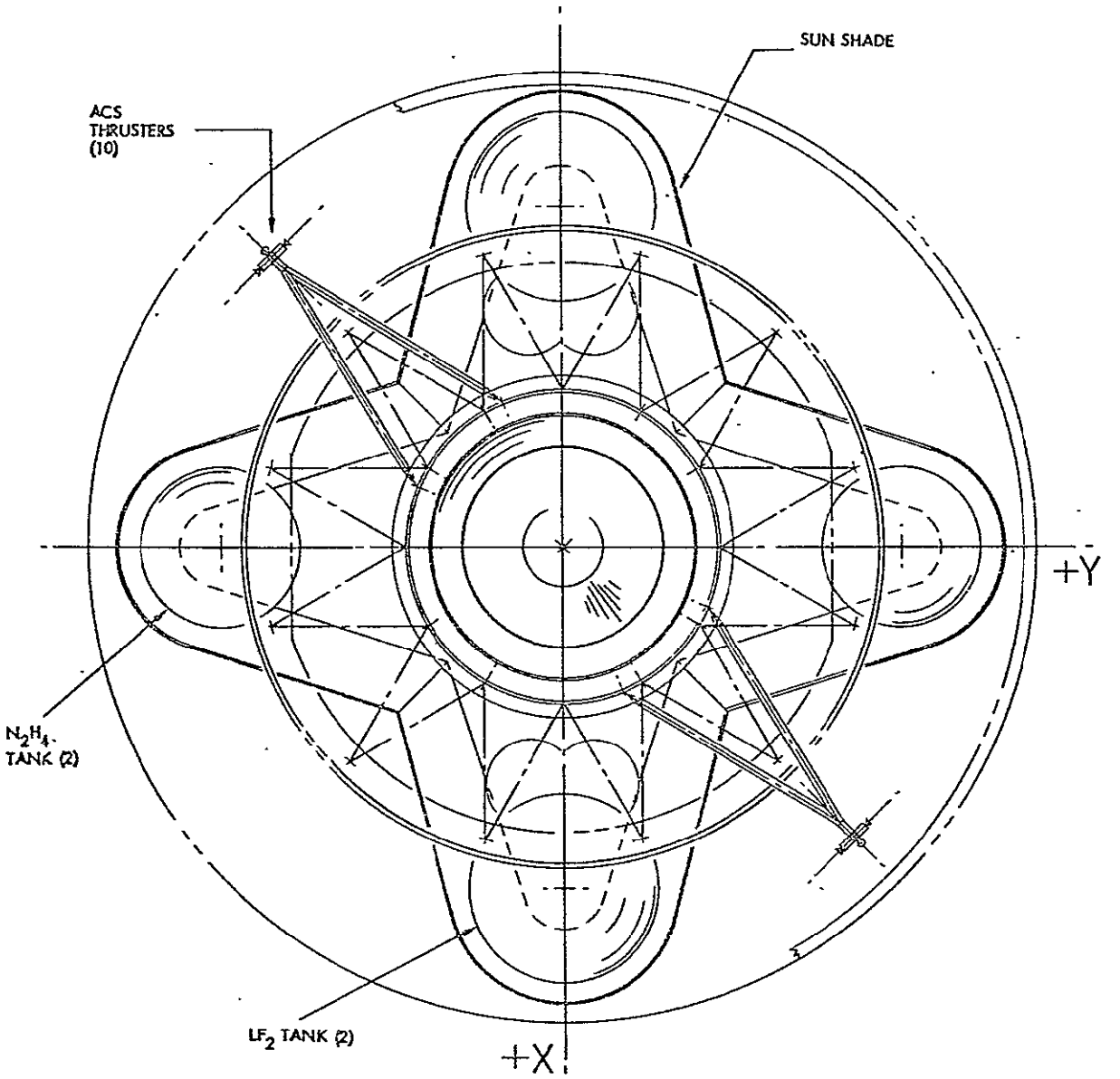

LOOKING FWD.

FOLDOUT FRAME 6

An interstage adapter truss supports the kick motor and the flight spacecraft on the 10-foot (3.05-m) Centaur interface mounting ring. A spin table is provided to spin up the kick motor and payload prior to separation from Centaur. The higher performance Space Tug/solid kick motor combination would be required for Uranus orbiter missions. The adapter truss design in that case is the same as for the Mercury orbiter, but with an added spin table.

The propulsion module is structurally identical to the tandem version used for the Mercury orbiter but requires the following modification of components:

- Replacement of the 800-lb_f (3560-Newton) main engine by the smaller 200-lb_f (890-Newton) unit, as necessitated by the lower structural load tolerance of deployed appendages (RTG support arms and magnetometer boom).
- Addition of a four-leaf sun shade extending beyond the high-gain antenna diameter, parallel to the X-Y plane, to protect the propellant tanks against solar heating.
- Omission of the sun shade and roll-up mandrels and two of four support arms. The two remaining support arms with their upper and lower mounting fixtures reversed are used to support two auxiliary thruster assemblies.
- The thruster assemblies (five thrusters on each arm: two fore/aft, two spin/despin and one radial thruster) are modified from the configuration used on the Mercury orbiter to conform with the modified support structure and to match the different center-of-mass locations.

Spacecraft operation is constrained to avoid prolonged side-sun illumination of the propellant tanks at angles greater than 15 degrees from the Z axis, because of limited sun shade coverage. During some time intervals occurring twice in the early transfer phase the earth-spacecraft-sun angle exceeds 15 degrees. As a compromise dictated by propellant-tank thermal control requirements, downlink communication via the high-gain antenna is interrupted during these periods but can be maintained either via the low-gain or medium-gain antennas since communication distance is still reasonably small. High bit rate telemetry is generally not required during these periods in any case.

Enlargement of the sun shades to cover a greater range of side-sun angles and, thereby, to reduce the constraint on communications coverage, is hindered by Shuttle cargo bay size limitation. An extension of the sun shade by deployable skirts would be feasible if further study should establish a firm requirement.

4.4.5 Mass Properties of Module A

Tables 4-5 and 4-6 list mass-property characteristics of Module A for space-storable and earth-storable propulsion systems, respectively. The upper half of each table gives data for the tandem arrangement of propulsion modules in the Mercury orbit mission with the Pioneer Venus spacecraft as payload. The lower half gives corresponding data for the single stage application in outer planet orbit missions, with the Pioneer outer-planet spacecraft as payload.*

Full propellant tanks were assumed in the outer-planet application, although actually because of limited earth launch-vehicle capabilities some of the propellant would probably be off-loaded or used during launch to augment injection energy.

Mass properties of the payload vehicles assumed in the analysis are those specified by NASA at the beginning of the study. They do not necessarily represent the most up-to-date values for each vehicle. Weight and mass-distribution estimates for the propulsion modules are based on values derived from structural analysis (see Appendix C). Subsequent performance iterations of each vehicle (to be presented in Section 7) give some reduction of propulsion module inert and propellant masses that are not reflected in Tables 4-5 and 4-6.

The results show that both the space-storable and earth-storable versions of Module A satisfy the principal spin-stability criteria in single stage and tandem stage arrangements, namely:

a) For short-term stability in the initial (stowed) configuration the moment-of-inertia ratios I_z/I_x and I_z/I_y must both be either greater or smaller than 1.0.

*Weight summaries of Modules A and B will be presented separately, see Section 4.9.

Table 4-5. Module A — Space-Storable Propellant Configuration Mass-Properties Characteristics

Condition	Weight (lb)	$\bar{Z}$[1] (in.)	Moment of Inertia (slug-ft^2)			Inertia Ratio		
			I_x	I_y	I_z (Spin)	I_z/I_x	I_z/I_y	$2I_z/I_x+I_y$
Module A - Inbound Configuration[2]								
At separation - stowed	4182	-26.1	2733	2743	2937	1.07	1.07	1.07
At separation - deployed	4182	-26.1	2911	2904	3265	1.12	1.12	1.12
At first module burnout - deployed	2836	-8.8	1629	1840	2056	1.26	1.12	1.19
At second module ignition - deployed	2490	-1.2	1305	1524	1945	1.49	1.28	1.38
At second module burnout - deployed	1144	18.1	640	642	736	1.15	1.15	1.15
Separated spacecraft - deployed[3]	750	39.0	175	168	265	1.51	1.58	1.55
Module A - Outbound Configuration								
At separation - stowed	7050	-49.8	3051	3243	1478	0.48	0.46	0.47
At solid stage burnout - stowed	3050	-14.1	1359	1550	1262	0.93	0.81	0.88
After solid stage jettison - stowed	2600	-4.0	903	1095	1199	1.33	1.09	1.20
At liquid module ignition - deployed	2600	-4.0	1211	1560	1973	1.63	1.26	1.43
At liquid module burnout - deployed	1254	15.9	624	807	1045	1.67	1.29	1.46
Separated spacecraft - deployed[4]	900	30.0	430	605	946	2.20	1.56	1.83

Notes:

[1] Longitudinal center of mass ($\bar{Z}$) referenced from the spacecraft/propulsion module separation plane. Minus values are below the reference plane; positive values are above this plane.

[2] To minimize large differences in the transverse inertias (I_x, I_y), the fuel and oxidizer tanks in the first module are rotated 90 degrees relative to the fuel and oxidizer tanks in the second module.

[3] Pioneer Venus configuration.

[4] Pioneer 10/11 modified for outer planet missions.

Table 4-6. Module A – Earth-Storable Propellant Configuration Mass-Property Characteristics

Condition	Weight (lb)	$\bar{Z}^1$ (in.)	Moment of Inertia (slug-ft^2)			Inertia Ratio		
			I_x	I_y	I_z (Spin)	I_z/I_x	I_z/I_y	$2I_z/I_x+I_y$
Module A - Inbound Configuration[2]								
At separation - stowed	6900	31.4	4281	4290	5295	1.24	1.24	1.24
At separation - deployed	6900	31.4	4383	4376	5478	1.25	1.25	1.25
At first module burnout - deployed	4350	13.2	2100	2681	3188	1.52	1.19	1.33
At second module ignition - deployed	3850	6.8	1679	2276	2977	1.77	1.31	1.51
At second module burnout - deployed	1300	-14.2	642	651	687	1.07	1.06	1.06
Separated spacecraft - deployed[3]	750	-39.0	171	164	261	1.53	1.59	1.56
Module A - Outbound Configuration								
At separation - stowed	8400	43.6	3913	4533	2952	0.75	0.65	0.70
At solid motor burnout - stowed	4400	13.3	1862	2481	2736	1.47	1.10	1.26[4]
After solid module jettison - stowed	3960	6.7	1424	2044	2675	1.88	1.31	1.54
At liquid module ignition - deployed	3960	6.7	1732	2510	3449	1.99	1.37	1.63
At liquid module burnout - deployed	1410	-12.9	700	891	1159	1.66	1.30	1.46
Separated spacecraft - deployed[5]	900	-30.0	430	605	946	2.20	1.56	1.83

Notes:

[1] Longitudinal center of mass ($\bar{Z}$) referenced from the spacecraft/propulsion module separation plane. Minus values are below the reference plane; positive values are above the plane.

[2] To minimize large differences in the transverse inertias (I_x, I_y), the fuel and oxidizer tanks in the first module are rotated 90 degrees relative to the fuel and oxidizer tanks in the second module.

[3] Assumes a spin-stabilized Pioneer Venus configuration

[4] Will require attitude control and dynamic analysis since inertia ratio goes from <1.0 to >1.0 during solid burn.

[5] Pioneer 10/11 modified for outer planet missions.

b) For long-term stability in the deployed configuration these ratios must be greater than 1.0 in all stages of propellant depletion. In general, the ratio should be at least 1.1 to provide a 10 percent margin for small distribution changes in flight and other uncertainties.

To achieve these results several changes in propellant tank location became necessary during the propellant module design iteration. The final configurations are those shown in the design drawings, Figures 4-9, 4-12, and 4-13. The tanks are placed as far from the spin axis as possible within the diameter constraints of the Shuttle cargo bay allowing space for a payload shroud (see Section 4.8), and as high on the module in the Z direction as possible without interfering with payload vehicle design features.

To minimize differences in the transverse moments of inertia (I_x, I_y) due to the difference in oxidizer and fuel mass the two modules mounted in tandem for the Mercury mission must be rotated relative to each other so that the fuel tanks of the upper module are stacked above the oxidizer tanks of the lower module, and vice versa. Adverse thermal control consequences due to the proximity of cryogenic and non-cryogenic propellant tanks in the space-storable case must be prevented by adding more thermal insulation to the fuel tank covers. With the nearly equal I_x and I_y values that can be achieved in this manner, dynamically unstable conditions during which one of the moment-of-inertia ratios (I_z/I_x) is greater than 1 and the other one (I_z/I_y) less than 1, or vice versa, can be circumvented.

Transition from the stowed to the deployed configuration can generally not be accomplished without passing briefly through an unstable condition, with $I_z/I_x > 1$ and $I_z/I_y < 1$, or vice versa. Transients occurring during the transition phase, including the effects of the despin thrust maneuver and appendage deployment, and the destabilizing effects on mass distribution of non-rigid appendages require further analysis.

Further mass distribution improvements are possible by reduction of the propulsion module height. This would permit reduction of lateral dimensions at least in a 1:1 ratio. It would also reduce the total center-of-mass shift along the Z axis which amounts to almost 4 feet (1.2 m) in

the tandem configuration assuming that the second propulsion module is retained. Reduction of center-of-mass shift simplifies auxiliary thrust requirements.

A shorter propulsion module height would also be desirable to reduce the inert mass (the reduction factor is about 5 pounds per inch, or 0.89 kg per cm per module) and to decrease the size of the deployed sun shade. A principal factor in adopting the height of 45 inches (114.3 cm) was the length of the 800-lb_f thruster assembly. A side-mounted engine valve assembly and a possible shortening of nozzle length (at some reduction of engine performance) are being contemplated as options for further design tradeoffs.

4.4.6 Arrangement of Auxiliary Propulsion Thrusters

In the selected design the auxiliary small thrusters required for precession control, spin rate control and small ΔV maneuvers are relocated from the payload spacecraft and placed on the propulsion module, using two support trusses attached on opposite sides of the central cylinder, as illustrated schematically in Figure 4-14. Five thrusters are mounted on each support arm:

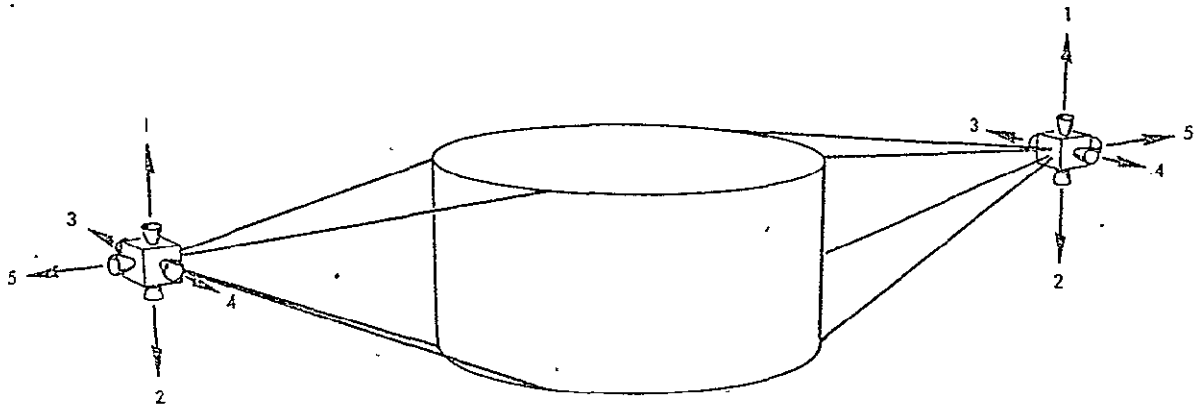

1, 2 PRECESSION CONTROL AND FORE/AFT ΔV CONTROL
3, 4 SPIN/DESPIN AND REDUNDANT LATERAL ΔV CONTROL
5 PULSED LATERAL ΔV CONTROL (CANTED FOR CM - SHIFT COMPENSATION)

Figure 4-14. Schematic of Auxiliary Thrusters on Module A

- A pair of thrusters for precession control and fore-aft ΔV maneuvers
- A pair of thrusters for spin/despin maneuvers, and
- One radial thruster for lateral maneuvers, operating in the pulsed mode.

Compared with the complement of six auxiliary thrusters on Pioneer 10/11 this configuration adds

a) Redundant spin/despin thrusters, necessitated by the greatly extended mission life and frequent spin rate changes

b) Redundant radial thrusters for lateral ΔV maneuvers. Use of these thrusters or pairs of spin/despin control thrusters for lateral maneuvers obviates spacecraft reorientation from the nominal earth-pointing position, and thus permits uninterrupted downlink communication to earth.

Placement of the auxiliary thrusters on the propulsion module rather than the payload spacecraft permits reduction or elimination of cross-coupling effects in the radial thrust mode caused by a large center-of-mass offset along the Z axis and thus simplifies the maneuver sequence. Performance penalties associated with cross-coupling compensation maneuvers in the case of large center-of-mass offsets are also being avoided by this thruster relocation.

The locations and thrust axes of the radial thrusters are selected such that their lines of force bracket the total range of center-of-mass locations along the Z-axis. This is illustrated in Figure 4-15. The thrusters are controlled to operate with differential pulse lengths in accordance with the predicted mass-center location so that the resultant net thrust force per spacecraft revolution always passes through the mass center and unwanted precession torques are cancelled. This technique is similar to one used in TRW's Pioneer Jupiter Orbiter/Probe spacecraft design (Reference 7) to meet the radial thrust vector alignment problem associated with center-of-mass shifts due to propellant depletion and entry probe separation. In the present design the lateral thrust is generally not purely radial but is oriented at a cant angle that varies with the state of propellant depletion, as a function of time.

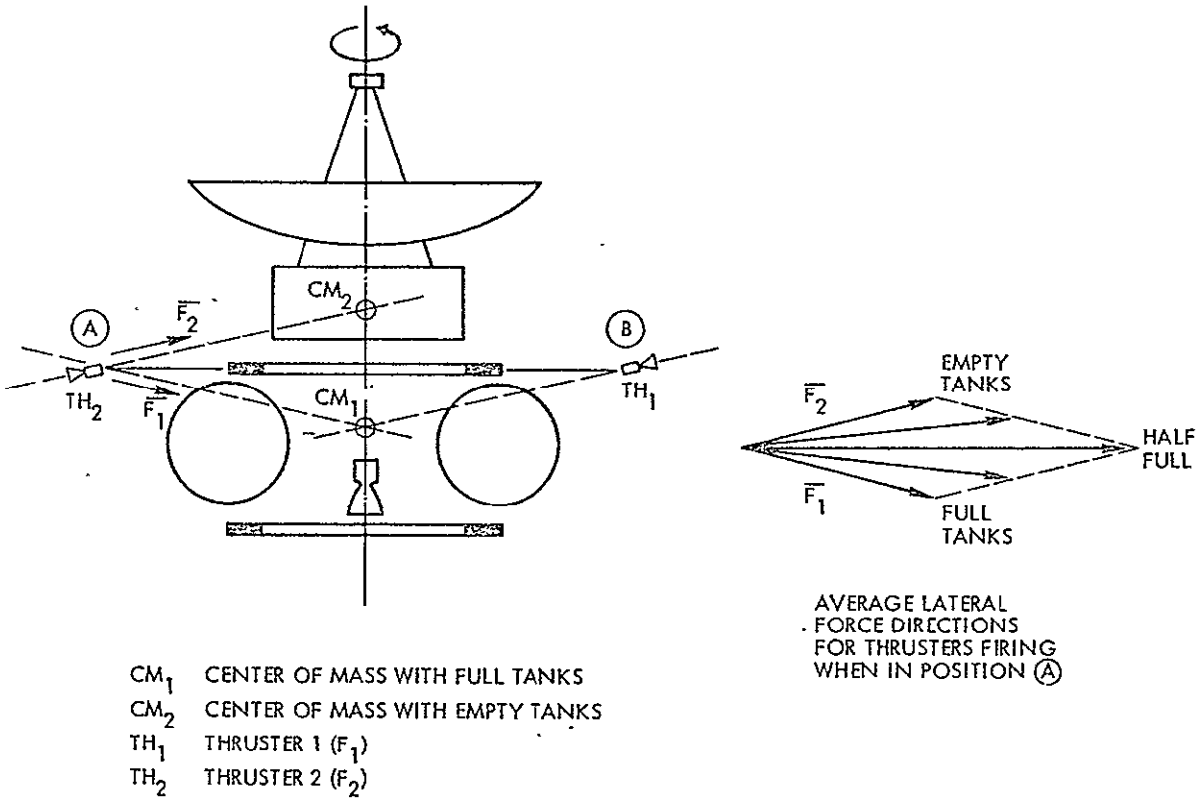

Figure 4-15. Pulsed Lateral Thrust with Center-of-Mass-Shift Compensation

As shown in the design drawings for the Mercury and outer planet orbiter propulsion module configurations (Figures 4-9 and 4-13) the radial thrusters are canted to meet the thrust offset cancellation objective. In the Mercury orbiter configuration the auxiliary thrusters are placed at the upper and lower ends of two of the sun shade deployment mandrels at opposite sides of the propulsion module. In the outer-planet orbiters, the thrusters are placed at the end of two support arms which are attached to the central cylinder. The support arms are identical to those used for the sun shade deployment mandrels, but with their upper and lower ends reversed.

The auxiliary thrusters on the space-storable propulsion module use monopropellant hydrazine making use of the module's spare fuel tank capacity as explained in Section 5. These thrusters are of the 1-lb_f (4.45-Newton) type flown on Pioneer 10 and 11. The earth-storable

system uses the larger (2- to 5-lb_f, 8.9 - to 22.3-Newton) AJ10 bipropellant thrusters being currently developed by Aerojet under a USAF contract. (See also Table 4-4.)

4.5 SELECTED DESIGN FOR MODULE B (THREE-AXIS STABILIZED SPACECRAFT)

4.5.1 Configuration for Mercury Orbiter

Figure 4-16 shows the selected space-storable propulsion module design for three-axis stabilized payloads (Module B) arranged in tandem for the Mercury orbiter mission. The side view shows the stowed configuration in the Shuttle cargo bay, attached to the projected Space Tug. A solid kick motor is not needed for this mission. The end view is shown on the right.

The payload is the Mariner 10 Venus Mercury flyby spacecraft (MVM) which was launched in 1973 and performed three successful close Mercury encounters in 1974/75 separated by 176-day intervals. Like the Mercury orbiter, the MVM spacecraft is designed for closest solar-approach distances of 0.31 AU, i.e., Mercury's perihelion. Several small design changes of the payload spacecraft had to be adopted to accommodate the propulsion module. Primarily, these changes are related to the spacecraft orientation mode which requires that the thrust vector and, hence, the spacecraft centerline (Z axis), be pointed perpendicular to the sun line. The frontal sun shade used by MVM is not compatible with the required thrust orientation during the Mercury orbit insertion maneuver and other major maneuvers; a side sun shade is used instead. As a consequence, the side-sun orientation is maintained in cruise as well as in the thrust phases.

During the cruise phase the axis of the solar array (spacecraft Y axis) is normal to the plane of motion. The articulated high-gain antenna therefore has an unobstructed view of earth most of the time. The nominal cruise orientation is resumed after the orbit insertion maneuver. Spacecraft, thrust vector, solar array and antenna pointing requirements will be discussed in greater detail in Section 4.6.

The propulsion module configuration is quite similar to that of Module A, using a hybrid structure consisting of a central cylinder and

lateral tank support trusses. Although lateral spreading of the propellant tanks, required in Module A for proper mass distribution, is not a consideration in Module B, the arrangement is nevertheless preferable for effective load transfer from vehicles placed above the propulsion module to those below, in addition to handling loads contributed by the propellant tanks that form part of the module. The multi-mission commonality requirement and the application of the module in single and tandem stage arrangements are additional factors to make this configuration the preferred design.

The choice of four spherical tanks was previously discussed as preferable to make the tank diameters and, thus, the module height as small as possible. As in Module A, each propellant tank support truss is attached to the tank at two lateral mounting bosses for efficient tank-to-truss load transfer. The dimensions (length and tube wall thickness) of the struts assure effective isolation of the cryogenic LF_2 tanks from the warm N_2H_4 tanks.

The main struts and diagonal stabilizers are attached to the reinforcement rings at the upper and lower ends of the support cylinder. These rings distribute the discrete truss loads evenly into the cylindrical shell and across the separation joints.

The double-gimballed 800-lb_f (3560-Newton) main thrust engine is mounted inside the central cylinder, enclosed by a radiation reflector and supported by a thrust cone of 45-degree half angle. The cone is attached to the support cylinder along a reinforcement ring half-way between the two separation rings that close off the cylinder at each end. The large 800-lb_f engine is the one selected for the Mercury mission; a smaller one is used in the outer-planets orbiters.

Vee-band separation joints are used to connect the tandem modules to each other and to the launch vehicle adapter truss as in the design adopted for Module A.

4.5.2 Propellant and Pressurant Tanks

The same design as in Module A was adopted to attach the four helium pressurant bottles in pairs to the LF_2 tanks and provide thermal

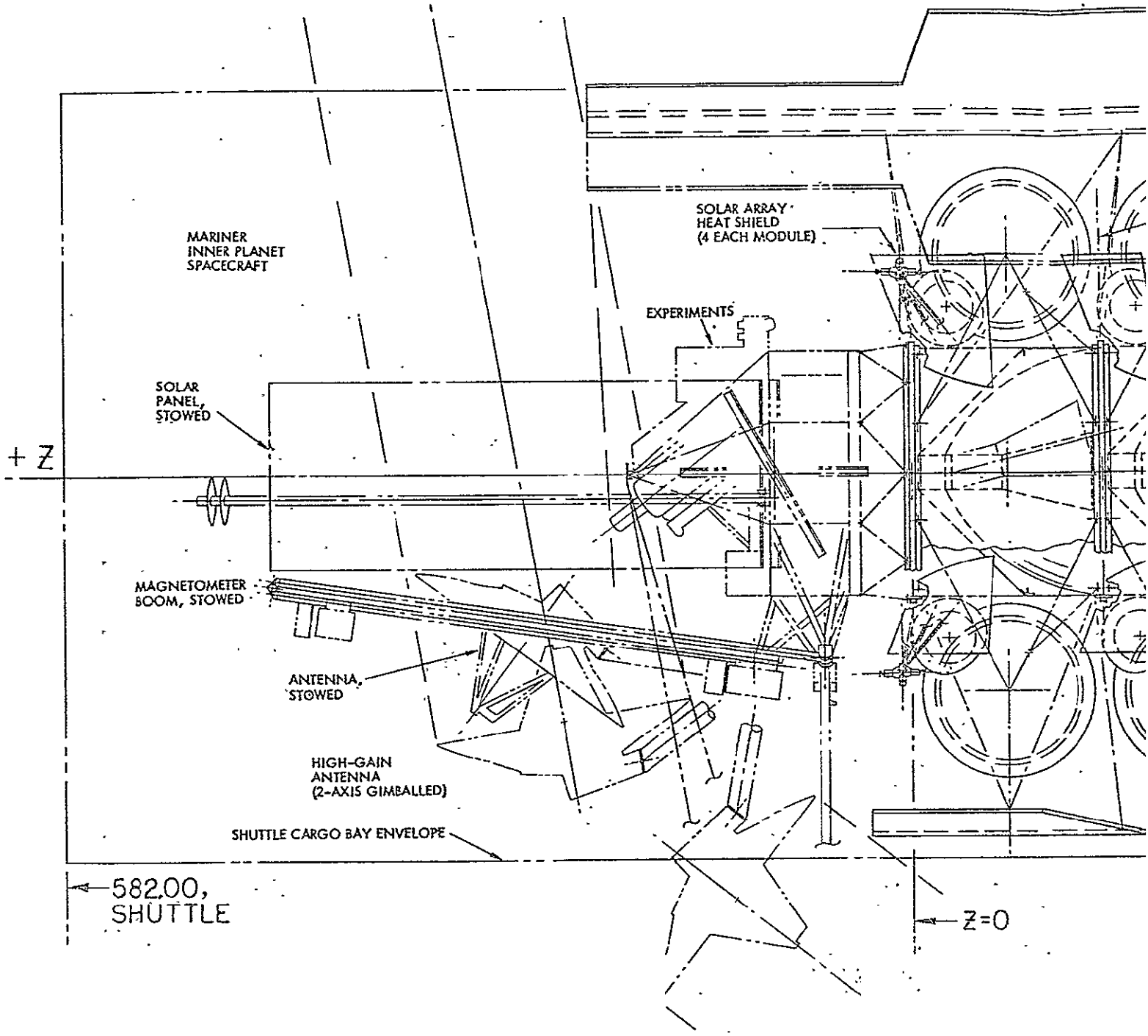

FOLDOUT FRAME 1

SPACE-STORABLE PROPELLANTS

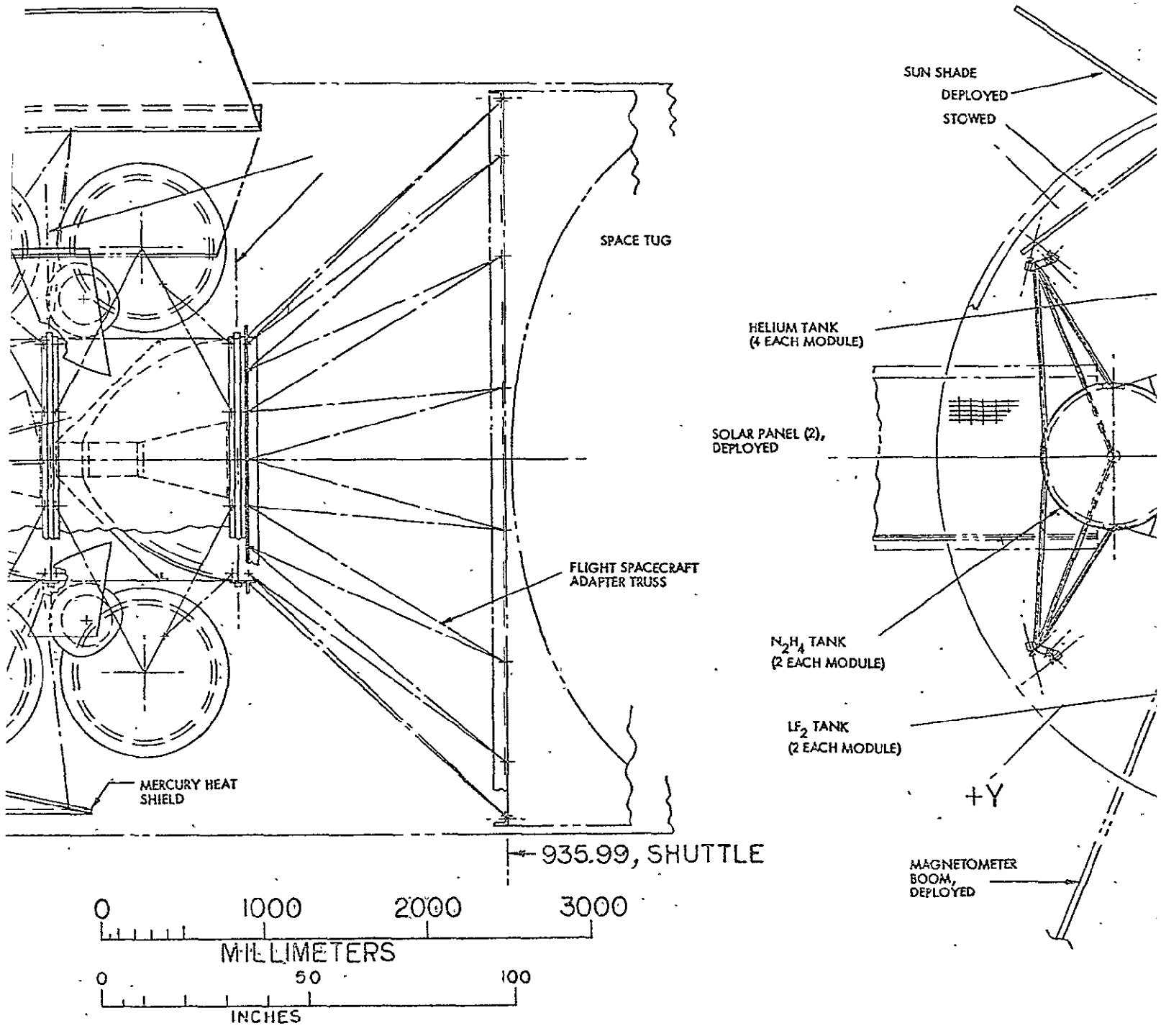

FOLDOUT FRAME 2

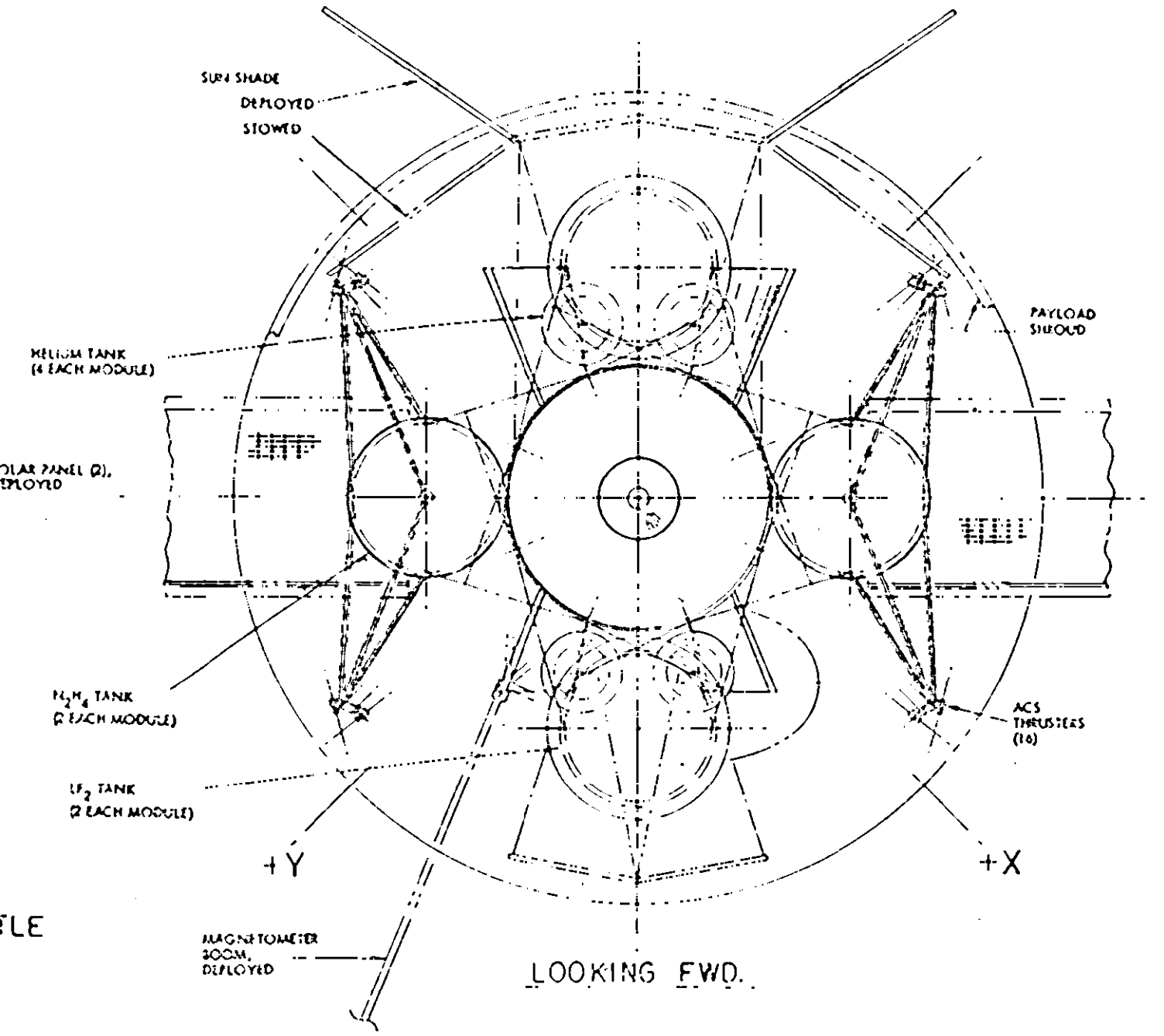

Figure 4-16. Propulsion Module B Configuration for Mariner Mercury Orbiter

FOLDOUT FRAME 3

coupling in the case of space-storable propellants. (In the earth-storable propulsion system design the four pressurant tanks are mounted individually near the propellant tanks.)

Fuel tank thermal insulation is provided by multilayer super-insulation blankets. No insulation blankets are used on the cold oxidizer tanks to permit effective radiation to the outside of heat accruing from unavoidable sources and, thus, to maintain proper thermal balance at the specified cryogenic storage temperature. Again, as in Module A, the cold tanks and nearby propulsion system components are enclosed by a foam layer to prevent frost formation during ground hold.

The tanks are enclosed by secondary walls (see Section 4.4.2) as a safety measure and for added meteoroid impact protection.

Propellant acquisition is effected passively through capillary devices in the N_2H_4 tank. This tank supplies auxiliary thrusters that are operated initially in the propellant settling mode, prior to the bipropellant engine ignition. This method is more reliable in long life missions than using positive expulsion bladders, and permits propellant acquisition for the LF_2 tanks without capillary devices (screens, etc.) thereby avoiding potential materials compatibility problems (see also Section 5).

4.5.3 Sun Shade Design

The sun shade shown in the design drawing (Figure 4-17) provides continuous protection of both the propulsion module and the payload spacecraft against side-sun exposure in the cruise and maneuver attitudes.

Shaped in the manner of a "keystone" with a narrower upper part, it leaves the solar panels unshaded provided the spacecraft Z-axis/ orientation remains nearly normal to the sun line.

Prior to launch the hinged side sections of the sun shade are stored by inward deflection to fit within the available cargo bay envelope. After launch the side sections are spring-deployed outward, by a 70-degree rotation, to increase the cold space viewing factor of the cold tanks (especially the tank of the upper propulsion module) and thus

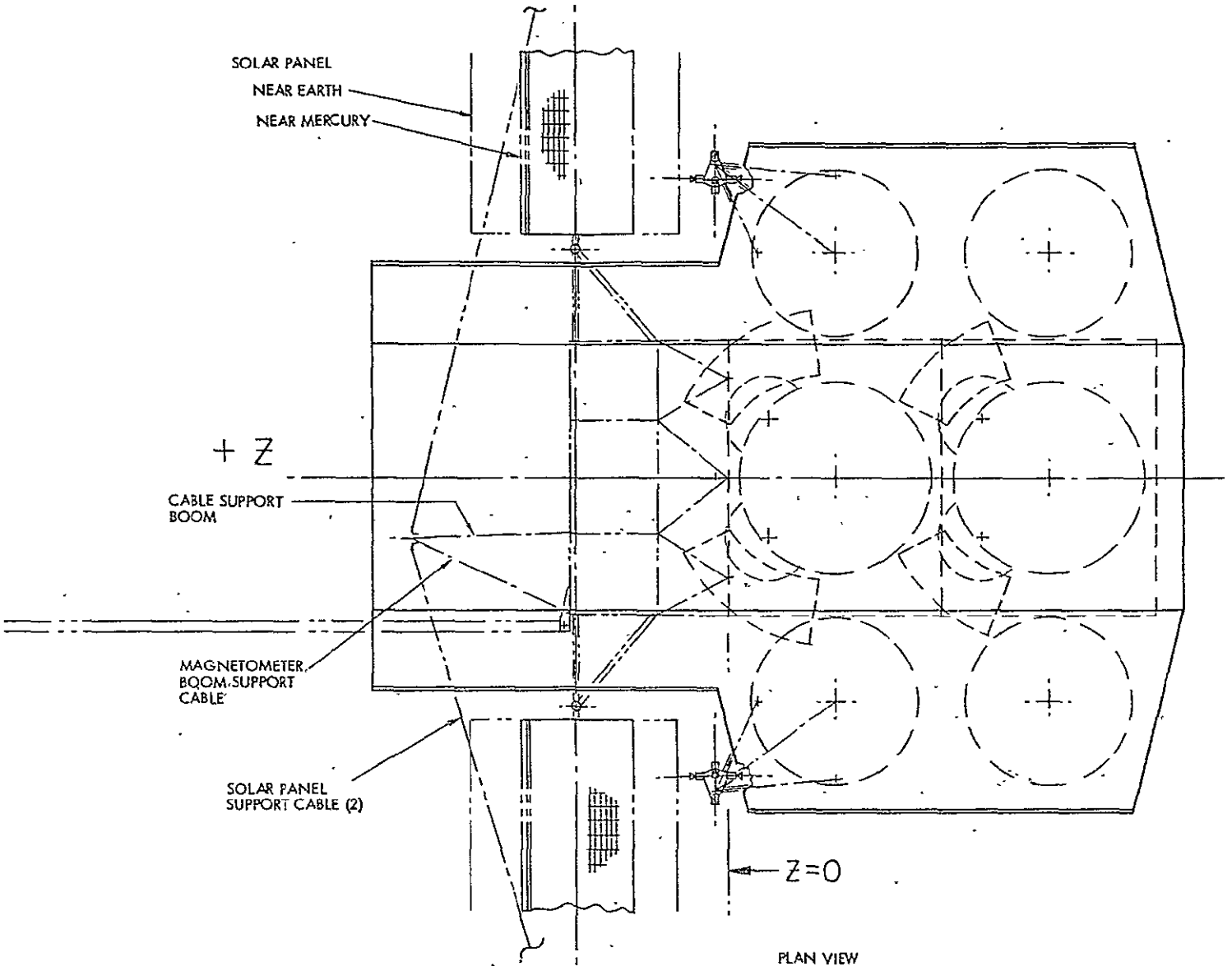

PLAN VIEW

FOLDOUT FRAME

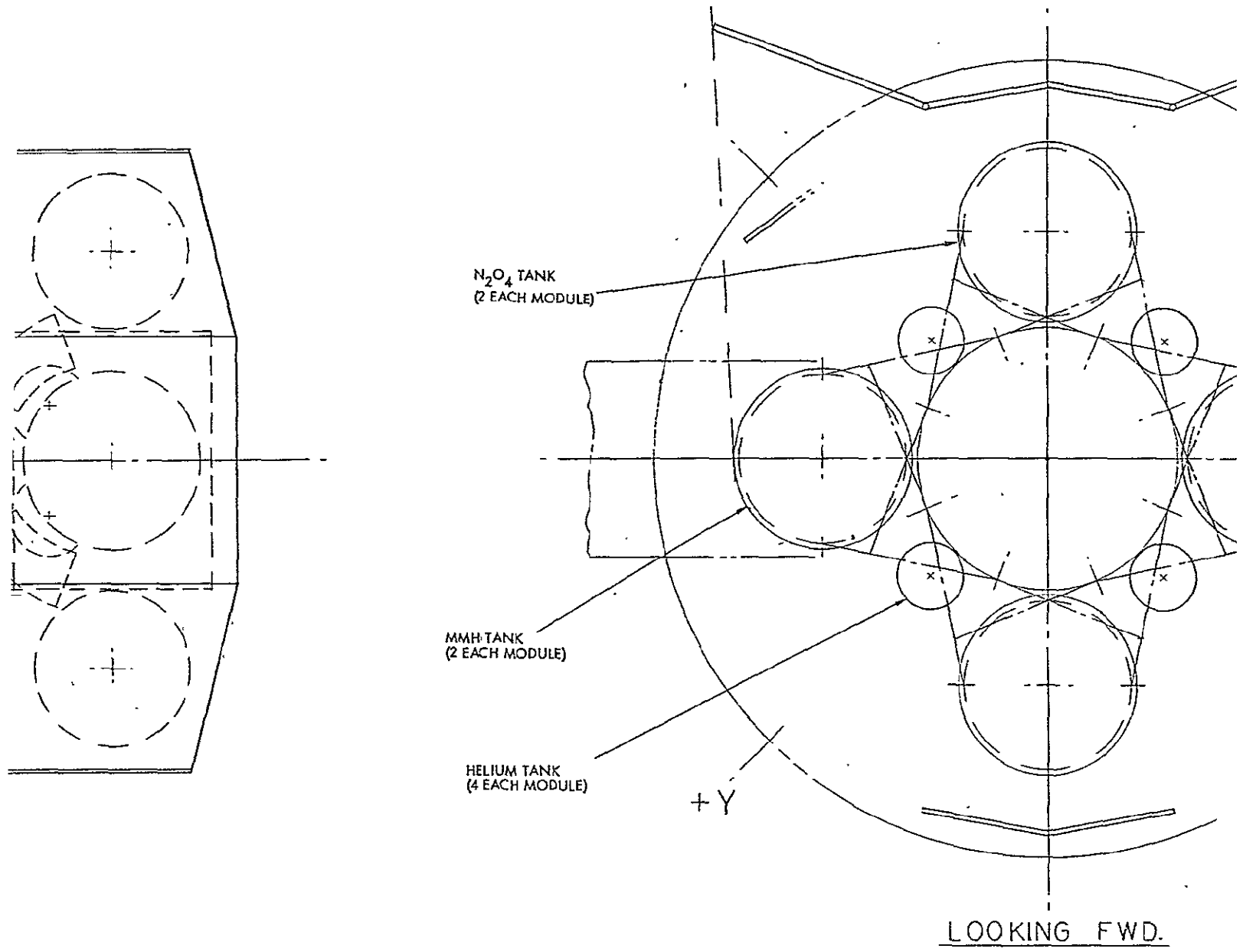

Figure 4-1

FOLDOUT FRAME 2

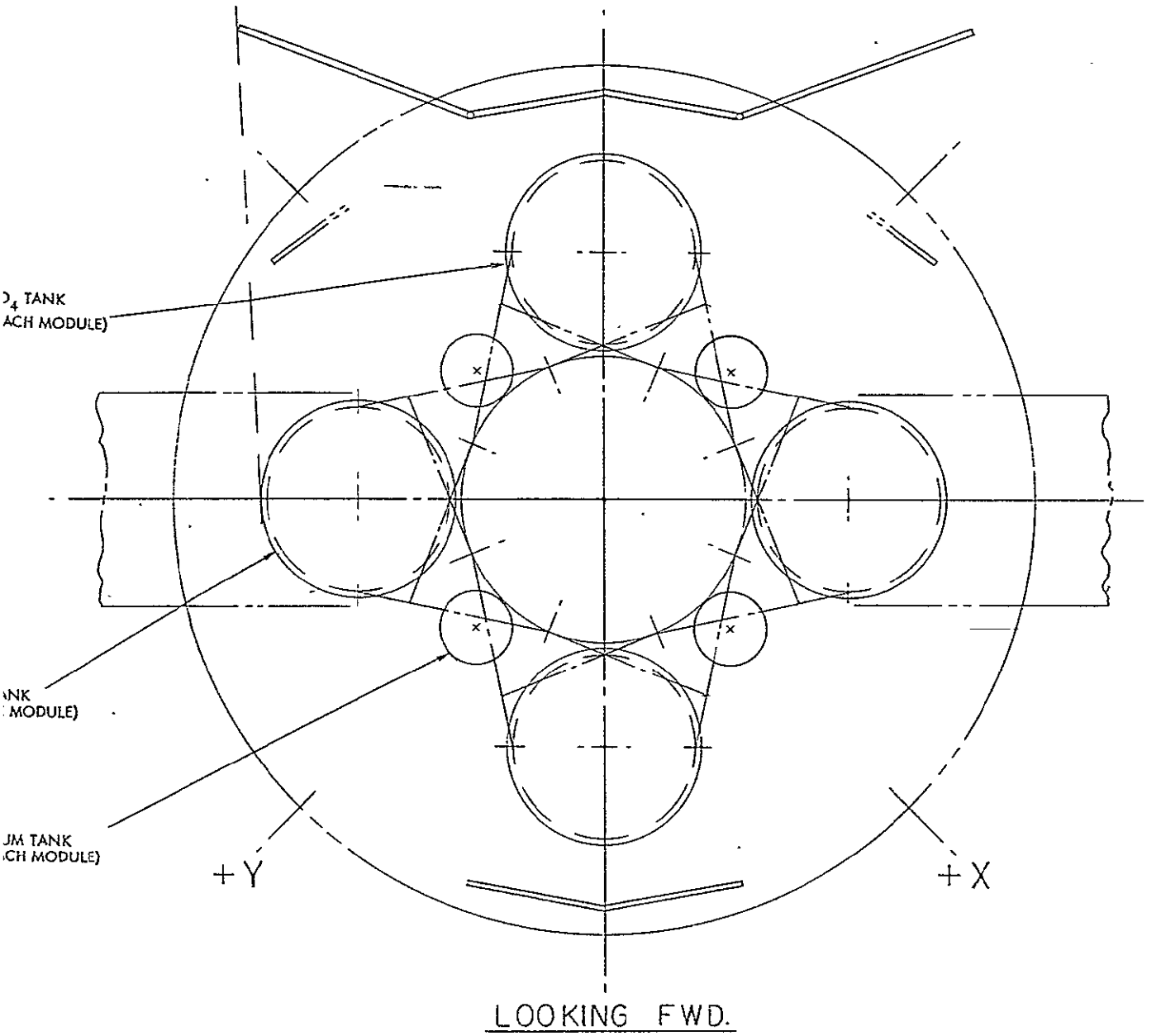

Figure 4-17. Sun Shade Configuration of Propulsion Module B for Mariner Mercury Orbiter

FOLDOUT FRAME 3

to permit effective heat radiation from these tanks to maintain the specified cryogenic temperature. The sun shade uses Beta cloth, backed by Kapton and multilayer aluminized Mylar, which is stretched over the fixed and movable frames that support the sun shade.

4.5.4 Other Heat Shields

Several other heat shields are required to prevent exposure of the uninsulated cold tanks to IR radiation, primarily from the solar panels and from the surface of Mercury during day-side passes.

As shown in the design drawing, two conic-segment shields are provided for each LF_2 tank to block heat radiation from the solar panels. These shields leave a sufficient cold space viewing factor to the tanks for outward heat radiation.

In addition, a local heat shield is provided for the upper LF_2 tank mounted on the side opposite the sun shade (spacecraft X-axis) to protect it against Mercury dayside heat flux. The lower tank needs no shielding since it is jettisoned along with the lower propulsion module before Mercury orbit insertion is completed. It will therefore not be exposed to the dayside IR radiation flux.

The shields consist of tubular frames over which flexible sheets of Beta cloth backed by an insulation blanket are stretched. Like the sun shade, the Mercury heat shield is supported by a lightweight truss attached to the central cylinder end rings. The side shields are directly attached to the cylinder walls.

In the earth-storable version of the module these auxiliary heat shields can be safely omitted.

4.5.5 Module B Configuration for Outer Planet Orbiters

Figure 4-18 shows the outer planet orbiter application of Module B with space-storable propellants. The payload is a Mariner MJS class outer-planets spacecraft. The Shuttle upper stage combination required for these missions is the Space Tug/SPM (1800).

The interstage adapter truss supports the kick motor and the flight spacecraft on the 14.5-foot (4.42-m) diameter Space Tug payload

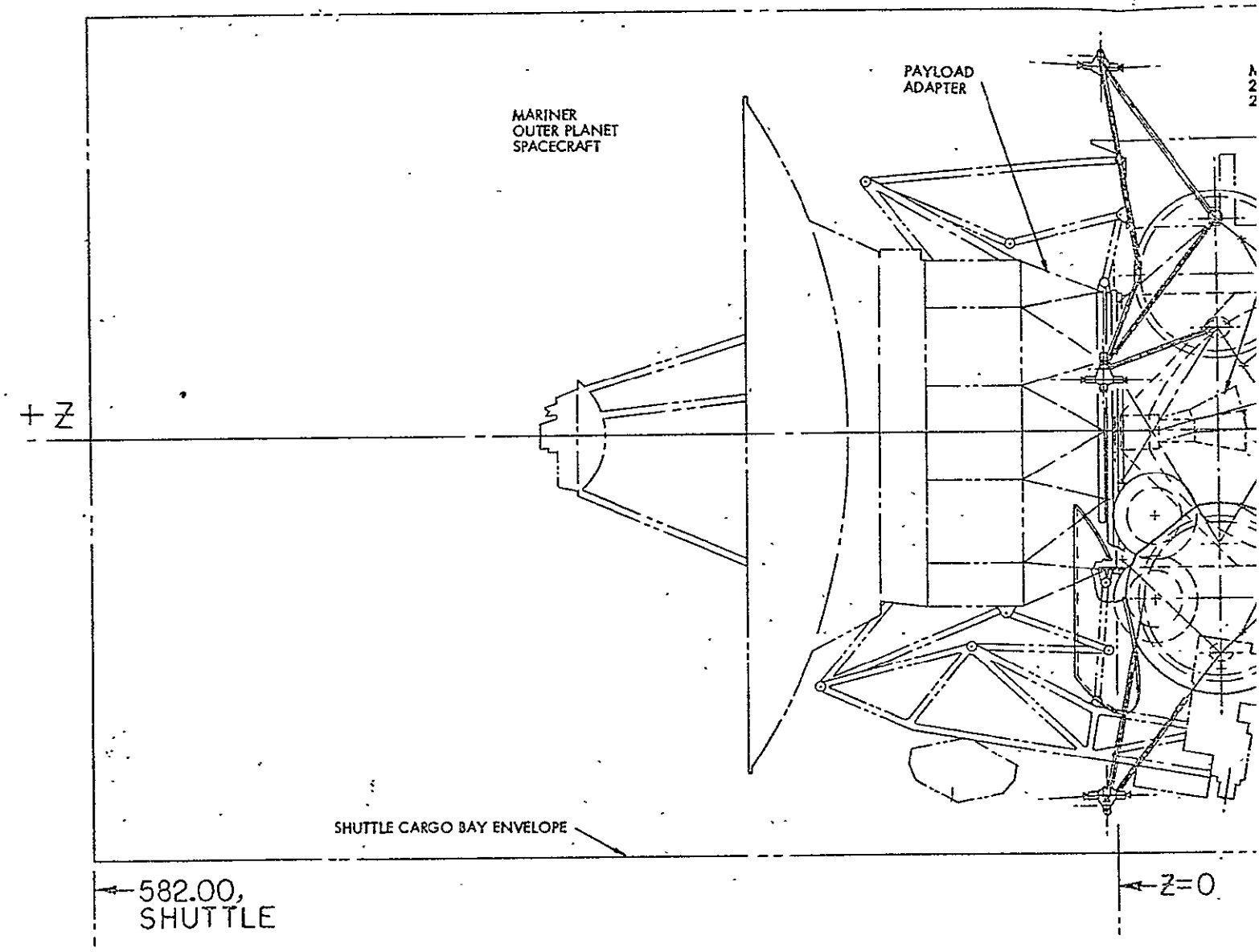

FOLDOUT FRAME

SPACE-STORABLE PROPELLANTS

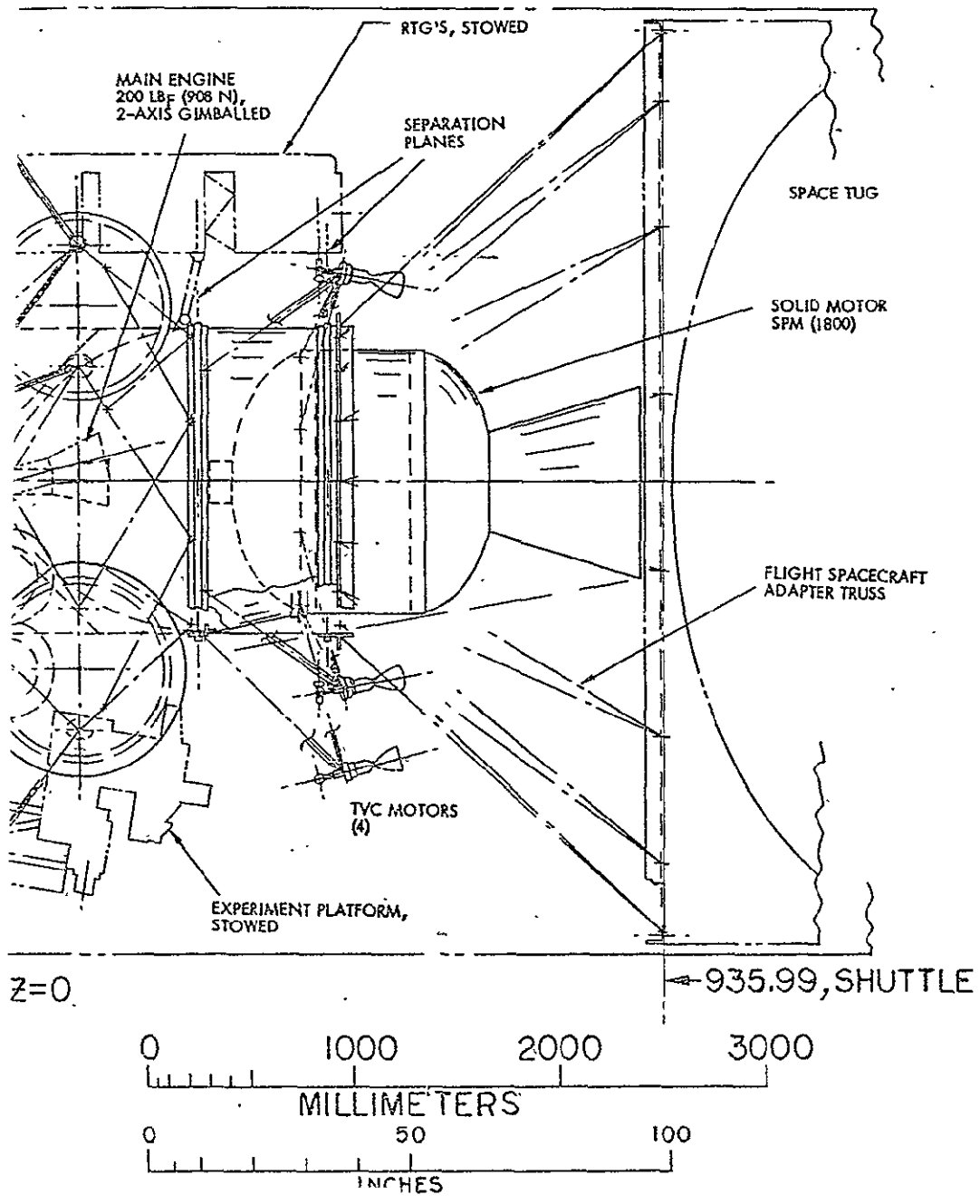

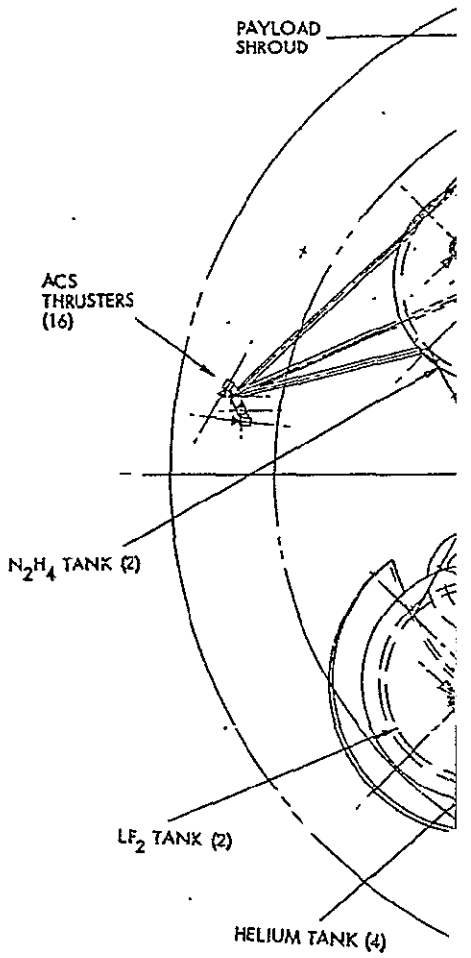

FOLDOUT FRAME 2

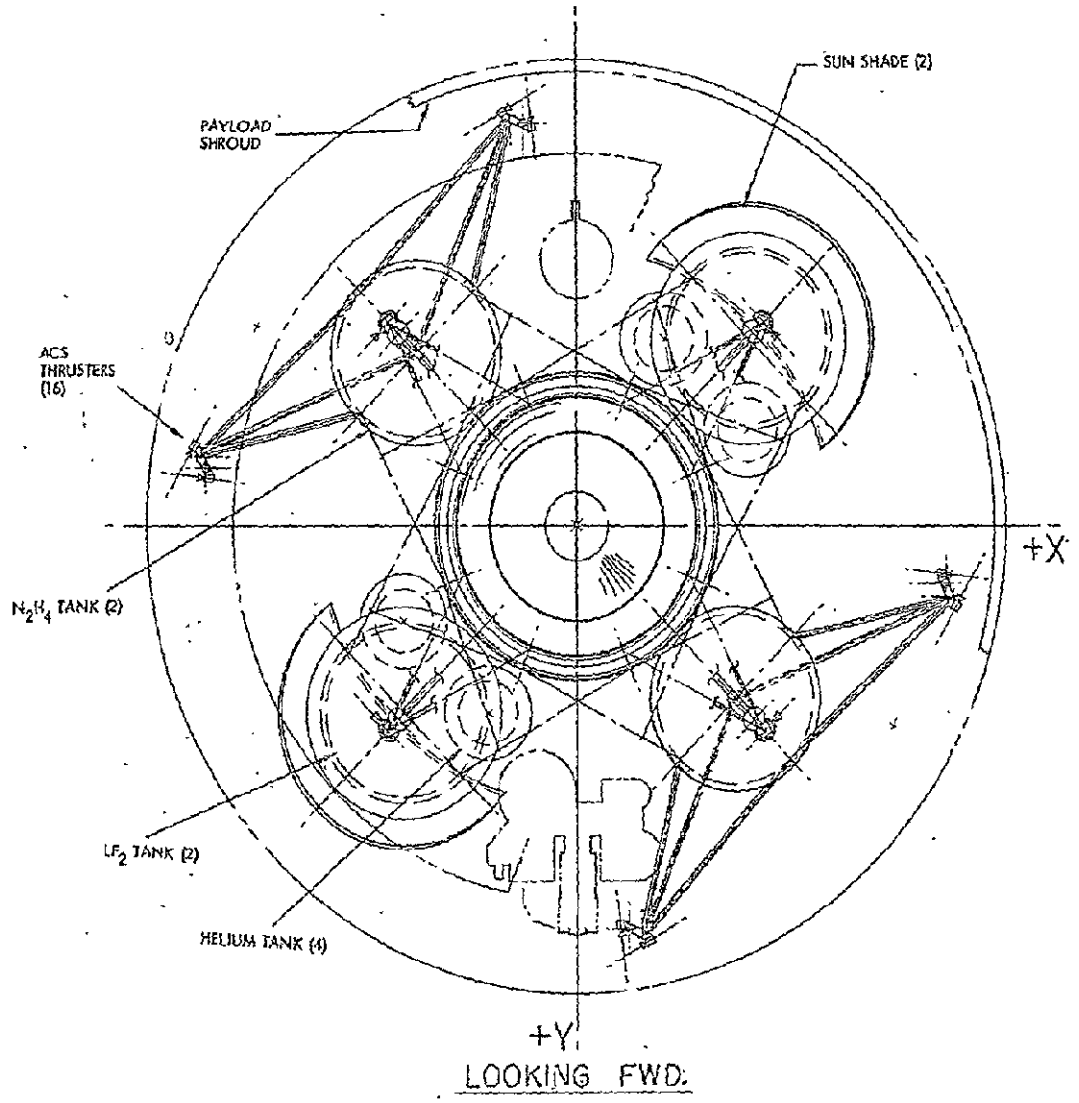

Figure 4-18. Propulsion Module B Configuration for Mariner Outer-Planet Orbiter

mounting flange. The adapter truss design is the same as for the Mercury orbiter where the solid kick stage was omitted.

The propulsion module is structurally identical to the tandem version used in the Mercury mission except for these minor modifications:

- Replacement of the 800-lb_f main engine by the smaller 200-lb_f unit, as necessitated by the low structural load tolerance of deployed appendages (RTG support arm, scientific platform support arm, and experiment booms)
- Omission of the large sun shade and other shields that are required only in the Mercury mission
- Addition of small sun shades to protect the LF_2 tanks individually against direct sun illumination at times when the sun is off the spacecraft Z axis and the tanks would no longer be shaded by the high-gain antenna dish.

Spacecraft operation is constrained to avoid Z-axis orientations at angles more than 15 degrees from the sun line in the plane containing the fluorine tanks. At some time intervals occurring twice during the early transfer phase, the earth-spacecraft-sun angle exceeds 15 degrees. As a compromise dictated by thermal control requirements, downlink communication via the high-gain antenna is not continued during these intervals, but can be maintained via the low- or medium-gain antennas, since communication ranges are still reasonably small. High bit rate telemetry is generally not required during these periods, in any case.

4.5.6 Mass Properties of Module B

Tables 4-7 and 4-8 list mass properties of Module B for space-storable and earth-storable systems, respectively. The first part of each table gives data for the tandem arrangement of propulsion modules in the Mercury orbiter; the second part gives corresponding data for the single-stage outer-planet orbit missions.*

Assumptions made in the Module A mass properties analysis (see Section 4.4.4) also apply in the Module B analysis.

*Weight summaries are presented separately in Section 4.9.

Table 4-7. Module B — Space-Storable Propellant Configuration Mass-Property Characteristics

Condition	Weight (lb)	$\bar{Z}$[1] (in.)	Moment of Inertia (slug-ft^2)		
			I_x	I_y	I_z
Module A - Inbound Configuration[2]					
At separation - stowed	6600	-30.1	3269	3678	2858
At separation - deployed	6600	-31.6	3090	3550	3250
At first module burnout - deployed	4420	-13.8	1691	1920	2026
At second module ignition - deployed	3928	-7.5	1305	1521	1886
At second module burnout - deployed	1748	11.3	549	572	673
Separated spacecraft - deployed	1248	23.9	302	344	518
Module B - Outbound Configuration					
At separation - stowed	8590	-47.5	3372	3049	2062
At solid stage burnout - stowed	4590	-21.9	1753	1430	1849
At liquid module ignition - deployed	4172	-8.0	3833	1453	4000
At liquid module burnout - deployed	1992	7.8	3009	643	2778
Separated spacecraft - deployed	1500	16.8	2816	452	2640

Notes:

[1] Longitudinal center of mass ($\bar{Z}$) referenced from the spacecraft/propulsion module separation plane. Minus values are below the reference plane; positive values are above this plane.

[2] Fuel and oxidizer tanks of both propulsion modules are oriented along the same transverse axes.

Table 4-8. Module B — Earth-Storable Propellant Configuration Mass-Property Characteristics

Condition	Weight (lb)	$\bar{Z}$[1] (in.)	Moment of Inertia (slug-ft^2)		
			I_x	I_y	I_z
Module B - Inbound Configuration[2]					
At separation - stowed	11240	-36.1	5956	5947	6505
At separation - deployed	11240	-37.0	5750	5791	6894
At first module burnout - deployed	6926	-18.0	2541	3271	3973
At second module ignition - deployed	6248	-12.9	2001	2789	3706
At second module burnout - deployed	1934	8.4	630	684	789
Separated spacecraft - deployed	1248	23.9	302	344	519
Module B - Outbound Configuration					
At separation - stowed	10950	-42.2	4809	3971	3899
At solid motor burnout - stowed	6950	-22.1	2941	2103	3684
After solid module jettison - stowed	6510	-19.0	2655	1817	3622
At liquid module ignition - deployed	6510	-13.2	4882	2379	5835
At liquid module burnout - deployed	2196	5.3	3111	744	2911
Separated spacecraft - deployed	1500	16.8	2816	452	2640

Notes:

[1] Longitudinal center of mass ($\bar{Z}$) referenced from the spacecraft/propulsion module separation plane. Minus values are below the reference plane; positive values are above this plane.

[2] Fuel and oxidizer tanks in lower module are rotated 90 degrees relative to fuel and oxidizer tanks in the second module.

4.5.7 Arrangement and Use of Auxiliary Propulsion Thrusters

In the selected design the small auxiliary propulsion thrusters required for attitude control and trajectory corrections are relocated from the payload spacecraft and placed on the propulsion module support arms attached to the fuel tanks on opposite sides of the propulsion module.

With four clusters of four thrusters mounted on support arms on opposite sides of the propulsion module (see end view in the design drawing, Figure 4-16) the total number is the same as in the original Mariner spacecraft design. The thrusters are arranged to serve partially redundant functions in pitch, yaw, roll and ΔV maneuvers.

The radial thrusters used for lateral ΔV maneuvers have small cant angles such that their respective lines of force bracket the total center-of-mass shift due to propellant depletion and staging. Thus, lateral thrust maneuvers can be performed with little or no effect on pitch or yaw control channels by appropriate combination of radial thruster pairs, i.e., by a technique similar to that devised for lateral maneuvers in the case of Module A (see Section 4.4.5).

The propulsion module alignment with the X and Y body axis of the payload spacecraft differs by 45 degrees in the Mercury and outer planet orbiters. This is dictated by different tank location criteria in the "inbound" and "outbound" configurations. In the inbound configuration the cold LF_2 tanks are placed on the sunward and anti-sun side of the spacecraft for best thermal protection. A 45-degree change of module alignment relative to payload spacecraft X and Y axes is necessary in the outbound configuration to provide space for the RTG and experiment platform support arms in the stowed configuration. The auxiliary thrusters are arranged geometrically in a configuration that is compatible with the different propulsion module alignments in the two mission classes.

Note that the thruster assemblies are configured to avoid any exhaust plume impingement in both applications.

In the tandem arrangement of two propulsion modules used in the Mercury mission the auxiliary thrusters and their support structures are omitted from the lower module.

4.6 DEPLOYMENT AND OPERATING MODES

Principal deployment and operating modes of propulsion Modules A and B in inbound and outbound missions will be discussed in this section to the extent required to show mission feasibility. Emphasis in the discussion will be placed on the space-storable propellant version of the propulsion modules. Reference to specific mission profile requirements and constraints is required especially for the Mercury orbiters, to explain deployment and operating modes adequately; this mission (subsection 4.6.1 and 4.6.3) will therefore be covered in geater detail than the others.

4.6.1 Module A Inbound Mission

The Mercury orbiter configuration differs from the outer-planet orbiter primarily in using two propulsion modules in tandem and requiring deployment (and occasional retraction) of the large cylindrical sun shade.

Separation of the burned-out first propulsion module during Mercury orbit insertion is similar to the separation from the launch vehicle upper stage employing identical Vee-band separation devices. The lower-module separation must be performed with minimum loss of time because of the critical influence of any delay on the insertion maneuver efficiency. With a nominal thrust level of 800 lb_f the propellant mass penalty due to a delay in first module separation and second module thrust initiation is about 25 kg per minute.

Deployment of the cylindrical sun shade by centrifugal action must be performed at earth departure, immediately after separation from the Shuttle upper stage and completion of the spacecraft spin-up maneuver. With a nominal spin rate of 10 rpm desired in the cruise mode the pre-deployment rate must be slightly higher (about 11.2 rpm) to allow for the rate reduction caused by the sun-shade deployment.

The sun shade must be retracted to the stowed condition prior to all main thrust maneuvers and redeployed after the maneuver. Upon completion of Mercury orbit insertion, with only one propulsion module remaining, the shade no longer requires deployment to the maximum radius as previously discussed. This has the advantage of reduced

shade deformation during precession maneuvers and more effective protection of the LF_2 tanks against Mercury day side thermal radiation. It also reduces solar pressure unbalance.

During dayside passages with maximum heat flux, i.e., passages near the subsolar region of the planet, which occur seasonally about every 3 months, LF_2 tank protection can be further improved by nearly complete sun shade retraction. Further analysis is required to determine whether these additional retraction and deployment sequences are actually necessary.

The configuration selected for Module A meets all orientation requirements of the Mercury orbiter mission with regard to

- Thrust pointing for effective orbit insertion
- Thrust pointing for secondary maneuvers
- Thermal protection
- High-gain antenna pointing
- Scientific instrument pointing.

The required orientation modes and sequences are described below.*

Cruise Mode

During the transfer and planetary orbit phases nominal spin axis orientation is normal to the heliocentric plane of motion (Figure 4-19). This assures effective thermal protection by the sun shade and permits unobstructed earth pointing of the despun antenna dish within a small range of elevation angles. Maximum positive or negative elevations (±13 degrees) occur when the spacecraft (and Mercury) is at inferior conjunction relative to earth and, at the same time, at maximum northern or southern heliocentric latitude. Owing to Mercury's orbital inclination these latitudes are ±7 degrees. The Pioneer Venus despun antenna is designed for elevation angles of ±20 degrees. The sun shade, even when fully deployed, gives the antenna an unobstructed downward view of about 20 degrees. After orbit insertion, with the shade only partially deployed, this increases to 30 degrees downward.

*See also Appendix G.

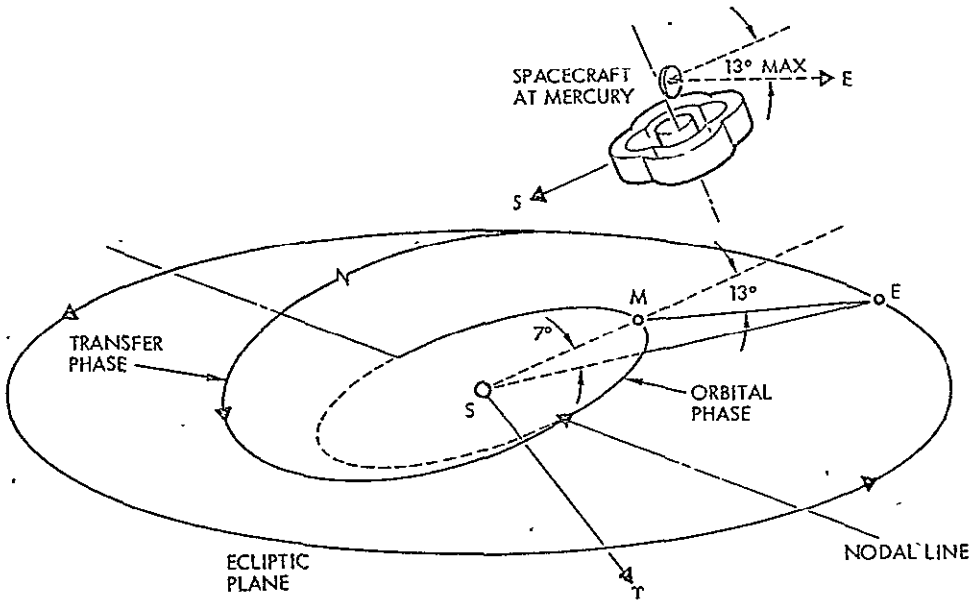

Figure 4-19. Nominal Spacecraft Orientation and High-Gain Antenna Pointing Geometry (Earth and Mercury at Inferior Conjunction)

Off-nominal spacecraft orientations are acceptable provided that side-sun thermal protection and high-gain antenna coverage of earth are not lost as a result. Figure 4-20 illustrates the relevant three-dimensional pointing requirements in spherical projection. The spacecraft spin axis, Z_s, is constrained to be in the plane normal to the sun line, shown in the spherical diagram by the circle C_o. In the left diagram the spin axis is in the nominal orientation, normal to the heliocentric orbit (C_1) at point Z_o. In this orientation the ±13-degree zone of possible relative earth positions is fully covered by the ±20-degree high-gain antenna deflection range. If the spin axis is tilted by an angle δ from the nominal orientation Z_o to position Z_t as shown in the diagram on the right, the high-gain antenna provides coverage only as long as earth's relative position is in a limited range of longitudes on both sides of the intersection of the two circles C_1 and C_2 formed by the sun line. This means that earth must be close to inferior or superior conjunction. The range of earth's longitudes and, therefore, the time interval during which the spacecraft may remain in the off-nominal attitude without losing high-gain antenna coverage, depends on the tilt angle δ and on the earth's relative heliocentric latitude north or south of the spacecraft's orbital plane (circle C_1). For example, with a 45-degree tilt angle and

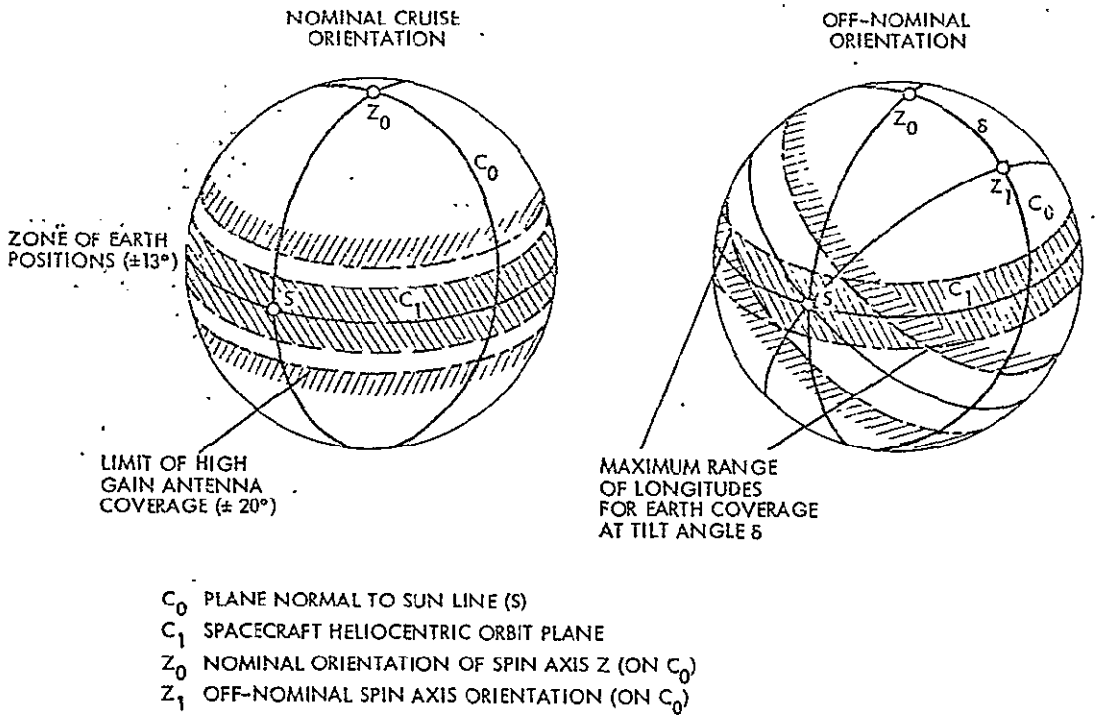

Figure 4-20. Earth Coverage by High-Gain Antenna in Nominal and Off-Nominal Cruise Orientation for Pioneer Mercury Orbiter

earth close to C_1 the range of relative longitudes for which earth coverage is provided by the ±20-degree antenna elevation angle range amounts to ±28 degrees. With earth 10 degrees north or south of C_1 the range of longitudes reduces to ±17 degrees from the sun or anti-sun line.

These factors are relevant for any spacecraft operations that require off-nominal orientation, e.g., for orbital maneuvers or scientific observations.

Orbit Insertion Mode

The orientation required for Mercury orbit insertion differs from the nominal cruise orientation. Thrust vector pointing options are related to the choice of approach trajectory for a given hyperbolic approach velocity $\overline{V}_\infty$. Figure 4-21 shows a set of approach hyperbolas and periapsis locations for an approach velocity vector pointing slightly more than 90 degrees from the sun which is typical for the mission options being considered in this study (SPA > 90 degrees). The aim angle θ_{AIM} indicated in the B-plane, at left, determines the inclination of the approach orbit.

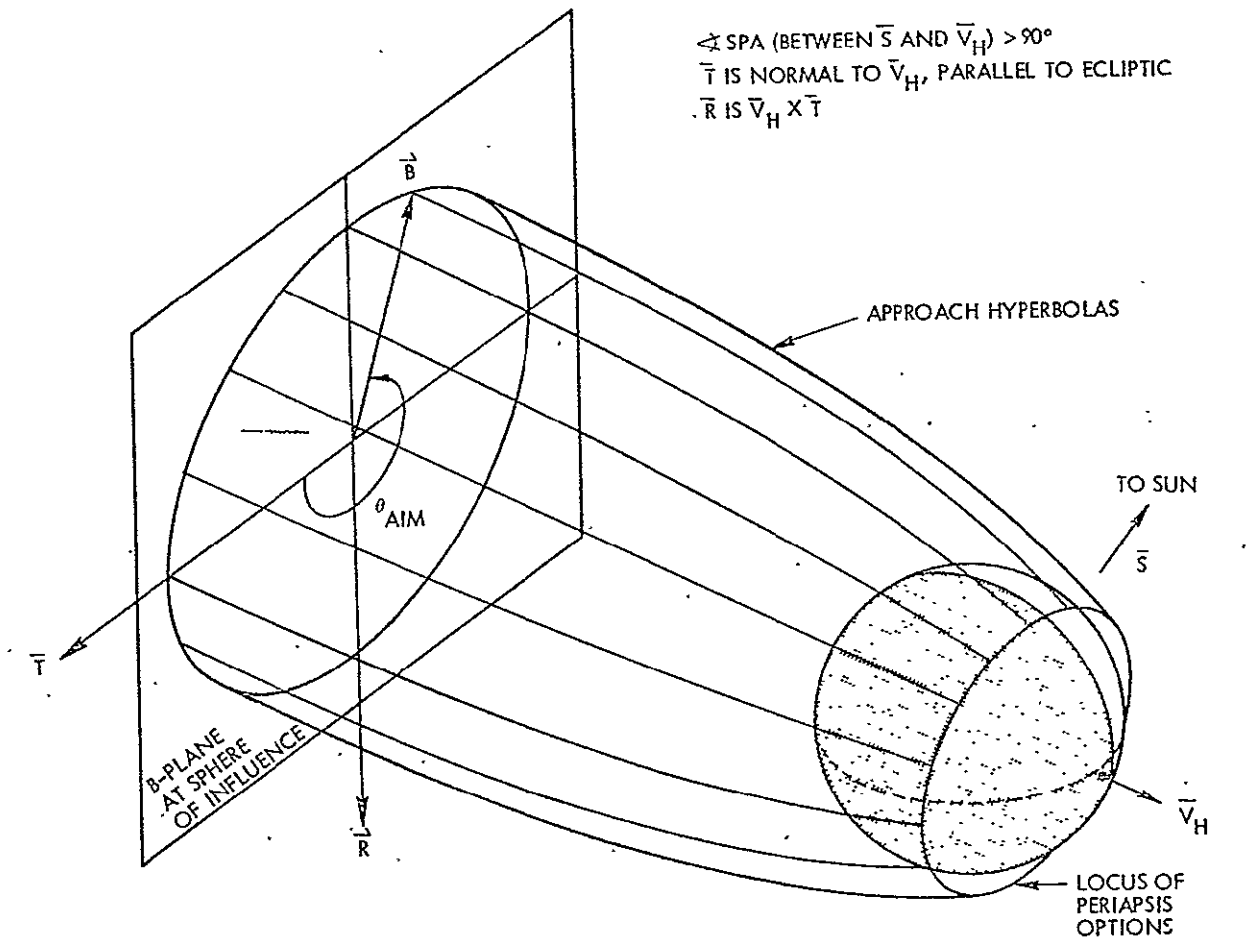

Figure 4-21. Mercury Approach Targeting Options*

Figure 4-22 illustrates the three-dimensional relations between approach trajectory options, retro-thrust pointing options, and side-sun protection constraints, in terms of a spherical projection. The spacecraft is assumed to be at the center of the diagram. The sun line (-S), the projection of the ecliptic (E), the north ecliptic pole (N_E), the approach velocity vector ($\bar{V}_\infty$), several approach trajectory traces, their aim angles (θ_{AIM}) and periapsis locations are indicated on the sphere. (The projection shown covers mostly the anti-solar side of the spacecraft.) The side-sun protection constraint is indicated by the circle C_o normal to the sun line. The spin axis Z (and the thrust vector $\bar{F}$) must be located on C_o, and should also be in the plane of motion for most effective orbit insertion.

*Adapted from Reference 10.

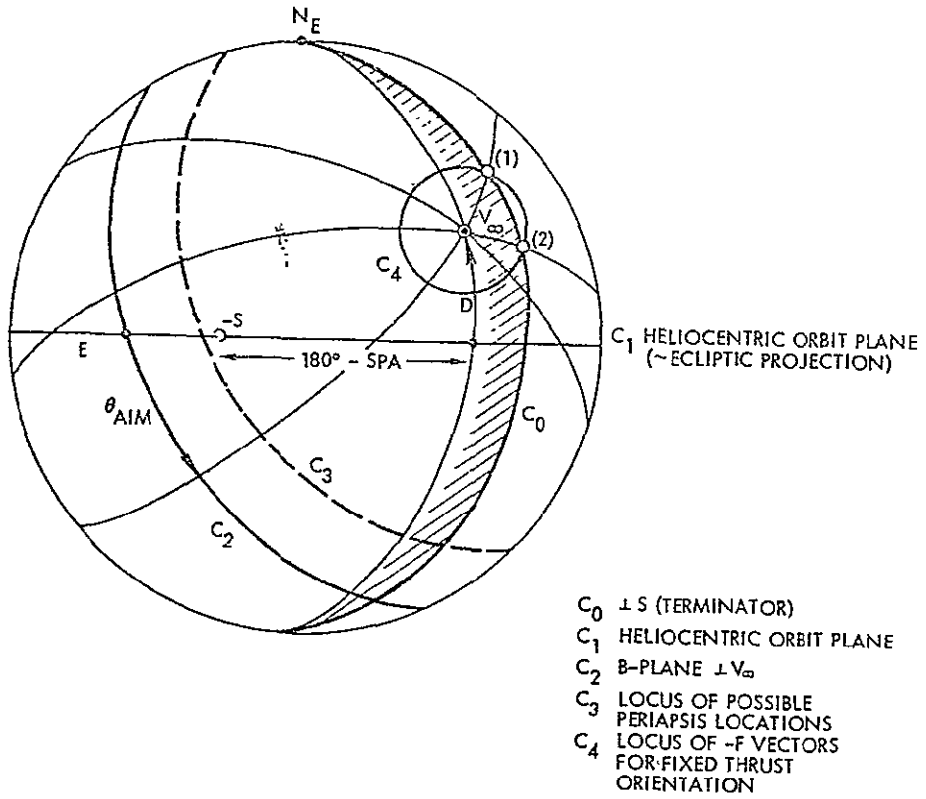

Figure 4-22. Pioneer Mercury Orbiter Trajectory Traces and Orbit Insertion Geometry

Since a fixed thrust orientation is adopted for the spinning spacecraft, as discussed in Section 3, the optimum orientation is tangential to the approach hyperbola at periapsis. In Figure 4-22 this is indicated by a locus of points 90 degrees from the respective periapsis locations of the trajectories associated with the given V_∞ vector. This locus, a small circle C_4 around $\overline{V}_\infty$, usually intersects the circle C_o and, if so, defines two possible thrust orientations, (1) and (2), that satisfy both the thermal protection and optimum fixed thrust pointing criteria. Orientations indicated by circle C_4 are actually those of the negative thrust vector, $-\overline{F}$. These characteristics are representative of orbit injection conditions which would occur with a transfer trajectory launched on 19 June 1988.

The selected mission opportunity (launch 12 March 1988, arrival 26 March 1990) has encounter characteristics shown in Figure 4-23 that differ somewhat from the usual conditions described above. With the

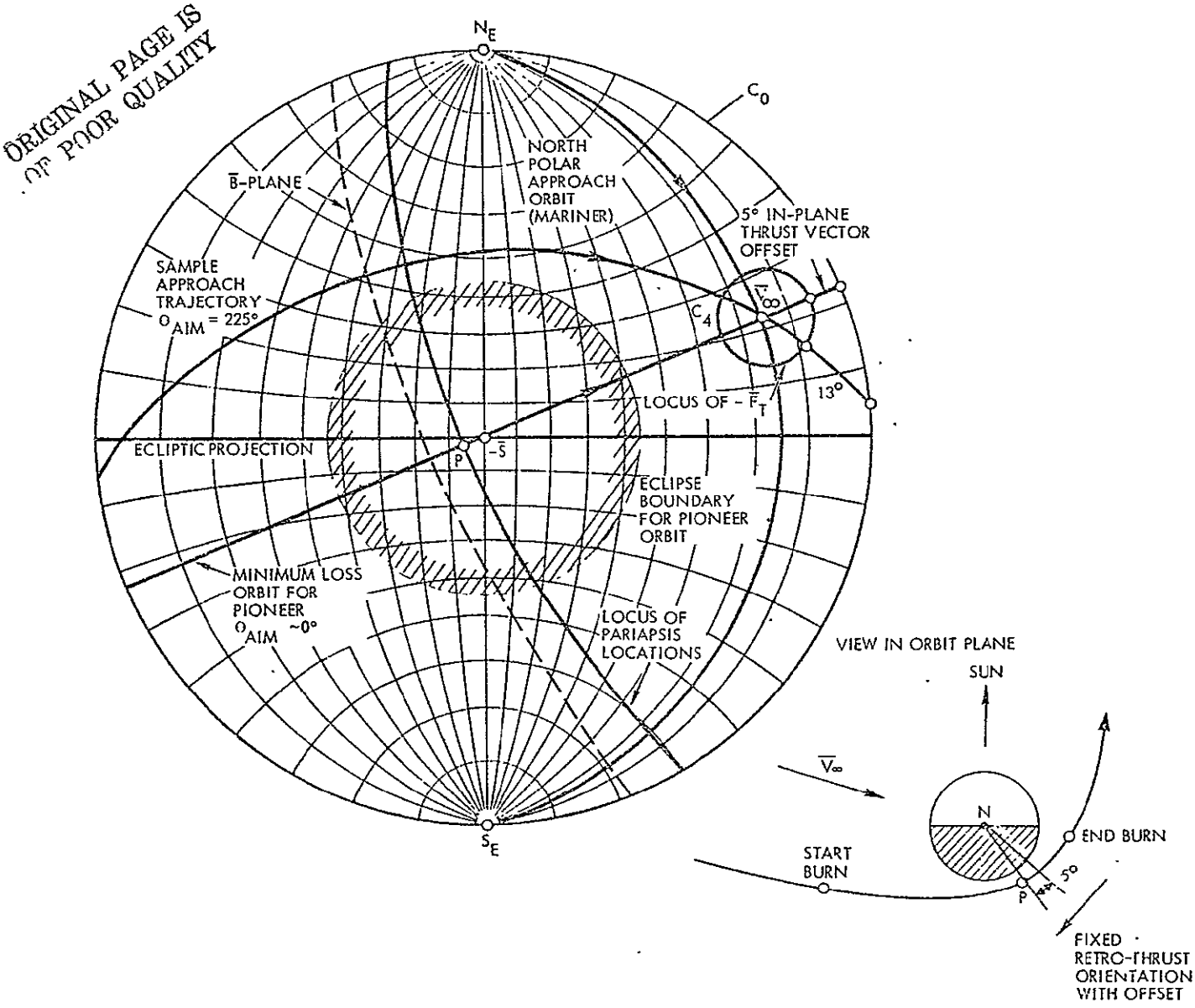

Figure 4-23. Encounter and Orbit Insertion Geometry for Mercury Orbiter (Mission Option II)

orientation of $\bar{V}_\infty$ given by SLA = 104.5 degrees and an optimum thrust vector locus (circle C_4) of only 9-degree radius, the two loci C_o and C_4 do not intersect in this case. The thrust vector must therefore be offset from the optimum orientation by a small angle in order to comply with the side-sun protection constraint C_o. This means that the thrust is tangential at a point about 5 degrees beyond the periapsis of the approach hyperbola as illustrated by the trajectory diagram at the lower right in Figure 4-23. The resulting maneuver performance penalty is about 2 percent for space-storable, and 2.5 percent for earth-storable propellants for the systems investigated.

If a polar orbit were chosen, the performance penalty would be nearly 6 percent, since an appreciable out-of-plane thrust component is required to meet the side-sun protection constraint under these arrival conditions.

The selected aim angle and thrust orientation identified in Figure 4-23 correspond to an orbit inclination of 22 degrees, and a periapsis located almost exactly above the anti-solar point. The apoapsis is located above the subsolar point. With this orientation of the apsidal line and the large distance at apoapsis (26,300 km for e = 0.8) thermal radiation from Mercury during dayside passage is of no consequence in the initial orbit phase. However, with the rotation of the sun line relative to the line of apsides, thermal flux affecting the spacecraft during dayside passages changes seasonally and reaches a maximum within 44 days, i.e., after half a period of Mercury's orbital revolution, when the sun line orientation is reversed. Therefore, a major orbit change maneuver is required in advance to prevent a build-up of unacceptably large flux levels (see below).

In the selected orbit insertion mode earth communication is disrupted because of a) the occurrence of earth occultation during part of the insertion maneuver, and b) the antenna gimbal angle limitation discussed previously in connection with Figure 4-20. At the arrival date earth is about 30 degrees west of the sun and close to the spacecraft's plane of motion. With the spacecraft in the thrust attitude, tilted nearly 70 degrees from the nominal cruise orientation, earth elevation in spacecraft coordinates is -27 degrees, thus exceeding the gimbal angle range of the despun antenna.

It should be noted that even by selection of a polar orbit, to avoid earth occultation during the orbit entry phase, downlink communication cannot be maintained since earth elevation angles in the tilted spacecraft coordinates are -25 and -29 degrees for approaches over the north or south pole, respectively.

Other Maneuver Modes

Periapsis altitude must be increased by at least 2000 km to reduce the exposure to heat flux during dayside passages, requiring an

apogee maneuver of about 120 m/sec. For best efficiency the maneuver should be performed with a thrust orientation normal to the apsidal line, i.e., the same as the retro-thrust orientation at orbit insertion. Since the sun line orientation changes at a rate of 6.2 degrees per day it is necessary to perform the apogee maneuver soon after arrival to assure side-sun protection during the maneuver. With the lower propulsion module jettisoned the sun shade (in the retracted configuration) permits sun angles of up to 20 degrees off the normal side-sun orientation without exposing the propellant tanks to direct illumination. Incidence of reflected sunlight limits the off-normal sun orientation to values of about 10 to 15 degrees. This means that the apoapsis maneuver must be executed within a few days after arrival to minimize performance penalties.

Downlink communication via the high-gain antenna will again be disrupted during the apoapsis maneuver since earth elevation in spacecraft coordinates exceeds the gimbal range and changes at a rate of about -3 degrees per day.

Other main thrust maneuvers of limited magnitude may be desired during the mission to vary orbital characteristics in accordance with scientific observation objectives, e.g., to change sequences and timing of solar corona observations on entering or exiting from solar eclipse. The above discussion has shown the nature of the pointing constraints that affect maneuver capabilities.

The velocity matching maneuver required during the first Venus swingby (see Reference 11) involves a total velocity change of about 220 m/sec in a direction 30 to 45 degrees from the sun line. In this instance the spacecraft can be safely reoriented to the desired maneuver attitude for the short time interval involved. At Venus' solar distance (0.72 AU) the rate of tank temperature increase does not exceed 1.7°C per hour, even with direct solar illumination in the required maneuver orientation.

Small orbit corrections in the vicinity of Mercury require thrust orientations that cannot be predicted. In order to retain the side-sun protection a combination of axial and radial thrust must generally be employed in these maneuvers to meet arbitrary orientation requirements.

Experiment Pointing

The nominal cruise attitude is consistent with typical experiment pointing objectives at Mercury, especially at the low orbit inclination selected for the reference mission. Spin-scan observation of the planetary surface is most effective in this attitude. However, off-nominal attitudes can also be employed at times provided that earth coverage can be maintained by the high-gain antenna (see Figure 4-20).

4.6.2 Module A Outbound Missions

No special deployment sequences are required for the propulsion module in the outer-planet orbiter application. However, as in the Mercury orbiter case, higher-than-nominal spin rate is required during main thrust phases to increase attitude stability and stiffen the deployed spacecraft appendages. Previous Pioneer orbiter studies have shown spin rates of 10 to 15 rpm to be appropriate during thrust phases with equivalent thrust levels.

In contrast with the Mercury orbiter application, the outer planet missions use a solid kick motor for interplanetary injection, spun up to 60 rpm by a spin table on the launch vehicle interstage adapter. After separation from the burned-out solid motor and before deployment of Pioneer spacecraft appendages a departure velocity augmentation maneuver is performed by the propulsion module using available excess propellant capacity. After the maneuver the spin rate is reduced and spacecraft appendages are deployed to initiate the cruise phase.

Cruise Mode

During the transfer and orbital mission phases the spacecraft maintains a nominal cruise orientation, with the spin axis pointing at earth to maintain continuous communication coverage via high-gain antenna. The only exception occurs during the early part of the transfer phase when earth pointing would cause side-sun exposure of the propellant tanks. Thus, during the first 60 days of transfer and again, during the interval between 100 and 230 days from launch, the spin axis orientation is restricted to an angle of 15 degrees from the sun line, and communication coverage is provided by the low-gain or medium-gain antenna.

Orbit Insertion Mode at Saturn

Orbit insertion at Saturn can be performed in the earth pointing mode by proper targeting of the approach trajectory, thereby minimizing performance losses due to non-tangential thrust.

The approach trajectory and hence, the initial planetary orbit at Saturn are inclined 30 to 40 degrees relative to the planet's equator. This permits planetary exploration at intermediate latitudes and out-of-plane observation, e.g., polarization and opacity measurements, of Saturn's rings.

Apoapsis Maneuver at Saturn

Because of the low periapsis distance selected for orbit insertion (2.5 Saturn radii), an apoapsis maneuver is required to increase this distance and, thereby, to avoid spacecraft exposure to excessive ring particle flux in the subsequent mission phase, after the inclined orbit is changed into a near-equatorial orbit. The apoapsis maneuver can be executed in the same (earth-pointing) mode as the orbit insertion maneuver. The nominal initial orbit dimensions of 2.5 x 61.6 Saturn radii (R_S) imply a ΔV expenditure of 206 m/sec to raise the periapsis to 4 R_S, or 332 m/sec to raise it to 5 R_S.

Orbit Plane Change at Saturn

A major ΔV expenditure (600-900 m/sec) is required to perform the plane change to a near-equatorial orbit. This maneuver will also be performed at or near apoapsis (the optimum location depends on several orbital parameters), and with a thrust orientation nearly normal to the initial orbit plane. Communication coverage is not possible during this maneuver phase, since the high-gain antenna is pointing nearly 90 degrees from the earth line.

Other Maneuver Modes

Combination of axial and radial thrust by auxiliary propulsion thrusters permits small ΔV maneuvers in arbitrary directions while nominal cruise orientation is maintained. The combined thrust mode will be used during midcourse corrections and orbit trim maneuvers at Saturn.

Use of repeated swingby of the satellite Titan will permit orbital plane changes as well as apsidal rotations. Thus the particles and fields environment of the planet can be explored more effectively. Data of a concurrent study by JPL* show the utility of these encounters in a largely nonpropulsive mission sequence. An ample propellant supply carried by the propulsion module will add flexibility and corrective maneuver capability to these encounters. Generally, several ΔV maneuvers are required per encounter 1) for approach guidance, 2) for post-encounter corrections. All corrections can be performed in the cruise attitude.

Uranus Mission Modes

The cruise and thrust phase operating modes for the Uranus mission are comparable with those of the Saturn mission except for different orbital entry options at Uranus and the omission of an orbital plane change requirement. Also, because of the less known ephemeris of Uranus, approach guidance maneuver requirements will probably be larger than at Saturn. Close encounters with Uranus satellites will also be more difficult to accomplish.

Figure 4-24 shows two orbit orientation options at Uranus that offer different exploration opportunities of the unusual physical environment of the planet caused by the 97-degree polar axis tilt. The orbits shown in the diagram can be achieved by posigrade (I) or retrograde (II) orbital entry. Both are approximately in the ecliptic plane. However, only one of these (orbit I) permits orbit injection in the earth-pointing mode. A comparative assessment of the two options indicates the following:

- Option I permits two distinct passes through the postulated bow shock and magnetopause configuration in addition to the initial passage by the arrival hyperbola.
- Option I is better for close observation of the dayside of the planet.

*Personal communication by Dr. Phil Roberts of JPL.

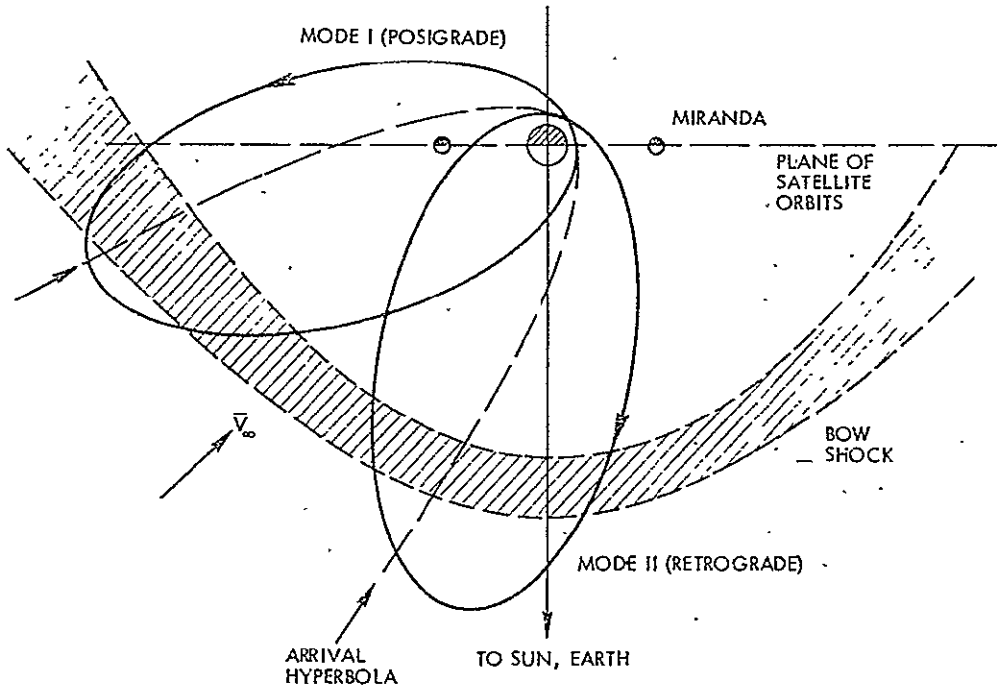

Figure 4-24. Two In-Plane Options of Uranus Orbits for Given V_∞-Orientation

- Option II provides less interesting passages because of its nearly symmetrical orientation relative to the sun line.
- Option II offers the possibility of expanding the orbit toward close encounters with at least Miranda at 4.8 Uranus radii, perhaps even Ariel (7.1 R_U). Significant orbit modifications via satellite encounters are probably impractical in any case.

4.6.3 Module B Inbound Mission

Deployment

After launch and separation from the Shuttle upper stage the appendages of the MVM payload spacecraft and the movable sections of the side-sun shield are deployed. The appendages remain deployed during main thrust application with guy wires providing support to the weakest structures (solar panels and magnetometer boom).

Staging of the lower propulsion module during the Mercury orbit insertion phase is accomplished routinely. However, to avoid a performance penalty the time elapsing between first stage burnout and second stage ignition must be held to a minimum.

As in the MVM mission the solar panels are rotated for thermal protection from the initial orientation normal to the sun (at 1 AU) to a maximum deflection angle of 75 degrees on closest solar approach. Rearrangement of the solar panel rotation joints from the MVM configuration provides the same range of rotation in the Mercury orbiter, shifted by 90 degrees to accommodate the nominal side-sun orientation of the spacecraft. The supporting guy wires are attached on the back of the solar panel to avoid solar cell shading and mechanical interference. The guy wires are deployed from a common reel held by a support mast on top of the spacecraft.

Cruise Mode

In the nominal cruise orientation used in the transfer phase and Mercury orbit phase the spacecraft Z-axis is normal to the sun line. The axis of the solar array (X-axis) is normal to the heliocentric plane of motion. With the long dimension of the side-sun shield extending in Z-axis direction this orientation provides a more unobstructed high-gain antenna view to earth than the cruise orientation used in the MVM mission where the Z axis was pointed normal to the plane of motion. In principle, both orientations are acceptable in the Mercury orbiter mission. The final choice depends on the preferred orientation of the stellar reference sensor. A disadvantage of north-south orientation of the solar panels is the potential stray light interference with Canopus or Vega tracking by the star sensor.

Mercury Orbit Insertion Mode

The Mercury arrival geometry discussed in Section 4.6.1 permits two orbit insertion alternatives for the non-spinning spacecraft:

a) Insertion into a low inclination orbit with the same thrust pointing mode as the spinning Pioneer orbiter

b) Insertion into a polar orbit approaching either over the north or south pole (with aim angles θ_{AIM} = -90 or +90 degrees).

The first mode requires a fixed thrust with 5-degree offset from the optimal orientation with a small performance loss, as discussed in connection with Figure 4-23.

The second mode permits the use of a nearly optimal variable thrust pointing program suitable for onboard storage and execution by the Mariner attitude control system. As a general rule, avoidance of performance losses in Mariner missions is even more important than in Pioneer missions because of the large payload weight difference of the two spacecraft families and the sensitivity of propellant requirements and, hence, propulsion module sizing to such losses. Consequently, insertion into a polar or near-polar orbit is to be preferred if this is consistent with thermal control requirements.

As discussed in Section 4.6.1 (Figures 4-21 and 4-23) the approach velocity vector $\overrightarrow{V}_\infty$ of the selected reference trajectory is oriented 104.5 degrees from the sun line. The declination of $\overrightarrow{V}_\infty$ is 22 degrees. Orbit insertion into a polar or near-polar orbit requires a deviation of the Z axis from the exact side-sun orientation by a 12-degree rotation about the X axis in order to avoid a performance loss due to non-coplanar thrust. This 12-degree offset can be accepted without adverse thermal effects, since with the selected propulsion module configuration the fluorine tanks remain shielded against direct sun illumination, while only a small section of the upper fuel tanks is exposed.

Compared with the low-inclination orbit adopted for the Pioneer orbiter, the polar orbit adopted for Mariner permits better coverage of surface features and environmental phenomena by the scientific instruments, especially magnetospheric phenomena at high latitudes.

The two arrival options, north or south polar, result in the Mercury orbits illustrated in Figure 4-25. The northern approach places the periapsis near the north pole (77 degrees north latitude), the southern approach places it at 61 degrees south latitude. Both orbits are of equal value scientifically, and are subject to nearly the same thermal flux at the time of subsolar passage, about 20 days after arrival.

Earth occultation is avoided during orbit insertion and begins only one week after arrival at Mercury.

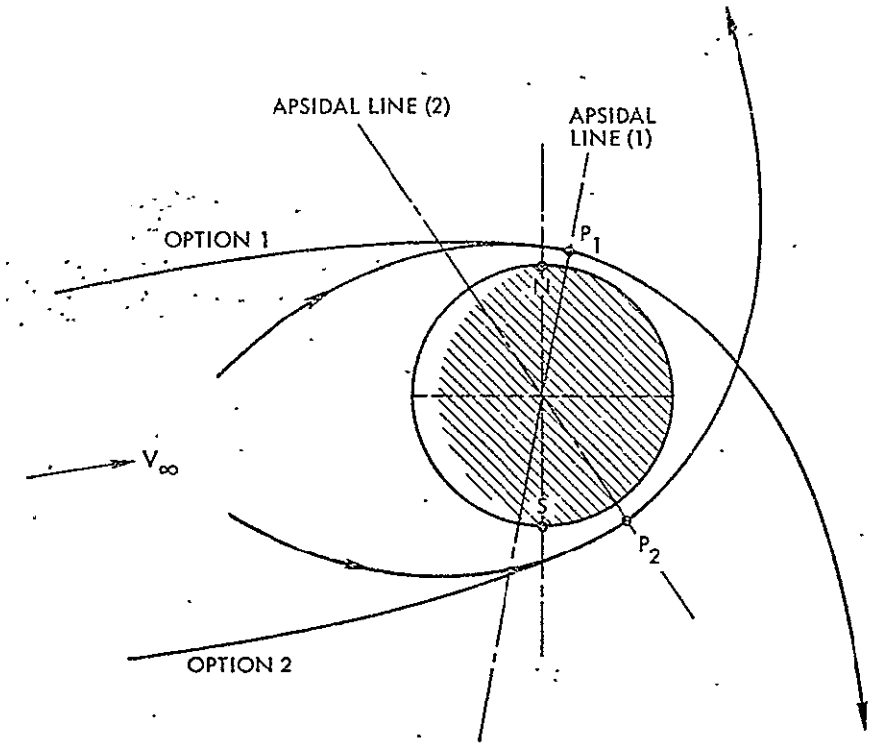

Figure 4-25. Two Arrival and Orbit Orientation Options for Mariner Mercury Orbiter

Apoapsis Maneuver

An increase from the initially selected 500-km periapsis altitude is necessary to alleviate the thermal flux from Mercury during subsolar passages that occur about 20 days after arrival and subsequently at 40- to 60-day intervals. With periapsis locations near the north or south pole (see Figure 4-25) the spacecraft altitude at subsolar passage would be at least 1500 to 2000 km even if no periapsis-raising maneuver was performed. Thus, maneuver requirements tend to be smaller (at least initially) than for the low-inclination orbit selected in the case of Pioneer. A periapsis altitude increase of about 1000 km, requiring a 60 m/sec velocity increment at apoapsis is considered adequate in the Mariner case. The maneuver should be performed immediately after arrival to avoid out-of-plane thrust losses due to sun-line rotation and maneuver attitude constraints if the maneuver was delayed, as explained in the Pioneer orbiter case.

Actually, changes in periapsis altitude due to solar gravity perturbation affect the apoapsis maneuver requirement and must be taken into account. Based on results from the Martin Marietta study (Reference 10) shown in Figure 4-26, the north-polar approach option (θ_{AIM} = 270 degrees) results in an orbit in which periapsis altitude increases at an average rate of about 9 km per day; the south-polar option (θ_{AIM} = 90 degrees) produces a periapsis altitude decline of about 5 km per day. The latter case requires a larger apoapsis maneuver not only to avoid excessive dayside heat fluxes, but also to prevent surface impact. Repeated periapsis raising maneuvers at intervals of 44 or 88 days may be preferred to retain the initially established orbit characteristics, e.g., for effective in-situ exploration of geophysical (hermiophysical) phenomena close to the planet.

Figure 4-26 also shows that for the low-inclination orbit (θ_{AIM} = 0 degree) that was selected for the Pioneer orbiter the evolution of periapsis altitude has no appreciable effect on apoapsis maneuver requirements.

Antenna Pointing

Earth view by the high-gain antenna is restricted in the -Z direction by the propellant tanks and the Mercury heat shield, and in the -Y direction by the upper extension of the sun shield. The unobstructed field of view to earth in the Y-Z plane is shown in Figure 4-16. Spacecraft reorientation by a 180-degree rotation around the sun line places the antenna in a position where about 120 degrees of additional heliocentric longitude is opened for earth viewing. This spacecraft reorientation must be performed twice per earth-Mercury synodic period, i.e., at intervals of 58 days on the average, to permit nearly uninterrupted communications coverage by the high-gain antenna.

A residual ±10-degree angular range in the Y-Z plane remains inaccessible for earth viewing when earth and Mercury are near superior conjunction due to field-of-view obstruction by the sun shade. Figure 4-27 shows earth maximum and minimum obscuration times as function of obscuration angle, corresponding to spacecraft locations at

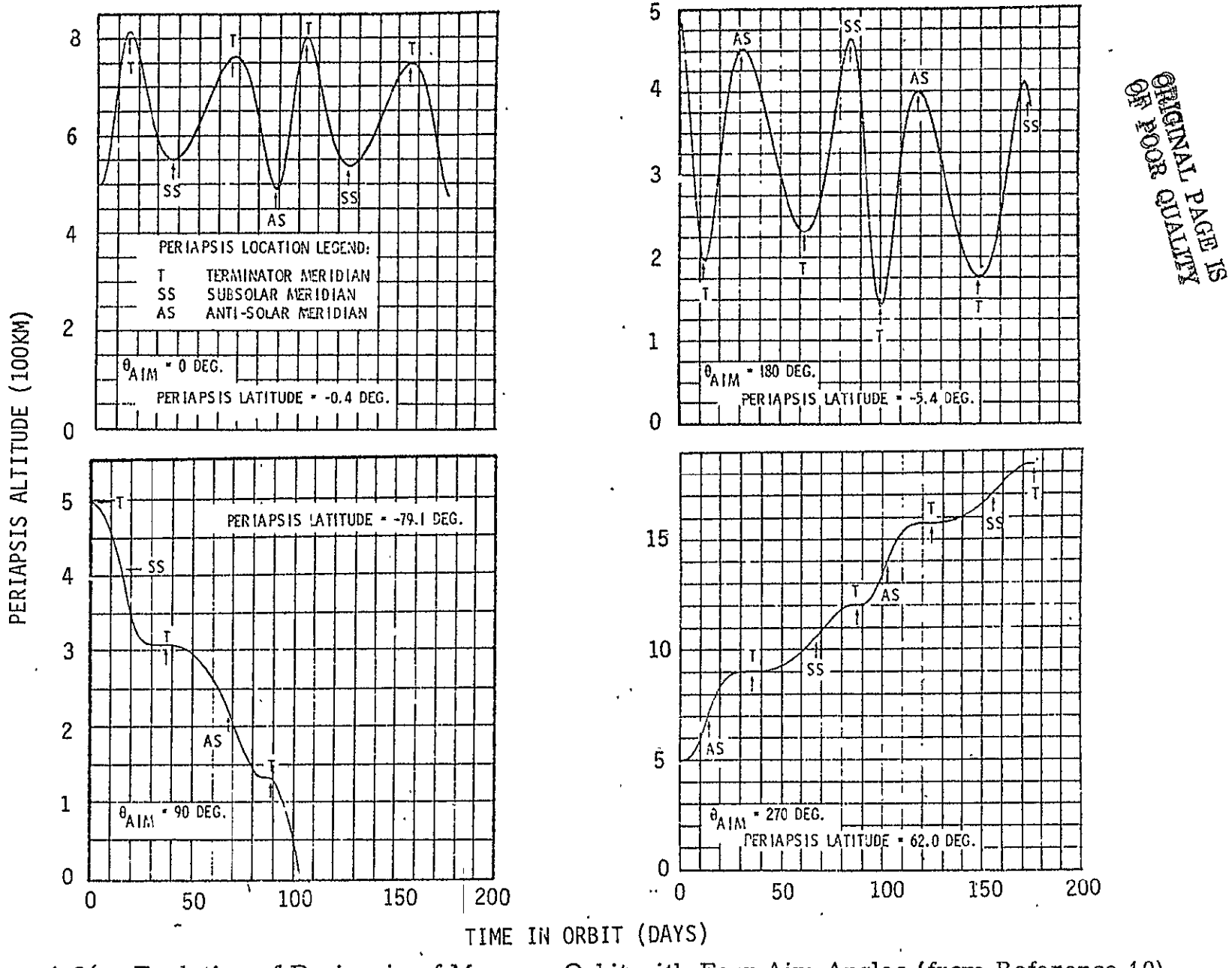

Figure 4-26. Evolution of Periapsis of Mercury Orbit with Four Aim Angles (from Reference 10)

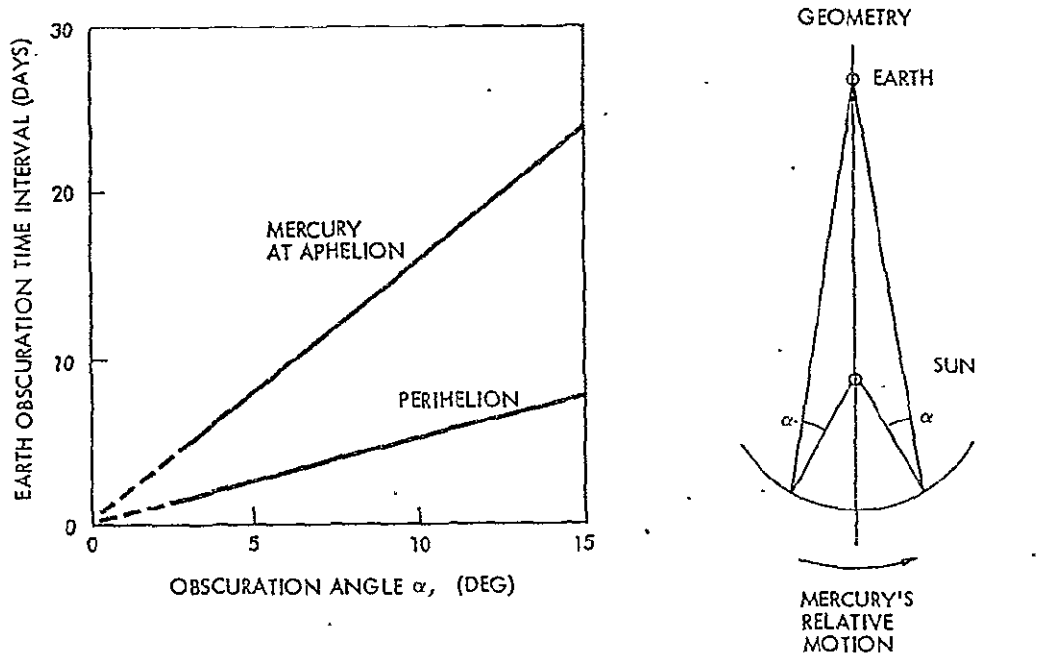

Figure 4-27. Communication Gap in Vicinity of Earth-Mercury Superior Conjunction

Mercury aphelion and perihelion, respectively. These times range between 5 and 16 days for an obscuration angle of 10 degrees.

Note that some of this communication gap is due to inability to receive useful radio signals within ±3 degrees of the center of sun's disk because of corona effects. A wider range of earth-spacecraft-sun angles perhaps as large as ±10 degrees is excluded to avoid focusing sun rays on the antenna feed, depending on design details. It can therefore be concluded that a significant communication gap is to be expected, not necessarily related to propulsion module accommodation and viewing geometry constraints.

4.6.4 Module B Outbound Missions

Deployment

The flight spacecraft is injected into the interplanetary trajectory by the solid kick motor SPM (1800) under the control of the payload spacecraft's attitude control subsystem. This method, already adopted for the MJS 1977 spacecraft, saves weight and cost for redundant guidance and control subsystem components but requires incorporation of an additional control mode into the system's attitude control computer.

After separation from the solid kick motor the flight spacecraft remains in the stowed configuration to perform a departure energy augmentation maneuver. Subsequently, the hinged RTG and experiment platform support arms and the experiment booms are deployed, and the vehicle assumes the cruise orientation.

Cruise Mode

In this mode the spacecraft is oriented with the Z axis (and hence, the fixed high-gain antenna dish) pointing at earth, and the X and Y axes in a roll attitude corresponding to star sensor alignment with respect to Canopus as reference star.

The spacecraft maintains this attitude throughout the mission (transfer and planetary orbit phases) except for interruption by main thrust maneuvers; by roll maneuvers required for planetary observation; and during the early part of the transfer phase when side-sun illumination of the propellant tanks is to be avoided (see discussion of Module A outbound mission cruise mode in Section 4.6.2).

Orbit-Insertion Mode

In principle, the spacecraft can perform orbit insertion at Saturn and Uranus in the earth-pointing mode, thereby retaining uninterrupted communications coverage before and during the maneuver, similar to the Pioneer outer-planet orbiter (Reference 6).

If desired for more effective orbit insertion or mission flexibility, e.g., for an orbital mission profile not consistent with earth pointing during orbit insertion (see Figure 4-24, Uranus orbit option II), the maneuver can be performed in any other attitude. For this it uses pitch and roll gyros to control departure from and return to the nominal cruise attitude, and to hold the commanded off-earth orientation during the maneuver phase.

Other Maneuver Modes

Major maneuvers using the propulsion module main engine include:

- An apoapsis maneuver at Saturn to raise periapsis altitude prior to orbital plane change. (Titan swingby maneuvers can be used to assist in orbit modifications.)

- A plane change maneuver at Saturn to convert the initial inclined orbit into a nearly equatorial orbit
- Maneuvers associated with satellite encounters at Saturn, possibly also at Uranus.

Reorientation from the cruise attitude is generally required except in the case of the periapsis raising maneuver at Saturn.

Small maneuvers for midcourse corrections, approach guidance and orbit trim can generally be performed through combined use of axial and lateral auxiliary thrusters, thereby avoiding repeated reorientation and loss of communications coverage.

4.6.5 Dynamics and Attitude Control of Module B

Dynamic characteristics and attitude control requirements of the three-axis stabilized system were analyzed to identify operating modes peculiar to the combination of payload vehicle and propulsion module(s), and to determine propellant mass allocations. The results presented in this section include:

- Limit-cycle characteristics
- Compensation of solar pressure unbalance
- Propellant mass settling and balancing
- Thrust vector gimballing requirements.

Limit-Cycle Operation

In the long-life missions considered here the propellant mass required for sustained limit-cycle operation exceeds other attitude-control propellant requirements, namely 1) those for spacecraft alignment with the changing earth or sun line and 2) those for orienting the spacecraft to and from a desired main-thrust maneuver attitude.

The propellant weight for pulsed attitude control thruster operation to maintain spacecraft orientation within a specified limit cycle deadband $\pm\theta_{LC}$ is given by

$$W_{P_{LC_i}} = \frac{F^2 \dot{t}_F^2 \ell t_M}{2 \theta_{LC} I_{sp} J_i} \quad (1)$$

for each axis of control, denoted by the subscript i, where

F = thrust force (each thruster)

t_F = pulse duration

ℓ = moment arm of thruster pair

t_M = mission duration (in seconds)

I_{sp} = specific impulse for pulsed thrust

J_i = moment of inertia around X, Y, Z axis, respectively.

Equation (1) applies to a symmetrical limit cycle with no external perturbing torque. The number of cycles is given by

$$n = \frac{1}{4} \frac{\dot{\theta}_{LC}}{\theta_{LC}} t_m = \frac{F t_F \ell}{8 \theta_{LC} J_i} t_M \quad (2)$$

where $\dot{\theta}_{LC}$ is the rate of change of θ between pulses. Each limit cycle includes two thrust applications.

Table 4-9 lists representative propellant expenditures and the number of limit cycles for typical Saturn and Uranus orbiters using either earth-storable or space-storable propellants, based on the following system characteristics, with hydrazine assumed as propellant:

F = 0.2 lb_f (0.91 N)

t_F = 0.03 seconds

ℓ = 12.8 ft (3.9 m)

θ_{LC} = 0.25 deg for fine pointing 0.75 deg for coarse pointing (during cruise)	limit-cycle rotations around X, Y axes
= 0.50 deg for fine pointing = 1.0 deg for coarse pointing	rotation around Z axis

Table 4-9. Limit-Cycle Characteristics of Mariner/Module B in Typical Saturn and Uranus Orbit Missions

Mission	Propulsion System Type	Number of Limit Cycles per Axis ($\times 10^3$)			Total Limit-Cycle Propellant kg (lb_m)
		X	Y	Z	
Saturn Orbiter	Earth-storable	51	160	29	23.8 (52.4)
	Space-storable	66	209	37	30.0 (66.2)
Uranus Orbiter	Earth-storable	56	152	33	23.9 (52.6)
	Space-storable	80	213	45	32.3 (71.2)

Assumptions:

- Saturn orbiter: 5-year transfer, 3-year orbit
- Uranus orbiter: 8-year transfer, 2-year orbit
- Limit cycle deadband:
  Coarse pointing X, Y axis 0.75 deg Z axis 1.0 deg
  Fine pointing 0.25 deg 0.5 deg
- Coarse pointing during cruise and 90 percent of orbit phase
  Fine pointing during 10 percent of orbit phase
- Minimum impulse bit: 0.2 lb_f thrust x 0.03 sec = 0.006 lb-sec (0.027 N-sec)
- Monopropellant hydrazine thrusters operate at 110 sec specific impulse in 30 millisec pulse mode.

I_{sp} = 110 sec (for 0.03 sec pulse length)

J_x, J_y, J_z as defined in Table 5-9.

For the Saturn mission a 5-year transfer time and 3-year orbital life is assumed; for the Uranus mission a transfer time of 8 years and orbital life of 2 years. Fine pointing is used during 10 percent of the orbital mission phase. Propellant expenditures range from 24 to 32 kg (52 to 71 lb_m). The number of limit cycles around the axis with the lowest moment of inertia (Y axis) is 209,000 and 213,000 for the two missions, respectively.

To limit the propellant expenditures and the number of pulses, a low thrust force and pulse duration was assumed. As noted in equation (1) the propellant mass increases with the square of the impulse bit, $F \cdot t_F$. Thus if both the thrust force and pulse duration were increased by 50 percent, with the impulse bit increasing from 0.006 lb sec (0.027 N sec) to 0.0135 lb sec (0.061 N sec), the propellant expenditure would increase by a factor of 5 and thus become prohibitively large.

Compensation of Solar-Pressure Unbalance Torque

In the Mercury orbiter mission, limit-cycle oscillations around the axis of the solar array (X axis) are affected by the strong solar pressure unbalance torque due to the offset of the sun shade center-of-pressure from the mass center. The limit cycles are no longer symmetrical and require only one pulse per cycle, i.e., equation (1) does not apply in this case. The propellant consumption is given by

$$W_{p_{SP}} = \frac{M_{SP} \cdot t_M}{I_{xp} \cdot \ell} \tag{3}$$

where

$M_{SP} = A_{diff} \cdot S \cdot Z_{offset}$ = solar-pressure unbalance torque

ℓ = moment arm of thruster pair

A_{diff} = differential area of sun shade and solar array varying with solar array rotation off the sun line

Z_{offset} = varying center-of-pressure offset from center of mass, due to propellant depletion and staging

S = solar pressure = S_o/r^2, with
$S_o = 0.92 \times 10^{-7}$ lb/ft^2 (2.18×10^{-7} N/m^2) at 1 AU.

The propulsion module design data give average solar-pressure unbalance torques of 0.32×10^{-4} ft-lb during the transfer and 1.413×10^{-4} ft-lb during the orbital phase (0.44×10^{-4} and 1.96×10^{-4} m-N) for the space storable system; 0.41×10^{-4} and 1.71×10^{-4} ft-lb (0.57×10^{-4} and 2.37×10^{-4} m-N) for the earth-storable system, respectively. Table 4-10 lists the propellant consumption for symmetrical limit cycles around the Y and Z axes, and for solar pressure unbalance compensation around the X axis for a Mercury orbiter with 2-year transit time and 2-year orbital life, assuming that fine pointing is required during 20 percent of the orbital life. Solar pressure compensation accounts for up to 50 percent of the total expenditure.

Table 4-10. Limit Cycle and Solar Pressure Compensation Propellant (in kg and lb_m) for Mariner/ Module B Mercury Orbit Mission

Propulsion System Type	Transit Phase		Orbit Phase		Total Propellant
	Solar Pressure Compensation (X Axis)	Symmetrical Limit Cycles (Y, Z Axes)	Solar Pressure Compensation (X Axis)	Symmetrical Limit Cycles (Y, Z Axes)	
Earth-storable	1.37	0.91	5.70	9.25	17.23
	(3.0)	(2.0)	(12.6)	(20.4)	(38.0)
Space-storable	1.08	1.95	3.96	13.79	20.78
	(2.4)	(4.3)	(8.7)	(30.4)	(45.8)

Assumptions:
- 2 years in transit, 2 years in orbit
- Thrust force 0.2 lb_f (0.91 N), pulse duration 0.03 sec
- Specific impulse 110 sec for 0.03 sec thrust duration
- Limit cycle deadband (Y, Z axes): coarse pointing — 1.0 deg (during cruise and 80 percent of orbit phase)
  fine pointing — 0.5 deg (during 20 percent of orbit phase)

Propellant Mass Settling and Equalization

A short period of low-thrust operation by the auxiliary (forward thrusting) axial thrusters is required to assure propellant settling prior to initiation of main axial thrust. This is necessary because

a) Initially the propellant mass may not be located over the drain vent, e.g., as a result of previous low thrust maneuvers in opposite direction

b) There may be a major initial mass unbalance between the two oxidizer or the two fuel tanks. This can be corrected by the propellant settling maneuver.

Even with the propellant mass located on the tank side opposite the drain vent, capillary ducts ("galleries") in the N_2H_4 tank are sufficient to initiate auxiliary thrust operation by the monopropellant thrusters. In the fluorine tanks the use of capillary ducts is avoided because of potential material corrosion problems in long life missions. Thus the propellant settling mode is mandatory in the space-storable application but also desirable in the earth-storable application for reasons stated under b) above.

Thrust Vector Gimballing

Thrust vector misalignment torques around the X and Y axes are nulled through activation of the two main-engine gimbals. With four propellant tanks adopted for Module B the largest gimbal deflections are required to compensate for unbalance of the propellant masses in opposite tanks. Conceivably an extreme condition could occur due to a slow propellant shift from one to the other tank, assuming the tanks are partially empty. Normally, the manifold lines between the tanks are closed off during main-thrust dormancy periods. However, they are interconnected in preparation for a main thrust maneuver. These conditions can be minimized by a propellant settling and equalization maneuver as discussed in the preceding paragraph.

Figure 4-28 illustrates the thrust vector offset angle required to control propellant mass unbalance. The angle is defined by

$$\alpha = \tan^{-1} \frac{X_p}{\ell_c - \ell_G} \cdot \frac{M_p}{M_T} \qquad (4)$$

where

X_p = tank distance from centerline

ℓ_c = height of mass center of entire spacecraft above tank location

ℓ_G = height of gimbal axis above tank location

M_p = differential propellant mass between left and right tank (unbalance mass)

M_T = total spacecraft mass.

Under extreme conditions a major propellant mass unbalance is possible during cruise and orbit phases such that the required offset angle α could increase to values greater than 20 degrees. Practical upper gimbal angle limits are 8 to 10 degrees.

Table 4-11 lists representative values of maximum mass unbalances $M_{P_{max}}$ that are within the correction capability of a gimbal angle of 8 degrees. These values change during the transit and orbit phases as a result of the changing total spacecraft mass M_T and center-of-mass location ℓ_T due to propellant depletion and staging. The table also shows

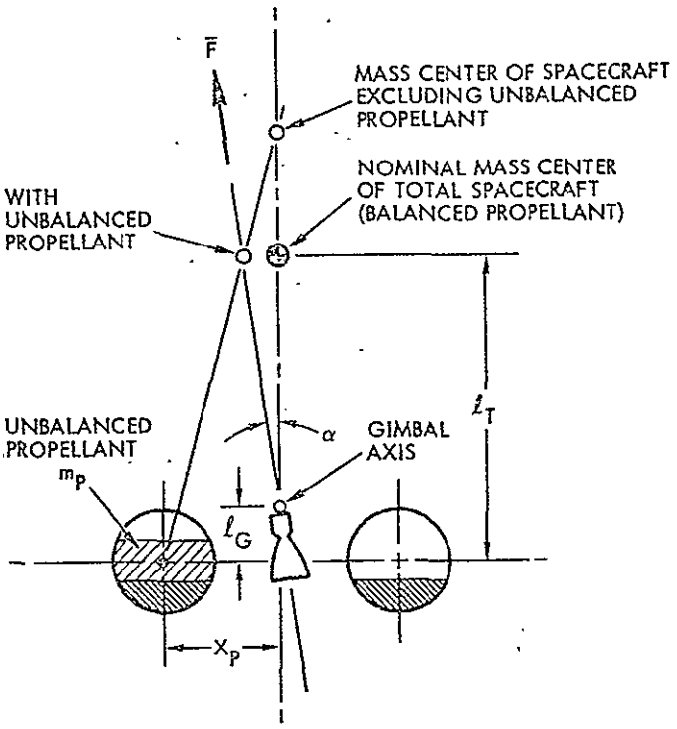

Figure 4-28. Thrust Vector Gimbal Deflection with Propellant Unbalance

Table 4-11. Maximum Permissible Propellant Mass Unbalance Controllable by 8-Degree Thrust Gimbal Deflection

Mission and Propellant Type	Mission Phase	Propellant Mass[1]		Maximum Permissible Unbalance Mass
		Oxidizer	Fuel	
Mercury Orbiter				
Earth-storable propellants	Transfer	614	364	425
	Orbit	27.2	18.1	83.0
Space-storable propellants	Transfer	292	203	294
	Orbit	27.2	18.1	83.9
Outer Planet Orbiter				
Earth-storable propellants	Transfer	614	364	96.6[2]
	Orbit	163	109	110[2]
Space-storable propellants	Transfer	292	203	90.2[2]
	Orbit	109	72.6	104[2]

[1] Each tank

[2] Propellant mass unbalance can exceed controllability limit: requires propellant equalization before main thrust initiation

the propellant mass contained in one oxidizer and one fuel tank, to indicate the potential for unacceptable mass unbalance conditions. It is apparent that propellant equalization prior to thrust initiation is necessary under these conditions.

Any residual mass unbalance is quickly reduced to zero after thrust initiation, with excess propellant flowing from the more fully to the less fully loaded tank achieving hydrostatic equilibrium.

4.7 PAYLOAD SPACECRAFT MODIFICATIONS AND INTERFACE REQUIREMENTS

Accommodation of the propulsion module(s) affects the payload spacecraft and requires configuration changes and subsystem modifications to various degrees depending on the specific mission to be performed. One of the ground rules followed in selecting the propulsion module design was to hold the impact on the payload spacecraft to a modest level.

In the foregoing sections, most of the required modifications of the payload spacecraft and interface requirements were discussed in the context of structural design, operational modes, attitude control, thermal interfaces, influence on communication performance, and power requirements. In the following paragraphs specific modifications and interface requirements for Pioneer class and Mariner class payloads and those affecting payload spacecraft in general will be summarized.

4.7.1 Spacecraft Modifications of Pioneer Class Spacecraft

Pioneer Inbound Mission

The required changes are primarily those imposed by the use of the large spin-deployed sun shade, i. e., influence on spacecraft dynamics and attitude control, and by the greater proximity to the sun in a Mercury orbiter mission than that for which the payload spacecraft was originally designed. The last requirement necessitates a change from the cylindrical to a conical configuration of the Pioneer Venus solar panels. In principle, the nominal cruise orientation and the communication mode of the despun, articulated high-gain antenna are retained in the new mission application.

The following specific changes in the payload vehicle are required in addition:

- Relocate thermal louvers to top of payload spacecraft
- Provide payload instrument insulation against spacecraft heat
- Eliminate auxiliary propulsion tanks, thrusters, etc., and place on propulsion module.

Pioneer Outbound Missions

The basic orientation and operation modes of the Pioneer outer planet spacecraft are preserved. However, the fundamentally different mass properties resulting from the addition of the propulsion module place the center-of-mass significantly below the deployment plane of the Pioneer spacecraft appendages. This necessitates the addition of a deployment counterweight to the magnetometer boom. A simultaneous boom deployment sequence is required.

Strengthening of the deployed appendages which cannot be retracted for high thrust operation becomes necessary and is accomplished partly by structural reinforcement and partly by spin rate increase. (The spin-rate increase is also required for increased attitude stability in the presence of unavoidable small torques due to thrust vector offsets from the center of mass.)

Thermal control design changes are necessary because of radiation blockage due to addition of the propulsion module. A detailed analysis of thermal balance will be required to determine whether the originally aft-facing louvers should be relocated on the side walls of the central equipment module.

The following specific changes in the payload vehicle are required:

- Relocate bottom-mounted payload instruments
- Remove auxiliary propulsion system and place on module
- Strengthen RTG and magnetometer booms to withstand 1/6 g maximum acceleration and magnetometer boom to accept larger deployment load

- Add deployment counterweight to magnetometer boom
- Provide spin-up logic to 15 rpm for thrust phases
- Relocate low-gain antenna and boom (possibly to aft structure of propulsion module if not jettisoned)
- Avoid side-sun conditions early in transfer phase by using low-gain/medium gain communication capabilities
- Possibly lengthen magnetometer boom because of stronger spacecraft magnetic field.

4.7.2 Modifications of Mariner Class Spacecraft

Mariner Inbound Mission

The payload spacecraft was originally designed to operate with its centerline pointing at the sun, using a frontal sun shade to protect all spacecraft elements but the solar array and the high-gain antenna. The Mariner Mercury orbiter, constrained to side-sun orientation by the dynamics of the orbit entry maneuver at Mercury, must use a side-mounted sun shade. This shade rather than the frontal sun shade is also used to protect the spacecraft during the cruise phase.

The solar array must be reoriented in accordance with the side-sun attitude requirement. Side-sun orientation of the spacecraft is compatible with earth coverage by the articulated high-gain antenna. A deployment arm extension is required to provide for better earth viewing past the propulsion modules and the side-sun shade.

For structural stiffening of the deployed solar panels against axial acceleration two guy wires are used, held by a support mast at the top of the experiment platform. The mast also supports the deployed magnetometer boom by a separate guy wire.

The following specific changes in the payload vehicle are required:

- Remove front sun shade and replace by side shade
- Relocate solar panel support structure
- Extend solar array rotation capability to conform with stowage and side-sun facing requirements

- Add guy wire supports and center mast to support solar panels against 0.48 g thrust acceleration
- Extend high-gain antenna boom deployment arm as required to give unobscured view to earth at all times
- Relocate magnetometer boom to clear side sun shade
- Remove auxiliary propulsion system and place on module.

Mariner Outbound Missions

The basic orientation and operation modes of the Mariner outer-planet spacecraft are preserved. The maximum thrust acceleration of only 0.1 g is small enough to be tolerated by the deployed RTG and experiment support booms which therefore need no structural strengthening. Experiment booms such as the 40-foot (12.2-m) magnetometer boom may require structural reinforcement or must be retracted during main thrust applications.

The following specific changes in the payload vehicle are required:

- Relocate low-gain antenna and boom (possibly to aft structure of propulsion module if not jettisoned)
- Strengthen magnetometer boom and possibly lengthen it because of stronger spacecraft and propulsion module magnetic fields
- Avoid side-sun conditions early in transfer phase
- Remove auxiliary propulsion system and place on propulsion module.

4.7.3 Design and Configuration Changes Affecting All Payloads

In addition to the specific changes discussed in the two preceding subsections, the following design and configuration changes are required on all payload spacecraft:

- Add data handling and telemetry capability for propulsion system engineering data
- Add command capabilities for propulsion module operation including automatic sequences as required

- Add electrical interfaces, modify electrical distribution and add propulsion module control electronics
- Add thermal control design features, especially in Pioneer Mercury orbiter (designed only for 0.7 AU solar approach distance); modify thermal control louver layout, etc.
- Add micrometeoroid protection as required by mission profile
- Modify payload instrument support features as required by propulsion module attachment
- Increase power capacity to meet heating requirements of propulsion module; provide for increased pulsed loads of added pyrotechnics and solenoids or servo-driven valves. Modify overall power budget as required.
- Change attitude control electronics to reflect new mass properties and large mass property changes, including staging effects.

4.8 ACCOMMODATION ON SHUTTLE ORBITER

Launch of Pioneer and Mariner class interplanetary spacecraft by the Shuttle orbiter and its upper stages imposes payload accommodation and interface requirements that are outside the scope of the present study. This study only addressed specific technical problems involved in accommodating the propulsion modules as part of the payload. Concurrent studies by Jet Propulsion Laboratory (Reference 5) have covered accommodation of Mariner class vehicles in greater depth.

Of particular concern are handling, loading, integration and general safeguarding of propulsion modules containing large amounts of hazardous propellants, especially fluorine. Safety of the Shuttle orbiter must not be compromised by this propellant load. The problem area was the subject of a concurrent separate TRW study sponsored by JPL (Reference 8). Results obtained in that study are reflected in the conclusions presented here.

4.8.1 Conformance with Cargo Bay Dimensions

Approximately half of the length of the cargo bay is used by the Shuttle upper stage which may be of the Centaur or Transtage class or, for higher performance requirements, the projected Space Tug.

Figure 4-29 shows typical stowage arrangements for Pioneer class Mercury and outer planet orbiters in the Shuttle cargo bay, assuming a Centaur D-1S upper stage. The deployment mechanism at the aft end of the cargo bay includes a trunnion on which the upper stage pallet can be rotated to the erect position, 45 degrees from the Shuttle centerline. It uses some of the available cargo bay length. Figure 4-30 shows the upper stage rotating 45 degrees from the stowed to the deployed configuration. The next step in the launch sequence, separation of the upper stage/payload vehicle stack from the cargo bay with the aid of the Shuttle manipulator arm, is not shown in the figure.

The configuration drawings (Figures 4-9, -13, -16, and -18) showed that the cargo bay provides ample space for the stowed payload vehicle because of reasonably short modules and interstage adapters. Table 4-12 lists the total length of each payload stack above the interstage adapter for the Pioneer and Mariner class vehicles both for inbound and outbound missions and the remaining unused cargo bay length.

4.8.2 Structural Interfaces

An important consideration in selecting the propulsion module configuration was to minimize bending loads by keeping the overhanging payload vehicle stack reasonably short. Structural analysis presented in Appendix C indicates that loads on the support structure, even for the heaviest gross payload weight considered, are not so large as to require a lateral support against the hull of the Shuttle, or an extended support pallet. This simplifies installation of the payload vehicle on the Shuttle orbiter and avoids attachment provisions on the side of the propulsion module.

Table 4-13 summarizes pertinent structural load characteristics during Shuttle launch, based on the acceleration load profile presented in Table 4-3. Structural analysis (Appendix C) showed that ascent loads are critical for central support cylinder and tank support truss design. The high forward-pointing accelerations that would occur during emergency landing are critical for the design of the separation rings and Vee-bands. These loads are alleviated by the fact that prior to abort

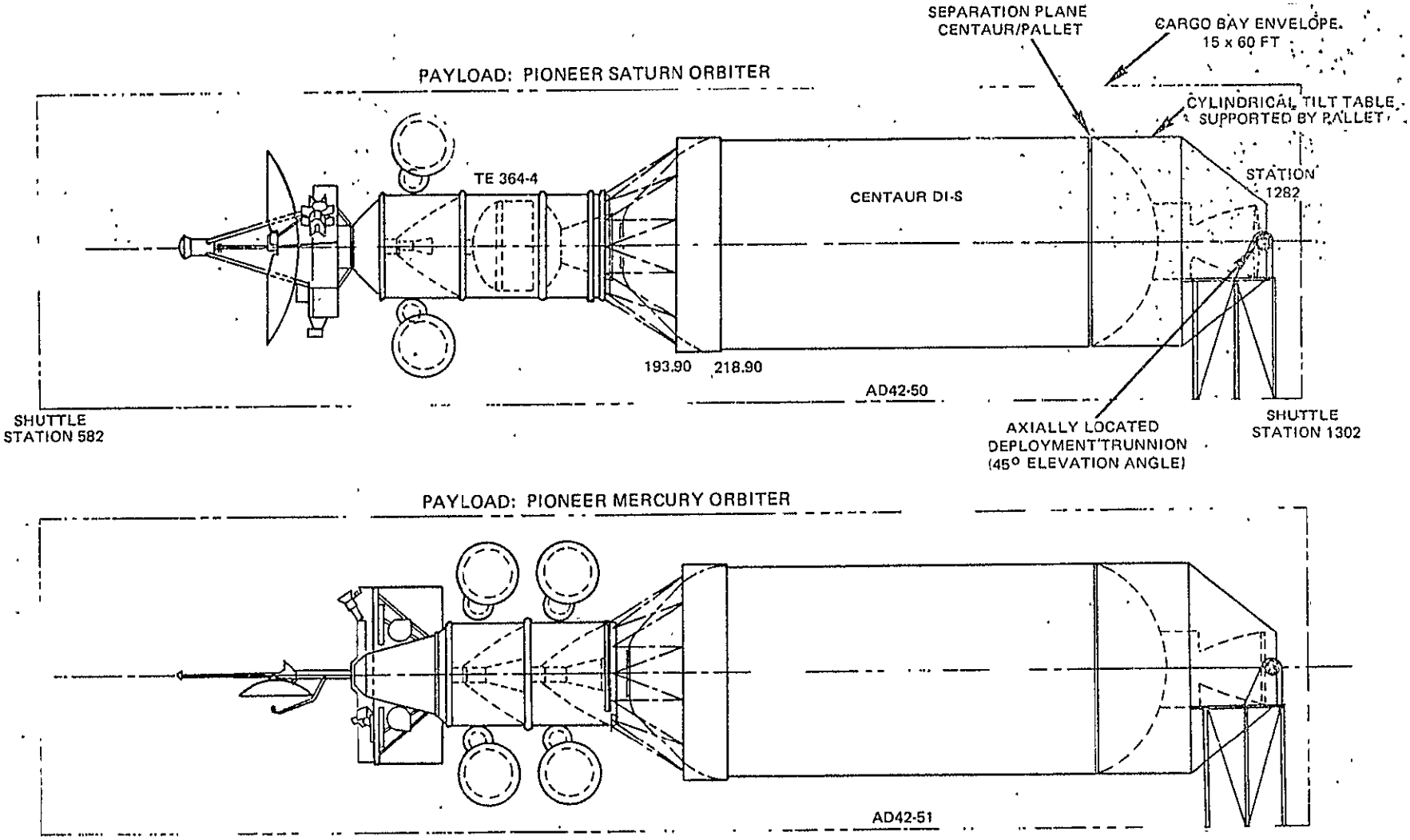

Figure 4-29. Stowage of Pioneer Class Spacecraft in Shuttle Bay

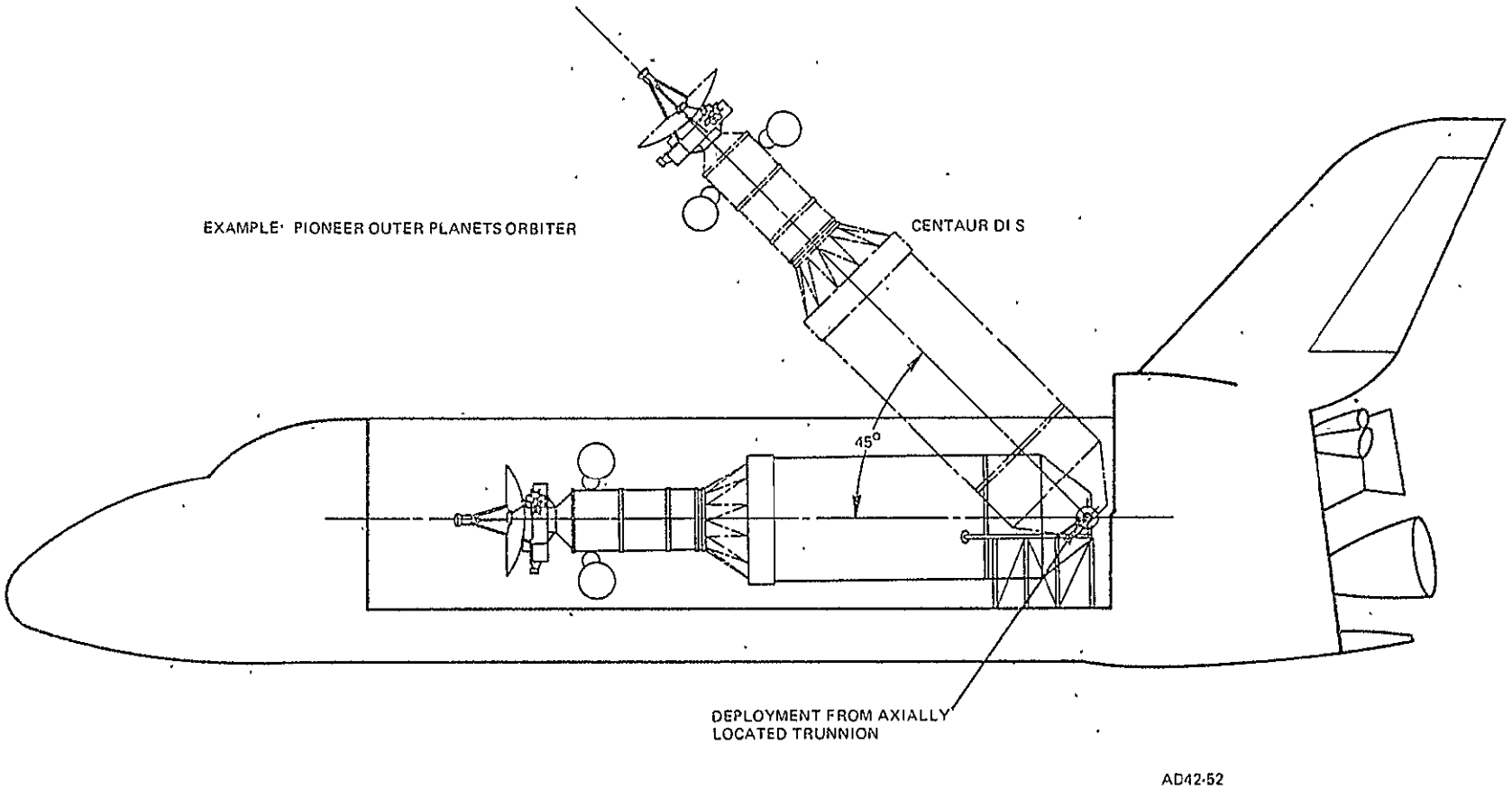

Figure 4-30. Deployment Procedure of Shuttle Upper Stage with Pioneer Orbiter

Table 4-12. Height of Total Payload Stack and Unused Cargo Bay Length for Three Mission Classes

Mission	Propulsion Module Type	Shuttle Upper Stage Assumed	Payload Stack Elements[1]	Total Height of Payload Stack[2] m (ft)	Unused Cargo Bay Length[3] m (ft)
Mercury orbiter	A	Centaur D-1S	P_{in} + 2 PM	6.23 (20.42)	2.01 (6.58)
	B	Space Tug	M_{in} + 2 PM	6.58 (21.58)	0.79 (2.58)
Outer planet orbiter	A	Centaur D-1S/SPM	P_{out} + 1 PM + SPM	6.05 (19.83)	2.16 (7.08)
	B	Space Tug/SPM	M_{out} + 1 PM + SPM	4.93 (16.17)	2.46 (8.08)
Comet missions	A	Centaur D-1S/SPM	P_{out} + 1 PM + SPM	6.05 (19.83)	2.16 (7.08)
Low ΔV-range	B	Space Tug/SPM	M_{out} + 1 PM + SPM	4.93 (16.17)	2.46 (8.08)
High ΔV-range	A	Centaur D-1S/SPM	P_{out} + 2 PM + SPM	7.45 (24.42)	1.02 (3.33)
	B	Space Tug/SPM	M_{out} + 2 PM + SPM	6.07 (19.92)	1.32 (4.33)

[1] Legend: P_{in}, P_{out}, M_{in}, M_{out} - Pioneer, Mariner, inbound, outbound

[2] Payload stack height measured from launch vehicle interstage adapter separation plane

[3] Data based on projected location of payload mounting flange of Centaur D-1S (Shuttle Station 946.18) and Space Tug (Station 935.99)

all propellants will be dumped overboard for safety reasons. The gross mass of the propulsion module(s) is thus reduced by up to several thousand kilograms.

Table 4-13. Structural Load Characteristics During Shuttle Launch*

Structural Elements and Loads		Module A		Module B	
		SS	ES	SS	ES
1. Central Support Cylinder					
Critical load condition		⑤	⑤	⑤	⑤
P_{EQ}	(lb_f)	100,600	64,400	168,500	103,800
M.S. on buckling		0.21	0.05	0.17	0.17
2. Main Tank Support Struts					
Critical load condition		⑤	⑤	⑤	⑤
Compression	(psi)	61,830	64,400	66,300	52,300
M.S. on compression		0.91	0.05	0.80	1.06
3. Separation System (Vee-band)					
Critical load condition		①, ②	①, ②	①, ②	①, ②
Required preload on band	(lb_f)	9,860	5,220	10,200	8,300
M.S. (preload)		0.26	1.39	0.22	0.50
Preload plus tension	(lb_f)	14,790	7,830	15,300	12,450
M.S. (tension)		0.35	1.55	0.30	0.60

Notes: Loading conditions are identified in Appendix C (see also Table 4-3).
① crash (axial loads), ② crash (lateral loads), acting in combination,
③ landing, ④ boost, ⑤ liftoff.
Stiffness critical design for support struts, Item 2, results in high margin of safety on compression
All loads are derived for Modules A and B in tandem
Propellant masses are those from first design iteration, Table 4-1 (conservative estimates)

*For detail and nomenclature, see Appendix C

4.8.3 Shuttle Safety Implications

Results of the concurrent study by TRW of safety implications of launching payload spacecraft with liquid fluorine propulsion systems have been reflected in the design concept. Of particular interest are the following:

- All handling and loading procedures must be conducted with the caution appropriate for handling hazardous propellants in large quantities
- Thermal protection of the cryogenic tanks is required during ground hold to avoid excessive temperature increase and overpressure
- Remote warning provisions must be available to alert ground handling and Shuttle crews of the occurrence of a leak, especially of fluorine
- Double-walled tanks are used for propellant retention in the event of a leak
- Provisions for safe dumping of propellants (especially liquid fluorine) must be available on the launch stand to prevent hazardous exposure of crews and equipment in the event of a leak
- Rapid disposal of propellants during the ascent and orbital phases must be possible in emergencies using available exhaust ports on the Shuttle hull.

Propellant dumping becomes necessary during the ascent or orbital phases either due to unsafe conditions on the propulsion module or as part of the abort preparation for other reasons. The oxidizer and fuel will be disposed of sequentially to preclude a hypergolic reaction. The corrosive oxidizers N_2O_4 or LF_2 dissipate rapidly on exhaustion from the dump line and thus do not pose a hazard to the Shuttle orbiter or any equipment carried by it.

Further discussion of safety implications and disposal of propellants will be presented in Appendix B.

4.8.4 Shuttle/Propulsion Module Interface Provisions

Figure 4-31 schematically illustrates interface provisions required to accommodate the propulsion module(s) on the Shuttle orbiter. It shows a coolant line for liquid nitrogen, to be used during ground hold for maintaining the cryogenic temperature on the LF_2 tanks; dump lines which separately connect to the oxidizer and fuel tanks; an electrical umbilical connector for power supply and control of the propulsion module prior to separation from the launch vehicle; and the structural interfaces at the launch vehicle adapter.

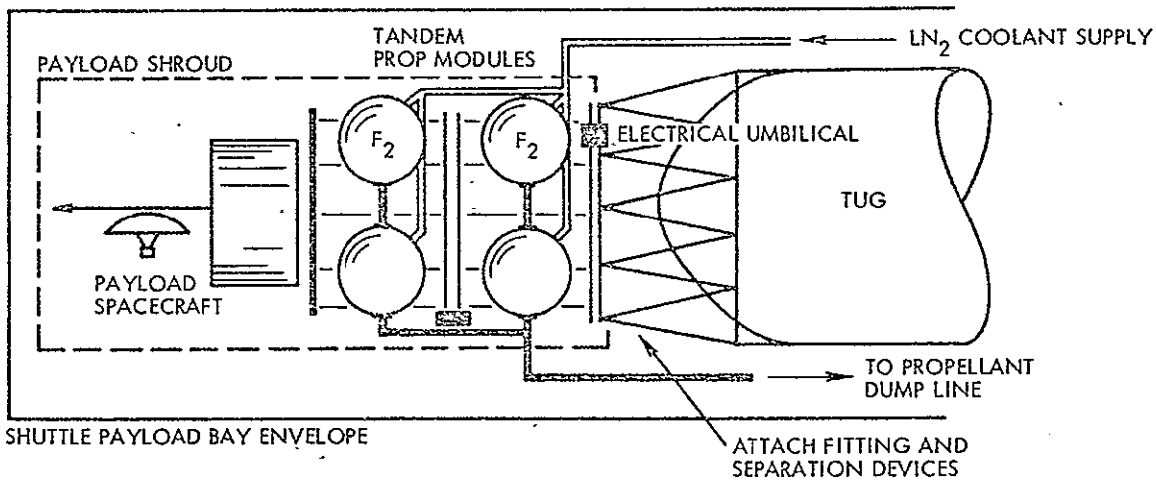

Figure 4-31. Shuttle Interfaces Schematic Considered in Propulsion Module Design

The JPL study (Reference 5) indicates a requirement for a payload shroud, primarily to protect against contamination and acoustic vibrations during the launch phase. Two options were explored by JPL (see Figure 4-32 and 4-33):

a) A disposable shroud removed from the Shuttle bay with the payload spacecraft and jettisoned prior to upper stage ignition

b) A reusable shroud remaining in the Shuttle cargo bay; extrication of the payload vehicle from the shroud by way of open clamshell doors.

Tradeoffs required in selecting shroud configurations involve weight, complexity, and cost. Study of shroud designs was outside the scope of this study. As seen on the design drawings, sufficient lateral space was allowed to install a shroud between the Shuttle bay and the payload vehicle.

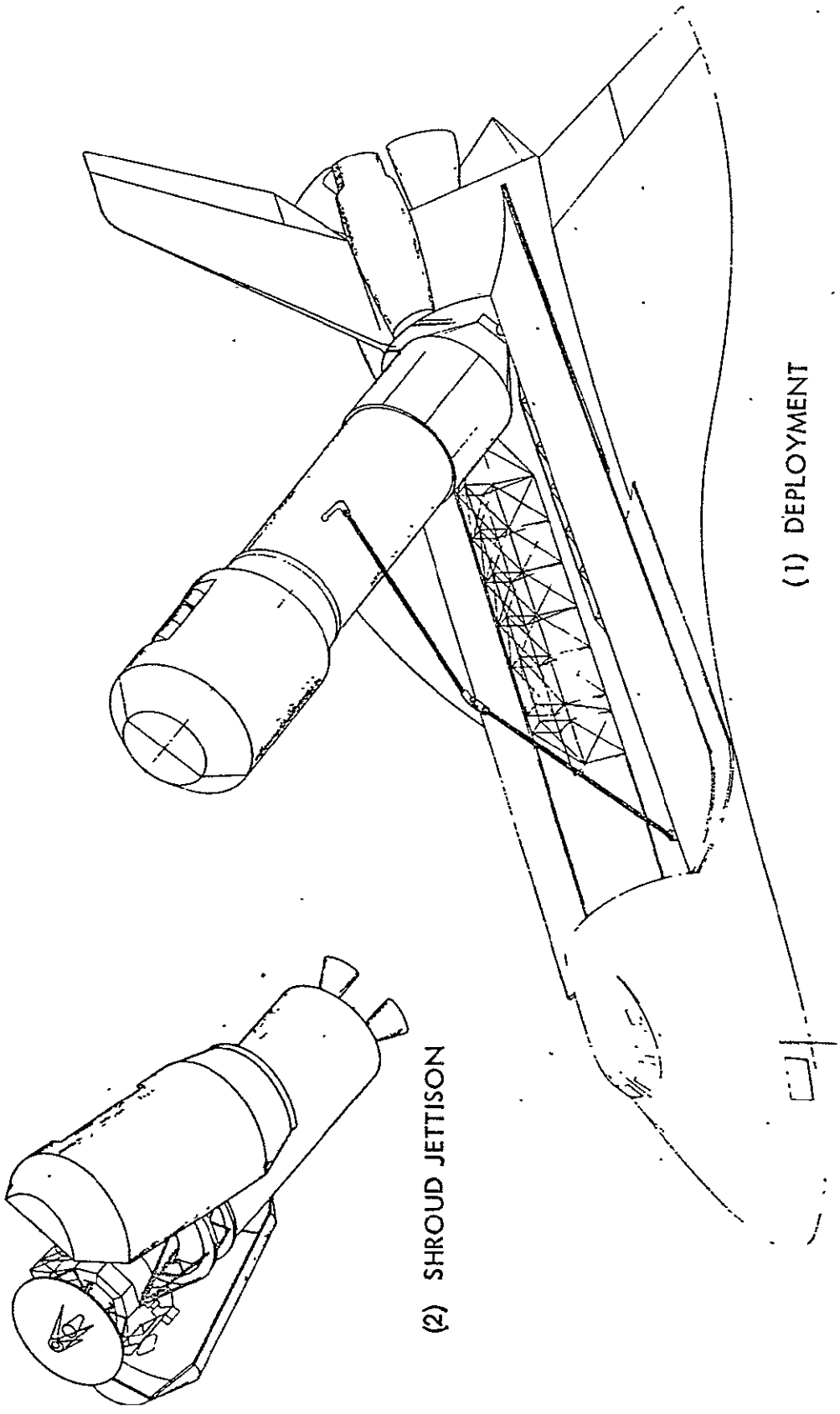

Figure 4-32. Disposable Shroud Concept (From JPL Study, Reference 5)

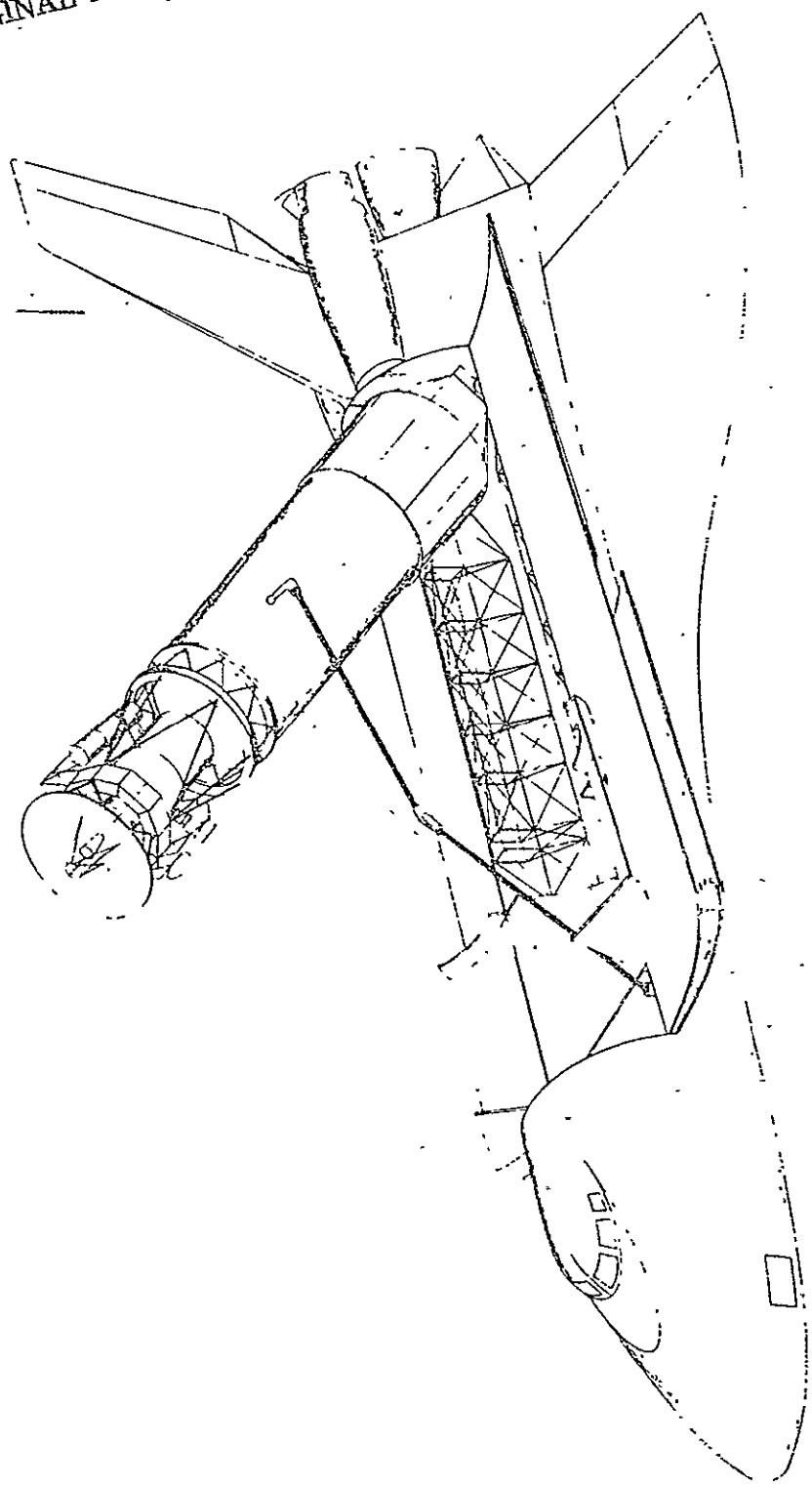

Figure 4-33. Reusable Shroud Concept (From JPL Study, Reference 5)

4.9 PROPULSION MODULE WEIGHT SUMMARY

Weight estimates for propulsion Modules A and B for space-storable and earth-storable propulsion systems are listed in Table 4-14. These estimates reflect the results of structural analysis (Appendix C) and include the updated results from the performance iteration (see Section 3.2). The total weights are in reasonably close agreement with inert weights used in the last step of the performance iteration.

Weight estimates for sun shades and support vary between 33 and 60 lb_m for the four propulsion module designs. The weight of ACS thruster assemblies (10 for Module A, 16 for Module B) is included in the propulsion subsystem. The comparatively low unused propellant weight (1 percent) is explained by the absence of expulsion bladders and the avoidance of surface tension devices in Module A (teardrop tanks) and in the oxidizer tanks of Module B. The weight estimates are conservative, allowing a 10 percent margin for structural weight uncertainty and 6 percent for overall weight contingencies.

Table 4-14. Multi-Mission Propulsion Module Weight Summary in kg (lb_m)

Component	Module A				Module B			
	Earth-Storable		Space-Storable		Earth-Storable		Space-Storable	
Structure	77	(170)	59	(130)	91	(200)	68	(150)
Primary	60	(132)	47	(104)	73	(160)	54	(120)
Secondary	10	(22)	6	(14)	10	(21)	7	(16)
Uncertainty (10%)	7	(16)	5	(12)	9	(19)	6	(14)
Propulsion Subsystem	89	(197)	74	(163)	118	(260)	100	(220)
Propellant tanks[1]	39	(87)	29	(65)	52	(115)	39	(85)
Helium tanks + helium	20	(44)	11	(24)	23	(51)	15	(33)
Engine	12	(26)	16	(35)	12	(26)	16	(35)
Gimbal system	-	-	-	-	10	(22)	10	(22)
Propellant control system	5	(12)	5	(12)	5	(12)	5	(12)
Lines and fittings	5	(10)	5	(10)	5	(10)	5	(10)
Heaters and RIIU's	1	(2)	1	(1)	1	(2)	1	(1)
ACS thruster assemblies	7	(16)	7	(16)	10	(22)	10	(22)
Thermal Insulation	5	(10)	5	(12)	4	(8)	4	(8)
Sun shade and Support[2,3]	18	(39)	27	(60)	15	(33)	15	(33)
Contingency (6 percent)	11	(25)	10	(22)	14	(30)	14	(25)
Propulsion Module Weight (dry)	200	(441)	176	(387)	241	(531)	198	(436)
Usable Propellant	894	(1971)	551	(1215)	1272	(2804)	781	(1722)
Unused Propellant	9	(20)	5	(12)	13	(28)	8	(17)
Total Inert Weight	209	(461)	181	(399)	254	(559)	205	(453)
Total Module Weight (Wet)	1103	(2432)	732	(1614)	1525	(3363)	986	(2175)

(1) Includes 20 percent for secondary tank wall

(2) Weights stated are for Mercury orbiters. Outer-planet orbiters require about 12 kg less for this item.

(3) Heat pipe would lead to about 10 kg weight reduction in Module A (space-storable)

5. PROPULSION SYSTEM DESIGN

5.1 DESIGN APPROACH, SYSTEM CONSIDERATIONS, AND TRADEOFFS

The propulsion system design approach followed in this study first established parametric characteristics for use in performance calculations, then defined preliminary configurations based on currently available technology or projected technology advances, and then finalized the four designs (i.e., for two payload classes each with two propellant combinations). Conservative design techniques were used to the extent possible. Study constraints specified by NASA are listed in Table 5-1.

Table 5-1. Specified Propulsion Module Characteristics and Design Constraints

A.	Propellants shall be F_2/N_2H_4 (fluorine/hydrazine) and N_2O_4/MMH (nitrogen tetroxide/monomethyl-hydrazine).
B.	The mixture ratio shall be nominally 1.5 for F_2/N_2H_4 and 1.65 for N_2O_4/MMH. Variation about these nominal values shall be made in order to achieve equal volumes of oxidizer and fuel tanks, taking into account the densities, residuals, and ullages for propellants.
C.	The thrust level of Module A shall be no greater than that which will result in a final acceleration of 0.4 earth g for the smallest payload, 340 kg (750 lb_m). The thrust level of Module B shall be determined from considerations of the effects of acceleration on the payload vehicle and on the penalties incurred due to finite thrust during capture at Mercury.
D.	The specific impulse shall in each case be assessed on the basis of thrust level, chamber pressure, expansion ratio, nozzle cooling requirements, and other factors that affect overall performance.
E.	Propellant tanks shall be nonvented and be designed with a burst safety factor of 2.
F.	Pressurization systems for oxidizer and fuel shall be separate and be designed to match the requirements peculiar to the propellant served. The pressurants shall be high-pressure helium unless it can be demonstrated that circumstances dictate another choice.
G.	The selection of materials for propellant tanks shall be based upon long-life compatibility of propellant and material, stage performance, and cost.
H.	Each multi-mission module shall have multiple restart capability to accommodate midcourse maneuvers, powered swingbys, planet orbital injection, orbital plane changes, and possibly orbital trim maneuvers.

Principal design and operations requirements include:

- Long storage in transit and between thrust operations up to 10 years storage in transit (References 1, 2)
- Long-life reliability
- Space Shuttle safety
- Severe thermal environment on the Mercury mission
- Numerous physical and thermal radiation interfaces with the payload spacecraft, the Shuttle orbiter and its upper stages.

For the earth-storable (N_2O_4/MMH) propellant combination, the entire design of the propulsion system was based on flight-proven technology. The design concept reflects TRW's experience with such earth-storable propulsion systems as the Multi-Mission Bipropellant Propulsion System (MMBPS) and was influenced by JPL's Mariner and Viking propulsion system designs which use comparable technology.

For space-storable propulsion systems, the design approach draws on the propulsion system previously studied by TRW under JPL contract NAS7-750, "Space-Storable Propellant Module Thermal Technology," (Reference 4) and on recent LF_2/N_2H_4 propulsion system developments by JPL. The design approach in this case cannot be based on flight-proven technology (at least not for fluorine). However, the design concepts formulated are consistent with ground test experience gained on technology programs for rockets and other systems using LF_2.

Design of the four stages was accomplished by:

- Selection of preliminary specific impulse and mass scaling characteristics
- Calculation of required propulsion system size
- Establishment of module (stage) configuration consistent with acceptable mass balance and flight stability criteria
- Layout of major propulsion elements, i.e., tankage and engine
- Definition of propulsion component characteristics
- Definition of actual propulsion component sizes.

The design progressed from tankage and pressurization considerations to engine considerations and engine design. As technology decisions were made, the basis for system parameter optimization was established. Key system parameter selections were engine thrust, chamber pressure, and nozzle area ratio.

5.2 SYSTEM DESCRIPTION

Key propulsion parameters are listed in Table 5-2. Schematic diagrams of the earth-storable and space-storable propulsion systems are shown in Figure 5-1. These schematics reflect a) the experience described above, b) concurrent work by TRW on JPL contract 954034 "Study of Safety Implications for Shuttle Launched Spacecraft Using Fluorinated Oxidizers," (Reference 8) and c) results of the present study.

The LF_2/N_2H_4 schematic is derived from that in contract NAS7-750 (Reference 4) which served as a state-of-the-art reference and point of departure. The technology of N_2O_4/MMH and LF_2/N_2H_4 propulsion systems is summarized in Tables 5-3 and 5-4. Materials considerations are listed in Table 5-5.*

The propulsion systems consist of separate fuel and oxidizer pressurization, tankage, and engine subsystems.

The helium pressurization subsystem consist of tanks, isolation valves, fill valves, filters, regulator valves, an optional heat exchanger, check valves, and servicing valves.

The helium pressurization bottles are connected thermally to corresponding propellant tanks. A single, separable joint upstream of the tank isolation valve allows pressurization system disconnection.

The tank (or propellant containment) assembly consists of the propellant tanks, an emergency relief valve with double redundant burst discs, isolation valves at the tank outlet and at the pressurization inlet ports, and remotely operated fill and dump valves.

Engine assemblies consist of two propellant filters, two orifices for adjusting mixture ratio; two engine control valves; and a thrust chamber assembly consisting of an injector, a combustion chamber and

*see also the technology review in Appendix A

Table 5-2. Key Propulsion Parameters

Parameter	Module A		Module B	
	N_2O_4/MMH	F_2/N_2H_4	N_2O_4/MMH	F_2/N_2H_4
Thrust N (lb_f)				
Selected thrust				
Outer planets orbiters	900 (200)[1]	900 (200)[1]	900 (200)[2]	900 (200)[2]
Mercury orbiter	3600 (800)[2]	3600 (800)[2]	3600 (800)[2]	3600 (800)[2]
Mass kg (lb_m)				
Module propellant, usable	894 (1966)	551 (1212)	1272 (2798)	781 (1718)
Module inerts	209 (460)	175 (385)	247 (543)	198 (435)
Payload spacecraft mass, inbound/outbound	340/408 (750/900)	340/408 (750/900)	550/680 (1213/1500)	550/680 (1213/1500)
Throw mass, inbound/outbound	549/617 (1208/1357)	515/898 (1133/1975)	797/927 (1753/2040)	748/878 (1646/1932)
Total initial mass	2547 (5603)	1792 (3942)	3588 (7894)	2508 (5518)

[1]Selection based on acceleration limit (rounded down)

[2]Selection based on upper size limit (800 lb_f in all cases)

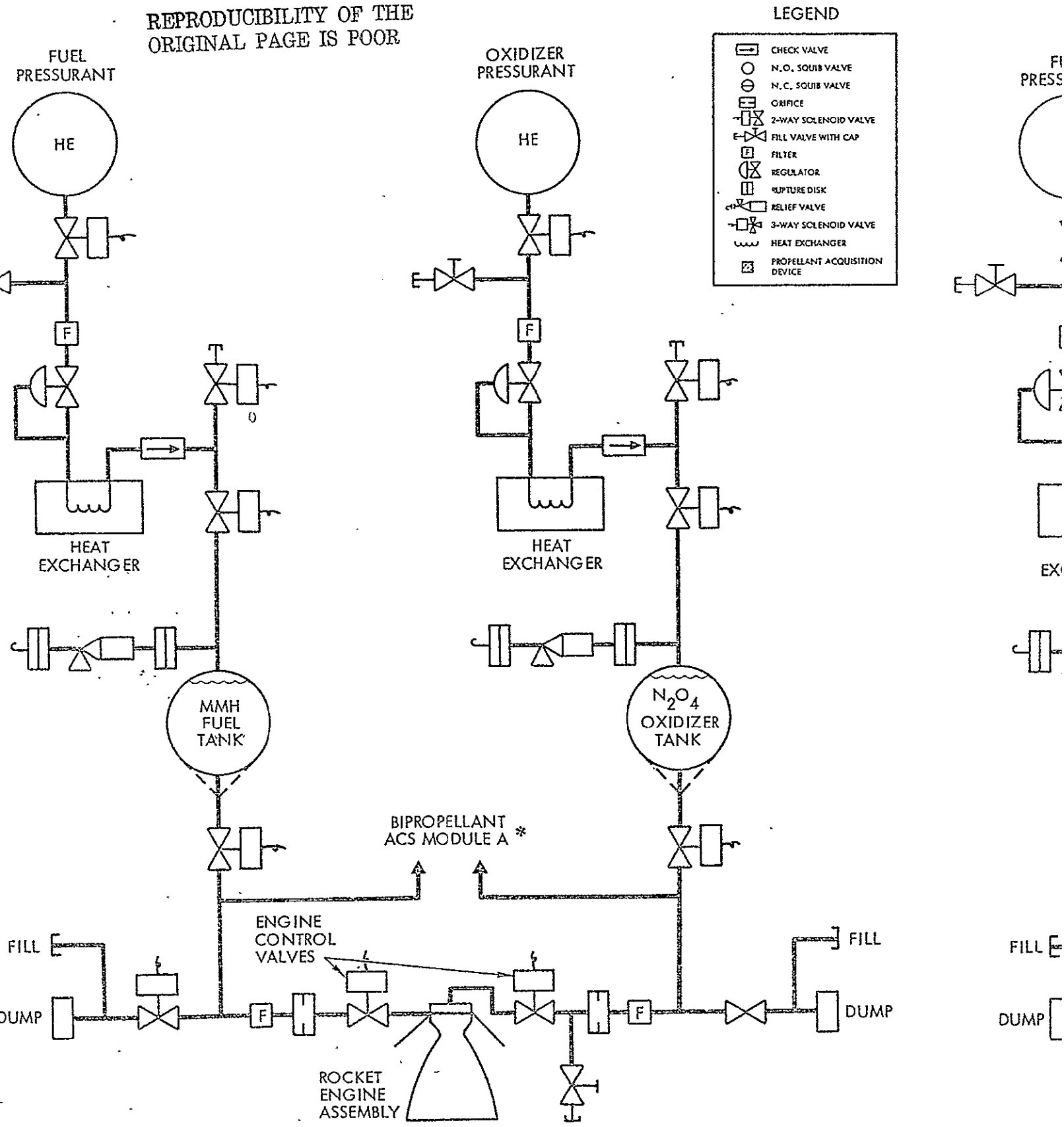

MODULE B USES SPACECRAFT ACS

A. N_2O_4/MMH SYSTEM SCHEMATIC

FOLDOUT FRAME 1

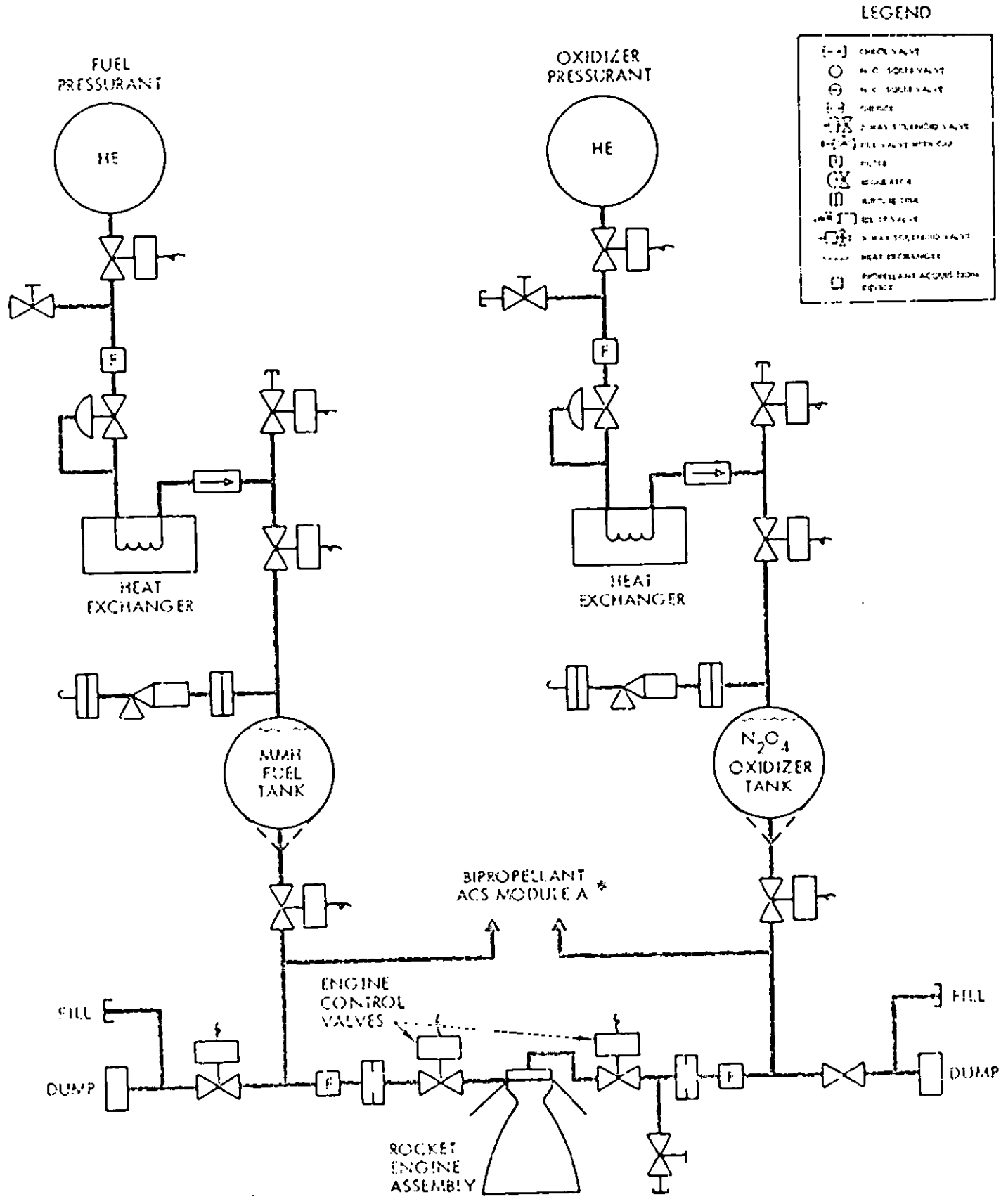

MODULE B USES SPACECRAFT ACS

A. N_2O_4/MMH SYSTEM SCHEMATIC

FOLDOUT FRAME 2

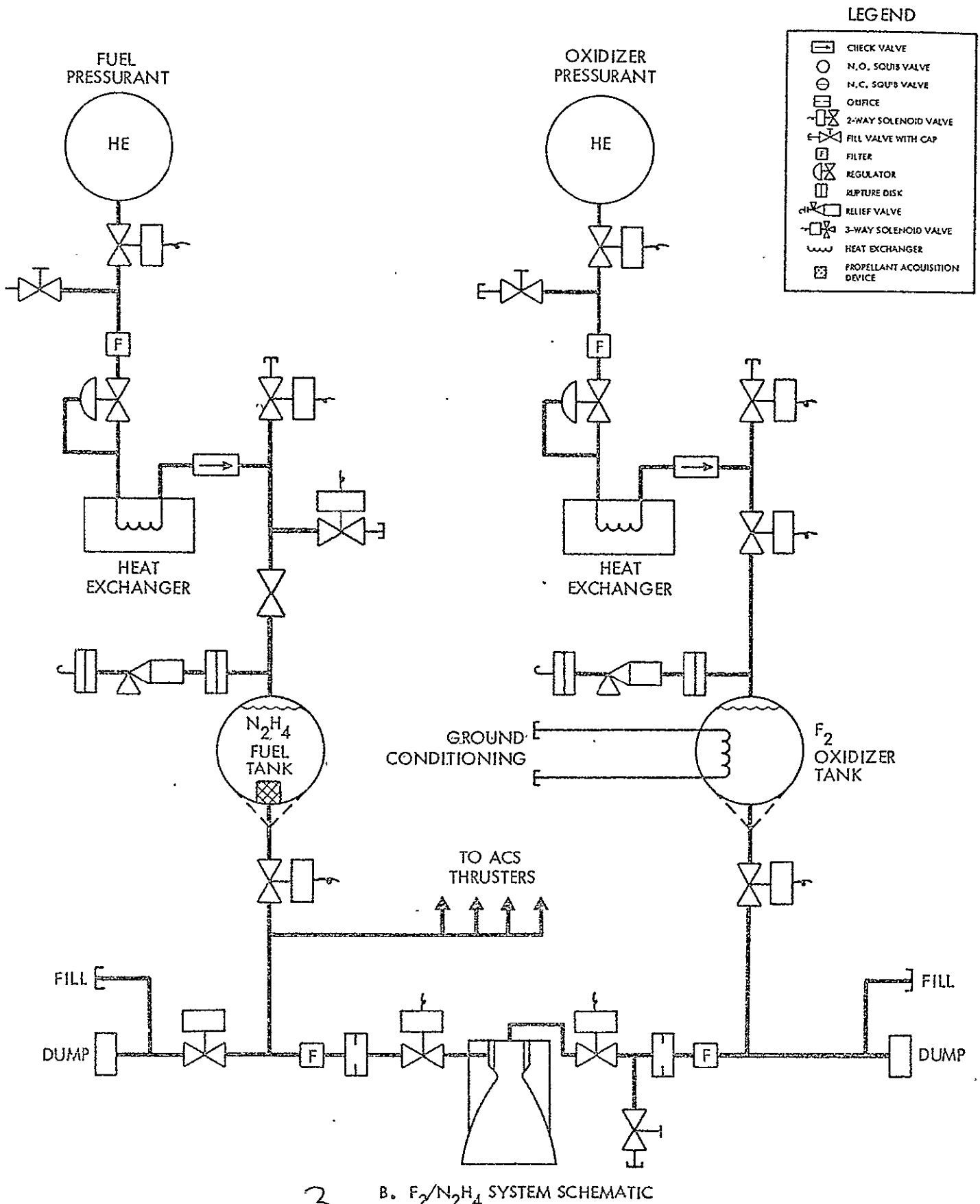

B. F_2/N_2H_4 SYSTEM SCHEMATIC

FOLDOUT FRAME 3

Figure 5-1. N_2O_4/MMH System Schematic

Table 5-3. Summary of N_2O_4/MMH Propulsion Technology

Component Area	Existing Technology (e.g., Mariner Mars '71)	Other Available Technology	Selected Technology
Propellant containment material kPa (psi)	Heat treated 6 Al-4V titanium σ_y = 1,120,000 - 1,225,000 (160,000 - 175,000), SF_B = 2	Alunimum, cryoformed stainless steel	6 Al-4V titanium σ_y = 1,120,000 (160,000), SF_B = 2
Pressurant containment	Annealed 6 Al-4V titanium	Heat treated 6 Al-4V titanium (160,000 psi)	Heat treated 6 Al-4V titanium
Pressurant isolation	Pyrotechnic-actuated piston shears parent metal	Electric motor actuated	Electric motor actuated
Propellant isolation	Pyrotechnic-actuated piston shears parent metal	Electric motor actuated	Electric motor actuated
Propellant acquisition	Bladders and standpipe	Centrifugal, surface tension	Settling by RCS/centrifugal
Engine operating modes	Bipropellant	Bipropellant/monopropellant dual mode	Bipropellant
Engine cooling method	Boundary layer conduction radiation nozzle, I_{sp} = 288 sec	Radiation cooled or ablative, I_{sp} = 296 sec	Radiation cooled I_{sp} = 296 min
Thermal control	Absorptivity emissivity control	Radioisotope heater units	Absorptivity/emissivity - inbound, RHu - outbound
Micrometeoroid protection	Aluminum honeycomb	Beta (quartz fiber) cloth	Titanium bumper or Beta cloth
Structure	Beryllium tube truss, magnesium and steel fittings	Titanium tube truss - aluminum fittings	Titanium tube truss - aluminum fittings
Typical Earth-Storable Performance Characteristics			
I_{sp}, sec	288-296 steady state		296^+ minimum, 310 nominal
Stage mass fraction, propellant/stage	0.85 approximately		Should be development goal

Note: σ_u ultimate strength, σ_y yield strength, SF_B burst safety factor

Table 5-4. Summary of Space-Storable Propulsion (F_2/N_2H_4) Technology

Technology Area	Imminent Technology	Other Available Technology	Selected Technology
Propellant containment	6 Al-4V titanium	2219 aluminum or nickel liner	6 Al-4V titanium (double-wall for LF_2)
Propellant isolation	Aluminum, nickel or gold metal-to-metal seals		Nickel metal-to-metal seal
Propellant acquisition	Capillary devices	Settling by RCS	Settling by RCS or centrifugally
Engine operating modes	Bipropellant or dual mode		Bipropellant
Engine cooling method	Graphite/ablative with throat insert	Graphite radiation cooled, pyrolytic or other graphite	Graphite/ablative
Propellant thermal control/micrometeoroid protection	PBI insulation, Beta cloth overwrap	Aluminum honeycomb	PBI insulation, Beta cloth overwrap
Expected Performance Characteristics			
I_{sp}, sec	363-376		370 minimum, 376 nominal
Stage mass fraction	0.85 approximately		Should be technology goal

Table 5-5. Materials Selection* for Use with LF_2

Application	Candidates	Status	Selected
Tankage	Titanium 6 Al-4V	Promising - under investigation	Titanium,** may use nickel liner
	Aluminum 2219	Promising	
	Stainless steel	Proven for ~8 years service on ground	
Lines	Titanium	If available	Titanium** or nickel liner
	Stainless steel 304L	Alternate	
	Monel		
Controls	Nickel alloys	Preferred	Propellant isolation
	Stainless steel	Often used. Should be satisfactory for this application except propellant isolation valve.	Engine oxidizer valve, if not nickel

*In passivated state with propellant-grade LF_2

**Tentative, based on JPL test data

deLaval nozzle. Engine assemblies are separable by a single joint upstream of the propellant filter on the engine assembly.

Thrust is initiated by opening the pressurant and tank isolation valves, allowing time for line filling and stabilization, and actuation of the engine control valves. Thrust is terminated by closing the engine control valves. Prior to main thrust initiation, a short period of auxiliary thrust operation is required on the three-axis stabilized system (Module B) to assure propellant settling (see Section 4).

In the case of an extended shutdown where oxidizer is trapped in the propellant line between tank and engine, the line can be cleared by venting first fuel, then oxidizer, to space. Depending on the thermal characteristics of the final configuration, such dumping of fuel may not be necessary.

5.3 PROPELLANT STORAGE AND ACQUISITION

5.3.1 Tankage Requirements and Materials

Placement of tanks and selection of the four-tank configuration was discussed previously in Section 4. Table 5-6 summarizes requirements for the tanks. The tankage material selected for the earth-storable

Table 5-6. Propellant Storage Criteria

Requirements

F_2, N_2O_4, N_2H_4 and MMH propellants

Micrometeoroid protection

Propellant tanks shall be nonvented and be designed for a burst safety factor of 2

Propellant tank/attachments designed for 3-g launch acceleration (upper stage acceleration of about 5 g)

Potential requirement for 9-g crash landing

Suggested Additional Criteria (determined in the study):

Up to 10-year storage

System designed for storage at less than 1/4 operating pressure

Pressurized tanks shall not fragment in the event of failure (leak-before-burst criterion)

Minimum number of components "wet" with oxidizer during Shuttle transportation

A possible requirement for propellant dump capability to be determined

Typical Operating Characteristics for Propellant Tanks are:

Operating pressure, typical 21.3 bar (300 psia)

Storage pressure, maximum 1-11.2 bar (14.7-165 psia)

Storage conditions, typical, in transit to planet

	Temperature °C (°F)	Vapor Pressure bar (psia)	Blanket Pressure bar (psia)
F_2	-188 (-306.6)	1 (14.7)	None
N_2O_4	21.2 (70.1)	1 (14.7)	He at 1 (14.7)
N_2H_4	25 (77)	0.02 (0.278)	He at 1 (14.7)
MMH	25 (77)	0.065 (0.960)	He at 1 (14.7)

N_2O_4/MMH propellants is 6A1-4V titanium alloy, used on the TRW MMBPS, JPL Mariner, and JPL Viking propulsion systems.

For the space-storable LF_2/N_2H_4 combination, recent testing by JPL indicates the suitability of 6A1-4V with LF_2. This titanium alloy, significantly lighter than aluminum alloy 2219 and other materials has been selected for its higher system performance.

5.3.2 Propellant Acquisition

Module A

Main propellant acquisition for Module A is provided by centrifugal force for both main propellants. For the N_2O_4/MMH system, bipropellant ACS thrusters operating from the main propellant tanks are used. For the LF_2/N_2H_4 system, monopropellant ACS thrusters operating from the main N_2H_4 tank are used.

Module B

Propellant acquisition for Module B main propellants (LF_2/N_2H_4 or N_2O_4/MMH) is provided by settling thrust from the ACS system, except for the N_2H_4 tank which uses a capillary device. In the LF_2/N_2H_4 stage the same capillary device also feeds the ACS system. For the N_2O_4/MMH system, both propellants are settled by the monopropellant ACS operating from a separate N_2H_4 tank containing a capillary device.

The use of capillary acquisition devices is considered permissible in the fuel tanks but not in the oxidizer tanks. Other techniques, including the use of a "trap tank" and check valve (to trap enough propellants so the main thruster can provide its own settling), have been used on previous systems. However, they were rejected because they require considerable development and may introduce reliability problems.

These selections for Modules A and B were based on the following reasons:

1) Teflon bladders are used for earth-storable propellants in present N_2O_4/MMH systems. Teflon compatibility with LF_2 is not suitable for LF_2 applications. In addition, bladders and capillary acquisition devices require significant effort to develop and have possible failure modes.

2) No suitable data is available to confirm the suitability of capillary devices with either N_2O_4 or LF_2 for storage periods as long as 10 years. There is a possibility of malfunctions due to corrosion products from the capillary ducts which could clog filters or engine injectors downstream. Thus, capillary acquisition devices were limited to the more benign N_2H_4 tankage on the basis of reliability and least technical risk (Reference 33). The Martin Company indicates the possible

feasibility of capillary devices for LF_2 by immersion tests of such devices for test periods of 30 days. However, the corrosion mechanism of LF_2 acting over longer periods (up to 10 years) and stress corrosion was not considered. TRW tests of aluminum and titanium materials in LF_2 indicated significant corrosion continuing after several months (Reference 18).

5.3.3 Propellant Tankage Configuration – Spinner

For Module A, the spinning spacecraft, initial propellant position is known. Centrifugal force orients the propellants away from the spin axis. After axial thrust has been applied, propellants settle into a position which depends on the relative centrifugal and axial acceleration forces.

Tanks having conical drainage spouts tangent to the sphere both at the lowest point (when it is in a vertical attitude) and at the outermost point (for the spinning case) are recommended. This allows propellant acquisition and complete drainage under all conditions of spin and acceleration and during ground handling with minimum use of tank penetration and welds. The use of teardrop-shaped tanks with 90-degree included angle conical spouts is simple, reliable, and consistent with the goals of this study. This acquisition and drainage technique is used on hydrazine tanks in a spin-stabilized earth orbiting spacecraft built by TRW.

5.3.4 Propellant Tankage Configuration – Three-Axis Stabilized System

The three-axis stabilized payload vehicle operates in a limit-cycle attitude-control mode with initial propellant position unknown. Some positive propellant acquisition method or settling by the attitude control system is required.

A small spout at the bottom of the tank allows complete drainage in ground handling and in flight. Propellant settling thrust is required prior to main engine operation and can be accomplished with a hydrazine thruster as described earlier.

5.3.5 Redundant Tank Wall for Oxidizers

Because of the potential hazard of leakage of LF_2 or N_2O_4 oxidizer into the shuttle cargo bay, use of a double wall tank was considered in other studies as a safety precaution (Reference 8). For this study, it was assumed that a double wall would be required by NASA for LF_2 but not for N_2O_4. The second fluorine tank wall would also require passivation. With adequate spacing the second wall can serve also as a micrometeoroid bumper shield. The weight of such a wall is estimated to be about 25 percent of the basic tank weight.

5.3.6 Propellant Storage Thermal Effects

Thermal Operating Conditions

For best engine operation, the propellants must be at predictable temperatures so that flow rates are reproducible. The earth-storable propellants can be maintained at a comfortable range above freezing by insulation and heaters.

The liquid fluorine for the outbound missions and Mercury mission with Module B, can be maintained at a convenient temperature near its normal boiling point. Thermal analysis of the Pioneer class Mercury orbiter (tandem configuration, Module A) indicated that space storage of liquid fluorine must be accomplished at a higher temperature than for the outbound missions. By using a deployed cylindrical sun shade of 15-foot radius with the selected configuration, the lowest fluorine storage temperature that can be achieved is about 117°K (-250°F). At this temperature, vapor pressure is 11.2 bar (165 psia) and specific gravity of the liquid fluorine is only 1.25.

With this increased storage temperature, the propellant tanks must be large enough to accommodate the fluorine at this temperature and the engine must operate with the fluorine in this condition.

The temperature margin during launch and deployment is at least 30°C (55°F) assuming 86°K (-305°F) storage on the ground. Less pressurization gas will be required since vapor pressure augments this function.

As a consequence, the design chamber pressure of the engine always must exceed the vapor pressure (approximately 11.2 bar (165 psia)). The desired engine combustion chamber pressure thus is at least 200 psia. This also conforms with preliminary chamber-pressure optimization results dictated by other factors. The current state of technology suggests limiting the design chamber pressure to 13.6 bar (200 psia).

5.3.7 Tank Size and Mixture Ratio

Tank sizes were dictated by propellant requirements of the Mercury orbiter mission with a 10 percent additional total volume above the margins required for thermal expansion, outage, ullage, etc. Further constraints were equal tank size for cost effectiveness as required by study guidelines.

The resulting propellant storage conditions are shown in Table 5-7. Storage conditions for earth-storable propellants are comparable to present systems. Tank size allocations are given in Table 5-8.

The desired mixture ratio for the earth-storable propellants was achieved without difficulty. However, thermal expansion of the LF_2, caused by the high temperatures near Mercury, decreases the LF_2/N_2H_4 misture ratio below optimum of 1.5 if tanks were fully loaded originally. The near-optimum mixture ratio of 1.5 still could be achieved by increasing the tank size or by putting all propellant reserve (20 percent) in the N_2H_4 tank and using part of the fuel as monopropellant in the auxiliary thrusters. The latter solution permits flexibility in fuel (N_2H_4) allocation between primary and auxiliary thrust functions and helps to maintain a favorable mixture ratio in spite of the large margin of LF_2 thermal expansion.

5.4 PRESSURIZATION SUBSYSTEM

Pressurization subsystem weight is significant because the volume of gas at tank pressure must generally equal the volume of the propellant tank. The weight of the pressurant helium bottle approximates the weight of the tank.

Table 5-7. Propellant Storage Conditions

Properties	F_2	N_2H_4	N_2O_4	MMH
Assumed maximum storage temperature, °K (°F)	130 (-230) Vapor pressure = 300 psi*	322 (120)	322 (120)	322 (120)
Specific gravity at maximum temperature	1.1	0.98	1.375	0.84
Density at maximum temperature, kg/l (lb/ft^3)	1.0 (68.6)	9.98 (61.5)	1.375 (85.8)	0.84 (53.0)
Operating nominal temperature, °K (°F)	85.5/117 (-306**)/(-250***)	294 (70)	294 (70)	294 (70)
Specific gravity****	1.5	1.01	1.45	0.87
Density at nominal temperature, kg/l (lb/ft^3)	1.5/1.25 93.6/78***	1.01 (62.4)	1.45 (90.5)	0.87 (54.3)
Mixture ratio, equal volume*****	F_2/N_2H_4 1.50		N_2O_4/MMH 1.69	

*Based on conservative assumption that propellant can expand until vapor pressure equals maximum tank operating pressure during Shuttle ascent and preseparation phase in orbit. This allows approximately 18°F of heat rise from a Mercury heat pulse.

**Normal boiling point

***Mercury orbiter only

****At nominal temperature

*****Tanked for maximum temperature, nominal tank sizing

Table 5-8. Tank Size Allocations for Equal-Volume Tanks

F_2/N_2H_4 Tank Volume = MPU*/4 x 904 kg/m^3 (56.5 lb/ft^3)

N_2O_4/MMH Tank Volume = MPU/4 x 797 kg/m^3 (49.8 lb/ft^3)

Items included in tank volume margin (percent):

	LF_2	N_2H_4	N_2O_4	MMH
Thermal expansion	36.3	3	5.5	3.6
Outage	1	1	2	2
Ullage	0	6	1	1
Acquisition	0	0	1	1
Propellant reserve	0	20	9	11
Miscellaneous	1	1	1	1
	38.3	31	19.5	19.6
Mixture ratio, equal-volume tanks	1.50		1.69	

Conclusions:

1) Tank sizing o.k.
2) Mixture ratios can be as shown above
3) I_{sp} performance previously presented
4) No need to change conservative assumptions if 10 percent propellant reserve
5) Common tanking of RCS propellant further improves F_2/N_2H_4 mixture ratio

*MPU - mass propellant usable

The weight can be lowered if exhaustion of pressurant occurs prior to exhaustion of propellant causing tank pressure to fall at the end of the operations. This slightly reduces thrust and limits maximum thrust acceleration of the vehicle. With separate helium pressurization systems for fuel and oxidizer, storage bottle material, storage pressure, storage temperature, and the need for a heat exchanger are main considerations.

Titanium alloy 6 Al-4V was selected for pressurant bottles. The potential weight savings of fiber composites does not justify the additional costs and technical risk involved in long-period storage. For the earth-storable propellants N_2O_4 and MMH cryogenic storage of pressurant is unnecessary. For liquid fluorine, cryogenic storage of the pressurant is essential. For example, storage at room temperature increases bottle weight by the ratio of the storage temperatures (e.g., for room temperature versus 86°K (-305°F), the ratio is $\frac{294°K\ (530°R)}{86°K\ (155°R)} = 3.42$). For the LF_2 pressurant tank, pressurant storage at cryogenic temperatures with pressurant bottles thermally connected to the LF_2 tank was selected. A good thermal path prevents the helium from becoming overpressurized during ground and launch operations or because of thermal conditions at Mercury.

Heat exchange sources to raise the temperature of the helium prior to its application to the propellant were evaluated because expansion in the helium pressurant bottle results in chilling of the helium remaining in the bottle; the quantity of helium needed depends on its temperature in the propellant tank; and use of helium with a lower temperature than the propellant can overpressurize the tank after a firing.

The preferred range of temperature differences between the pressurant gas and cryogenic propellants is typically from 0 to 56°K (100°R) over propellant temperature. Potential heat sources are the propellant being used, engine heat, and heat in the structure. The selected method is use of the N_2H_4 to heat the pressurant.

5.5 ENGINE DESIGN

5.5.1 Design Considerations

Desired characteristics for the engines based on mission requirements and state-of-the-art practice are summarized in Table 5-9.

Table 5-9. Desired Engine Characteristics

Characteristics	Module A		Module B	
	N_2O_4/MMH	LF_2/N_2H_4	N_2O_4/MMH	LF_2/N_2H_4
Propellant to consume, kg (lb_m)	894 (1967)	551 (1212)	1272 (2798)	781 (1718)
Thrust levels, outbound/Mercury, N (lf_f)	900/3600 (200/800)	900/3600 (200/800)	900/3600 (200/800)	900/3600 (200/800)
Chamber pressure, bar (psia)	7-14 (100-200)	14 (200)	7-14 (100-200)	14 (200)
Mixture ratio	1.6	1.5	1.6	1.5
Operating duration, sec	2852/713	2278/569	4057/1014	3230/807
Allowable cooling methods	Radiation, ablative, regenerative, duct	Graphite lined, ablative	Radiation, ablative, regenerative, duct	Graphite lined, ablative
Selected cooling method	Radiation	Graphite lined, ablative	Radiation	Graphite lined, ablative
Specific impulse, sec				
Deliverable, sec	295-300	376	300-310	376

For the earth-storable propellant combination N_2O_4/MMH, directly applicable data and data on the closely related N_2O_4/Aerozine 50 (A-50) propellant combination is available. From this data, parametric data can be directly taken or scaled.

After the stage was defined, existing hardware was evaluated. Key propulsion system tradeoffs are thrust, engine operating (chamber) pressure, and engine nozzle area ratio.

5.5.2 Selection of F_2/N_2H_4 Engine Thrust

The Module B spacecraft performing the Mercury orbit insertion maneuver is the most thrust sensitive of the four possibilities. Therefore an analysis was first made to size the engine for this application, then the resultant design was optimized and evaluated for the other applications.

The engine weight effect shown in Figure 5-2 (bottom) was estimated to be a linear function of thrust with a coefficient, $\frac{\partial W}{\partial F}$, of 13.6 kg/kN (29.9 lb_m/225 lb_f). For thrust levels above 5000 N (1125 lb_f) an additional structural penalty was added to account for module design modifications required to accommodate the larger engine.

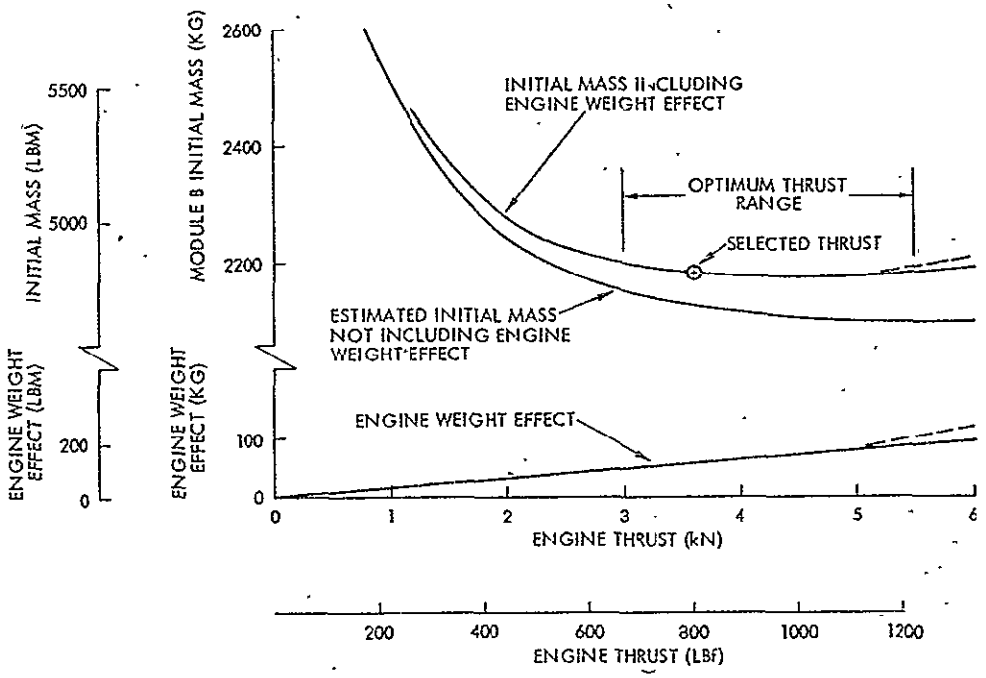

Figure 5-2. Weight Vs. Thrust Level (Module B, Mercury Orbiter)

Figure 5-2 also shows the estimated initial module mass for a Module B spacecraft performing the Mercury orbit insertion maneuver without reflecting the engine weight effect. This curve was determined as a function of thrust for a two-stage spacecraft of fixed payload, structural factor, and specific impulse and reflects the greater gravity losses associated with lower thrust (see Sections 3 and 4). The combined effect of engine weight and initial vehicle mass as a function of thrust, obtained by adding the two curves, can be summarized as follows: 1) for thrust levels below 2000 N (450 lb_f) the effect on initial mass predominates, and further reduction of thrust would cause significant spacecraft weight penalties; 2) for thrust levels above 6000 N (1350 lb_f), engine weight and propulsion module structural design considerations more than offset the savings in gravity loss, with the net effect of an increase in spacecraft weight; 3) there is a flat optimum thrust range between 3000 N (670 lb_f) and 5500 N (1240 lb_f) where the effects tend to cancel each other. Since the selection of thrust level is not critical in this range, a thrust of 3600 N (800 lb_f) was selected pending evaluation of other criteria.

For the Module A spacecraft, the general shape of the curves is similar to those shown in Figure 5-2, except that for this lighter-weight spacecraft, the optimum thrust range falls between 1875 N (410 lb_f) and 3600 N (800 lb_f). Hence it is feasible to use the same 3600 N (800 lb_f)-thrust engine for the Module A spacecraft with a minor weight penalty of only about 5 kg (11 lb_m).

Engine Volume Considerations

The initial propulsion module design concept of Module A allowed a total length of approximately 81 cm (32 in.) for the LF_2/N_2H_4 propulsion system, and 86 cm (34 in.) for the N_2O_4/MMH propulsion system, based on the assumption that stage length is dictated by the outer tank diameter. Similarly, for Module B the allowable length is 91 cm (36 in.) for the LF_2/N_2H_4 propulsion system and 96 cm (38 in.) for the N_2O_4/MMH propulsion system. The diameter of the cylindrical shell containing the engine is 147 cm (58 in.) for both modules.

As shown in Figure 5-3, a 3600 N (800 lb_f) thruster can easily meet these constraints for chamber pressures of 13.6 bar (200 psia).

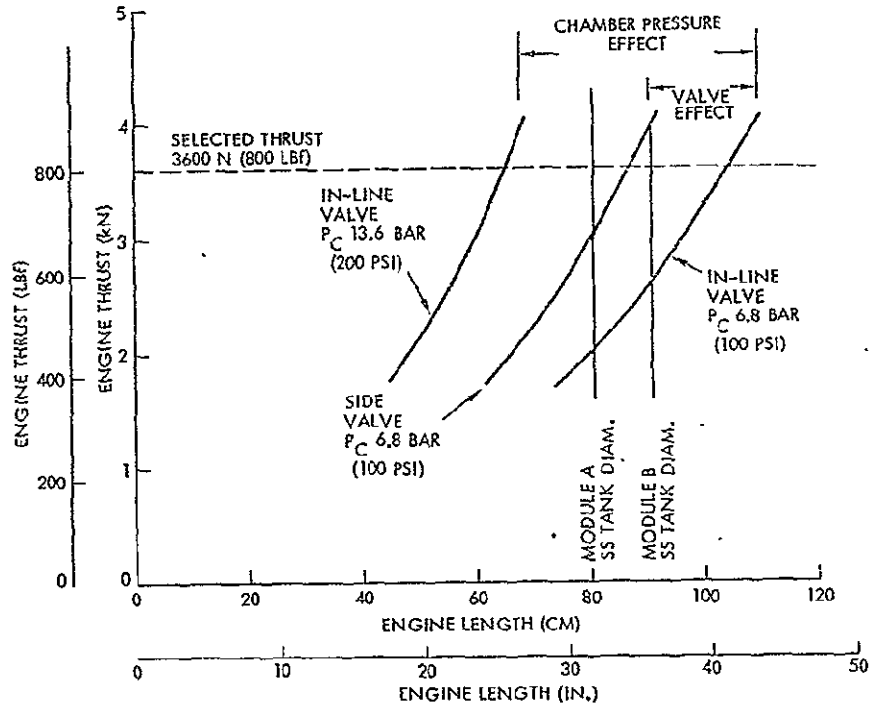

Figure 5-3. Main Engine Thrust Vs. Total Length

Side mounting of the propellant valve would permit a chamber pressure of 6.8 bar (100 psia) at a thrust of about 3100 N (700 lb_f) or 3600 N (800 lb_f) at a chamber pressure of approximately 10.9 bar (160 psia). Therefore, volume considerations do not significantly restrict engine thrust selection.

Subsequent design iteration of the propulsion module structure made it preferable to increase the stage height to 114 cm (45 in.) for both Modules A and B. This permits even greater freedom of choice for engine assembly length and mounting provisions. However, the above results indicate that a significant height reduction could be accommodated if necessary (e.g., for improved mass distribution) without unduly restricting the engine design.

Thrust Level Constraints Imposed by Payload Spacecraft

Thrust level tolerance of the payload spacecraft structure, especially the deployed appendages is quite limited, as previously...

discussed in Section 4 (see Table 4-2). In all cases except for the Pioneer Mercury orbiter, where the payload (Pioneer Venus spacecraft) is designed to withstand several g's of thrust acceleration, these structural load tolerances impose limits on the choice of main engine thrust level. This leads to selection of two different thrust levels, 900 N (200 lb_f) and 3560 N (800 lb_f), for the outbound- and inbound-mission propulsion modules (A and B), respectively. As previously shown in this section (see Figure 5-2) the selection of 800 lb_f is nearly optimum for the Mercury orbiter missions. A thrust level of 200 lb_f is as large as can be tolerated without major payload structure redesign by the outer-planet orbiters and is large enough to hold orbit insertion losses to a reasonably low level (see Appendix F).

5.5.3 Chamber Pressure Selection

Chamber pressure selection for the LF_2/N_2H_4 engine was made on the basis of weight optimization which included the effects of chamber pressure on engine weight, specific impulse, and on propellant tank, pressurant gas, and pressurant tank weights. Figure 5-4 shows the results of this analysis. A chamber pressure of 5.44 bar (80 psia) was selected as a base point and weight differences were calculated for each of the variables as a function of chamber pressure. Assumptions used in these calculations were as follows:

1) The propellant tank pressure was assumed to equal the chamber pressure plus 6.8 bar (100 psia).

2) For propellant tank pressure below 15 bar (220 psia) the tank walls are minimum gage and therefore tank weight is constant for pressures below this amount.

3) Pressurant and pressurant storage weight are combined and are a linear function of pressure over the entire range.

4) The engine weight effect was derived from data given in Reference 17. This reference determined the weight of an ablative LF_2/N_2H_4 engine of 4080 N (600 lb_f) thrust for a chamber pressure range of 5.44 bar (80 psia) to 13.6 bar (200 psia). The data was extrapolated to 3600 N (800 lb_f) by increasing engine weight by 33 percent. The shape of the curve reflects two opposing effects characteristic of ablative

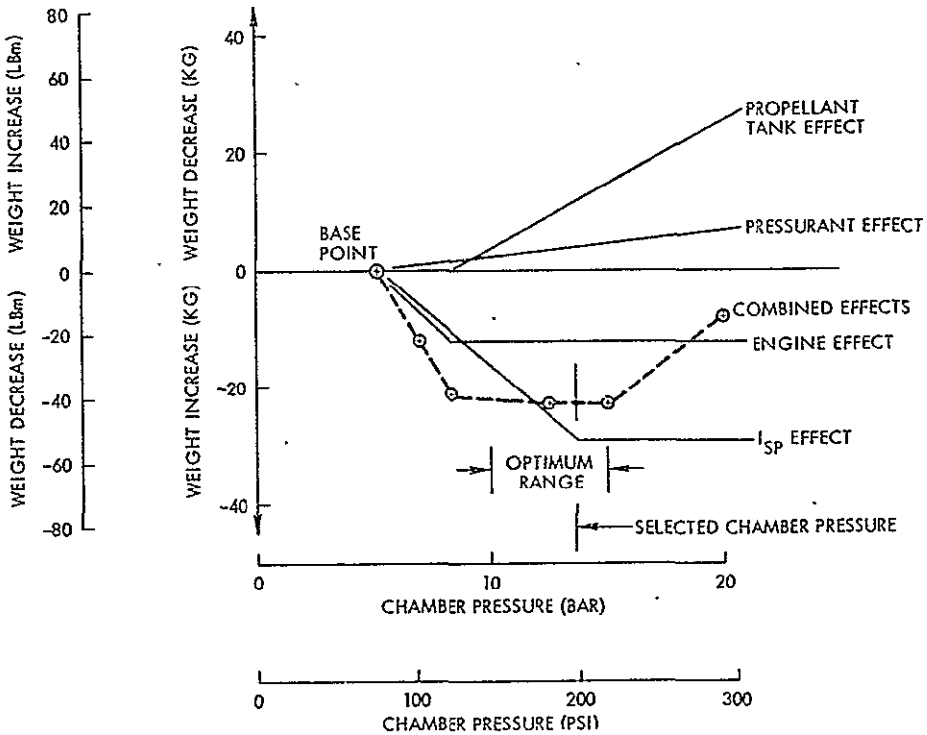

Figure 5-4. Propulsion Module Inert Weight Vs. Chamber Pressure (Earth-Storable System)

thrusters. As the chamber pressure increases, the size of the nozzle decreases, tending to decrease the engine weight. However, increasing the chamber pressure also increases heat transfer rates which in turn increases the required ablative material thickness. In the region between 5.44 bar (80 psia) and 8.2 bar (120 psia) the predominant effect is a decrease in nozzle size and engine weight with increasing chamber pressure. However, above 8.2 bar (120 psia) the two effects offset each other, and engine weight remains essentially constant.

5) The effect of specific impulse was determined on the assumption that each second of specific impulse was equivalent to 2.1 kg (4.6 lb_m) of inert weight. The specific impulse was calculated on the basis of a fixed area ratio of 60. With that assumption specific impulse is only a function of the kinetic reaction effect of pressure. I_{sp} is nearly constant above a pressure of 13.6 bar (200 psia).

Combining all of these effects shows that the optimum (minimum weight) occurs in the range of 10.1 bar (150 psia) to 13.6 bar (200 psia).

A similar analysis was performed for the N_2O_4/MMH engine. The results are shown in Figure 5-5. The pressurant and propellant tank effects are both linear over the range of interest and are shown as a

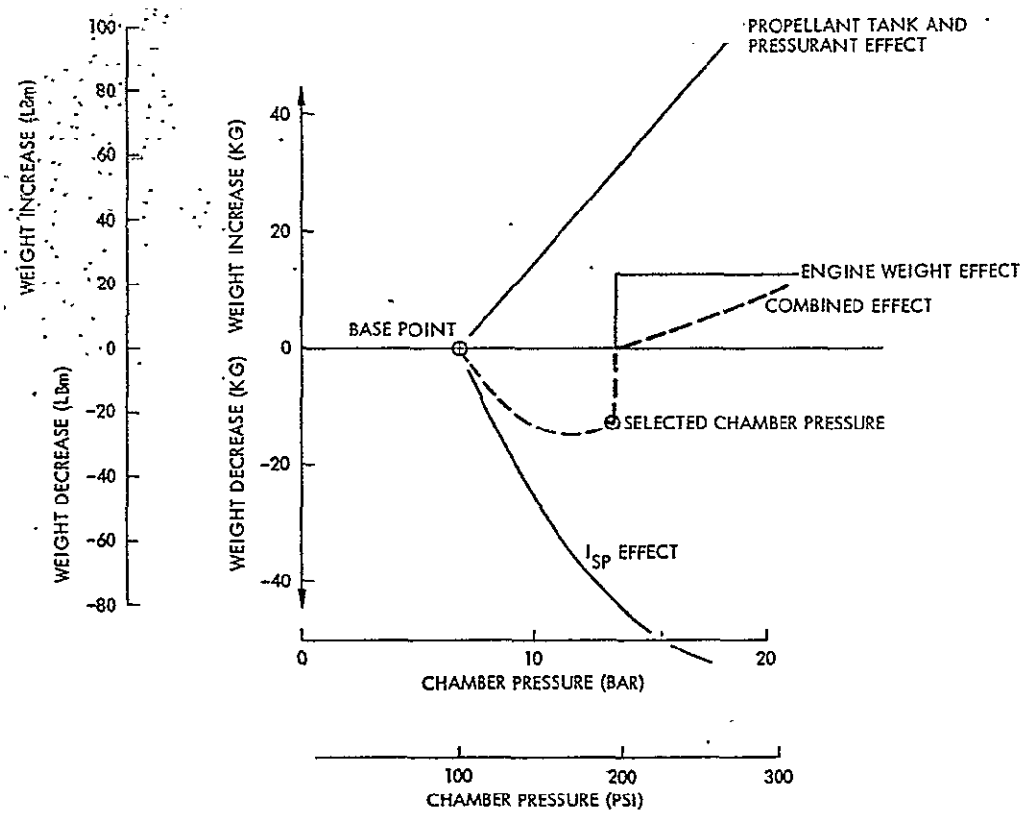

Figure 5-5. Propulsion Module Inert Weight Variation Vs. Chamber Pressure (Space-Storable Systems)

combined single curve. The engine weight was estimated on the following assumptions:

1) Below a chamber pressure of 13.6 bar (200 psia) the thruster is radiation-cooled, above 13.6 bar (200 psia) it is ablatively cooled. (This assumption is generally consistent with current high-temperature material technology.)

2) For radiation-cooled engines in this thrust class most of the weight is in the valves, injector, and combustion chamber. The weight of these components are thrust sensitive but relatively insensitive to chamber pressure. Therefore it was assumed that over the range of interest, 5.44 bar (80 psia) to 13.6 bar (200 psia), the weight of the thruster remains constant.

3) For the ablatively cooled engines, the basic engine weight was estimated to be 11.4 kg (25 lb_m) heavier than the radiation-cooled engine. For reasons previously discussed with regard to the LF_2/N_2H_4 engine, it was assumed that between 13.6 bar (200 psia) and 20.4 bar (300 psia) the engine weight is constant.

4) The specific impulse assumption for the N_2O_4/MMH engine was based on a constant exit area rather than a constant area ratio. This assumption results in a more significant effect than was used for the LF_2/N_2H_4 engine analysis.

The combined effect shows that the optimum point is at 13.6 bar (200 psia) with a flat range between 10.1 bar (150 psia) and 13.6 bar (200 psia). Hence the selection of a chamber pressure of 13.6 bar (200 psia) is suitable for both engine types.

5.5.4 Area Ratio Selection

To determine the optimum area ratio for the 3600 N (800 lb_f) engine, the increase in payload capability due to increase in specific impulse with increased area ratio was traded against the concomitant increase in engine nozzle weight. The specific impulse variation with area ratio was based on I_{sp} versus ϵ data given in Figure 5-6.

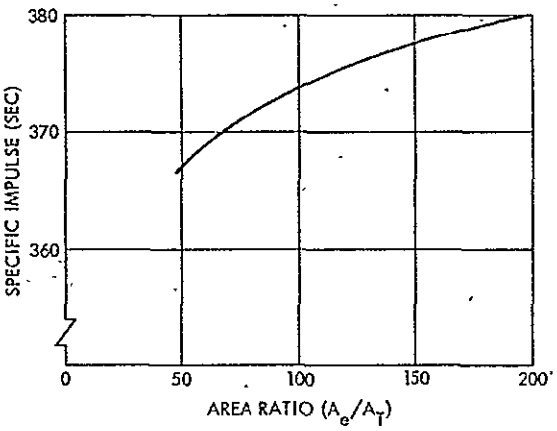

Figure 5-6. Variation of Specific Impulse with Nozzle Area Ratio

The trade ratio for payload weight and I_{sp} is 2.08 kg/sec (4.6 lb_m/sec). The nozzle weight varies with the area ratio as expressed by

$$W = 3.35 \left(\frac{\epsilon}{52}\right)^2$$

This relation is derived from the following assumptions:

1) The nozzle is a cone with a 15-degree half angle
2) The nozzle has a constant skin thickness of 0.32 cm (0.125 in.)
3) The material density is 2.25 g/cm^2 (140 lb_m/ft^3).

The results of the analyses, shown in Figure 5-7, indicate that the optimum value of ϵ is approximately 100. This area-ratio fits the available envelope and was selected for both engine sizes used in Modules A and B.

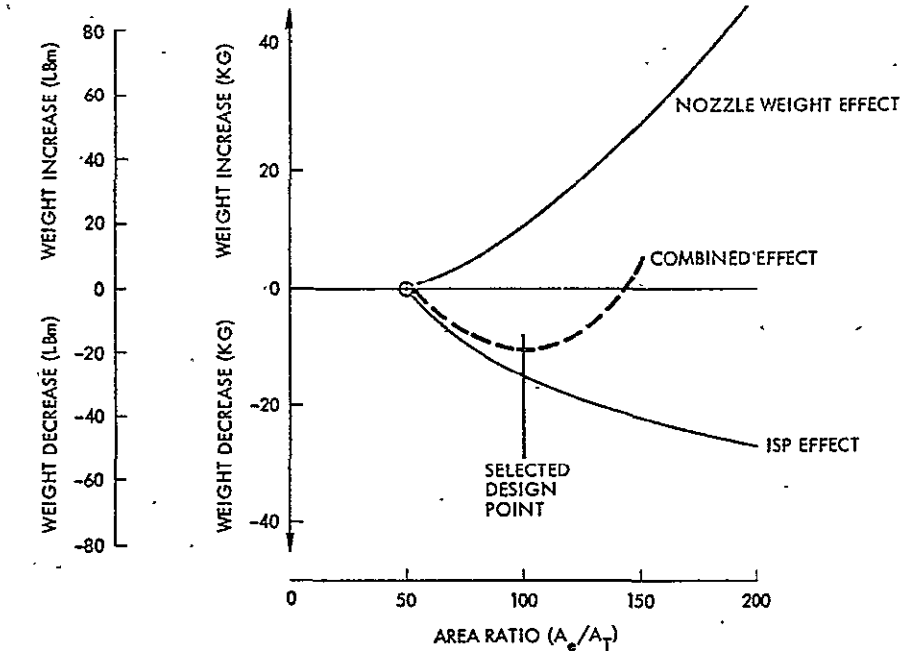

Figure 5-7. Propulsion Module Inert Weight Variation Vs. Nozzle Area Ratio

6. ENVIRONMENTAL PROTECTION AND RELIABILITY

In this section the thermal and micrometeoroid environment in which the multi-mission propulsion module is to operate will be discussed and environmental protection approaches will be presented. This section also includes a brief discussion of reliability requirements of long life missions and approaches used for reliability enhancement.

Because of the variety of mission classes, payload spacecraft types, and propulsion module designs investigated it was not possible within the scope of this study to cover environmental and reliability factors in depth. Only factors critical to mission success are identified and analyzed.

6.1 THERMAL ENVIRONMENT

The mission classes encompassed by this study present thermal environments that vary from negligible external heat input at Uranus distance (19.2 AU) to 10.6 solar constants at Mercury's perihelion distance (0.31 AU), plus potentially large infrared radiation from Mercury's dayside. Under these extreme environmental conditions propellants must be maintained within specific temperature ranges to limit vapor pressure, prevent freezing and decomposition, and achieve near-optimal propellant utilization, at a favorable mixture ratio. Permissible temperatures range from -300 to -230°F (-184 to -146°C) for liquid fluorine, and between -60 to +40°F or -51 to +44°C (lower limits) and 100°F or 38°C (upper limit) for earth-storable propellants.

Because of the low radiation potential of the fluorine tanks at the selected temperatures, effective protection or isolation against external heat input from sources such as solar flux, spacecraft heat dissipation and heat from other components of the propulsion module, is essential. Earth-storable propellants, on the other hand, must be thermally protected to prevent freezing and to minimize heater requirements.

6.1.1 Mercury Thermal Radiation

Of particular concern in the Mercury orbit mission is the spacecraft's exposure to high solar heat flux on one side, and to high Mercury thermal flux on the opposite side whenever it passes close to the subsolar

region. Figure 6-1 shows thermal radiation contours at Mercury (from the previously quoted study by Martin Marietta, Reference 10).

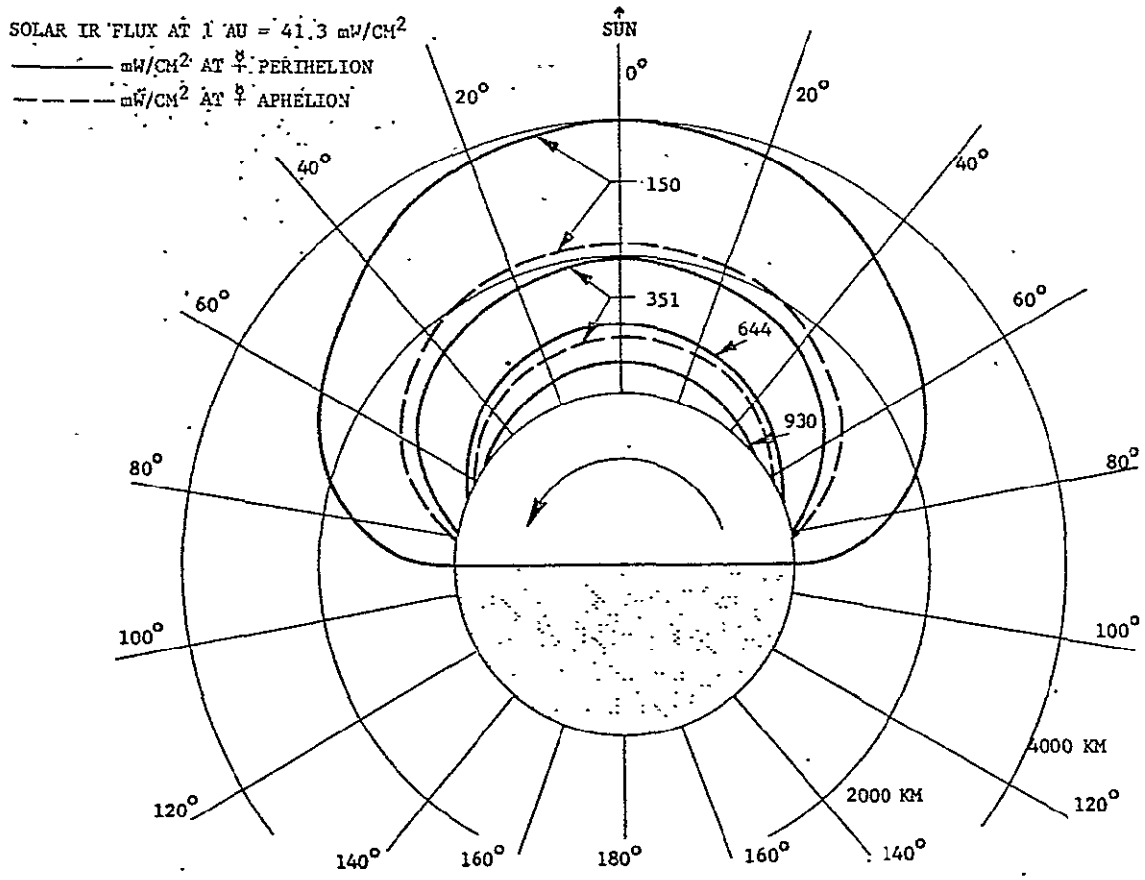

Figure 6-1. IR Radiation Contours, Surface to 4000 km Altitude (from Reference 10)

In contrast to the solar flux the planetary heat flux is not collimated, being distributed over solid angles as large as 1.5π steradians at low orbital altitudes. Heat shield protection against planetary flux is less effective than against solar flux, and a mission profile must be selected that avoids passes of the subsolar region at the very low initial periapsis altitude of 500 km (see Section 4).

The heat flux during passes of the subsolar region was integrated to determine the total thermal input for low and intermediate altitudes. Figure 6-2 shows the heat flux as a function of time from periapsis for the specified initial orbit with eccentricity of 0.8 and periapsis altitude of 500 kilometers, and for a modified orbit with 2500 kilometers altitude ($e = 0.71$). Worst-case thermal conditions corresponding to Mercury's

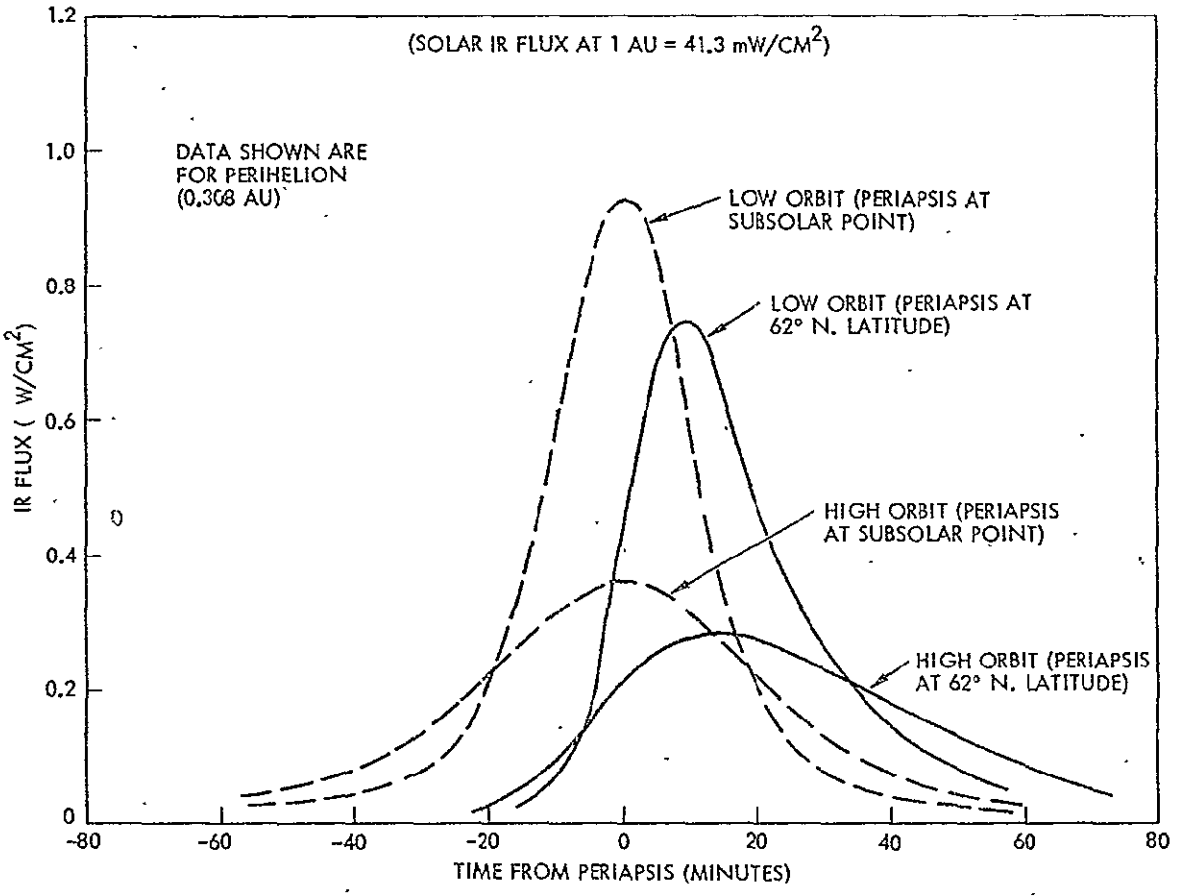

Figure 6-2. Mercury Orbit IR Flux Time Histories

perihelion distance are assumed. The diagram compares the flux time histories for polar orbits with periapsis locations at the subsolar point and at 62 degrees north latitude. The peak heat flux is reduced by 62 percent as a result of raising the orbital altitude but only by 19 percent as the result of periapsis latitude change. Integrated Mercury heat flux (in watt-minutes per cm^2) varies in the four sample orbits, as shown below.

Periapsis Location	Periapsis Altitude 500 km	2500 km
At subsolar point	29.2	21.1
At 62°N latitude	23.9	16.5

Actually, the integrated flux is not as much reduced by the altitude increase as might be expected since, due to the lower velocity at periapsis, the exposure time increases as noted in Figure 6-2.

These results were taken into consideration in defining heat shield requirements for the spinning and nonspinning propulsion modules and in determining the required periapsis raising maneuver to be performed by the spacecraft soon after arrival in Mercury's orbit. Thermal protection requirements also are a critical factor in selecting the orbit insertion mode at Mercury (see Section 4).

6.2 THERMAL CONTROL APPROACH

The thermal control approach used in the various mission classes and for the two propulsion module types have been discussed in Sections 4 and 5 in the context of design approaches. Of principal concern are the following factors:

- Thermal control of the cold fluorine tanks during Shuttle launch, ascent, and orbital phases
- Protection of cold tanks against heat inputs originating from the spacecraft or components of the propulsion module (warm tanks and engine assembly)
- Protection against external heat inputs from sun and Mercury
- Protection against plume heating
- Protection against heat soak-back during and after the main thrust phase.

6.2.1 Thermal Design Concept

A summary of thermal control requirements and approaches taken is given in Table 6-1. The thermal control design concept adopted for the F_2/N_2H_4 stage is shown in Figure 6-3. The fluorine and helium pressurant tanks are covered with nonporous foam. The N_2H_4 tank is insulated with multilayer aluminized Mylar. All propulsion components are insulated to maintain their required temperatures. Heaters must be provided to make up for the heat loss to space. For 1-meter diameter tanks, approximately 12 watts per tank are required to maintain a 20°C fuel temperature. Titanium struts are used for tank support. These

Table 6-1. Summary of Thermal Control Techniques Applied in Three Mission Classes

Thermal Control Requirement/Problem Area	Thermal Control Technique Used			
	Module A		Module B	
	SS[1]	ES[1]	SS	ES
Launch Mode				
LF_2 cooling - on ground	Use LN_2 coolant	-	Same as A/SS[1]	-
- in flight on Shuttle	Passive (thermal inertia)	-	Same as A/SS	-
Protection from RTG heat	← Water-cooled jackets on RTG's while in Shuttle bay →			
Mercury Orbit Mission				
Keep noncryogenic propellants warm	← Multilayer insulation blankets →			
	← Radioisotope and thermostat-controlled heaters →			
Keep LF_2 tanks cold	Minimize conductive heat input (long struts)	-	Same as A/SS	-
	Assure direct radiation of excess heat to space (no insulation blankets)	-	Same as A/SS	-
	Selective thermal coatings	-	Same as A/SS	-
Solar flux protection	← Spin-deployed sun shade →		← Side sun shade →	
Mercury IR radiation protection	← Spin-deployed sun shade →		LF_2 tank shield	
Shielding against solar panel heat	-	-	Local LF_2 tank heat shields	
Midcourse maneuver exposure to sun	Accept short-duration exposure (thermal inertia)		Same as A/SS	
Outer Planet Orbit Missions				
Keep noncryogenic propellants warm	← Multilayer insulation blankets →			
	← RHU's and thermostat-controlled heaters →			
Keep LF_2 tanks cold	Avoid side-sun early in transit	-	Same as A/SS	-
	Add frontal sun shade	-	Same as A/SS	-
Midcourse maneuver exposure to sun	Accept short duration exposure	-	Same as A/SS	-
Comet Rendezvous				
Rendezvous at R > 1 AU	← Same approach as in outer planet orbiters →			
Rendezvous extends to R < 1 AU (e.g., Encke, R_p = 0.34 AU)	← Use side sun shade (needs additional study) →			

[1] SS - space-storable propellants; ES - earth-storable propellants; A/SS - Module A with SS propellants

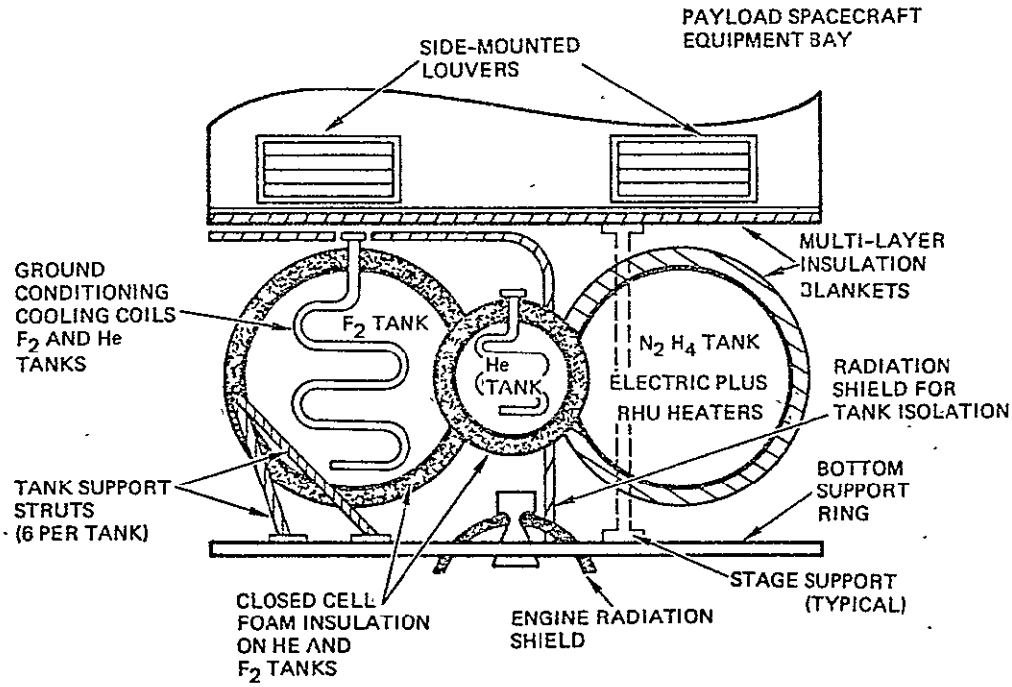

Figure 6-3. Stage Thermal Control Concept

struts are not insulated and are sufficiently long such that they in effect act as radiating fins and result in a slight heat removal from the LF_2 tanks (Reference 3).

Liquid nitrogen cooling of the fluorine tanks is required during ground-hold and perhaps also during Shuttle ascent and orbital operations. However, with an adequate tank volume margin for fluorine expansion liquid nitrogen cooling during transportation on the Shuttle may be avoidable (see Section 5). This question still requires further study.

Protection against heating from the stowed RTG's for outbound Pioneer and Mariner configurations is provided by water-cooled jackets around the RTG's. However, the RTG's will remain in close proximity of the fluorine tanks after separation of the stowed spacecraft from the Shuttle cargo bay, until appendage deployment upon completion of the interplanetary injection phase. A heat shield against radiative heat transfer from the RTG's must therefore be provided.

Return of the spacecraft to ground in the event of an abort would impose a severe heating problem from the RTG's which, at this time,

are no longer shielded by a cooling jacket; however, the necessity for dumping of propulsion module propellants prior to abort dictated by safety considerations eliminates this potential problem area.

Plume heating during the thrust phase of the solid propellant kick motor and during main engine thrust of the propulsion module has been considered as a potential thermal control problem. However, the burn time of the solid motor is so short that the heat pulse can be readily absorbed by the fluorine tanks. The main engine plume only gives negligible thermal inputs even during maximum firing periods of 25 minutes because of the low radiation intensity of the engine exhaust. Heat soak-back after a prolonged main thrust burning phase will require further analysis after the layout of propulsion system hardware, valve locations, and fuel lines are more fully defined.

6.2.2 Short-Term Sun Exposure of Fluorine Tanks

Short-term exposure of the fluorine tanks to solar illumination during off-nominal attitudes as required for the powered Venus swingby and other midcourse maneuvers can be tolerated without adverse thermal effects. Figure 6-4 shows LF_2 tank temperature rise per hour as a function of solar distance for a representative tank size and oxidizer weight. For the smaller propellant weights and tank sizes determined during the design iteration, the resulting rates of temperature rise would increase by about 10 percent from the data given in the figure. The short exposure of the tanks required during the Venus swingby maneuver will not increase the temperature by more than $6^{\circ}F$ and, therefore, does not present a problem. Terminal guidance before arrival at Mercury can probably be performed with auxiliary thrusters and therefore no reorientation from the cruise attitude is required. Tank exposure for even one hour at Mercury distances would lead to a temperature rise of $5^{\circ}K$ ($9^{\circ}F$) and should be avoided.

As a consequence of propellant depletion and the resulting reduction in the F_2 tanks' thermal inertia an increase of heating rates from the values given in Figure 6-4 will occur. Implications of this effect on operational modes (e.g., the question of propulsion module retention) require further study.

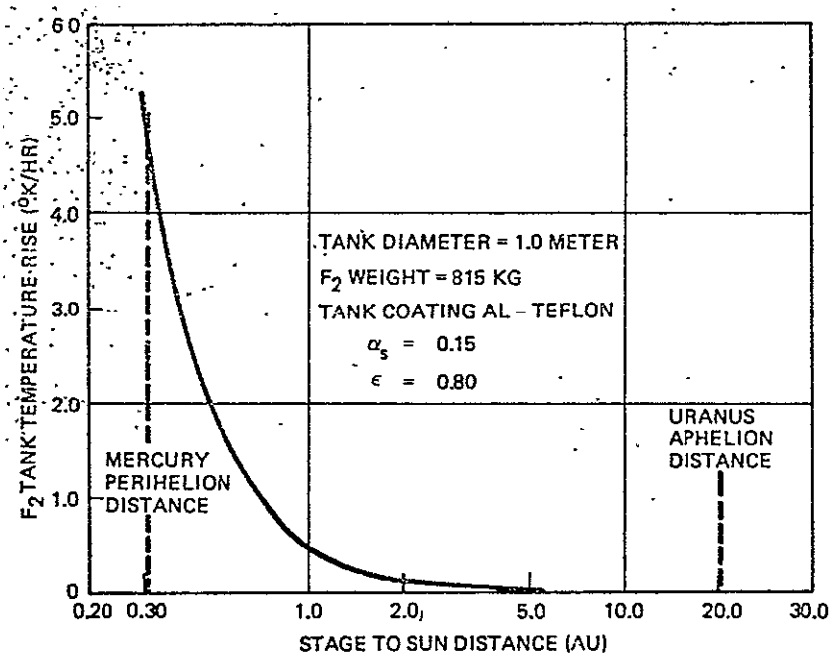

Figure 6-4. F_2 Tank Heating Rate Due to Side-Sun Exposure Versus Sun Distance

6.2.3 Analysis of Sun-Shade Sizing Requirement

A parametric analysis was performed to determine the required size of the sun shade. Figure 6-5 shows temperatures and view factors for the upper LF_2 tanks which have less view to space than the lower tanks. Results of the analysis indicate that a shade diameter of approximately 9.2 meters (30 feet) would be required. A differentiated pattern of thermal coatings is used for the LF_2 tanks such that inward-facing areas of each tank (which see primarily either the warm tanks or the spacecraft) have a low-emittance coating to minimize heat absorption from these sources. Surfaces with a better view to space have a high-emittance coating.

The sun shade has an outer layer of Beta cloth with a sheet of aluminized Kapton bonded on the inside. This results in a stable, low absorptance-high emittance surface. To minimize radiation to the LF_2 tanks, 20 layers of aluminized Kapton are then fastened to the back of the shade.

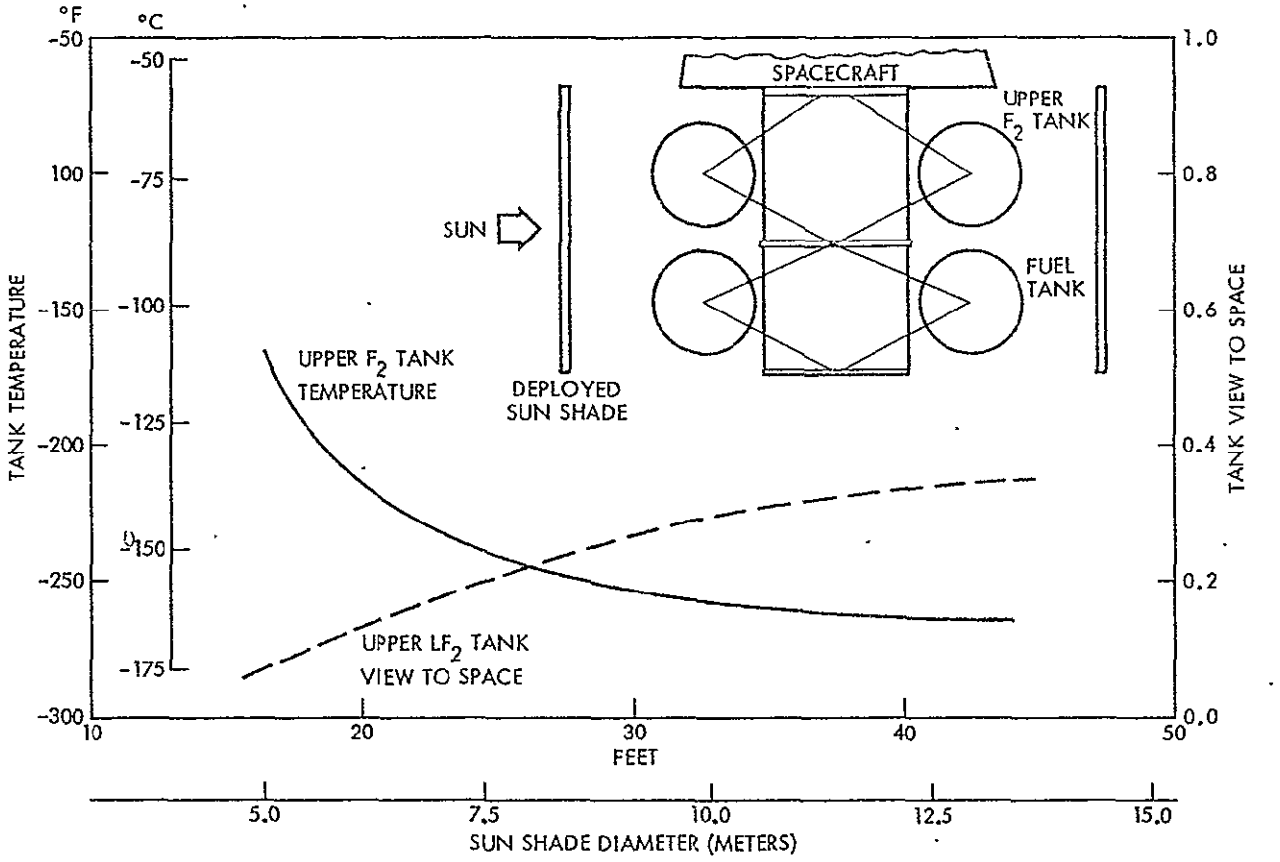

Figure 6-5. Effect of Sun Shade Diameter on LF_2 Tank Temperature

6.2.4 Fluorine Tank Thermal Control by Heat Pipes

Evaluation of the design concept for a spin-deployed cylindrical sun shade for Module A and consideration of development and test costs for this configuration have led to a search for possible alternatives that would use existing technology. The concept of a centrifugally actuated heat pipe for fluorine tank thermal control in the Mercury mission appears promising. However, this concept was introduced at a late stage in the study which allowed only a cursory examination of its characteristics. The technique is illustrated in Figure 6-6. The F_2 tanks are coupled to an aft-mounted radiator by nitrogen filled heat pipes. Because the spacecraft spin axis is normal to the solar vector this panel has a very low environmental heat input and can reject heat absorbed by the F_2 tanks at the low temperature required.

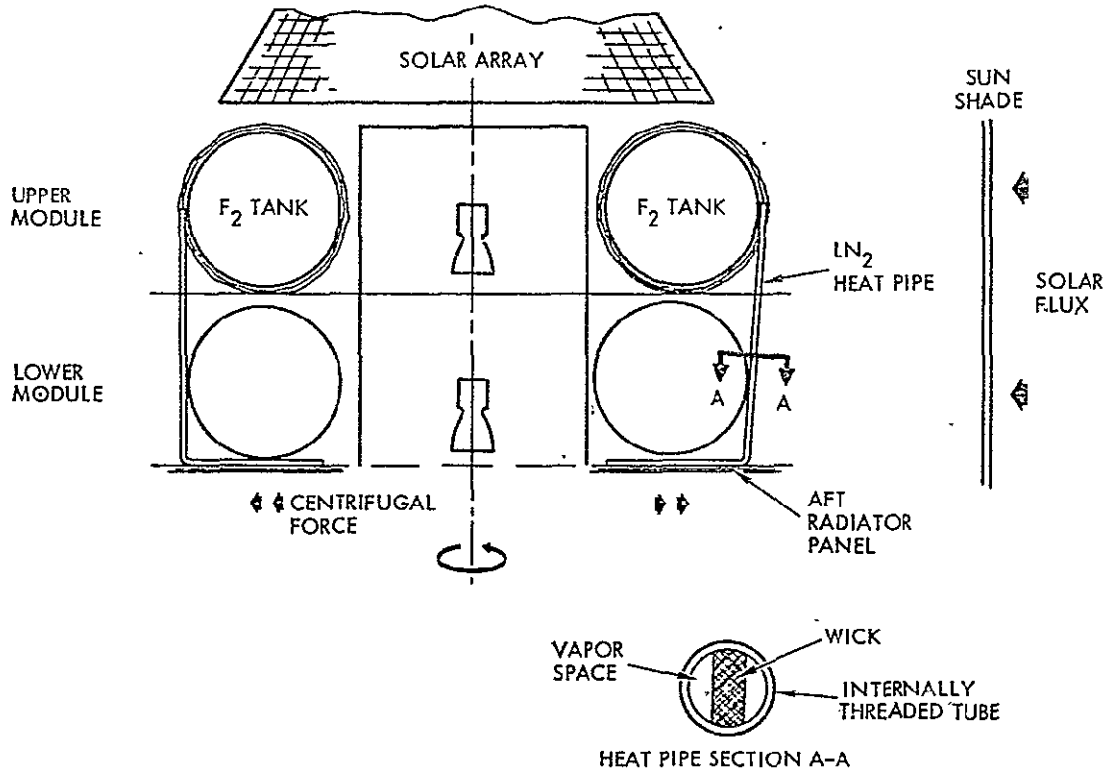

Figure 6-6. Heat Pipe Concept for LF_2 Cooling on Spinning Module

The heat pipes are attached to the outboard F_2 tank surface and configured such that the radiator plate is inboard. As a consequence, centrifugal action due to spacecraft spin motion aids in pumping the heat pipe working fluid, (LN_2), from the radiator, where it is condensed, to the F_2 tank where it is evaporated. A wick and internal threading provide liquid control and assure that the working fluid wets the heat pipe wall. Heat pipe operating pressure at -157°C (-250°F) will be approximately 300 psia.

Relying on centrifugal action to pump the coolant has the additional advantage of providing a "one-way" heat pipe. If the radiator becomes temporarily warmer than the F_2 tank, e.g., due to infrared radiation from Mercury, the heat pipe will not act in reverse direction and transfer heat into the LF_2 tank since such a reversal would involve a flow against the centrifugal force. The radiator or hot portion of the heat pipe will thus become depleted of liquid working fluid and the heat pipe action is suspended.

A potential problem with this design is the difficulty of ground testing in the flight configuration. The pipes would probably have to be tested individually and in an orientation such that earth's gravity force is partially neutralized. A tilted orientation by about 15 degrees against the horizontal would simulate the effect of spin action (0.25 g) on the radial segment of the pipe located at the radiator plate.

In the tandem arrangement the heat pipes for the upper module LF_2 tanks must extend across the separation joint and to the radiator plate at the bottom of the lower module. These pipes are broken when the lower module is jettisoned. A second heat pipe and radiator plate (confined to the upper module) will be necessary to provide thermal control during the rest of the mission if the upper module is to be retained.

This thermal control concept has the following principal advantages:

- Replacement of large spin-deployed sun shade by a smaller (stationary) one. This saves weight and cost and reduces operational constraints
- Elimination of moving parts, hence greater reliability
- Lower development risk; easier, less costly verification tests
- Reduction of solar pressure unbalance
- Fluorine tanks can now be covered by thermal blankets and thus be given more protection against temporary heat inputs
- The system can be designed for lower oxidizer temperature fluctuation and thus easier mixture ratio control.

6.3 MICROMETEOROID ENVIRONMENT

Micrometeoroids of cometary and asteroidal origin encountered by the spacecraft during the inbound and outbound missions can cause potential damage to exposed spacecraft components. In the context of this study, the possibility of propellant tank penetration by such particles and design approaches for tank protection are the principal concern.

An analysis of micrometeoroid exposure of the propulsion module indicated that probably the most severe environment is encountered

a) in the Saturn orbit mission, during ring plane crossings close to the planet, and subsequently, during the nearly equatorial orbit phase, even at increased periapsis distances.

b) in the Mercury orbit mission, due to extended exposure to increased meteoroid flux levels close to the sun.

6.3.1 Particle Impact Rates for Planetary Orbiters

With respect to the outbound cruise in the Saturn and Uranus orbit missions the following observations are relevant. Prior to the asteroid belt crossing by Pioneer 10 and 11 it was generally assumed that the particle flux in this region was many times denser than at earth's distance from the sun. Consequently, these spacecraft were designed to withstand the estimated relatively high flux at the densest part of the asteroid belt (10^{-3} particles per cubic meter of mass greater than 10^{-3} grams) in accordance with NASA's micrometeoroid spatial density model defined in SP-8038 (Reference 26).

Actually, the meteoroid impact measurements made by both Pioneer 10 and 11 indicate the penetration flux in the asteroid belt to be smaller by a factor of 3 than that near 1 AU, whereas the NASA model predictions suggested that it would be greater by a factor of 5.

These results are of great importance to the design of outer planet orbiters, particularly since they represent actual penetration measurements on exposed sheet metal samples of two thicknesses, rather than only visual observations of particles encountered.

Results of a calculation of particle impacts sustained during the crossing of Saturn's ring plane, based on the current NASA model of ring particle flux (NASA SP-8091, Reference 27) are shown in Figure 6-7. A solid line shows the estimated upper bound for a ring plane crossing at 2.3 planet radii under representative encounter conditions that are stated in the legend of the graph. A much less conservative estimate of the number of impacts sustained, using a 90th percentile particle flux estimate is shown by a dashed line. The upper bound of the number of particles of 0.01 gram or larger striking the protective shield would be about three per ring crossing. The 90th percentile flux estimate projects

RESULTS BASED ON: RING CROSSING AT 2.3 SATURN RADII
RELATIVE VELOCITY: 11.4 KM/SEC
VELOCITY COMPONENT ⊥ TO RING PLANE: 8 KM/SEC
INTERCEPT ANGLE RELATIVE TO SPACECRAFT -Z AXIS: 45 DEGREES
EXPOSED PROPULSION BAY AREA: 1.5M^2
ASSUMED PARTICLE DENSITY: 1 GRAM/CM^3

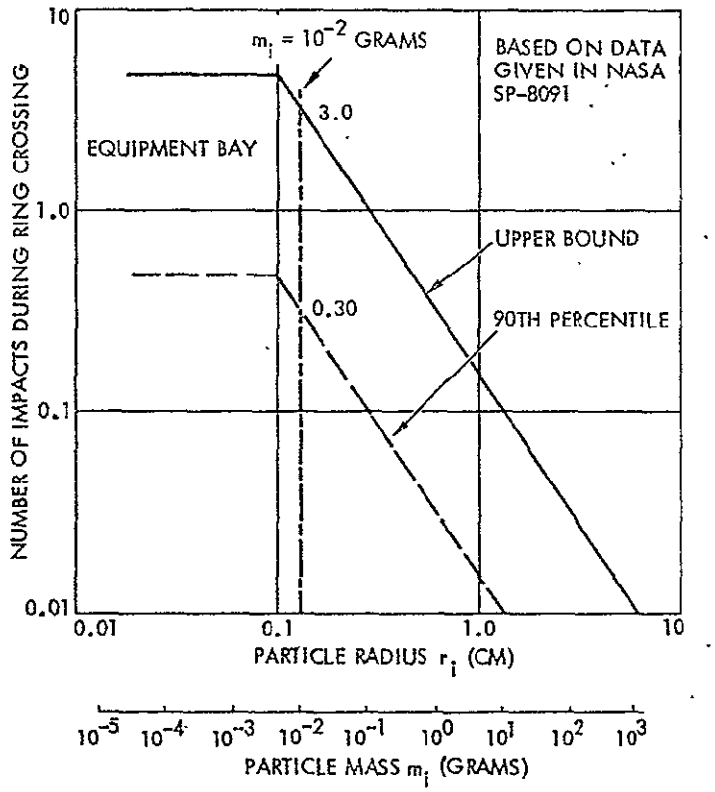

Figure 6-7. Estimated Impacts Sustained During Saturn Ring Crossing

only 0.3 particle impacts. Note that the assumed ring crossing distance of 2.3 Saturn radii is also on the conservative side since in the mission profile being considered the spacecraft will remain outside the perimeter of ring A, ($R = 2.29\ R_S$). Just inside this perimeter, i.e., 600 km closer to the planet, the estimated particle number density is six times greater than at 2.30 R_S. A closest approach distance of 2.5 planet radii was specified by the mission guidelines. By an appropriate aim point selection relative to Saturn's equator the ring plane crossing can be placed at considerably greater distances where the particle flux density is lower. A periapsis-raising maneuver, to be performed at the first apoapsis passage, will reduce the number of particle impacts during subsequent close approaches and later on, during the equatorial orbital mission phase.

Table 6-2 lists preliminary results of particle impact rate analysis for milligram-size particles using conservative estimates of particle flux at Saturn and Mercury. Reference areas for determination of the impact rates are the exposed cross sections of all four propellant tanks, totaling 1.1 and 2.6 m^2 for propulsion Modules A and B, respectively.

Table 6-2. Comparison of Estimated Micrometeoroid Impacts During Mercury and Saturn Orbit Missions

Mission	Exposure	Meteoroid Impacts ($m \geq 10^{-3}$ gm)			
		Module A (Area: 1.1 m^2)(1)		Module B (2.6 m^2)(1)	
		Low(2)	High(3)	Low(2)	High(3)
Saturn Orbiter	1 passage at 2.5 R_S	0.23	2.35	0.55	5.52
	1 passage at 4 R_S	0.08	0.79	0.19	1.86
	2 years in orbit (4) (periapsis 4 R_S)	1.96	19.60	4.65	46.5
Mercury Orbiter	1 revolution of Mercury (88 earth days)	0.050	0.16	0.11	0.37
	1.5 year at close solar distances (1 year in Mercury orbit + 0.5 year of transfer phase)	0.131	0.63	0.47	1.50

Notes
(1) Reference areas (1.1 and 2.6 m^2) are upper and lower cross-sectional areas of four tanks for Modules A and B.

(2) Low estimates correspond to 90 percentile of upper bound values for Saturn orbiter and to $R^{-1.5}$ law of micrometeoroid density for Mercury orbiter.

(3) High estimates correspond to upper bound values for Saturn orbiter and to $R^{-2.5}$ law of micrometeoroid density for Mercury orbiter.

(4) Two year orbit at Saturn assumes orbit insertion at 2.5 R_S and 22 subsequent passages at 4 R_S periapsis distance (32-day orbit period).

The low and high estimates for particle flux densities at Mercury use a distribution that depends on a $R^{-1.5}$ or $R^{-2.5}$ law of cometary meteoroid flux in interplanetary space as function of solar distance R. A less conservative assumption (R^{-1} law) would reduce the flux at Mercury's closest approach to the sun (0.308 AU) by a factor of about 1.8 compared with results obtained for the $R^{-1.5}$ law. While the Saturn mission profile can be modified by expenditure of extra propellant without sacrificing scientific objectives, the Mercury mission which is next

in severity from a particle impact standpoint could only be changed by reducing exposure time and hence scientific data return.

6.3.2 Particle Flux Near Comets

The particle flux environment in comet rendezvous mission requires further study. Flux densities vary with each comet and with the comet's activity level in the given encounter year. Some comets exhibit great changes in acitivity level between apparitions. The flux densities encountered in the rendezvous mission also depends strongly on solar distance, on spacecraft distance from the comet' nucleus and on the geometry and depth of comet tail penetrations to be performed by the spacecraft.

Results from an Encke (1984) rendezvous study by TRW (Reference 12) indicate a 10^{-3} gram particle flux of the order of 10^{-3} to 10^{-4} particles per m^2 per second at a distance of 20 km from the nucleus, i.e., an impact rate of about 0.1 to 1 particle per hour. The flux density varies inversely with the square of the nucleus approach distance. The particle impact hazard can thus be readily controlled by mission profile selection. Since the particles are of low density and are streaming at a low relative velocity, the effect of particle impacts is felt less strongly by the propulsion system than by other exposed subsystem components, especially scientific instruments. With respect to the propulsion module, the effect of particle impact and deposition (adhesion) is likely to be a degradation of thermal blankets or thermal coating effectiveness.

6.4 MICROMETEOROID PROTECTION APPROACH

The most vulnerable parts of the propulsion module are the propellant tanks. The micrometeoroid protection approach was aimed at giving the tanks adequate protection so as to survive impacts of particles in the 1 to 10-milligram mass range without damage. Impact probability of larger particles decreases by a factor of 3 per order of magnitude of mass increase in the Saturn ring environment and by a factor of 7 per order of magnitude in the interplanetary environment and at Mercury.

The design approach used to protect the propellant tanks relies on the protective containers (stainless steel or titanium) around the tanks

that have been adopted as safety device to preclude propellant leaks into the Shuttle bay. The skin of these outer vessels acts as micrometeoroid bumper with the outer tank wall spaced about 1 inch (2.54 cm) from the inner wall. The multilayer insulation blankets and, in the case of the LF_2 tanks, the foam layer and Beta quartz cloth covering provide additional shielding.

A skin thickness of 0.008 inch (0.2 mm) of the outer tank wall (6 Al-4V) at 1 inch spacing, provides effective bumper protection against 1 milligram particles, based on HEAO design data. Actually, a wall thickness of at least 0.02 inch (0.5 mm) is required for rigidity, extending the effectiveness of the micrometeoroid bumper against impact of particles of about 2 orders-of-magnitude greater mass. This should be adequate to give a high probability of preventing catastrophic impact damage even for the highly conservative estimates in Table 6-2.

6.5 RELIABILITY

Reliability criteria that are applicable to the design and operation of the multi-mission propulsion module, and to long-life planetary missions, in general, are outlined in this section, and design approaches adopted on the system and component levels to achieve a high mission success probability are discussed. The different mission environments, duty cycles and lifetime requirements to be met by the same propulsion system, and the introduction of advanced propulsion technology impose novel reliability problems which have been addressed in this study.

6.5.1 Reliability Criteria

6.5.1.1 Mission Environment

Thermal and micrometeoroid environments of the different mission types, and design approaches to protect the propulsion module against environmental damage or degradation were discussed in the preceding subsections.

The trapped radiation environment that might be encountered in the planetary orbit phase has been omitted from previous discussion. In the Saturn orbit mission, with closest approach distances of 2.5 R_S initially, and 4 R_S or greater after orbit modification, a sustained high-level flux

of charged particles that would degrade spacecraft components is unlikely. At Uranus, the specified initial periapsis of 1.1 R_U may expose the spacecraft to higher levels of particle flux, but any assumptions regarding the existence of such a flux at Uranus are only speculative. Nevertheless, a periapsis raising maneuver may be necessary early in the orbital mission phase.

Probably the most adverse environment of any of the missions from a reliability standpoint is the intense solar flux at Mercury which necessitates a complex thermal design with novel mechanisms and new failure modes, at least for the spinning spacecraft (Module A). As a mitigating factor, this mission is by far the shortest in the specified mission spectrum, and the spinning spacecraft is inherently simpler and, presumably, more reliable than the three-axis stabilized spacecraft type.

6.5.1.2 Lifetime

The propulsion module must be designed for a wide range of mission durations. The Mercury mission with a 2-year transit phase and, possibly, a 2-year orbital phase has the shortest duration; the Uranus mission, up to 10 years in transit and 2 years in orbit, the longest. All missions except the Mercury orbiter can be classified as long life missions. The scientific mission objectives can be achieved only upon arrival and successful orbit insertion at the target planet, during 1 to 2, or even 3 years in orbit. Design approaches to achieve high long life reliability will be discussed below.

6.5.1.3 Operational Phases and Cycles

The main engine is largely inactive during long intervals of the transit and orbital mission phases. However, the auxiliary (ACS) thrusters will be in use almost continuously. The propulsion module must therefore be maintained in operating condition throughout the mission. As previously discussed, the total number of ACS limit cycles required in the Mariner-class Uranus mission can be as large as 2×10^5 cycles in two of three channels.

A question that still requires further study concerns the possible alternative of keeping primary and auxiliary thrust functions separate, in order to raise overall propulsion system reliability.

6.5.1.4 Reliability Characteristics of Long-Life Missions

In a previous study performed by TRW under NASA Ames sponsorship (Reference 28) a general design approach for increasing reliability of Pioneer outer planet spacecraft in missions of 8 to 10 years duration was developed. A "fail safe" design policy was adopted in that study which is directly applicable to propulsion module long life requirements:

1) The system should be designed with appropriate redundancy, workarounds and backup capabilities which will eliminate as many electronic, mechanical, and electromechanical failure modes as sources of spacecraft failure as practical. When redundancy or backups are employed, circuits, interfaces between units, and switching circuits should be designed with fault isolation so that a failure in one unit does not propagate into, or does not interfere with the operation of, the redundant units or backup modes.

2) Electrical or electromechanical random single-point failures should be eliminated from equipment which must successfully operate at a high duty cycle throughout the mission, and from equipment which is especially critical to the success of the mission. For the purposes of this single-point failure criterion, failure or degradation from predictable wearout shall not be regarded as random, and the design should be capable of surviving a single-random failure in addition to expected wearout failures. Equipment subject to wearout shall be sized to accommodate the design life of 10 years.

The above design policy is intended as a guideline, but with some flexibility. In implementing the policy in specific cases, competing factors — such as cost, practicality, schedule, weight, redesign, or repackaging of existing equipment, possible introduction of higher probability failures, increased risks of operator errors, etc. — should be taken into account.

Figure 6-8 is an example of reliability versus weight tradeoffs in the Pioneer outer planets spacecraft design leading to discrete increments in reliability by optimum redundancy weight allocations in various subsystems. Figure 6-9 shows the estimated reliability improvement for the Pioneer spacecraft as a function of time. A similar approach is to be followed in the multi-mission propulsion module design.

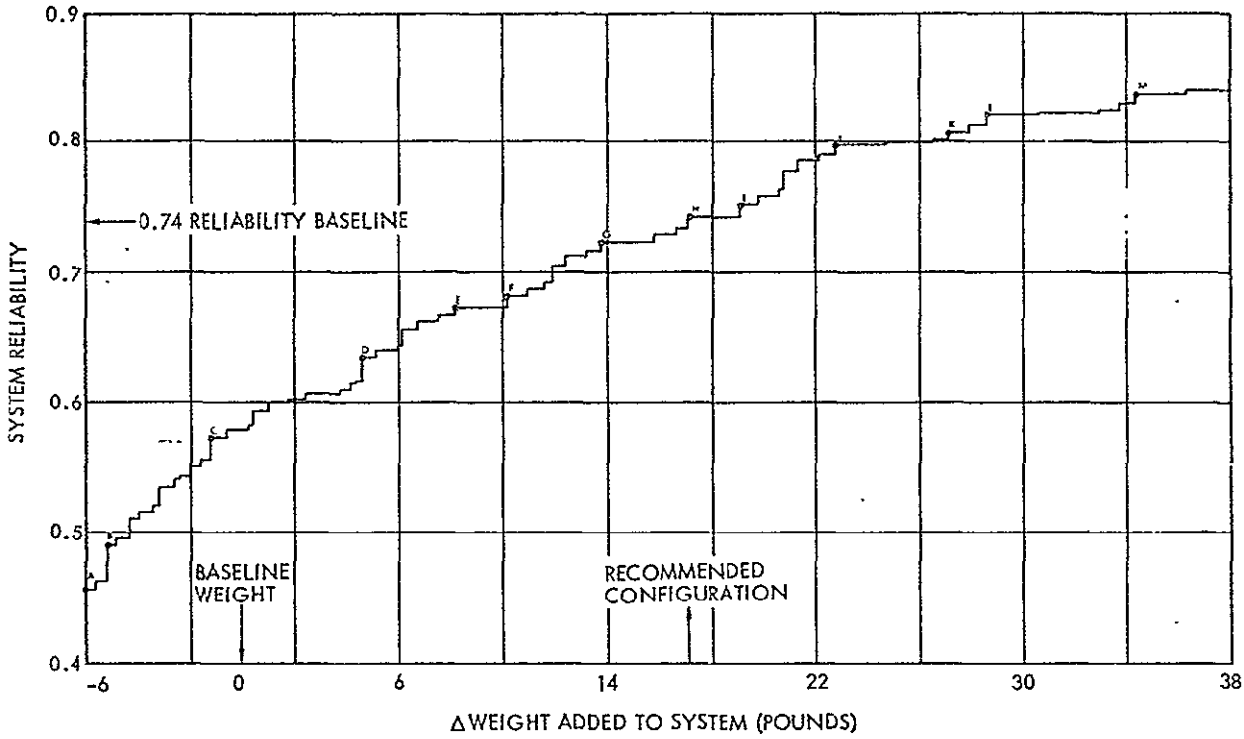

Figure 6-8. Summary of System Reliability/Weight Tradeoff (8-Year Mission)

Based on results of other recent system reliability studies by TRW (Reference 29) some general observations on long-life mission reliability are relevant in the context of the present study:

- Current reliability estimation techniques are conservative.
- Satellite and space probe failure predictions are consistently higher than failures experienced in flight. For example, Pioneers 6-9 and 10-11 have established a much higher reliability than predicted or specified.
- Underlying reasons for this discrepancy are piece-part failure rates and quality control data of early spacecraft still being used as major part of the data base. This introduces a heavy bias toward unrealistically high failure rates.
- Random failure rates approach a constant level as time increases (see Figure 6-10).
- Effect on propulsion module design philosophy
  - Maximize long-life mission reliability (e.g., Uranus orbiter) by minimizing design elements subject to wearout failure

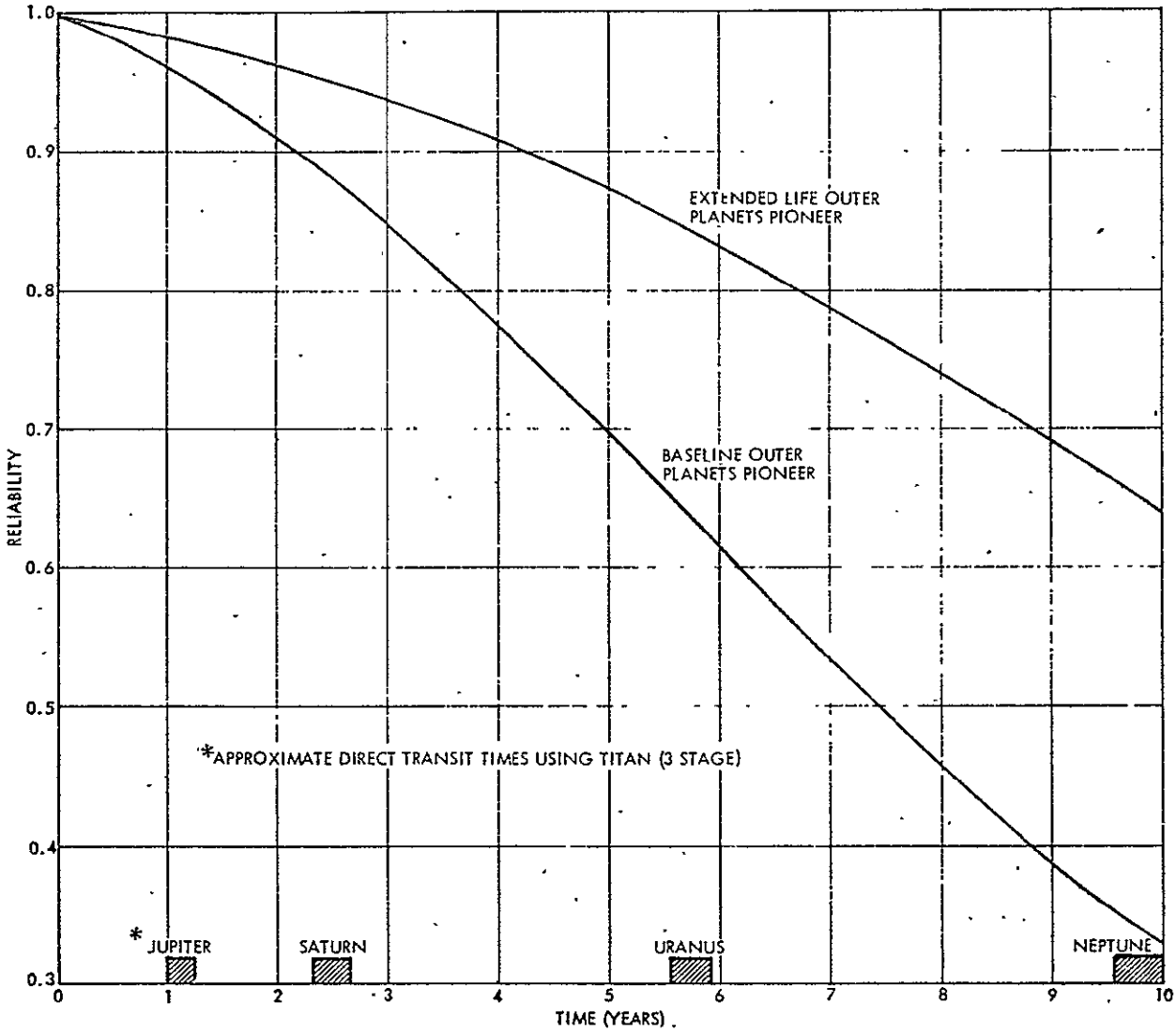

Figure 6-9. System Reliability Estimate for Long-Life Pioneer Mission

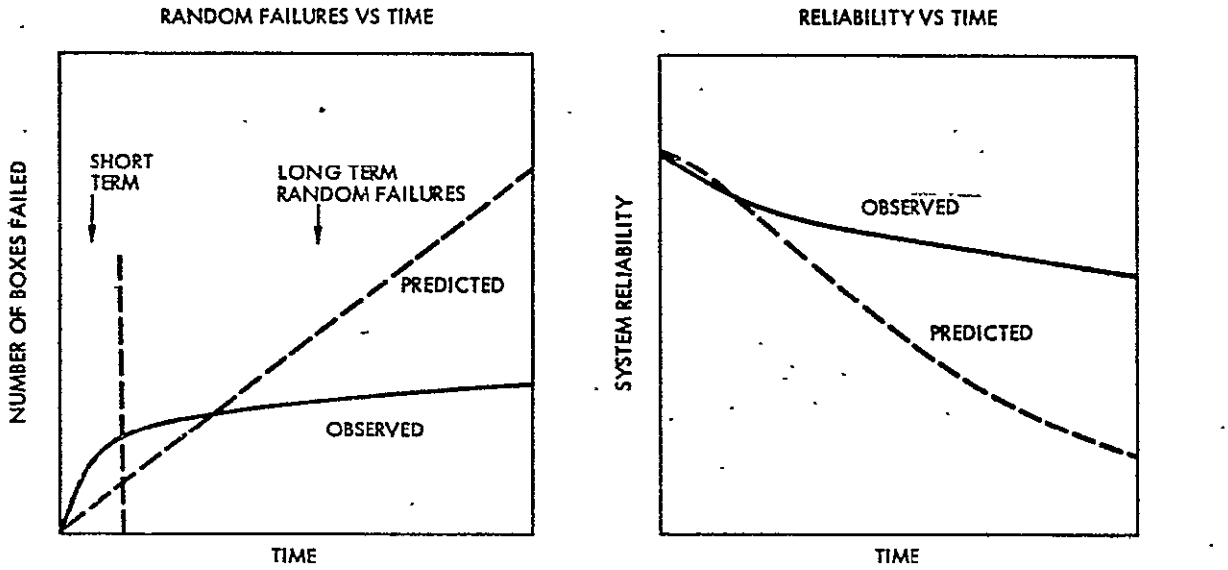

Figure 6-10. Typical Spacecraft Failure Rates and Reliability in Long Duration Missions (Qualitative Trends, Based on Recent TRW Systems Studies)

- If failures are primarily of random type then mission durations of 8, 9 or 10 years are not critically different from a reliability standpoint

- Long-life missions with high reliability should be feasible in mid-1980's without prohibitive extra cost.

To conclude this general discussion, it can be expected that with proper attention to redundant design and avoidance of predictable wear-out failures, the desired long-life reliability can be achieved. The design approach will be discussed in the following subsections.

6.5.2 Propulsion Module Design for Long-Life Reliability

6.5.2.1 Component Reliability

Mission durations range up to 10 years, while present systems have demonstrated operability for approximately 2 years. For 10-year durations, aspects usually not considered, such as propellant tank life under pressure and/or corrosion, will become important. Long-term operating life, and storage life, as well as combination effects also increase reliability requirements on other components.

A reliable, long-life system design must take into account best available data on environments to which the components will be exposed. The planetary orbiter missions will be performed after the environments at the target planet will have been sampled by previous flyby missions and will be fairly well understood. One exception will be the Uranus mission: a 1985 projected launch date would precede the encounter date of a Mariner Jupiter Uranus mission launched in 1979 or 1980.

Tradeoffs performed during this study considered equipment redundancies, competing technologies, weight, cost, and practicality of implementation. Real-time life testing in a simulated enviroment of components intended for very long mission life generally is not feasible. Therefore, some overdesign and/or component redundancy is needed. Primary reliability concerns in the conceptual design phase included propellant acquisition, pressurant regulation, valve actuator implementation, propellant isolation and corrosion effects on tanks and propellant lines. Problem areas needing further research during the subsequent technology and hardware development phases are listed in Section 6.5.3.

Propellant Storage and Acquisition

Corrosion is a principal concern in subsystems in contact with the oxidizer. Impurities, such as water, can aggravate oxidizer corrosivity and lead to a slow pitting that may cause slow leaks in tanks or valves. The selected design approach is to minimize the number of components that are exposed to the oxidizer and to keep tank pressure low in order to reduce stress-corrosion. The main tanks can remain unpressurized initially until first use.

During operation, the tanks are pressurized with warmed pressurant. This permits tank pressure to relax after isolation from the regulated source during periods of inactivity and reduces the potential for stress-corrosion.

Passive surface tension propellant acquisition devices suitable for N_2O_4, MMH and N_2H_4 tanks are currently being developed and perfected. As substitute for conventional expulsion bladders, they will avoid problems of leak, rupture, fuel and oxidizer corrosion, and degradation due to RTG radiation. They will thus provide much higher reliability in long-duration missions.

The state of the art in materials compatibility for LF_2 tanks is not highly developed. Capillary acquisition devices will therefore be avoided which could corrode and cause clogging of downstream filters, etc. In the spin-stabilized Module A a bladderless tank design using centrifugal action for propellant acquisition was selected. For the three-axis stabilized Module B, use of auxiliary thrusters (ACS thrusters) as settling rockets was chosen to accomplish propellant acquisition. For both LF_2 and N_2O_4 use, the same choice was made, although capillary devices are believed to be less problematic with N_2O_4. Capillary devices will be used in the hydrazine tanks which feed the ACS thrusters.

Valves

The chemical stability of ordnance material for squib-actuated isolation valves is another unknown for long space storage, especially in the RTG environment. Another concern is the power requirement for ordnance firing or, alternatively, the long-life integrity of wet slug

tantalum capacitors as charge-storage devices for ordnance-firing. Because of these concerns, solenoid and motor-actuated valves are preferred alternatives.

Pressure Regulators

The relative merits of conventional pneumatic pressure regulators and mechanical pressure switches operating in a bang-bang mode with an on-off valve were considered. Pneumatic regulators were selected, as a conservative approach since they are expected to have fewer, and better known failure modes.

6.5.2.2 System Reliability

Tank Leakage

In the unlikely event of propellant tank penetration by a micrometeoroid, approximately one-fourth of the propellant remaining in the module will be lost. However, depending on the time of occurrence the mission may still achieve a partial success. Such an event is more likely to occur after orbit insertion than during the transit phase, considering the micrometeoroid flux densities discussed before, and in this case would impair maneuvering capability for the remaining part of the orbital phase.

If the propellant loss should occur before arrival at the target planet the reduced ΔV capability may still permit successful orbit insertion, e.g., at Saturn. However, the mass unbalance resulting from a major propellant loss would lead to a large principal-axis tilt angle and, hence, loss of communication capability, in the case of spinning spacecraft.

To make use of the potential redundancy of the four-tank configuration selected, appropriate isolation of the two fuel tanks and two oxidizer tanks from each other is necessary. Otherwise, a leak occurring in one tank would cause the loss of the entire remaining fuel (or oxidizer) and pressurant. The isolation valves must be controlled automatically to prevent propellant in the undamaged tank from leaking out through the manifold line. Long communication time delays preclude timely remedial action by ground command in most cases.

With a partial loss of propellant, the main engine may have to operate at an off-nominal mixture ratio, at a significant performance loss. Since nominal mixture ratios are of the order of 1.5 to 1.6, loss of an oxidizer tank would cause the mixture ratio to change to $1/2 \times 1.6 = 0.8$. The engine can possibly be made to operate at a greatly reduced mixture ratio by programming the isolation valve to act as a secondary (bang-bang) pressure regulator. By lowering the oxidizer tank pressure to approximately 50 percent the remaining oxidizer and fuel can be utilized. The resulting specific impulse loss could be 20 or 30 percent. Loss of a fuel tank is even more severe since the main engine would not be operable with the resulting mixture ratio of $1.6/0.5 = 3.2$ (or 2.7 if the fuel reserve of 20 percent is taken into consideration). To restore the system to operational condition would require a partial venting of the oxidizer tanks. Further study is required to determine feasibility and implementation of such operating modes which would require a complex automatic onboard correction program.

Auxiliary Propulsion System Reliability

Wearout failures are to be expected, particularly in the ACS system, because of the large number of operating cycles required of each thruster during long-duration missions, both in spinning and nonspinning spacecraft applications. The maximum number of limit cycles per control channel of Module B in Saturn and Uranus missions are estimated in excess of 2×10^5. Pulsed thrust operations by Module A thrusters, while generally lower, still will be of the order of 10^5 cycles. Sufficient ACS thruster redundancy is provided to reduce the effect of single-point wearout failures on mission success probability. With a total of 16 ACS thrusters in Module B and 10 in Module A, several backup modes are available to retain full attitude-control and ΔV-correction capability after a single thruster failure, and at least partial capability in most cases as a result of an additional thruster failure in any channel.

Design Conservatism

To achieve high system reliability a conservative approach was used in defining the propulsion system design, including the following:

1) Use of separate pressurant systems for fuel and oxidizer

2) Use of a safety factor of 2.0

3) Use of a pneumatic gas regulator

4) Avoidance of thin-gauge materials (e.g., capillary devices in oxidizer tanks)

5) Unpressurized storage of the propellants during inactive mission phases

6) Use of heated pressurant to permit automatic pressure decay in propellant tanks after pressurant shutoff

7) Redundant sealing of tanks after each propulsion event to prevent minor corrosive leakages

8) Capability for venting of the engine lines to prevent corrosion

9) Inclusion of additional propellant reserve (10 percent) for contingencies.

6.5.3 Areas for Further Study and Research Related to Reliability

Recommended areas for further study include:

1) Mechanization schemes for optimum redundancy

2) Component and system design requirements related to controls redundancy

3) Component and system design requirements to provide partial (degraded) mission capability in the event of component failures.

The following areas require additional research and development:

1) Propellant corrosion (stress corrosion) of materials used in tanks and valves

2) Development of very high-reliability ACS thruster valves

3) All aspects of LF_2/N_2H_4 propulsion design

4) All aspects of system safety engineering, especially for LF_2/N_2H_4 (with emphasis on Shuttle launch requirements)

5) Design and utilization of double-wall tanks as related to system reliability aspects and safety during transport by Shuttle orbiter

7. SYSTEM PERFORMANCE ASSESSMENT

Characteristics of the selected propulsion module design for space-storable and earth-storable propellants were used to update earlier performance estimates for the various missions under consideration, following the iteration process outlined in Section 3 (see Figure 3-6). The results presented in this section show an appreciable performance improvement of the multi-mission propulsion module, sized for Mercury orbiter requirements, in the outer-planet orbiter and comet rendezvous missions.

7.1 INITIAL PERFORMANCE ESTIMATES AND PERFORMANCE IMPROVEMENT OPTIONS

Initial propulsion module size selections and inert weight estimates, based on Mercury orbiter requirements for two modules operating in tandem, were obtained by assuming the empirical scaling relations between propellant and inert weight given in Section 3.3. The first step in the iterative propulsion module sizing procedure resulted in generally unfavorable performance of the multi-mission module in outer-planet orbit and comet rendezvous missions since the tank sizes, and hence inert weights (listed in Table 5-1), were overly large.

A performance improvement in multi-mission applications of the propulsion module is achievable primarily by size and inert weight reduction. The following improvement options were explored:

1) Lowering the maneuver requirements for the Mercury orbiter and thereby reducing the size penalty for other missions

2) Reducing inert weight by design iteration and improved weight estimates based on structural analysis.

A reduction of the maneuver requirements for the Mercury orbiter resulted from adopting a less demanding mission mode with launch on 12 March 1988 (see Section 2.2.1) as reference mission. This mission mode was identified by NASA Ames Research Center during the study as a possible alternative to the mission mode specified initially, with launch on 19 June 1988. The new mission mode reduces ideal velocity requirements by about 350 m/sec and permits a more than proportionally

large size reduction of the propulsion module. This was used as the basis for resizing Modules A and B.

A change in initial orbit characteristics at Mercury (a lower periapsis altitude and higher eccentricity than specified in the study guidelines) would also contribute to a reduction of ΔV requirements and, hence, a size reduction of the multi-mission propulsion module. However, these options would a) increase the difficulty of approach guidance and b) compromise orbital stability and were omitted from further consideration.

7.2 UPDATED INERT WEIGHT ESTIMATES

Updated weight estimates of the four selected propulsion module designs were obtained on the basis of structural analysis (Appendix C) for the initially selected propellant weights. Results are shown in Figure 7-1. The updated inert weights follow a trend that differs markedly from the initially assumed scaling relations (shown by dashed lines). In the propellant mass range of interest this can be expressed approximately by

$$W_i = 0.1\ W_p + 120\ \text{kg}$$

for both the earth-storable and space-storable system designs. The fixed mass of 120 kg (265 lb_m) includes the sun shade and support structure used in the Mercury orbit mission, estimated as 27 kg (60 lb_m). For the outer-planet orbiters this value is about 15 kg (33 lb_m) lower.

Actually, the inert weights established by structural analysis do not depend linearly on propellant mass because of the following factors:

- Only the support trusses and tank weights vary in proportion to propellant mass
- The weight of the cylindrical center hull increases in proportion to the square root of the load since the design is based on critical buckling loads
- The heavy end ring structures on each propulsion module are essentially independent of propellant mass, being stressed by the crash load requirements of the Shuttle orbiter with propellant tanks empty.

This departure from the more usual structural weight characteristics of propulsion systems is due primarily to the tank mounting arrangement, the multi-mission/tandem configuration constraints, and Shuttle launch and abort load requirements. The tank mounting arrangement was adopted partly to facilitate load path separation with two propulsion modules mounted in tandem, partly to facilitate thermal separation of warm and cold tanks (in the space-storable propellant case), and partly to meet mass distribution constraints in the spinning Module A configuration.

Figure 7-1 shows that inert weights are reduced primarily for the earth-storable configurations for Module A and Module B where a performance improvement is most important.

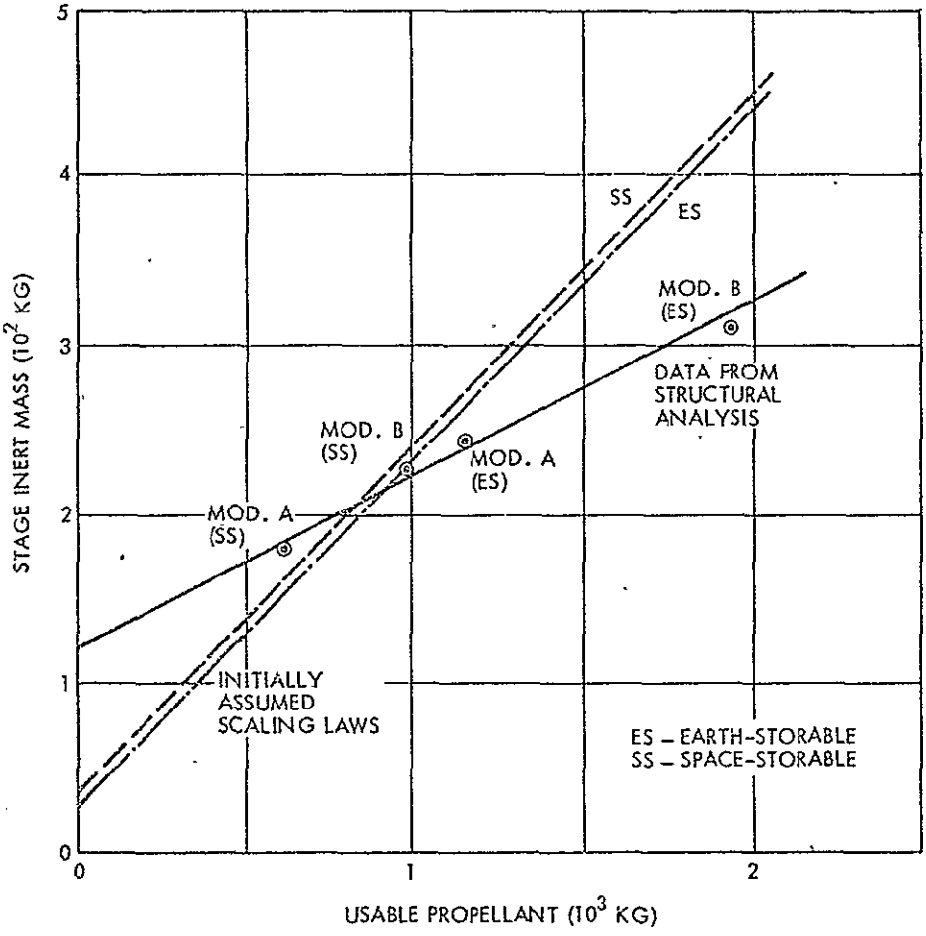

Figure 7-1. Initially Assumed and Revised Stage Inert Weights

Extending the results obtained for the multi-mission propulsion module to custom-designed modules leads to a similar scaling law, since the principal factors listed above give rise to a similar dependence of structural weight on propellant mass. Except for lower compression and bending loads during launch and lower tension loads during maximum survivable crash landing accelerations similar load profiles are in effect for a single propulsion module at a given propellant mass. The estimated reduction of fixed-weight components of the custom-designed stage leads to an inert weight scaling law of the form

$$W_i' = 0.1\ W_p + 80 \text{ kg.}$$

applicable to earth- and space-storable propellants.

7.3 MERCURY ORBITER PERFORMANCE

The revised scaling law was used to obtain updated propulsion module sizes and inert weights based on the modified Mercury orbiter maneuver requirements discussed above. Table 7-1 lists the resulting Module A and Module B mass characteristics and tank sizes for earth-storable and space-storable propellants. It also lists the injected gross spacecraft mass and indicates which launch vehicles are adequate to perform the mission. Comparison with the initial propulsion module data (Table 4-1) indicates a major size reduction in the earth-storable versions of Modules A and B.

The performance analysis of Module B assumed an optimum variable thrust vector pointing program for Mercury orbit insertion and determined the optimum thrust initiation time. Module A uses a fixed thrust orientation nearly tangential to the flight path at periapsis but only with a small in-plane thrust vector offset to satisfy the side-sun protection constraint (see Section 4.6).

7.4 PERFORMANCE COMPARISON OF EARTH-STORABLE AND SPACE-STORABLE SYSTEMS IN OUTER PLANET MISSIONS

7.4.1 Propellant Mass

Figures 7-2 and 7-3 show updated propellant-mass requirements for Pioneer and Mariner payloads with earth-storable and space-storable propulsion systems, as functions of flight time to Saturn and Uranus.

Table 7-1. Performance Characteristics of Mercury Orbiters (Launch 12 March 1988; C_3 = 25.8 km^2/sec^2)

Flight Vehicle, Propellant Type	Weight, kg (lb_m)			Candidate Shuttle Upper Stages (No kick stage required)	Injected Weight Capability kg (lb_m)
	Propellant Weight[1]	Inert Weight[1]	Gross Weight		
Pioneer (340 kg)/Tandem Module A[2]					
Earth-Storable	894 (1971)	209.4 (462)	2546 (5614)	Dual Transtage	3900 (8600)
				or Centaur D-1S	5250 (11,600)
Space-Storable	551 (1215)	175.1 (386)	1792 (3951)		
				or Titan 3E/Centaur D-1T (for reference only)	3300 (7277)
Mariner (550 kg)/Tandem Module B[3]					
Earth-Storable	1272 (2805)	247.2 (545)	3588 (7912)	Dual Transtage	4000 (8820)
				or Centaur D-1S	5300 (11,700)
Space-Storable	781 (1722)	198.1 (437)	2508 (5530)		

[1] Each module

[2] Module A uses fixed thrust orientation, 5 degrees offset from optimum (near-equatorial orbit)

[3] Module B uses variable thrust pointing program (near-polar orbit)

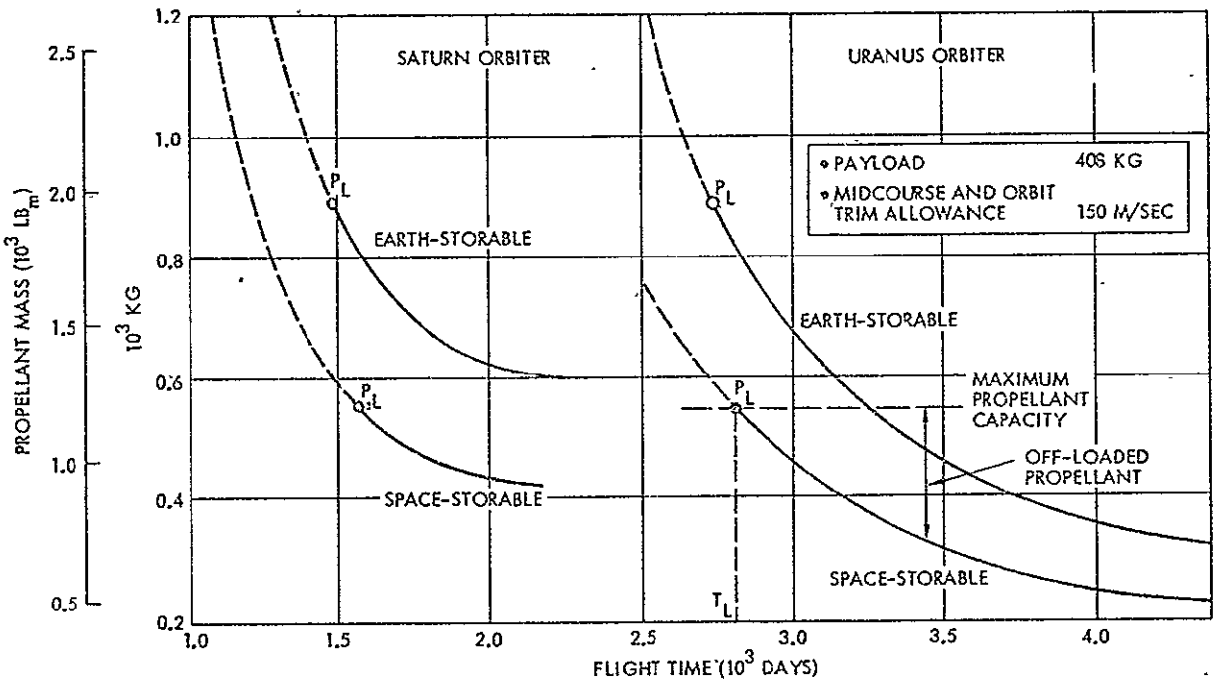

Figure 7-2. Propellant Requirements for Saturn and Uranus Orbiters (Pioneer Payloads, Multi-Mission Module)

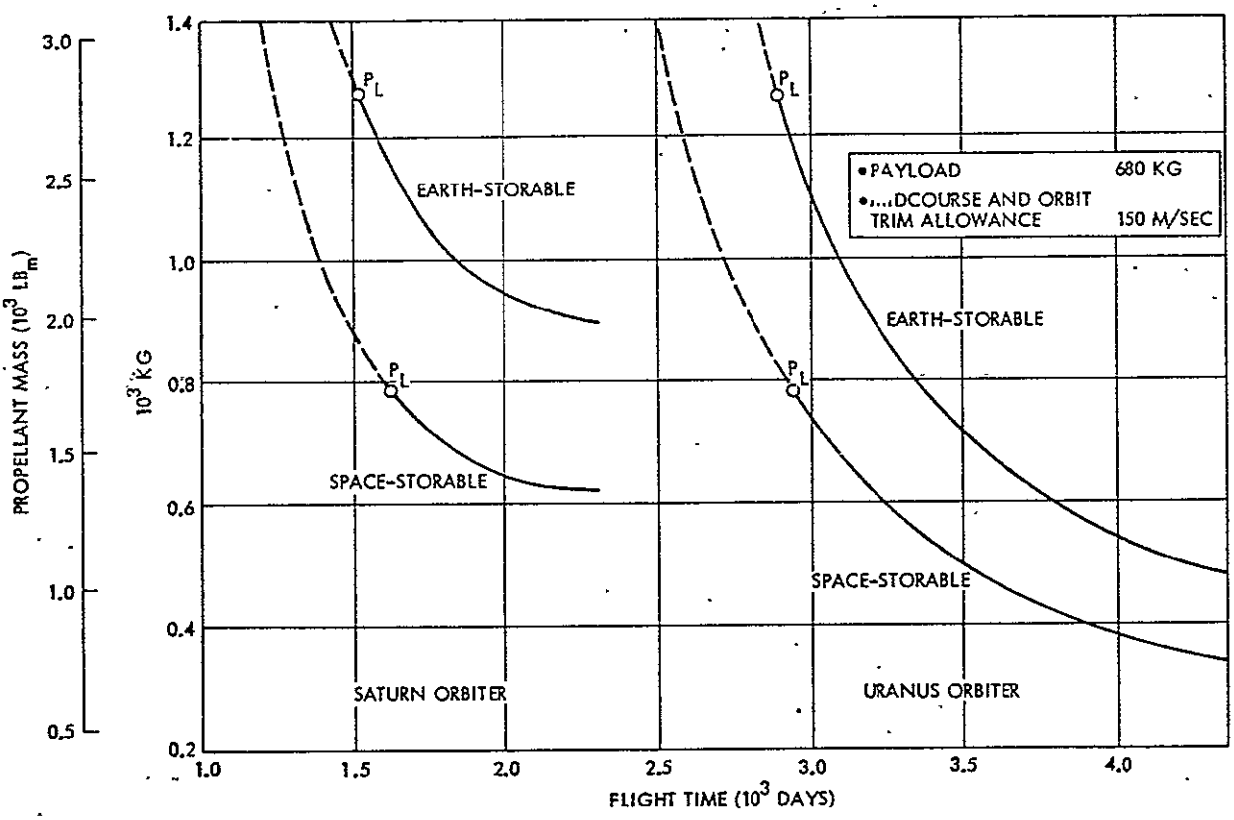

Figure 7-3. Propellant Requirements for Saturn and Uranus Orbiters (Mariner Payloads, Multi-Mission Module)

Only one payload weight (408 kg) is assumed as typical for Pioneer class, and one (680 kg) for Mariner class orbiters in deriving the propellant requirements shown in Figures 7-2 and 7-3. Other payload weights will be considered parametrically in Section 7.4.4. On each of these curves the propellant capacity of the multi-mission propulsion module is indicated by limit values P_L. These points also designate lower limits of achievable flight times (T_L) regardless of launch vehicle capability. The amount of propellant to be off-loaded for flight times greater than T_L is indicated by the difference between the required propellant mass and P_L.

7.4.2 Saturn Orbiter Performance

Performance characteristics of Saturn orbiters derived from the above propellant requirements are shown in Figure 7-4 for Pioneer and Mariner payloads, earth-storable and space-storable systems. The graph also provides comparisons of multi-mission and custom-designed

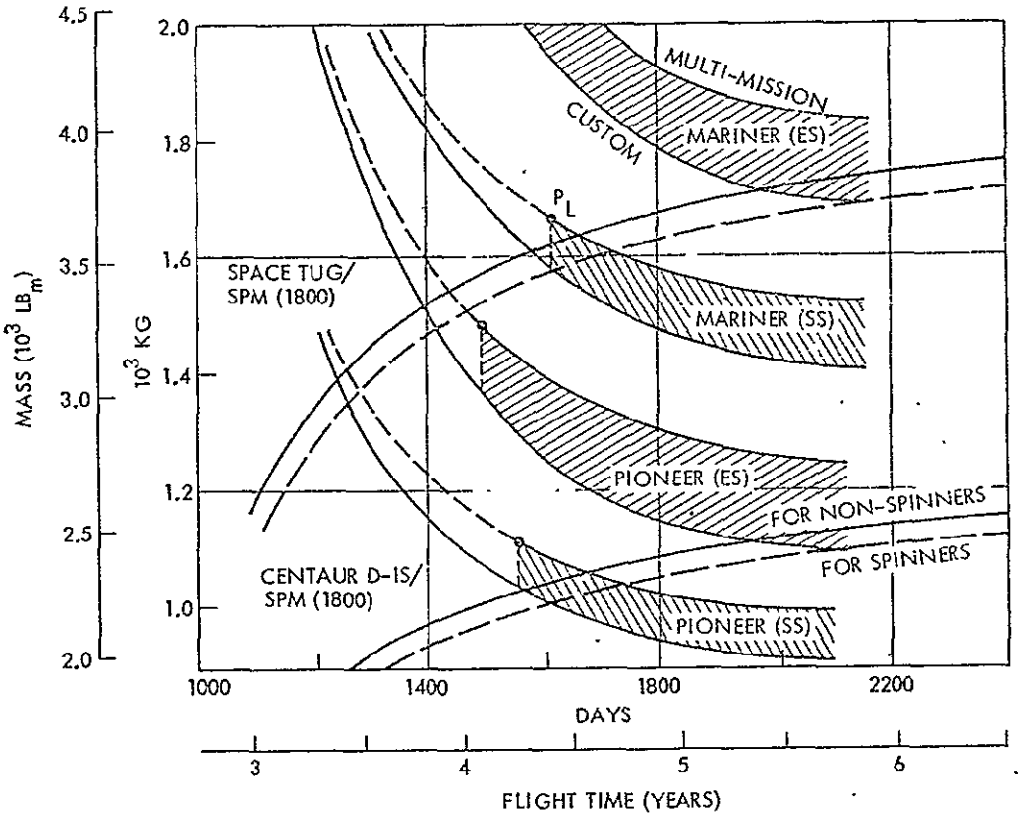

Figure 7-4. Performance of Pioneer and Mariner Saturn Orbiters. Earth-Storable (ES) and Space-Storable (SS) Propulsion Systems.

propulsion module performance. The shaded areas between the upper curves (multi-mission module performance) and the lower curves (custom-designed module performance) represent design options that are "customized" to some degree having a lower weight penalty than the multi-mission design.

The graph shows the injected weight capabilities of the launch vehicle candidates by a second set of curves, differentiated as to spinning and nonspinning payloads. Intersections with the corresponding payload performance curves determine the minimum flight times in each case. The lower limit of achievable flight times is not always determined by the intersection of payload and launch vehicle curves. In some instances, e.g., for Pioneer missions launched by Space Tug, the minimum flight time is actually determined by the time T_L that corresponds

to the maximum propellant capacity of the multi-mission module. Dashed curves extending beyond the propellant capacity limit do not represent actual performance characteristics but only indicate the (ideal) minimum flight time in the absence of the propellant limit ($P_{I'}$).

From these results it is apparent that the selected size of Module A is actually too small for most effective use of the Space Tug as upper stage for Pioneer Saturn orbiters. This means use of the multi-mission module imposes longer trip times to Saturn in exchange for reduced trip times to Uranus (see below).

To summarize Saturn orbiter performance characteristics, Mariner class spacecraft of 680 kg launched by Space Tug/SPM (1800) require flight times of 1600 days or much more depending on the type of propulsion module and bipropellants used. Pioneer class orbiters (408 kg payload) launched by Centaur D-1S/SPM (1800) require flight times of 1750 days and more. With Space Tug as launch vehicle, more appropriate for Pioneer orbiters with an earth-storable, multi-mission module, the minimum flight time would be 1480 days.

7.4.3 Uranus Orbiter Performance

Figure 7-5 shows the corresponding performance plot for Uranus orbit missions. Only the Space Tug/SPM (1800) performance curve is shown in this graph. The performance of a Centaur class upper stage would not be adequate for Uranus missions. Flight times range from about 2750 to 3860 days for Pioneer orbiters, and from 3450 to 3750 days for Mariner orbiters with space-storable propulsion assuming payload weights of 408 and 680 kg respectively. Mariner orbiters with earth-storable propulsion require at least 3840 days with a custom-designed propulsion module and about 4700 days with a multi-mission module.

These data do not reflect the use of the propulsion module for C_3 augmentation maneuvers which will be discussed below.

7.4.4 Effects of Payload Mass Variation and Change in Launch Vehicle Performance

Performance data shown in Figures 7-2 to 7-5 were based on the assumption of fixed payload weights for Pioneer and Mariner type spacecraft. Actually, a range of payload weights for each spacecraft family

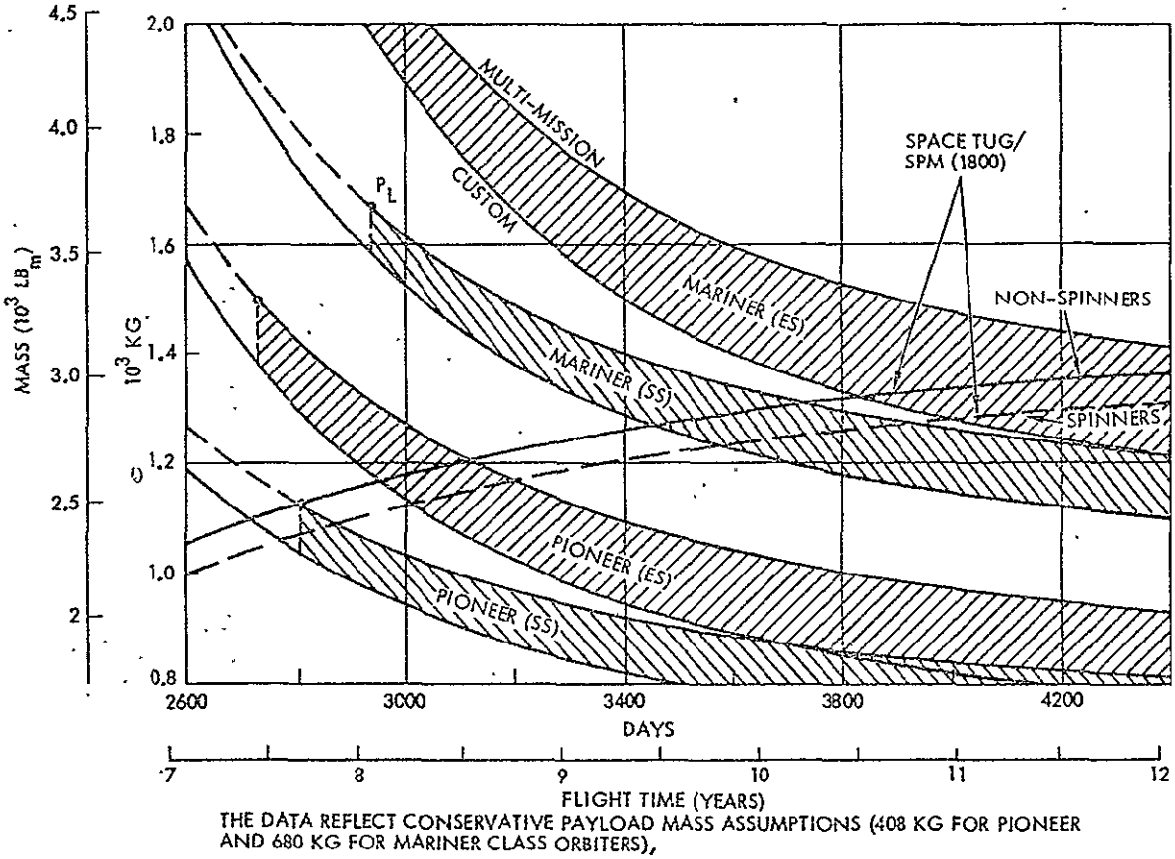

Figure 7-5. Performance of Pioneer and Mariner Uranus Orbiters. Earth-Storable (ES) and Space-Storable (SS) Propulsion Systems.

was specified in the work statement. Figures 7-6 and 7-7 show performance plots for parametric payload weight changes in Saturn and Uranus orbiters with multi-mission propulsion modules and space-storable propellants. It can be seen that the advantages of reducing payload weight in terms of minimum flight time are greater for missions to Uranus than to Saturn.

The format of these graphs permits direct analysis of the effect of launch vehicle performance variations to be expected in the future as Shuttle upper stages become more firmly defined. For convenient reference a set of launch vehicle performance characteristics is shown in Figures 7-6 and 7-7 together with the parametric payload curves. Depending on whether a spinning or nonspinning flight spacecraft is considered, the dashed or solid launch vehicle performance curves apply. Lower flight time limits T_L defined by propellant capacity are indicated

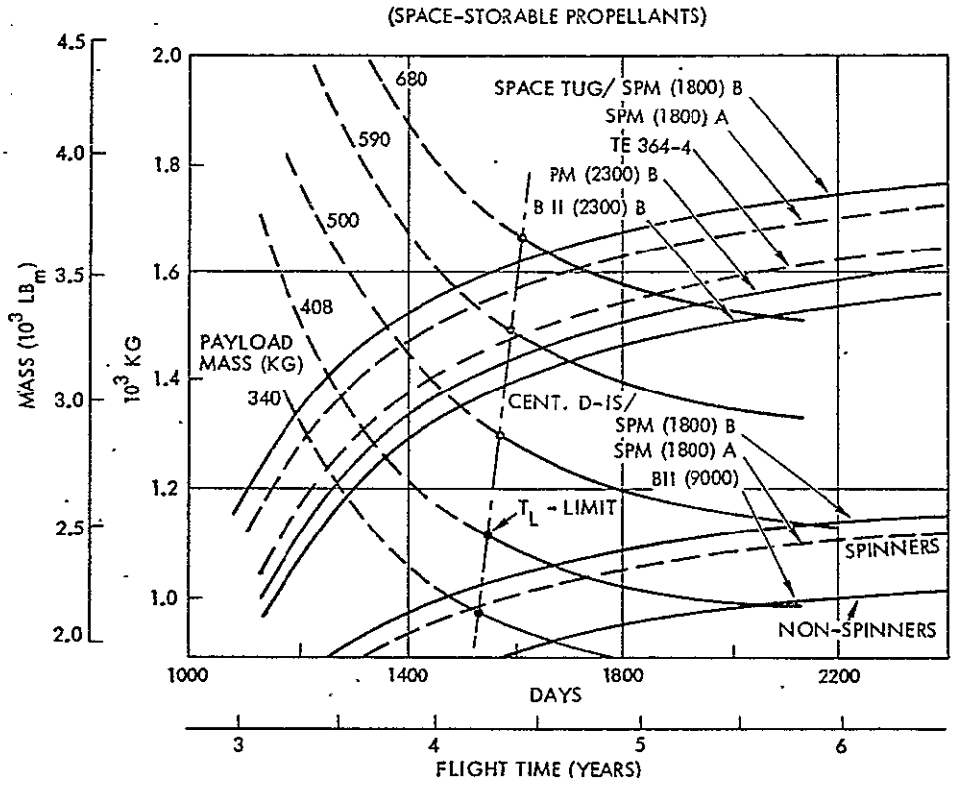

Figure 7-6. Saturn Orbiter Performance for Several Shuttle/ Upper Stage Candidates, with Payload as Parameter

in the graphs by (nearly vertical) dashed lines in the range of 1500 to 1600 days for Saturn orbiters, and in the range of 2800 to 2950 days for Uranus orbiters.

For Saturn orbiters the higher-performance upper stage candidates give flight times close to the T_L limits only for the upper range of payload mass. For the lower payload mass range the lower performance stages are more appropriate. In Uranus orbit missions the T_L limit is commensurate with or below the minimum flight times achievable by any of the upper stage candidates shown.

7.4.5 Performance Improvement by C_3 Augmentation Maneuver

The effect of C_3 augmentation (see Section 3.5) is significant primarily for missions of long duration where the slope of the performance curves in Figures 7-3 through 7-7 levels out, and the location of their intersections, designating minimum flight time, becomes increasingly

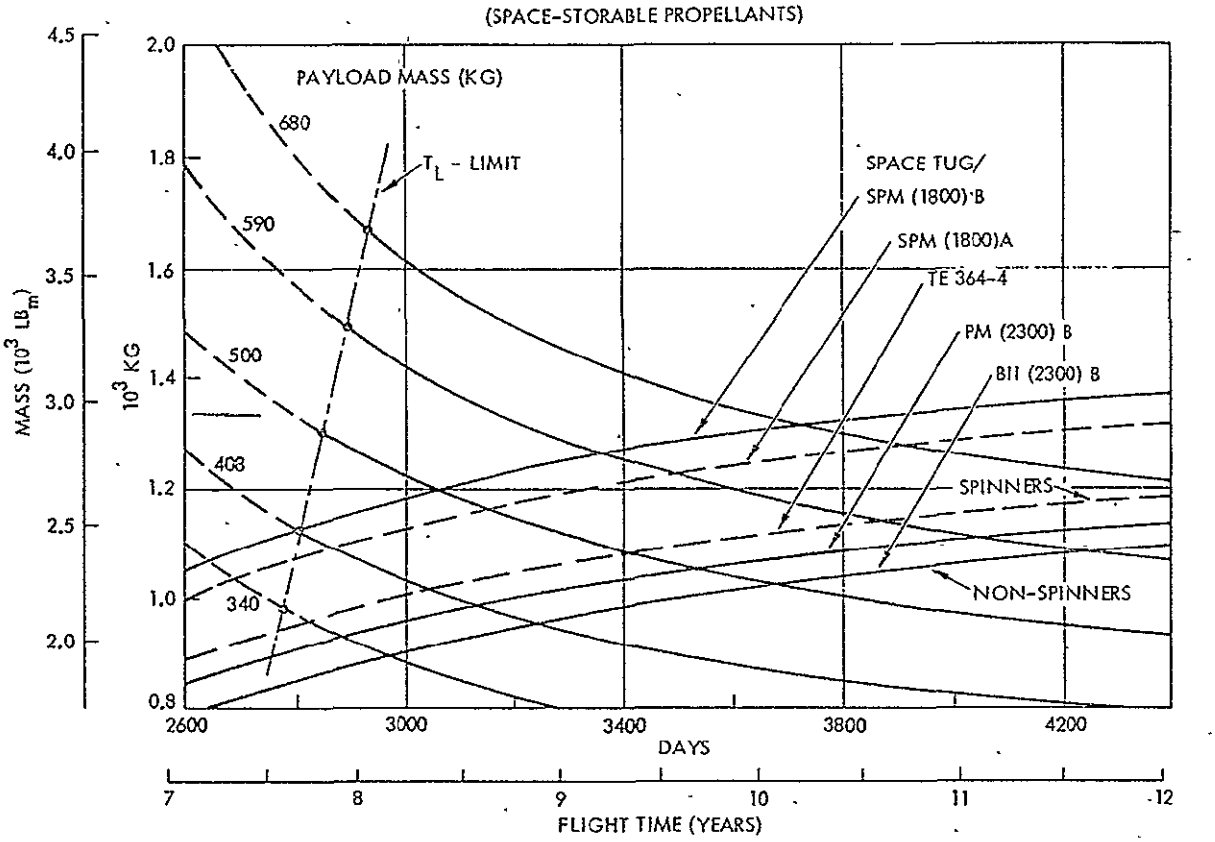

Figure 7-7. Uranus Orbiter Performance for Several Shuttle/ Upper Stage Candidates, with Payload as Parameter.

sensitive. Thus an augmentation of launch vehicle capability by 100 kilograms or more, achievable by an expenditure of several hundred kilograms of extra propellant, can produce flight time reductions of more than 150 days in Uranus missions with flight times of about 10 years.

This is illustrated in Figure 7-8 for three values of payload mass with Space Tug/SPM (1800) assumed as launch vehicle. The upper graph shows the propellant mass required without the C_3 augmentation maneuver (see scale on the right) as function of flight time and the off-loaded propellant, ΔW_p, available partly for C_3 augmentation and partly for meeting higher velocity requirements as flight time increases (left scale). The lower graph shows the launch vehicle performance curve with and without the augmentation maneuver, based on data previously discussed in Section 3.5 (Figure 3-16), and three payload curves. Even

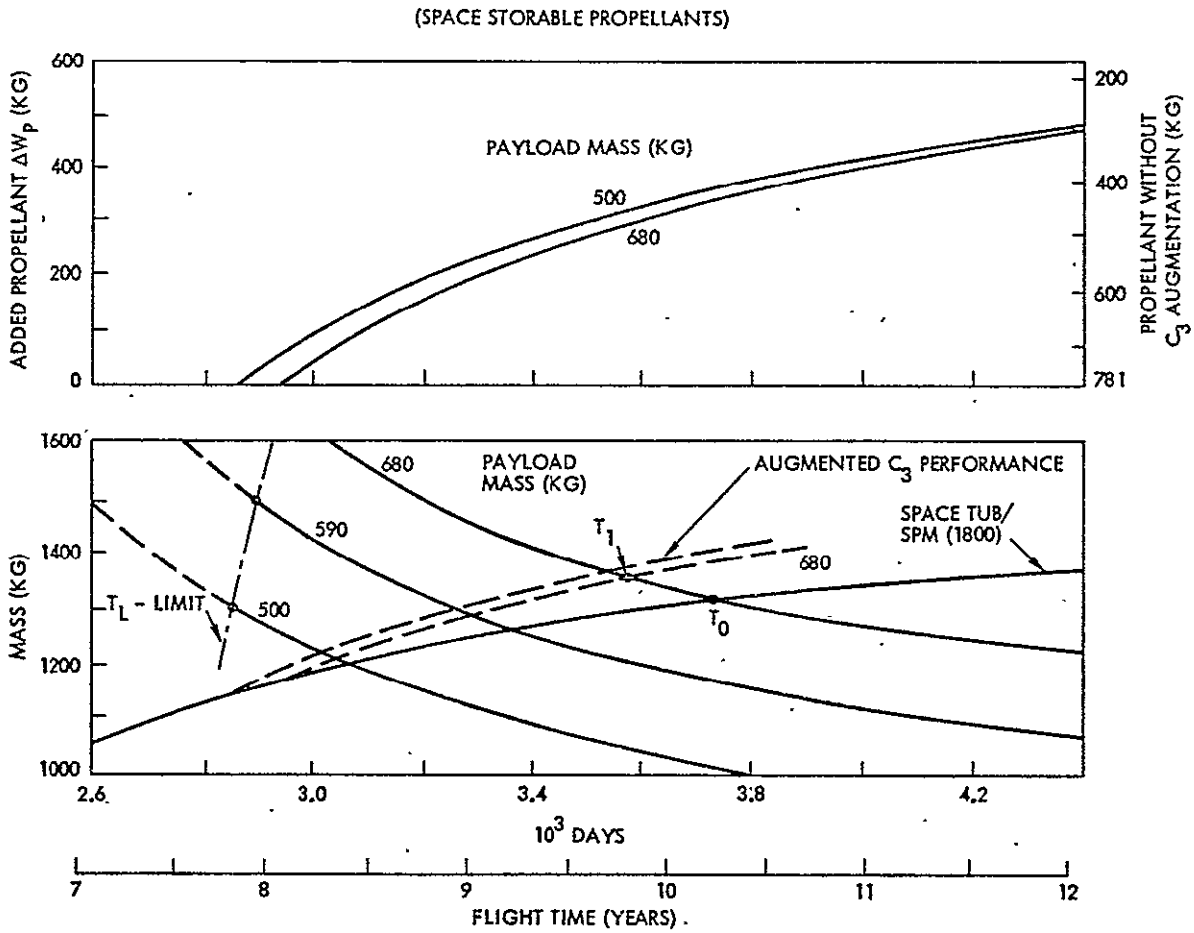

Figure 7-8. C_3 Augmentation Effect on Uranus Orbiter Performance

with the assumption of zero coast time between upper stage burnout and propulsion module ignition the flight time reduction is only modest and becomes progressively smaller with reduction of payload weight. Somewhat larger reductions would be achieved with lower performance launch vehicles.

Unfortunately, the very long flight times characteristic of Mariner Uranus orbiters with earth-storable propellants cannot be reduced to an acceptable range because of the very limited C_3 augmentation effect attainable by these propellants.

Table 7-2 summarizes applicability of the C_3 augmentation method and shows that it is of only limited usefulness partly because the propulsion module does not offer sufficient spare propellant capacity or the maneuver mode is too inefficient because of significant gravity losses with only 200 lb_f (890 N) of thrust.

Table 7-2. Applicability of C_3 Augmentation Technique

Propulsion Type, Mission Class and Module Type	Applicability of Technique	Remarks
• Earth-storable propulsion	No	Negligible benefit in all cases of practical interest
• Space-storable propulsion, multi-mission module		
- Saturn orbiter		
Module A	No	Negligible flight time reduction
Module B	No	Negligible flight time reduction if Space Tug/SPM (1800) available
	Yes	If only lower performance upper stage available and 180-day flight time reduction important
- Uranus Orbiter		
Module A	No	Negligible flight time reduction
Module B	Yes	If 160-day flight time reduction important enough
• Custom-designed propulsion Modules A or B, Uranus orbit missions	Yes	If 180-240 day flight time reduction is important enough

A practical objection to its use is the necessity for maneuver initiation immediately after launch vehicle separation. This implies the need for attitude control modes for Pioneer or Mariner spacecraft with appendages still stowed. For the selected propulsion module size the benefits attainable by the C_3 augmentation maneuver are too small to warrant the added design complexity and also the possible decrease in propulsion system reliability resulting from its implementation.

If the capacity of the solid kick stages used at launch were no greater than that of the Burner II (2300) or of the TE 364-4, the advantages of C_3 augmentation would no doubt outweigh the arguments against it.

7.4.6 Mission Characteristics Summary

Table 7-3 summarizes mission characteristics for representative (fixed) Pioneer and Mariner class payload vehicles in Saturn and Uranus

Table 7-3. Outer Planet Orbiter Performance Summary. Payload weight = 408 kg (Pioneer) and 680 kg (Mariner)

Payload	Propellants/ Module Type[1]	Trip Time[2] (days)	Propellant Capacity of MM Module kg (lb_m)	Propellant Mass kg (lb_m)	Inert Mass kg (lb_m)	Total Injected Mass kg (lb_m)
Saturn Orbiter						
Pioneer	ES/MM	1480[3]	894 (1971)	894[3] (1971)	617 (1360)	1511 (3332)
	CD	1400	-	910 (2007)	579 (1277)	1489 (3283)
	SS/MM	1720[4]	551 (1215)	480 (1058)	583 (1286)	1063 (2344)
	CD	1600[4]	-	480 (1058)	536 (1182)	1016 (2240)
Mariner	ES/MM	2160	1272 (2805)	930 (2051)	927. (2044)	1857 (4095)
	CD	1920	-	860 (1896)	846 (1865)	1706 (3762)
	SS/MM	1730	781 (1722)	725 (1599)	878 (1936)	1603 (3535)
	CD	1570	-	680 (1499)	828 (1826)	1508 (3325)
Uranus Orbiter						
Pioneer	ES/MM	3200	894 (1971)	570 (1257)	617 (1360)	1187 (2617)
	CD	3020	-	560 (1235)	544 (1200)	1104 (2434)
	SS/MM	2860	551 (1215)	510 (1125)	583 (1286)	1093 (2410)
	CD	2750	-	520 (1147)	540 (1191)	1060 (2337)
Mariner	ES/MM	4700	1272 (2805)	470 (1036)	927 (2044)	1397 (3080)
	CD	3840	-	575 (1268)	818 (1804)	1393 (3072)
	SS/MM	3750	781 (1722)	430 (948)	878 (1936)	1308 (2884)
	CD	3460	-	460 (1014)	806 (1777)	1266 (2792)

Notes:

[1] MM - Multi-mission; CD - custom-designed

[2] Does not reflect C_3 augmentation

[3] Dictated by maximum propellant capacity (50 kg launch weight margin)

[4] Launched by Shuttle/Centaur D-1S/SPM (1800)

orbit missions, including comparisons of spacecraft and propellant mass and flight times for space- and earth-storable propellants, and for multi-mission and custom-designed propulsion modules.

The bar graph, Figure 7-9, shows minimum flight times achievable in Saturn and Uranus orbit missions under the stated conditions.

In summary, the performance comparisons shown above indicate the following:

1) Flight time reductions achievable by space-storable propellants for a given Shuttle upper stage are very significant (1 to 2 years), particularly in the case of Mariner type payloads. For equal trip times, the increase in payload is about 100 kg.

2) In missions with Pioneer type payloads the flight time reduction is important but not nearly as great, typically ranging from 0.5 to 1.5 years in Saturn and Uranus missions, respectively. Payload advantages for trip times equal to those for earth-storable propulsion modules are also about 100 kg.

3) Only the use of space-storable propellants makes the multi-mission module concept, with its attendant cost economy, feasible and attractive in Mariner class missions.

4) In the case of Mariner missions to Uranus a space-storable multi-mission propulsion module would lead to unrealistically long flight times approaching that of a Hohmann transfer.

5) A lower-performance Shuttle upper stage, such as Centaur D-1S/SPM (1800) is adequate for Saturn missions by Pioneer class vehicles. However, in the case of earth-storable propellants a flight time increase of over 800 days would result, compared with an increase of only 400 days for space-storable propellants, assuming multi-mission modules in both cases.

6) C_3 augmentation by using excess propellant capacity of the multi-mission propulsion module can reduce flight times by up to about 180 days (or more under some circumstances) in Uranus missions. However, flight time reductions achievable are too small, in most instances, to warrant operational and reliability disadvantages associated with its implementation.

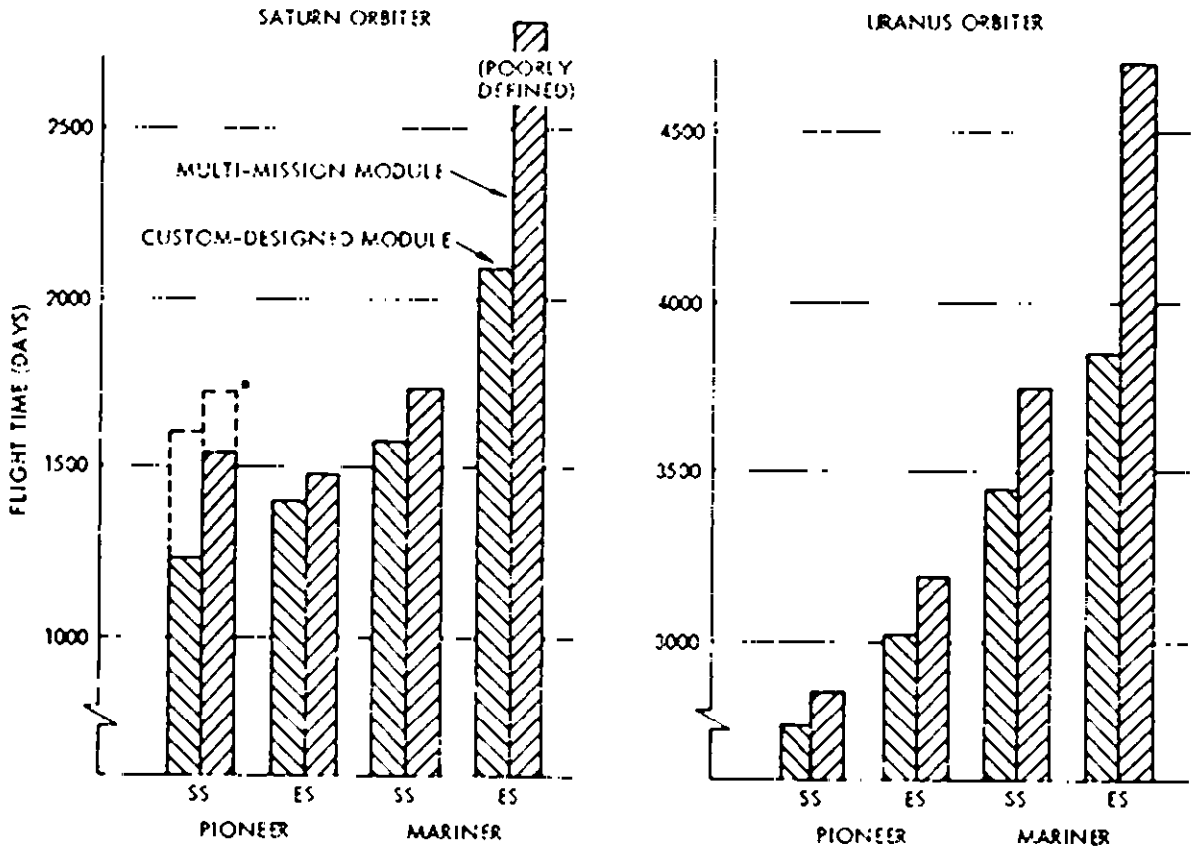

Figure 7-9. Flight Times for Saturn and Uranus Orbiters (Launch Vehicle Shuttle/Space Tug/SPM (1800) Except as Noted)

7.5 COMET MISSION PERFORMANCE

Comet rendezvous performance of the multi-mission propulsion Modules A and B was analyzed, based on the maximum propellant capacities and inert weight data listed in Table 7-1. Figure 7-10 shows curves of maximum payload weight capability as function of ΔV expenditure for earth- and space-storable systems. Specified ranges of Pioneer- and Mariner-class payload weights are indicated in the graph.

Total ΔV requirements for the seven comet rendezvous missions being considered are marked on the abscissa. They include the major midcourse (ΔV_2) and rendezvous maneuvers (ΔV_3) listed in Table 2-4.

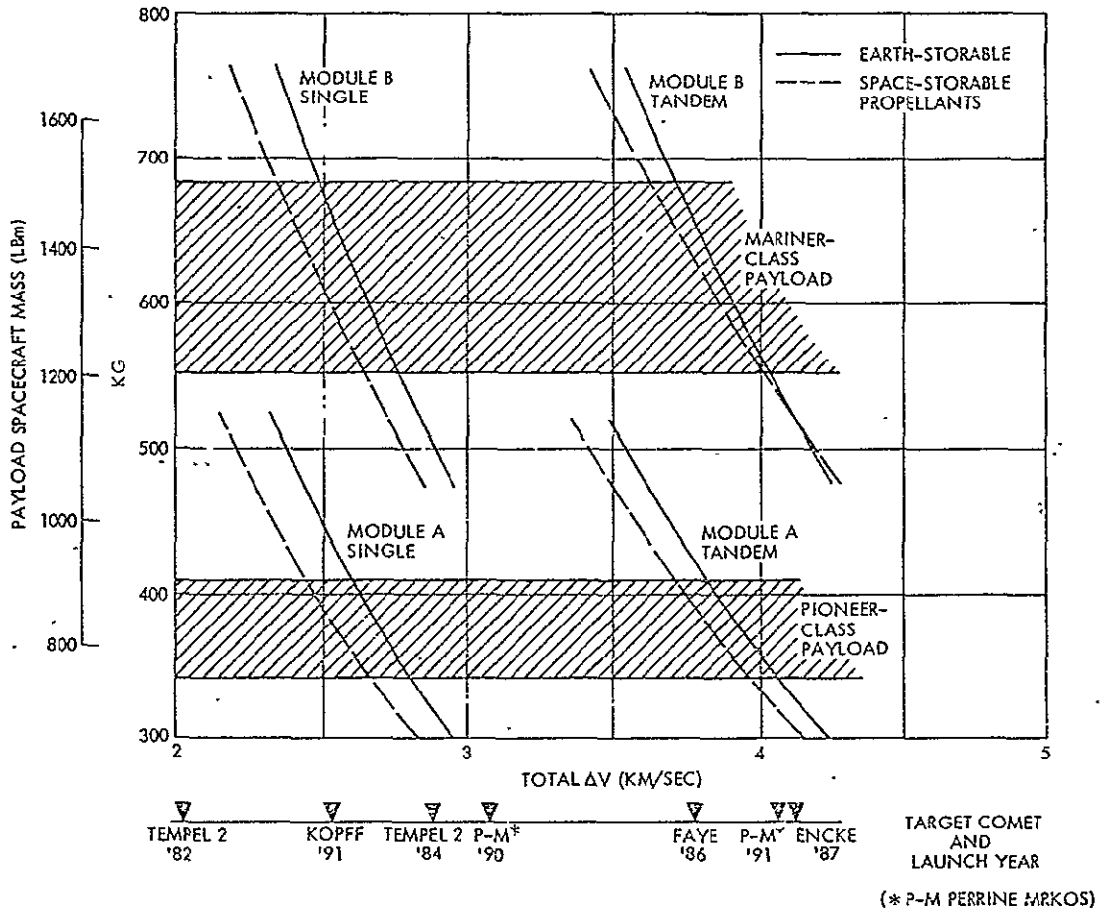

Figure 7-10. Payload Weight Capabilities of Single and Tandem Propulsion Modules in Comet Rendezvous Missions

plus 300 m/sec for guidance corrections and excursions at the comet. For Encke (having less uncertain orbital characteristics than the other comets) only 200 m/sec are assumed for extra maneuvers.

The chart shows that only two of the missions (Tempel 2, '82, and Kopff, '91) can be performed with a single propulsion stage. All others require the use of two stages in tandem. Missions with the highest ΔV requirements (Faye '86, Perrine Mrkos '91, and Encke '87) could be accomplished only by adding propellant capability and/or by reducing payload mass significantly, i.e., even below the lower limits of the Pioneer and Mariner payload mass ranges indicated in the chart. Note that the maximum ΔV capabilities of the earth- and space-storable propulsion modules do not differ much for these payload mass ranges since both modules were designed to handle a similar payload mass in the Mercury orbiter mission.

Table 7-4 lists weight characteristics of spacecraft with maximum payload weights in the Pioneer and Mariner class (408 and 680 kg, respectively) in the case of space-storable propellants. Evaluation of launch vehicle performance requirements shows that the four missions identified as feasible with these payload weights are within the performance range of Shuttle/Centaur/SPM (1800), except for the Mariner class mission to Perrine Mrkos (1990) which would require either a slightly larger (~200 kg) injected weight capability or a payload mass reduction of about 80 kg (176 lb_m).

Table 7-4. Characteristics of Comet Rendezvous Missions

Comet Mission	ΔV_{total}* (km/sec)	Number of Stages Required	Module Type	Propellant Weight		Initial Weight kg (lb_m)
				Stage 2 kg (lb_m)	Stage 1 kg (lb_m)	
1 Tempel 2	2.021	1	A	414 (913)	- -	997 (2198)
		1	B	623 (1374)	- -	1501 (3310)
2 Tempel 2	2.879	2	A	551 (1215)	159 (351)	1468 (3237)
		2	B	781 (1722)	285 (628)	2142 (4723)
3 Faye	3.760	2	A	551 (1215)	546 (1204)	1855 (4090)
		**	B	781 (1722)	845** (1863)	**
4 Kopff	2.521	2	A	551 (1215)	26 (57)	1335 (2944)
		2	B	781 (1722)	91 (201)	1948 (4295)
5 Perrine Mrkos	3.082	2	A	551 (1215)	240 (529)	1549 (3416)
		2	B	781 (1722)	403 (889)	2260 (4983)
6 Perrine Mrkos	4.062	**	A	551 (1215)	700** (1544)	**
		**	B	781 (1722)	1075** (2370)	**
7 Encke	4.110	**	A	551 (1215)	726** (1601)	**
		**	B	781 (1722)	1112** (2452)	**

*ΔV_{total} includes major midcourse (ΔV_2) and rendezvous maneuver (ΔV_3) plus 300 m/sec for guidance corrections and for excursions at comet. (For Encke only 200 m/sec of extra maneuver capability are allowable.)

**In these missions propellant requirements exceed tandem-stage capacity if payload mass of 408 (for Module A) and 680 (Module B) is assumed. Payload mass reduction of about 50 kg is required to make missions 3(B), 6(A and B), and 7(A) feasible.

7.6 AUXILIARY PROPELLANT REQUIREMENTS

Only preliminary estimates for auxiliary propellant requirements were obtained within the scope of this study. They include midcourse and orbit trim ΔV requirements of 450 m/sec for the Mercury orbiter

and 150 m/sec for the Saturn and Uranus orbiters. Table 7-5 lists propellant requirements for these maneuvers for the different mission classes, payload classes and propellant types considered. Propellant requirements for attitude control are also listed, based on data derived in Section 4-6 and on data derived in a recent TRW study of Pioneer Jupiter orbiters and Saturn/Uranus probe missions.

Propellant weights previously listed in Table 7-1 (Mercury orbiter) and 7-3 (outer-planet orbiters) include midcourse and orbit trim maneuver propellant for the above requirements. However, the weights listed in Table 7-5(a) are slightly larger to reflect the fact that actually only about one-half of these maneuvers can be performed by the main engines. The rest of the maneuvers require the use of auxiliary thrusters and are therefore performed less efficiently, namely at I_{sp} = 200 sec for monopropellant hydrazine thrusters in Module A (space-storable) and Module B (both earth- and space-storable) and at I_{sp} = 260 sec for bipropellant auxiliary thrusters in Module A with earth-storable propellants.

Attitude control (ACS) propellant weights listed in Table 7-5(b) range between 24 and 42 kg (52 and 93 lb_m). These weights were not included in the performance analysis since up to 80 percent of this propellant can be assumed as expended by the time the spacecraft reaches the target planet.

The effect of the added ΔV correction propellant on mission performance of the outer-planet orbiters can be assessed by considering half of this as added inert mass at the time of orbit insertion. The exchange ratio of added propellant mass to inert mass, $\partial W_p / \partial W_{inert}$, ranges from 1.0 to 1.5 in these missions. Thus, in the worst case a propellant mass of 20 to 30 kg must be added to compensate for the incremental auxiliary propellant mass remaining at orbit insertion. The effect is an increase of about 25 to 75 days in trip time to Saturn or Uranus, depending on the propellant expenditure time history.

More detailed study of auxiliary propellant weight characteristics and their effect on mission performance is required as mission characteristics in each case become more firmly defined.

Table 7-5. Auxiliary Propellant Requirements

a) ΔV Correction Maneuvers[1]

Propulsion Module	Transit Time (days)	Propellant Mass, kg (lb_m)			Remarks
		Transit Phase	Orbit Phase	Total	
Mercury Orbiter (ΔV = 450 m/sec)					
A – ES	735	210 (463)	45 (99)	225 (496)	Values are 30 to 80 kg larger than those reflected in total propellant mass in Table 7-1[2], [3]
SS	735	155 (342)	45 (99)	200 (441)	
B – ES	735	344 (759)	72 (159)	416 (917)	
SS	735	216 (476)	65 (143)	281 (620)	
Saturn Orbiter (ΔV = 150 m/sec)					
A – ES	1480	40 (88)	16 (35)	56 (123)	Values are up to 18 kg larger than those included in Table 7-3[2], [3]
SS	1720	30 (66)	17 (37)	47 (104)	
B – ES	2160	58 (128)	29 (64)	87 (192)	
SS	1730	45 (99)	25 (55)	70 (154)	
Uranus Orbiter (ΔV = 150 m/sec)					
A – ES	3200	32 (71)	16 (35)	48 (106)	Values are up to 18 kg larger than those included in Table 7-3[2], [3]
SS	2860	31 (68)	17 (37)	47 (104)	
B – ES	4700	43 (95)	29 (64)	71 (157)	
SS	3750	34 (75)	25 (55)	59 (130)	

[1] Assuming 1/2 of ΔV corrections occur in transit phase, 1/2 in orbital phase.

[2] Assuming 1/2 of correction maneuvers are performed by main thruster, others by monopropellant auxiliary thrusters. Reduced I_{sp} (200 seconds average) reflected in data.

[3] Only A/ES auxiliary thrusters use bipropellant, average I_{sp} = 260 sec.

b) Attitude Control Maneuvers

	Propulsion Module	Transit Time (years)	Orbit Time (years)	ACS Propellant, kg (lb_m) Solar Pressure Compensation[1]	ACS Propellant, kg (lb_m) Other[2]	Remarks
Pioneer Class Payloads	**Mercury Orbiter**					
	A – ES	2	2	10 (22)	20 (44)	Solar pressure compensation; see Figure G-6 (Appendix G).
	SS	2	2	15 (33)	16 (35)	
	Saturn Orbiter					Spin/precession propellant estimates extrapolated from TRW's Pioneer Saturn/Uranus Probe Study. (Reference 25).
	A – ES	4.7	3	-	28 (62)	
	SS	4.1	3	-	24 (53)	
	Uranus Orbiter					
	A – ES	8.8	1	-	42 (93)	
	SS	7.8	1	-	32 (71)	
Mariner Class Payloads	**Mercury Orbiter**					
	B – ES	2	2	17 (37)	8 (18)	See Table 4-10.
	SS	2	2	21 (46)	6 (13)	
	Saturn Orbiter					
	B – ES	5.9	3	-	24 (52)	See Table 4-9.
	SS	4.7	3	-	30 (66)	
	Uranus Orbiter					
	B – ES	12.9	1	-	24 (53)	See Table 4-9.
	SS	10.3	1	-	32 (71)	

[1] Solar pressure compensation for Mariner Mercury orbiter requires asymmetrical limit cycle (see Section 4.6).

[2] These data represent spin/precession maneuver propellant in Pioneer missions, symmetrical limit cycles and reorientations in Mariner missions.

7.7 PERFORMANCE NOMOGRAPHS

The nomographs shown in Figures 7-11 and 7-12 permit convenient parametric performance evaluation for space-storable and earth-storable propulsion systems, e.g., assessment of variations in launch vehicle characteristics, maneuver requirements, propulsion module inert weights, etc.

Curves shown in the upper left part of the nomograph represent two parameters of the rocket equation for impulsive maneuvers, namely, total spacecraft inert mass and usable propellant mass. The upper right part of the nomograph gives injected mass versus injection energy. Three launch vehicle performance curves are shown, others can be added. The lower right portion shows ΔV requirements for orbit insertion, plane change and midcourse maneuvers of Saturn and Uranus orbiters with flight time as parameter.

The example shown in Figure 7-13 gives the performance of a Saturn orbiter with a flight time of 1700 days and a total maneuver capability of 2300 m/sec. The injection energy requirement is 123 km^2/sec^2. The rectangle indicated by dashed lines determines the propellant mass, inert mass, and injected mass of the flight spacecraft corresponding to this trip time. Repeating this evaluation for other trip times leads to the dashed curve L_P shown in the upper left area of the nomograph. The combined inert weight of the multi-mission propulsion module and payload is indicated by a line designated L_M. The intersection P_T, of the dashed line, L_P, and the inert weight line, L_M, determines the minimum flight time achievable by the system. For missions with greater flight time, i.e., points on line L_P above the intersection, the propulsion module has a spare propellant capacity that can be read off the parametric lines W_{PR} between the intersect point, P_T, and the point of full propellant loading on line L_M. The example shown in Figure 7-13 indicates that with a total inert mass of 880 kg (Mariner payload plus propulsion module inerts) the full propellant load (780 kg) of multi-mission Module B is required to perform the Saturn orbit mission at the specified 1700-day trip time.

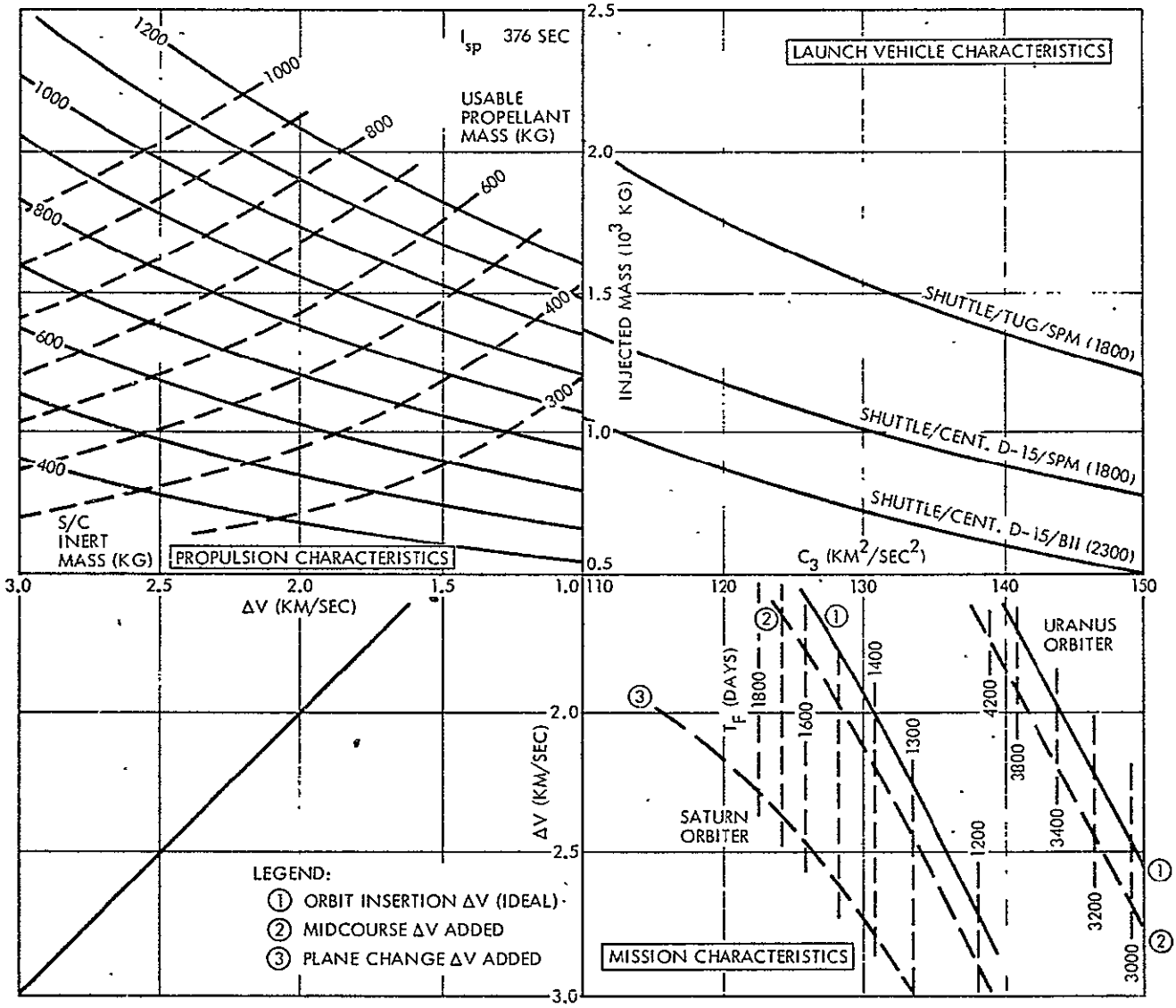

EXAMPLE: PIONEER URANUS ORBITER - SPACE STORABLE, MODULE A - SHUTTLE/TUG/SPM (1800)

T_F = 3040 DAYS, ΔV = 2.7 KM/SEC, C_3 = 149 KM^2/SEC^2

W_o = 1220 KG, W_{INERT} = 568 KG, W_{PR} = 652 KG

Figure 7-11. Mission Performance Nomograph (Space-Storable Propulsion)

Note that the upper left section of the nomograph does not reflect orbit insertion losses. These can be accounted for by an increase in actual ΔV requirements.

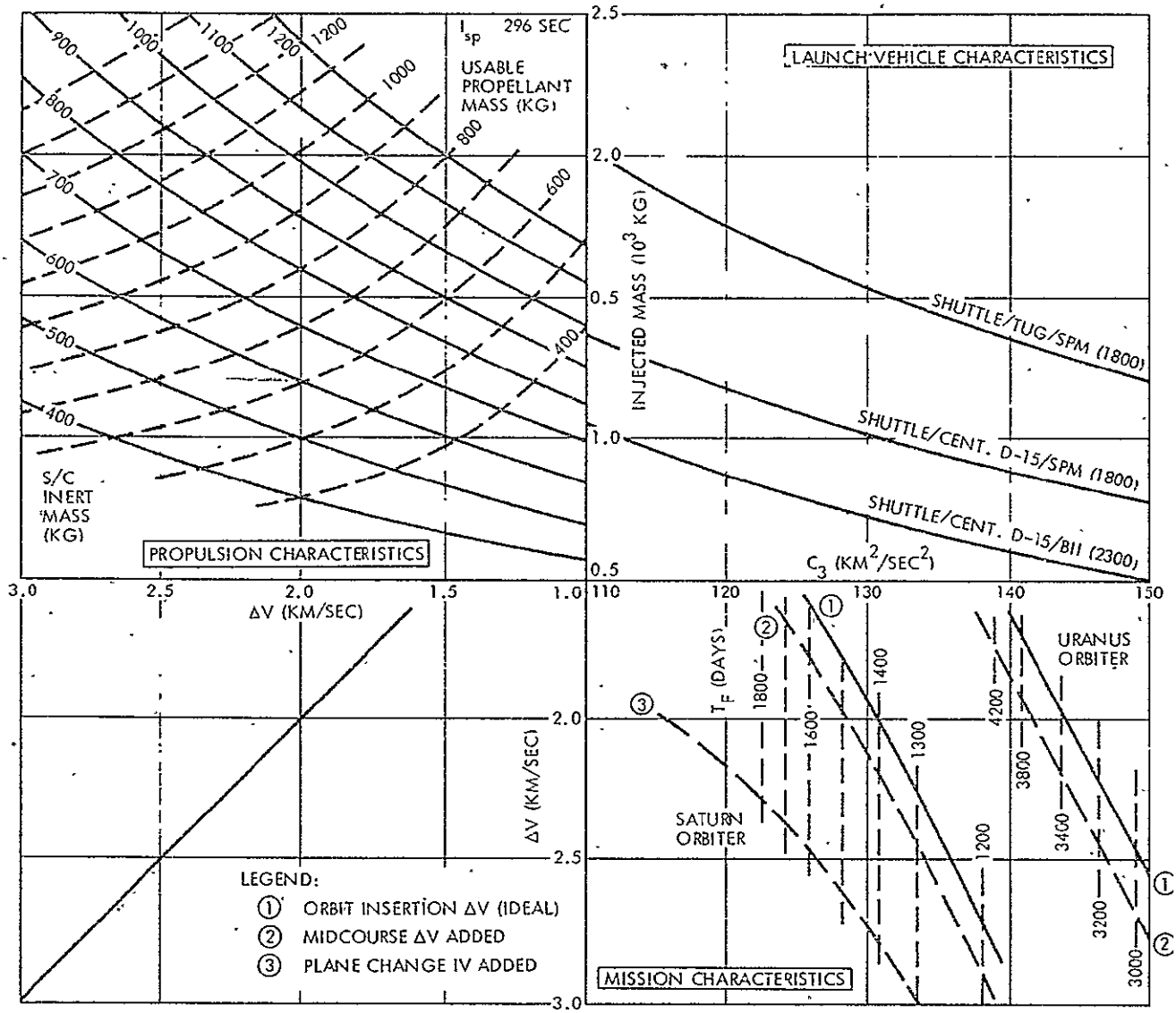

EXAMPLE: PIONEER URANUS ORBITER - EARTH STORABLE, MODULE A - SHUTTLE/TUG/SPM (1800)

T_F = 3600 DAYS, ΔV = 2.1 KM/SEC, C_3 = 143 KM^2/SEC^2

W_o = 1320 KG, W_{INERT} = 667 KG, W_{PR} = 653 KG

Figure 7-12. Mission Performance Nomograph (Earth-Storable Propulsion)

The data presented by the nomograph complement those given by the performance graphs shown in Figures 7-3 through 7-7, and facilitate the assessment of parameter changes and tradeoffs. They permit a determination of exchange ratios, for example, those between ΔV capability, inert mass and propellant mass.

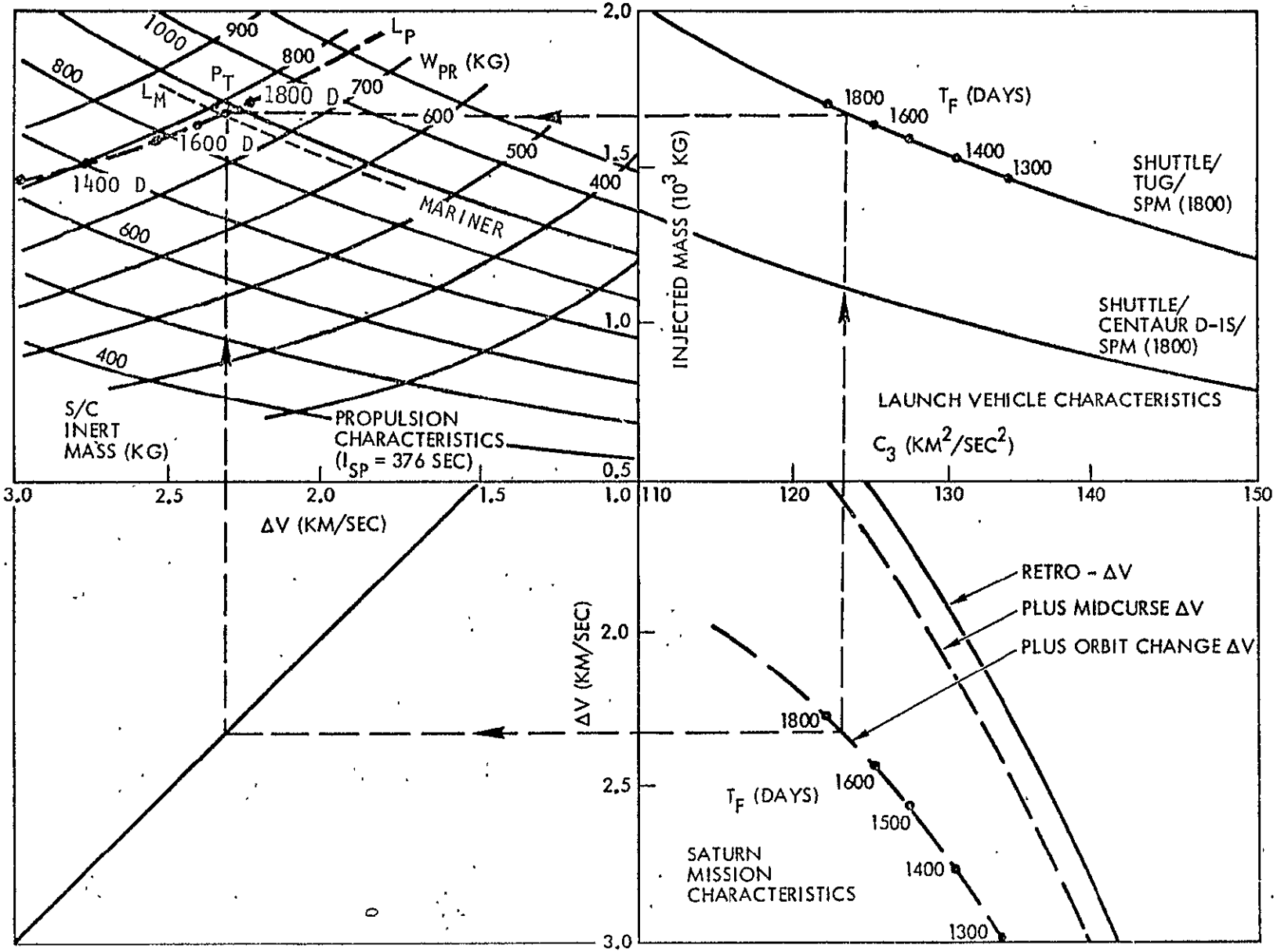

Figure 7-13. Mariner Saturn Orbiter Performance Example

8. DEVELOPMENT PLAN AND COST ASSESSMENT

8.1 PROGRAMMATIC CONSIDERATIONS

One of the principal objectives of the study was to assess the costs, both recurring and non-recurring of the four multi-mission chemical propulsion modules as a function of the number of missions they might serve, and to estimate the total time required to develop and bring the stages to operational status.

Development of a propulsion module for either a custom design for a specific mission or a multi-mission stage will begin from the technical (state-of-the-art) and hardware bases in effect at the time. Components such as rocket engines, valves and controls and, possibly, tankage may be adapted from other programs. However the time frame and new handling and interface requirements for Shuttle launch imply that most components are of new or modified design.

The new size, Shuttle launch requirements and long flight duration imply a full propulsion development cycle, even if an existing engine were to be used.

For N_2O_4/MMH propulsion systems, a complete technology base exists on which to start development except possibly for some aspects related to long life, e.g., corrosion and material life.

For LF_2/N_2H_4 systems, rocket propulsion hardware is in an advanced technology status with flight qualification of a system not yet accomplished, and a longer development cycle will be required than for N_2O_4/MMH. It is assumed that systematic technology development will continue, to be followed by a development program aimed at mission applications such as those considered here.

The main incentive for a multi-mission stage development is cost saving. For a single mission, a custom designed stage may have cost advantages, however slight, over a multi-mission stage. It also will have performance advantages because its design and size is optimized for this mission. Custom-designed stages will be almost identical except for tank size, and thrust level. Differences in development cost for custom and multi-mission stages then depend on 1) mission, 2) availability of hardware, 3) type and quantity of propellants.

Stages of N_2O_4 and MMH, and to a certain extent LF_2/N_2H_4, if developed soon, would undoubtedly utilize hardware adapted from the TRW MMBPS or JPL Mariner programs. In order to assess the costs for the multi-mission stages under the performance, reliability and safety requirements described previously (and in Appendix B), new propulsion stage costs were developed as an upper boundary.

In order to assess the multi-mission stage program cost relative to a minimum cost program, direct application of an existing stage (TRW's MMBPS) with only structural and thermal modifications and an unmodified, existing 90-lb_f engine was considered for comparison. Such a stage adaptation, suitable for a Pioneer Jupiter orbiter, launched from a Titan Centaur, was studied by TRW under NASA/Ames contract (Reference 7) and serves as a reference.

Between these cost levels will lie the various alternatives for propulsion system development. If development were to proceed on a mission-by-mission basis, each subsequent development may be less costly than the previous one but the total must obviously be greater than a single development.

Differences in the propulsion system hardware development items between the various stages are indicated by X's in the chart below.

	Module A		Module B	
	E.S. N_2O_4/MMH	S.S. LF_2/N_2H_4	E.S. N_2O_4/MMH	S.S. LF_2/N_2H_4
Gimballed engine			X	X
Bipropellant ACS	X			
ACS propellant in main tanks	X	X		
Capillary propellant acquisition (N_2H_4 only)		X		
Sun shade, deployable		X		
Cryogenic tank		X		X

It is expected that missions to the outer planets will be performed earlier than the Mercury missions. This places emphasis on the 900 Newton (200 lb_f) thruster development having a higher priority than 3600

Newton (800 lb_f) thrusters. (It should be noted that Mariner 9 used a 1300 Newton (300 lb_f) N_2O_4/MMH thruster which has a specific impulse of 290 sec.)

8.2 COSTING GUIDELINES

Four sets of costs and time requirements are anticipated for the four stages to be presented and shown in Section 8.1.

The following guidelines were used.

- Four baseline multi-mission stages were defined: A-N_2O_4/MMH, A-F_2/N_2H_4, B-N_2O_4/MMH, and B-F_2/N_2H_4
- Stages sized and optimized for an ambitious mission, the 1988 Mercury Orbiter 735-day flight, covered as a tandem application
- System performance of this configuration was assessed for the other missions
- Modified stage designs were prepared for the other missions using components from the baseline Mercury system
- A development start date of 1 January 1976, and a minimum-cost development schedule were established. This means a fairly short schedule for the N_2O_4/MMH system and a longer one for the F_2/N_2H_4 system. This date is suggested to establish early fixed-cost and state-of-the-art bench-marks for the study
- Development costs were generated on either/or (independent) basis not on the basis that two or more systems are started at once
- Cost estimates for the stages were related to TRW past programs. Labor, materials and overhead rate assumptions were mutually agreed upon with NASA as representing industry
- Costs were expressed in constant dollars based on a fixed date – 1 January 1975
- It was assumed that programs will be conducted in accordance with usual spacecraft propulsion development procedures
- Stage hardware is assumed to be delivered to the government to payload vehicle integration.

8.3 COST ELEMENTS

Key elements of propulsion development consist of:

1) The engine, often a pacing item

2) Tankage, including propellant acquisition devices

3) Valves and controls

4) Attitude control system.

Other aspects of the system development which may pace development of the type of system described here include:

1) Materials and processes for LF_2 use

2) The sun shade (used by the Pioneer Mercury orbiter).

The cost elements developed for this program are:

- Engine predevelopment
- Other predevelopment technology (i.e., valves, materials and processes)
- ACS development
- Engine development
- System development

Design and system definition studies are not included.

8.4 SUMMARY DEVELOPMENT SCHEDULE

8.4.1 N_2O_4/MMH Development Schedule

Figure 8-1 shows a typical development schedule for an N_2O_4/MMH propulsion stage. The first eight months shown represent an optional eight month technology cycle the purpose of which is to demonstrate the technology necessary to begin full development of a propulsion stage or module. If an existing engine can be used, the overall cycle can be shortened.

Time required from development go-ahead to flight-module delivery is 30 to 44 months with 36 months being typical. If an engine predevelopment is required then the cycle is 38-44 months. Aerospace ground-equipment deliveries can precede the flight hardware deliveries.

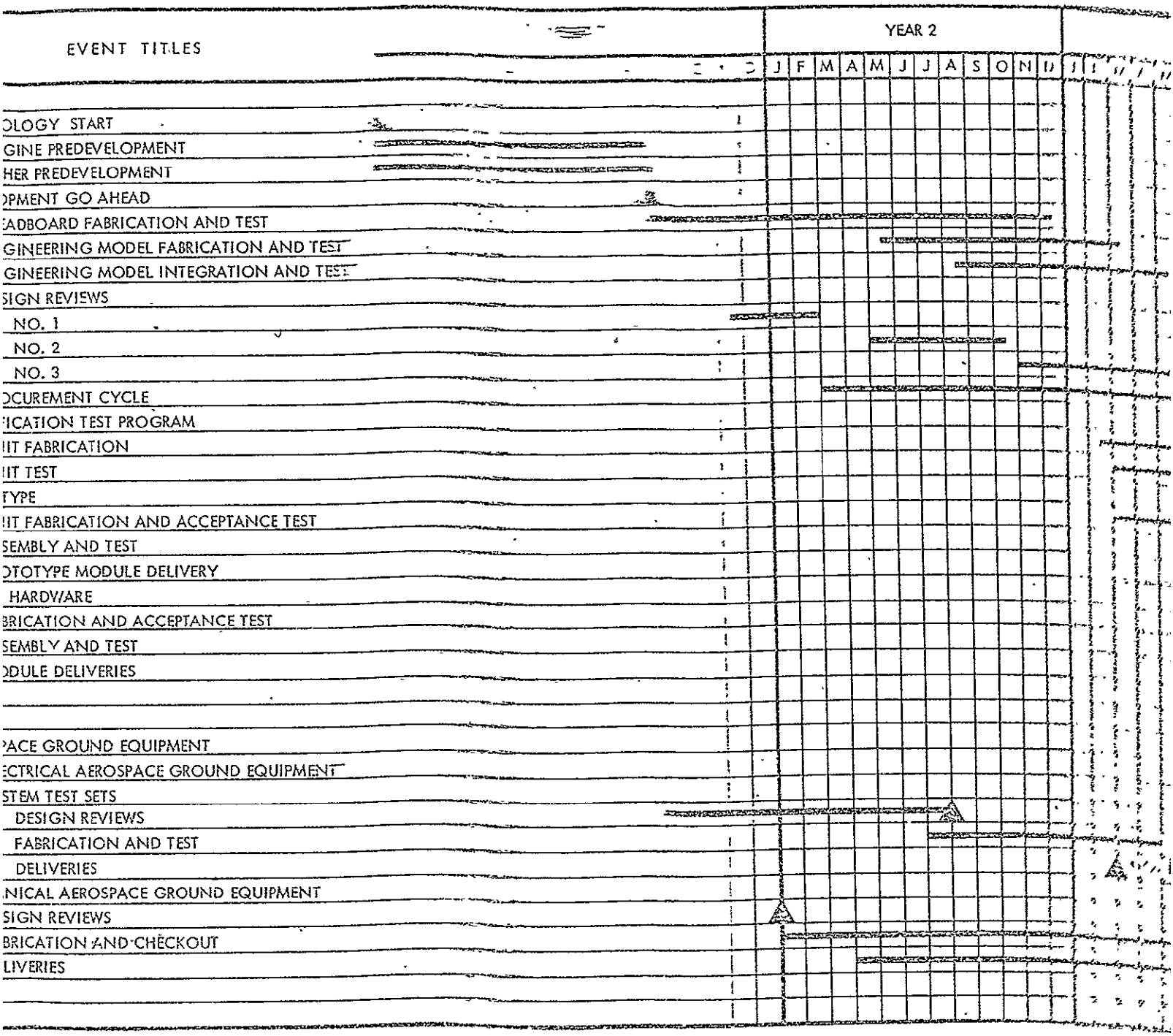

FOLDOUT FRAME

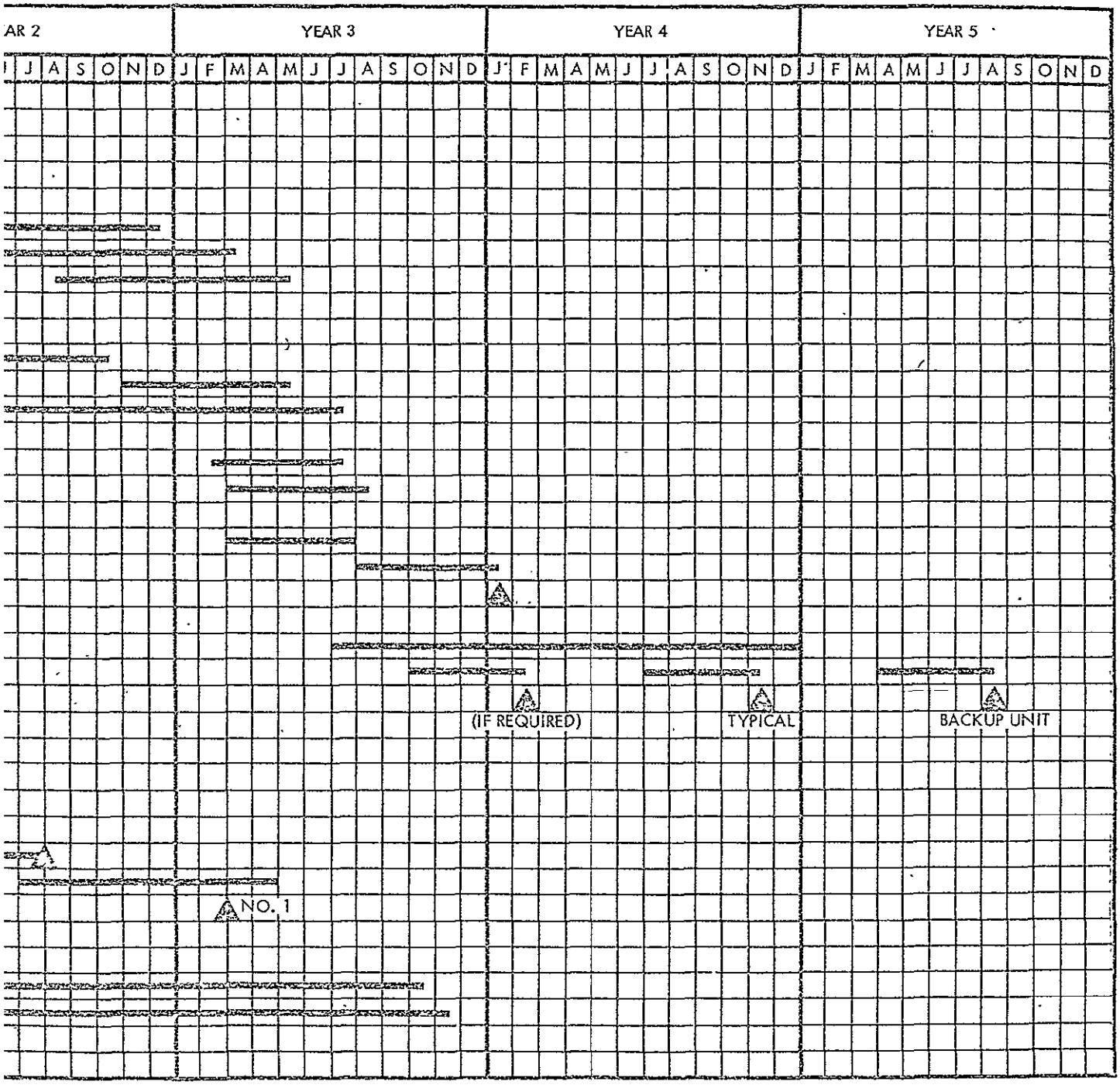

Figure 8-1. N_2O_4/MMH Milestone Schedule

FOLDOUT FRAME 2

LF_2/N_2H_4 Development Schedule

Figure 8-2 shows the schedule anticipated for development of an LF_2/N_2H_4 propulsion system. This development schedule is similar to that for N_2O_4/MMH except that technology work is mandatory. An estimated twenty months of technology work on engine demonstration, valve technology for engine and propellant isolation valves, and materials and processes will be needed before a development comparable with the N_2O_4/MMH program could be started.

Once started, the propulsion module development should progress with all deliberate speed from the base of technology established previously. Stretchout of the program would cause additional costs.

Duration of the F_2/N_2H_4 development program is thus approximately 50 to 53 months. This compares with approximately 38 to 44 months for N_2O_4/MMH system. These estimates are based on the assumption that no major technical difficulties are experienced.

Since technical risk is higher in the LF_2/N_2H_4 development program the longer technology period is recommended, so that technical questions can be resolved prior to full commitment.

Spacecraft development cycles can be even longer. An obvious conclusion is that if fluorine propulsion is needed in 4 or 5 years, the needed technology work should be instituted so that decisions can be made at an early date.

8.4.2 Custom Designed Propulsion Module

N_2O_4/MMH Propulsion Modules

Custom-designed propulsion modules developed to meet the same performance, reliability and safety requirements will be very similar in schedule and cost to a multi-mission module.

Cost savings in development would result from use of existing hardware. However, since each system must undergo system tests and because the urge to modify is ever present, large savings are not possible unless a complete propulsion system can be adapted.

Spacecraft propulsion systems which might be adapted include the JPL Mariner with 440 kg capacity (970 lb_m in 2 tanks), TRW's MMBPS

EVENT TITLES	YEAR 1												YEAR 2								
	J	F	M	A	M	J	J	A	S	O	N	D	J	F	M	A	M	J	J	A	S
TECHNOLOGY START	▲																				
ENGINE PREDEVELOPMENT/VALVE TECHNOLOGY/																					
MATERIALS AND PROCESSES																					
PREDEVELOPMENT VALVE AND MATERIALS																					
DEVELOPMENT GO AHEAD																				▲	
BREADBOARD FABRICATION AND TEST																					
ENGINEERING MODEL FABRICATION AND TEST																					
ENGINEERING MODEL INTEGRATION AND TEST																					
DESIGN REVIEWS																					
NO. 1																					
NO. 2																					
NO. 3																					
PROCUREMENT CYCLE																					
QUALIFICATION TEST PROGRAM																					
UNIT FABRICATION																					
UNIT TEST																					
PROTOTYPE																					
UNIT FABRICATION AND ACCEPTANCE TEST																					
ASSEMBLY AND TEST																					
PROTOTYPE MODULE DELIVERY																					
FLIGHT HARDWARE																					
FABRICATION AND ACCEPTANCE TEST																					
ASSEMBLY AND TEST																					
MODULE DELIVERIES																					
AEROSPACE GROUND EQUIPMENT																					
ELECTRICAL AEROSPACE GROUND EQUIPMENT																					
SYSTEM TEST SETS																					
DESIGN REVIEWS																					
FABRICATION AND TEST																					
DELIVERIES																					
MECHANICAL AEROSPACE GROUND EQUIPMENT																					
DESIGN REVIEWS																					
FABRICATION AND CHECKOUT																					
DELIVERIES																					

FULLOUT FRAME 1

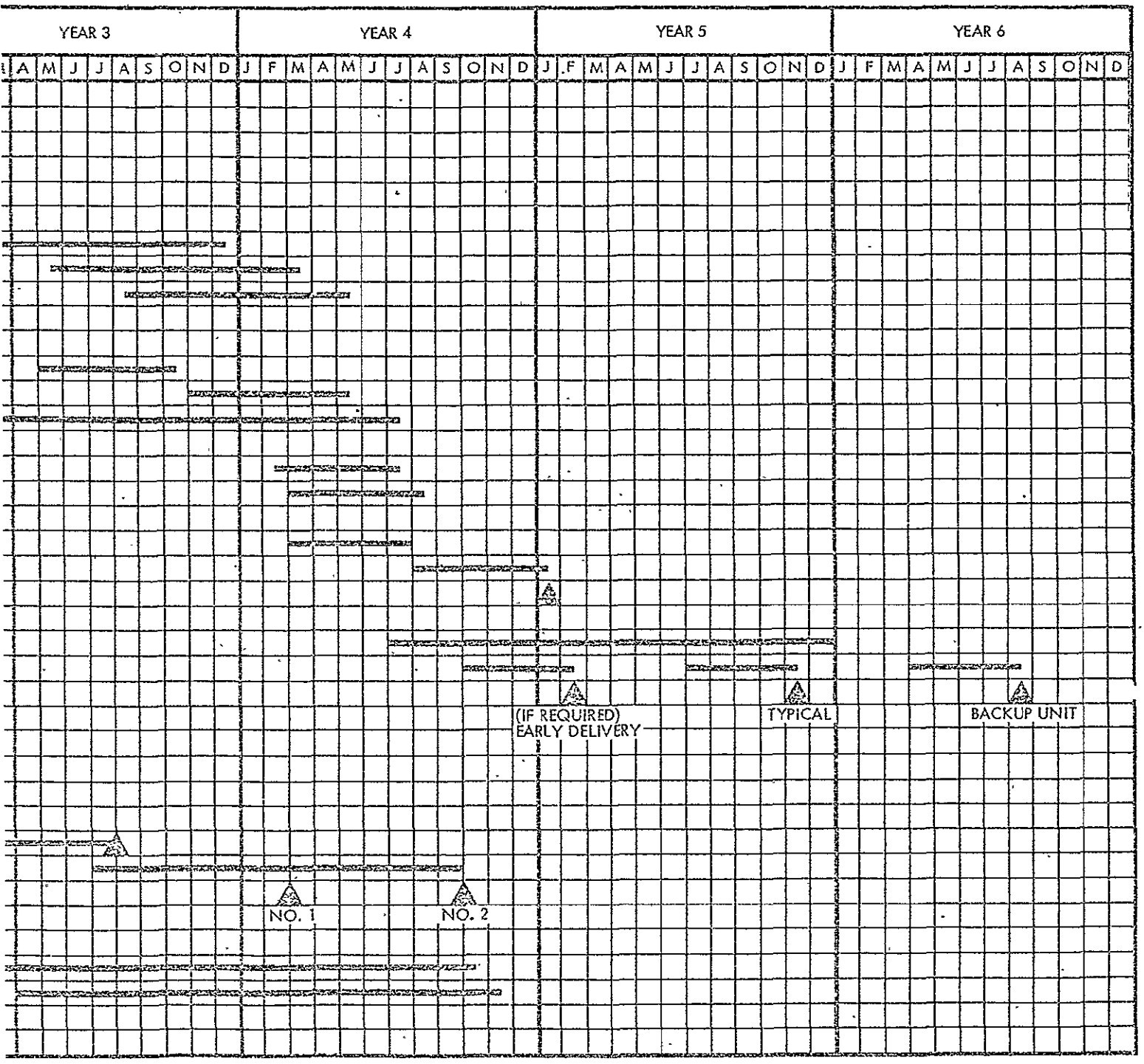

Figure 8-2. LF_2/N_2H_4 Milestone Schedule

FOLDOUT FRAME 2

600 kg (1300 lb_m in 4 tanks), or JPL Viking 1408 kg (3097 lb_m in 2 tanks) capacity sytems.

Orbiters based on these stages might be possible for the outer-planet missions with Pioneer and Mariner class payloads; however either would require major repackaging.

The estimated schedule and cost for an outer-planet orbiter based on repackaging components from these systems is 24-30 months and approximately 1/3 the cost of an all new multi-mission module or all new custom stage. Such a repackaged stage would have the following disadvantages compared with multi-mission stages.

1) Propellant expulsion bladders are of questionable reliability because of the long flight time

2) The system may not be suitable for Space Shuttle launch

3) It would not have as high a mass fraction or specific impulse.

Adaptation of any custom design to a new mission requiring a significant tank or structure change will require a lead time of at least 18-24 months to build, wring out, and qualify. Engine and control components can remain the same provided their original sizing is for the 800 lb_f level.

LF_2/N_2H_4 Propulsion Module

The first custom or multi-mission propulsion module to be qualified and flown using LF_2/N_2H_4 will incur significantly higher costs than subsequent modules. However, costs of subsequent adaptation and requalification should approach those of the N_2O_4/MMH stages. No existing stages can be used for adaptation. However, some use of existing hardware on the N_2H_4 system may be possible.

8.5 DEVELOPMENT COST ESTIMATES

Comparison of Multi-Mission and Custom Designed Propulsion Modules

Shuttle-launched custom stages built to the same performance, reliability and safety specifications as a multi-mission module, are very likely to have the same non-recurring cost. The difference in tank and test costs is insignificant within the accuracy of estimating. Recurring

cost would, of course be much higher for custom-designed stages. For custom-designed stages, system development, normally a non-recurring cost, would continue to be a recurring cost. Each new configuration would require $5-7 million to modify and requalify assuming a single hardware set for requalification.

Table 8-1 shows the estimated non-recurring and recurring costs for the systems considered. The earth-storable cost data represent an all-new system designed for Shuttle launch requirements. As a basis of recurring cost data a production run of 10 propulsion modules is assumed. Cost data given in the table represent recurring costs of 1 out of a total of 10 modules produced.

Table 8-1. System Cost Estimates for Multi-Mission Modules ($K)

Cost Elements	Module A		Module B		Repackaged Existing Earth-Storable
	New Earth-Storable	Space-Storable	New Earth-Storable	Space-Storable	
NON-RECURRING COST					
1. Configuration with 800-lb_f engine					
Predevelopment	450	2,996	450	2,996	
Module development	15,510	21,330	15,510	21,330	5,100
Sun shade		1,150			
ACS engine, bipropellant	1,640				
ACS monopropellant requal		250	250	250	
Gimbal actuators			300	300	
Total	17,600	25,726	16,510	24,876	
Alternate Configurations					
2. Module with existing 96-lb_f engine	15,650	-	15,560	-	5,100
3. Module with 200-lb_f engine	17,580	25,550	-	-	
4. Module with two engines) ngines (200- and 800-lb_f)	19,080	28,110	18,010	26,876	
RECURRING COST*					
Module system	1,170	1,470	1,170	1,470	920
Sun shade, acceptance		200			
10 bipropellant ACSE	273				
10 monopropellant ACSE		250			
16 monopropellant ACSE			400	400	
Gimbal actuators			100	100	
Total	1,443	1,920	1,670	1,970	1,170

*Based on a production run of 10 stages. Costs shown are for one stage.

Under non-recurring cost a breakdown of development cost items is given for Modules A and B with an 800-lb_f thrust engine. Costs for three alternate configurations are also listed but without a cost breakdown.

The recurring cost elements are very similar for each module irrespective of the type of configuration considered; thus only one set of cost data are listed in each case.

There is approximately $8.4 million cost difference between the F_2/N_2H_4 stage compared with the N_2O_4/MMH stage. Of this, approximately $3 million consists of technology expected to be needed to assure a low risk development, and $5 million is related to the additional engineering, hardware and test costs during development.

The sun shade required by the LF_2/N_2H_4 Module A is also a significant cost item.

Module A and Module B are not greatly different in physical size and have the same maximum thrust level. Except for the sun shade and fewer thrusters on the space-storable Module A they are similar in complexity. The only significant differences are in tank size. Lines, valves and engines could, and most likely would, be identical (and sized for 800 lb_f). Since there is little difference in equipment and complexity, development costs are very similar.

The repackaged existing stage is shown for comparison and represents the cost of repackaging the components of an existing N_2O_4/MMH propulsion system in a new structure, with a monopropellant ACS system and requalifying it for flight on Titan/Centaur as mentioned previously (Reference 7).

Table 8-2 lists the cost elements used to prepare Table 8-1. No facilities costs were included.

Figure 8-3 shows cumulative costs of multi-mission module procurement compared with single-module procurement for Module A with an earth-storable (left) and space-storable propulsion system (right) as function of the number of flights. These results are based on cost

Table 8-2. Cost Elements in $K (January 1976 dollars)

Cost Elements	N_2O_4/MMH		LF_2/N_2H_4		N_2O_4/MMH
	200 lb_f	800 lb_f	200 lb_f	800 lb_f	Repackaged
Predevelopment - nonrecurring					
1. Engine predevelopment	430	450	980	996	
2. LF_2 valve programs			1,000	1,000	
3. LF_2 materials and processes			1,000	1,000	
Predevelopment package	430	450	2,980	2,996	
Development - nonrecurring					
4. Module development (one engine)	15,510	15,510	21,330	21,330	5,100
5. Sun shade, Module A only			1,150	1,150	
6. ACS engine	1,640	1,640			
7. Gimbal actuators	300	300			
8. Monopropellant requalification	250	250			Included
Recurring*					
9. Main system, 1 each of 10	1,160	1,170	1,460	1,470	1,170
10. Sun shade			200	200	
11. Set of 10 bipropellant ACS engines	273	273			
12. Set of 10 monopropellant ACS engines	250	250	250	250	Included
13. Set of 16 monopropellant ACS engines	400	400	400	400	
14. Gimbal actuators, set of 2	100	100	100	100	

*Based on a production run of 10 stages. Costs shown are for one stage

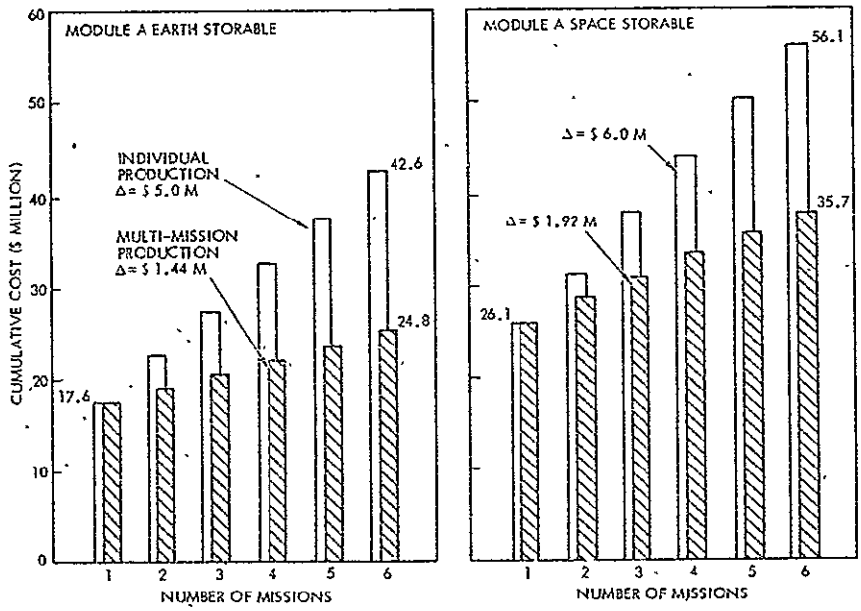

Figure 8-3. Comparison of Cumulative Cost of Individually Produced Propulsion Modules Vs. Multi-Mission Module Production

data in Table 8-1 and the incremental cost of $5 to 7 million for individual production mentioned earlier. The two bar graphs illustrate the rapid accumulation of higher costs in the individual procurement, amounting to differences of $17.8 million and $20.4 million for the earth- and space-storable systems, respectively, assuming 6 flights.

It should be noted, however, that programmatic decisions to be made by NASA regarding the possibility of procuring several stages at one time rather than individual procurement have not been reflected in this analysis. If multi-mission stages would be procured sequentially with an appreciable time elapsing between procurements, not all of the cost advantage depicted in Figure 8-3 would necessarily be realizable.

Table 8-3 lists cost elements for the repackaged existing stage. Costs presented here are based on the experience of TRW and other industry and government organizations. Accuracy of these earth-storable stage cost estimates is considered good, and may be conservative if many existing components can be found which meet the system specifications.

Table 8-3. Repackaged Stage Costs* in $K

1. Nonrecurring (1 set)	2,700
2. Nonrecurring propulsion cost-basic	1,400
3. Monopropellant (included)	-
4. System requalification:	
1 Set hardware	1,200
Qualification testing	1,450
Test tooling	370
System engineering	180
5. Structure	250
6. Thermal	250
7. Total recurring	5,100
8. Deliverable stage hardware (includes $250K for ACS thrusters)	1,170
	6,270

*This analysis is representative of repackaging an existing stage (see Reference 7)

9. NEW TECHNOLOGY REQUIREMENTS AND COST EFFECTIVENESS

9.1 TECHNOLOGY ADVANCES REQUIRED FOR MULTI-MISSION MODULE

A major study objective was to identify new technology items necessary or desirable to meet the performance objectives of the multi-mission module most effectively, and to assess their cost effectiveness.

New technology is necessary to accomplish some of the specified missions launched by the Shuttle and Shuttle upper stages. There is a critical need to conserve injected weight in some of the missions. The higher-performance, space-storable F_2/N_2H_4 propellant combination is needed to perform many of the Shuttle-launched missions with the IUS or even with the Space Tug. At the large propellant weight-to-inert weight exchange ratios typical for this mission range, a 100-kilogram saving in inert weight can yield up to 500-kilogram savings in total injected weight. Thus, the cost of propulsion technology development could avoid even more costly payload accommodation problems.

In this context, time is an important element. The multi-mission module flight programs are intended for the mid-1980's with the advent of Space Shuttle. Technology advances are achievable if development starts immediately. Available lead time must be factored into the technology-versus-cost assessment and could become a sensitive factor if underestimated.

The new technologies most necessary, and the benefits to be gained, are summarized in Table 9-1.

9.1.1 Deployable Sun Shade

For spin-stabilized (Pioneer class) spacecraft missions to Mercury using LF_2 as an oxidizer, an excessively high heat load would result if a sun shade were not used. The spin-deployed sun shade protects the tanks as they turn, yet allows them an adequate view factor to cold space.

In Mariner class missions a simpler, stationary sun shade with deployable wings is used which is not a new technology item.

Table 9-1. Summary of New Technology Requirements and Suggested Innovations

	Improvement	Category	Cost, $M
New Technology			
1. Deployable sun shade*		Essential for Module A for Mercury	1.150
2. LF_2/N_2H_4 800 lb_f engine technology	Demonstrate feasibility at I_{sp} = 370 + sec.	Essential for LF_2 Mercury missions	0.993
3. LF_2/N_2H_4 200 lb_f engine technology	Demonstrate feasibility at I_{sp} = 370 + sec.	Essential for LF_2 Mercury missions	0.981
4. Long-life isolation valves for LF_2		Essential for LF_2/N_2H_4 systems	1.000
5. LF_2 materials and processes technology	Determine compatibility and passivation	Essential for LF_2/N_2H_4 systems	1.000
6. Improved I_{sp} 200 lb_f N_2O_4/MMH engine	Demonstrate increase in I_{sp} state of the art to approximately 310 sec.	Beneficial	1.930
7. Improved I_{sp} 800 lb_f N_2O_4/MMH engine	Demonstrate increase in I_{sp} SOTA to approximately 310 sec.	Beneficial	1.950
8. Development of 2 lb_f N_2O_4/MMH ACS thrusters	Reduce ACS propellant approximately 1/3 for Module A with earth-storables	Beneficial	1.650
Suggested Innovations			
9. Technology of N_2O_4/N_2H_4 engine - 200 lb_f alternative to 6.	Allows common tanking of ACS and main propellant	Beneficial	2.430
10. Technology of N_2O_4/N_2H_4 engine - 800 lb_f alternative to 7.	Allows common tanking of ACS and main propellant	Beneficial	2.450
11. Development of 2 lb_f N_2O_4/MMH bimodal engine	Allows common tanking of ACS and main propellant	Beneficial	3.000
12. Technology of N_2O_4/N_2H_4 bimodal engine	Allows common tanking of ACS and main propellant	Beneficial	3.000

*Heat pipe would reduce cost to $0.2 million

9.1.2 Engine Development

LF_2/N_2H_4 800 lb_f Engine

An optimum Mercury mission necessitates an LF_2/N_2H_4 engine of the 800 lb_f (3600 N) class (see Sections 3, 7). No fully developed or qualified engine of this type exists. JPL has demonstrated a prototype with approximately 360-366 seconds of I_{sp} at the 600-lb_f thrust level, but further progress is required before starting a full development program. This engine is required for both Pioneer and Mercury class Mercury orbiters.

LF_2/N_2H_4 200 lb_f Engine

No fully developed LF_2/N_2H_4 engine exists at the 200 lb_f (900 N) level. This engine is essential for Pioneer and Mariner outer-planet orbiters.

9.1.3 Long-Life Isolation Valve for LF_2

Mission durations of 10 years or more require a suitable propellant isolation valve. The development of this valve is essential for all flights with LF_2. The valve must not contain any metallic materials that would be in contact with fluorine or in any possible fluorine leakage path. This valve also could function as a propellant dump valve if properly sized.

9.1.4 LF_2 Materials and Processes Technology

Tank containment and the use of LF_2 in a rocket engine over periods of 10 years raises unresolved questions of fluorine compatibility. Corrosion and pitting are the main concerns.

TRW has used an LF_2 stainless steel storage tank in ground-based operations for 8 years; however, an analysis of stainless steel compatibility and applicability in the orbiter missions has not been performed. Storage tests of about 1 year of aluminum and titanium alloys in liquid fluorine have yielded promising but not conclusive results.

Laboratory testing also must answer questions of passivation procedures for components before assembly and LF_2 tankage passivation before shipment.

9.1.5 Development of Improved N_2O_4/MMH Engines

200 lb_f Engine

Present engines for the N_2O_4/MMH propellant combination in the 90- to 300-pound (400 to 1300 N) thrust range have a specific impulse of 285 to 295 seconds. Higher specific impulses can be obtained. If a higher level of performance can be shown to have a relatively low cost, engine development may proceed on a firm technology base.

This technology is beneficial for Pioneer and Mariner class outer planets orbiters with N_2O_4/MMH.

800 lb_f Engine

An engine presently under development (Marquardt Shuttle RCS engine) for the N_2O_4/MMH propellant combination in the 800 lb_f (3600 N) thrust range has a specific impulse of 285 seconds. Higher specific impulse (up to 310 sec) can probably be achieved with further engine technology development. If demonstrated, this technology would greatly benefit Pioneer and Mariner class Mercury orbiters using N_2O_4/MMH.

9.1.6 Development of 2 lb_f N_2O_4/MMH ACS Thrusters and N_2O_4 10-Year Life Capillary Acquisition Device.

For Module A with the earth-storable propellant, increased payload performance can be obtained by use of bipropellant ACS. Development of a system with specific impulse performance of approximately 300 seconds appears technically feasible, and estimates indicate it could be flight qualified within 15 to 24 months. Its cost of $1,650K is included in Table 8-1.

9.1.7 Development of N_2O_4/N_2H_4 Engines

Development of N_2O_4/N_2H_4 engines would allow commonality of axial (ΔV) hydrazine fuel and ACS hydrazine with the result of flexibility and improved performance. A demonstration of engine performance and stability is considered in the cost estimates in Table 8-1.

Engine development could be initiated for a conventional liquid-liquid injector or a bimodal (also called dual-mode) engine. A

bimodal engine is more flexible than a conventional engine: it can perform maneuvers without oxidizer by operating on residual fuel at a lower thrust than with both oxidizer and fuel.

Technology development for a N_2O_4/N_2H_4 engine will benefit missions that are likely to use earth-storable propellants, particularly those that can be performed by Pioneer-class orbiters.

9.2 SUGGESTED INNOVATIONS

9.2.1 Concurrent Development of 200 and 800 lb_f Engines

The requirements and schedule of Module A suggest that, during the development phase, components should be sized for the 800 lb_f (3600 N) thrust level. The bipropellant valve designed for 800 lb_f also will be suitable for 200 lb_f.

Because missions to outer planets probably will precede Mercury flights, the 200 lb_f engine should receive a higher priority. However, if this engine were developed first, the valve might not be suitable for the larger engine.

Concurrent development would produce cost savings in program management, material procurement, design and engineering, and testing. Work could be coordinated and new skills shared. If both engines shared a common test setup, further savings would occur.

9.2.2 Concurrent Propulsion Module Development

Common Propellant

Development of two propulsion modules concurrently, e.g., earth-storable Module A and Module B, would be very economical. Valves and pressurization could be identical. Structures could have the same configuration. However, the larger load to be accommodated by Module B would require a reinforced central structure and stronger tank support struts than for Module A. Structural commonality would penalize Module A by at least 20 to 30 kg of increased inert mass. Module B would require engine gimbals and have 16 monopropellant thrusters instead of 10 bipropellant thrusters. Otherwise, except for the tanks, they would be similar. It appears that totally independent efforts would

cost several million dollars more if both Pioneer and Mariner missions to Mercury and outer planets were to be used.

Different Propellants

Concurrent development of stages with different propellants also is possible. Although the tank size for earth-storable is larger than for space-storable propellants, the fuel side of a N_2O_4/MMH system is quite suitable for use with N_2H_4. Since the selected configurations of Modules A and B are so similar, it appears that commonality of structure, fuel tank and engine compartment could be achieved. This might allow a beginning of the multi-mission module development before fluorine use has been approved.

9.2.3 Conversion from N_2O_4/MMH to LF_2/N_2H_4

A delayed conversion from N_2O_4/MMH to LF_2/N_2H_4 could be more costly because components will not have been designed to accommodate both propellants. Mission scheduling would also be adversely affected. If more than one type of stage is to be developed, an initial design approach with thermal characteristics suitable for LF_2/N_2H_4 and a tank size suitable for N_2O_4/MMH would be advantageous. However, overall desirability of such a development has not been established.

9.3 ESTIMATED NEW TECHNOLOGY EVOLUTION, SCHEDULE AND MILESTONES

The evolutionary schedule for N_2O_4/MMH depends on funding plans and normal lead times for hardware and engineering. For the LF_2/N_2H_4 combination, approximately $3,000,000 for predevelopment is required to allow full scale development starting in fiscal year 1978. Thus, no flights with LF_2/N_2H_4 systems could occur before mid-1981 (or, with more conservative spacecraft lead time estimates, not before 1982).

Figure 9-1 shows mileposts for a scenario of technological evolution of both types of propulsion systems, assuming prompt and adequate funding without undue haste in the conduct of the programs.

Figure 9-1 includes the schedule for repackaging existing components into a structural configuration similar to the earth-storable multi-mission module for launch on Titan/Centaur (see TRW's Pioneer Jupiter Orbiter Study, Reference 7).

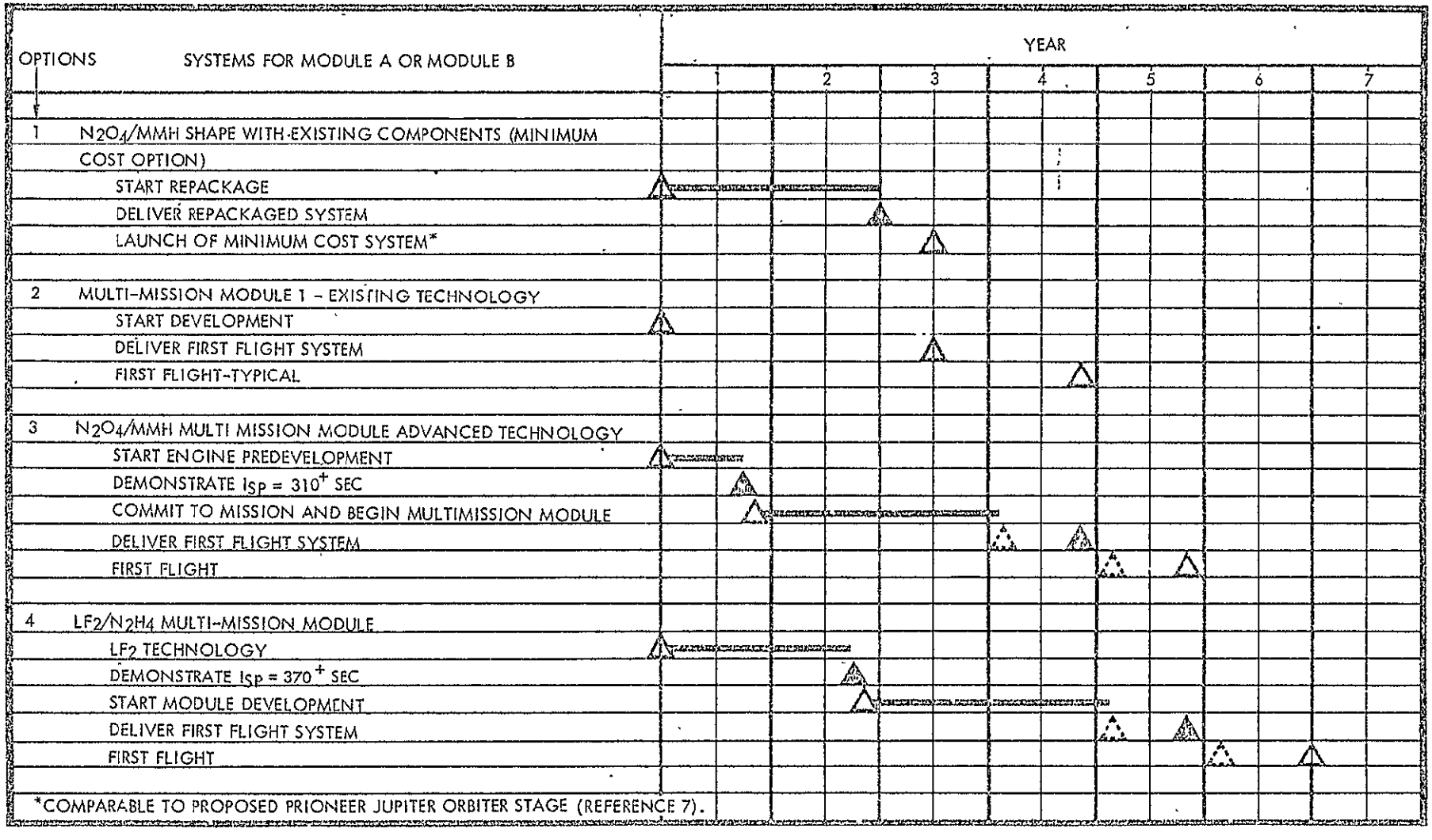

Figure 9-1. Availability Schedule of Propulsion Module Types

Six months later, an alternate, newer N_2O_4/MMH system with improved components could be ready. This stage could incorporate advanced technology except for using an existing engine.

Eight months later, a system with an improved engine could be available. If desired, N_2O_4/N_2H_4 engines could be available on the same schedule. A LF_2/N_2H_4 system could be available twelve months later.

9.4 COST EFFECTIVENESS ASSESSMENT

9.4.1 Qualitative Assessment

Instead of making a quantitative cost-benefit assessment, overall system performance improvements made possible by advanced propulsion technology will be considered in a more qualitative manner. A recent JPL study (Reference 2) evaluated cost-benefits accruing from increased ΔV capability in Jupiter and Saturn orbiter missions. A unit of value was defined and evaluated based on opinions of mission planners and scientists using a Delphi assessment technique. Examples of resulting mission benefits versus time in orbit at Jupiter and Saturn are shown in Figure 9-2a and b. In these cost-benefit graphs, the increment of scientific value, gained by extension of time in orbit and by additional orbital maneuvers, is estimated that accrues from the exploration of phenomena not observable in the preceding orbital phase. For example, in the Jupiter orbiter mission the initial (reference) ΔV requirement of 1375 m/sec establishes the orbit and permits continuation in the initial orbit for several years at a fixed rate of increase of scientific value per year. New maneuvers raising the total ΔV requirement to 1625, 1875, and ultimately to 2750 m/sec increase the rate of change of scientific value compared with the fixed rate of the mission with unchanged orbital characteristics.

Broadening of the scientific and programmatic figure of merit may include criteria such as the following:

- Payload mass increase
- Flight time reduction, with resultant increase in reliability and mission cost reduction

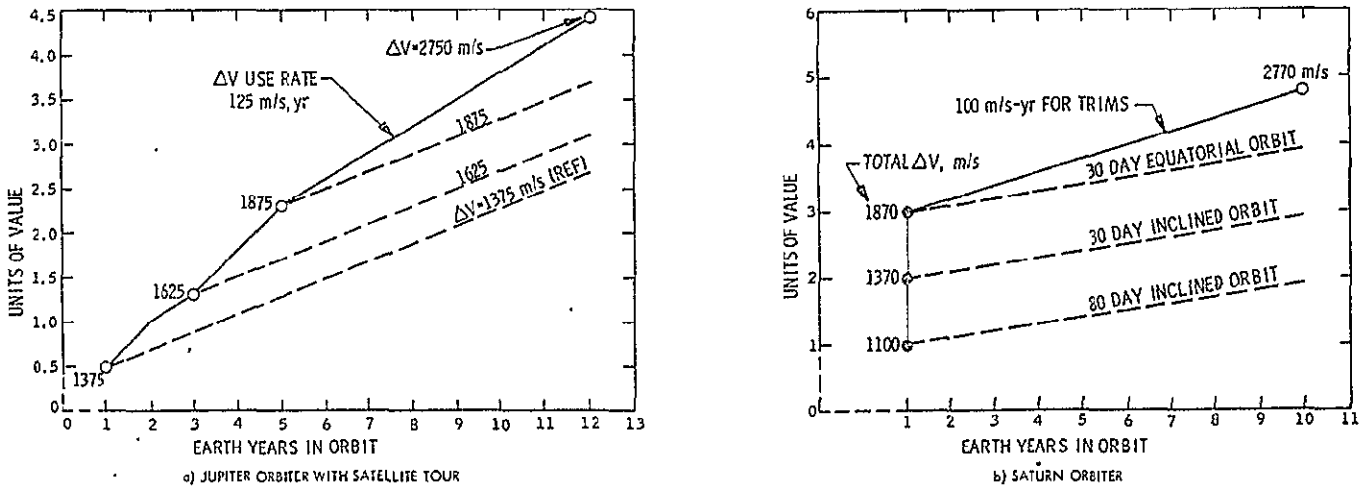

Figure 9-2. Benefit Functions for Planetary Orbit Missions*

*From JPL study, Reference 2

- Mission flexibility improvement, e.g., increase of the launch window
- Improved planetary exploration strategy permitting scientific results to be taken into account prior to making mission profile changes ("adaptive" mission strategy)
- Increased probability of success by permitting maneuvers to escape hazardous environmental conditions (e.g., change in periapsis altitude to avoid high particle flux, high thermal flux, or possible early impact on the planet surface)
- Reliability increase by adding weight for redundancy
- Payload cost reduction by relaxing weight and size constraints
- Reduction of the booster cost through lower launch vehicle performance requirements
- Achievability of missions that would not be feasible without the advanced propulsion technology.

Increased payload mass is a primary concern in mission planning and includes in part some of the other items listed above, such as added redundancy weight. Payload mass increase is inherent in the ability to perform planetary exploration by Mariner class rather than only Pioneer class orbiters with the possibility of accommodating more sophisticated instruments, such as higher-resolution image systems, on the nonspinning spacecraft.

Payload mass increase also implies cost reductions by permitting adaptation of existing subsystems and/or scientific instruments without costly redesign.

Another possible benefit of payload mass increase is the ability to carry a planetary entry probe to the target planet. The addition of the entry probe means primarily added takeoff weight, not added inert weight during the orbital entry maneuver. However, it also requires additional onboard equipment such as relay communication system, and other probe support hardware. Mounting of the entry probe does not necessarily increase the height of the flight spacecraft. In the nonspinning configuration one or several probes could be mounted off-center without imposing mass distribution problems.

Greater mission flexibility is of particular value in connection with the use of the Shuttle orbiter as launch vehicle. An increase in launch window duration made possible by increased spacecraft propulsion capability will make the tight turnaround schedule between Shuttle flights a less severe constraint on launch operations.

Adaptive strategy of planetary exploration is becoming a matter of increased interest to mission planners and scientific experimenters. In all missions being considered the physical environment and potential hazards existing at the target planet or comet are largely unknown at the start of the mission. With orbital periods of the order of 30 to 50 days in the case of outer planet missions there is wide room for orbit-to-orbit decision making on how to shape subsequent orbits by application of orbit change impulses. Many options exist for changing the orbital phase through repeated satellite encounters. A concurrent JPL study of Saturn orbiters (Reference 30), has established that major orbital plane changes and apsidel line changes can be achieved effectively by repeated flyby maneuvers of Titan with relatively small ΔV expenditures.

In comet rendezvous missions, maneuver requirements to explore the comet more fully after establishing rendezvous are quite modest, typically 100 to 200 m/sec, depending on the comet, the length of time of stay with the comet, and range of excursions to be performed. Previously these missions were believed to be the domain of solar electric propulsion and have been awaiting the advent of that technology. As shown by the performance assessment, a wide range of possible comet rendezvous missions can be performed and thus the cost effectiveness of introducing advanced chemical propulsion is greatly increased.

Table 9-2 lists advantages achievable by using space-storable instead of earth-storable propellants versus specific benefits accruing in terms of scientific mission yield, mission success probability, cost reduction and program management factors. These factors are given a tentative value ranking, and scores of maximum benefits are indicated for each category by circled figures.

Table 9-2. Rating of Advantages Achieved by Space-Storable Propulsion

Categories of Advantages Achieved / Specific Benefits →	Greater Science Returns	Less Development of Payload Instruments	Cost Reductions: Lower Spacecraft and System Cost	Cost Reductions: Lower Shuttle Utilization Cost	Cost Reductions: Lower Upper Stage Performance Required	Cost Reductions: Lower Mission Support Cost	Greater Mission Success Probability	Programmatic Advantages	Score
Payload increase	x x x	x x[1]	x[1]		x		x[2]	x[3]	(9)
Missions made feasible (Uranus, comets)	x x			x[4]	x			x	(5)
More missions achievable by multi-mission module			x x					x	3
Flight time reduction						x x	x	x	4
Launch window increase				x x			x	x	4
Increased ΔV capability/ adaptive mission profile (e.g., satellite encounters)	x x	x	x[5]				x x[5]		(6)
Hazard avoidance at destination (extra maneuvers)			x				x		2
Score	(7)	3	(5)	3	2	2	(6)	(5)	

Notes:

[1] Relaxed weight constraints on components

[2] Redundancy weight added for greater reliability

[3] Adaptation of existing hardware to other missions

[4] Additional Shuttle traffic

[5] Higher ΔV capability implies simpler navigation

9.4.2 Performance, Cost and Risk Considerations

Cost-effectiveness analysis must take into account three principal criteria from which a figure of merit can be derived, namely performance, cost and risk.

The performance criterion includes such factors as payload capability, flight time reduction, and extra maneuvering capability that will enhance scientific mission yield.

The cost criterion includes cost savings due to improved design approaches, simpler test procedures, etc., and reduced mission time. The latter aspect of cost reduction can be very significant. For example, in concurrent JPL studies typical mission cost per year of transit is assumed as $6 to 7 million, and cost per year in orbit (which requires more intensive ground operations and support) as large as $13 million.*

The risk factor includes development risk, mission success (or failure) probability, and safety considerations, especially those involving ground handling and launch of the system by the Shuttle orbiter. It interacts with performance characteristics since higher payload potential implies a greater redundancy weight allowance, and lower flight time implies higher success probability, as discussed in the preceding section.

For purposes of cost-benefit analysis the cost of technology improvement is accounted for as a separate item from the cost reduction achieved by this investment.

Table 9-3 lists major items of technology improvement identified in this study and cost estimates for this improvement, and assesses the benefits in each of the three categories (performance, risk reduction, and cost reduction) in matrix form. Only rough estimates of the benefit in terms of percentage improvement are given. Further study would be required to establish more detailed estimates. These data are then used to determine an estimated cost effectiveness ratio, defined as the sum of the three benefits, divided by the respective technology cost increments also in percent, viz.,

*Informal communication from R. Chase, JPL

Table 9-3. Matrix of Preliminary Cost-Benefit Estimates

Technology Improvement Item	Estimated Cost of Improvement, C_T		Estimated Benefits (percent)			Cost-Effectiveness Ratio CE	Priority of Development
	$M	%[a]	Performance $\Delta P/P_o$	Reduced Risk $\lvert\Delta R\rvert P_o$	Reduced Cost $\lvert\Delta C\rvert/C_o$		
1. Development of space-storable propulsion system (see Table 8-1)	8	16	30 to 100	10 to 20	10 to 20	1.9 to 8.8	High
2. Improved materials technology (e.g., LF_2 compatibility)[b]	3	6	10	10	10	5	High
3. Additional development of safety provisions for LF_2 ground handling and Shuttle launch[b]	2	4	-	10 to 20	-	2.5 to 5	High
4. Increased specific impulse of earth-storable propulsion systems (see Table 9-4)	2	4	10 to 15	-	-	2.5 to 3.8	Medium
5. Centrifugally actuated heat pipe for LF_2 tanks	0.2	0.7[c]	-	5	3[c]	11.4	High[c]
6. Bipropellant ACS thrusters in 9 to 20 N (2 to 5 lbf) range (see Table 9-4)[d]	1.6	3.2	5	5	3	4.1	Medium
7. Longer life ACS thrusters	1	2	-	10	-	5	High[e]
8. Improved long-life reliability design techniques	2	4	5	10 to 20	5	5 to 7.5	Medium

[a] Assumes total flight spacecraft cost of $50M (average between Pioneer and Mariner type missions) as reference

[b] These items for additional technology work, over minimum requirements subsumed under Item 1

[c] Required only for Pioneer Mercury orbiter. Reflects a lower reference cost ($30M) than other entries.

[d] Recognizes earlier bipropellant ACS thruster development by Aerojet Liquid Rocket Company (Reference 35)

[e] Required particularly for Mariner outer-planet orbiters

$$CE = \frac{\frac{\Delta P}{P_o} + \frac{|\Delta R|}{R_o} + \frac{|\Delta C|}{C_o}}{\frac{\Delta C_T}{C_o}}$$

Each contribution is assumed to carry an equal weighting factor.

The results show that the development of space-storable propulsion technology, additional development of F_2 safety provisions and materials technology, and longer-life ACS thrusters score high on this scale. Development of the heat pipe approach for LF_2 tank thermal control in the Pioneer Mercury orbiter mission, although a specialized requirement, stands out as having the highest cost effectiveness.

9.4.3 Figure-of-Merit Analysis Examples

A more detailed quantitative analysis was performed on several examples of cost benefits achievable by technology improvement.

The approach used here to evaluate cost effectiveness considers the ratio of payload increment to cost of technology improvement. By this approach, various technology improvements can be compared to each other and to the average cost of performance.

Table 9-4 lists five items of improvement in earth-storable propulsion technology, the payload gain ΔM achievable by each, the benefit-to-cost-ratio, the average cost of the payload, and the cost-benefit index given by

$$CE = \frac{\Delta M/M_o}{\Delta C_T/C_o}$$

This quantity is directly related to the ratio CE defined in the preceding section, being one of the components of the fraction defining CE.

Items 1 through 3 in Table 9-4 were incorporated in the design and in the cost schedules as they were clearly indicated as being necessary and desirable. Items 4 and 5 which involve the propellant combination N_2O_4/N_2H_4 are alternatives to Items 1 and 2 and involve some small amount of technical risk. They also depart from study guidelines which specified the more conservative choice of N_2O_4/MMH.

Table 9-4. Technology Benefit Analysis Examples (Earth-Storable Propulsion Technology Improvements)

Item	Technology Improvement	① Improvement Produced	② Exchange Ratio	③ Payload Gain (kg) ① × ②	④ Cost ($M)	⑤ Benefit Ratio (kg/$M) ③ ÷ ④	⑥ Mission Payload (kg)	⑦ Mission Recurring Costs ($M)	⑧ Average Cost of Payload ($M/kg) ⑦ ÷ ⑥	⑨ Cost-Benefit Index CB_M ⑤ × ⑧
1	200 lb_f engine development*	ΔI_{sp} = 15 sec								
	- Outbound Module A		1.86 kg/sec	27.9	1.93	14.45	408	100	0.245	3.5
	- Outbound Module B		2.81 kg/sec	42.2	1.93	21.88	680	100	0.147	3.2
2	800 lb_f engine development*	ΔI_{sp} = 25 sec								
	- Inbound Module A		2.42 kg/sec	60.5	1.95	31.06	340	100	0.294	9.1
	- Inbound Module B		3.53 kg/sec	88.3	1.95	45.25	550	100	0.182	8.2
3	2 lb_f ACS thruster development	Weight saving ~20 kg								
	- Inbound N_2O_4/MMH Module A		~1 kg/kg	20.0	1.64	12.20	340	100	0.294	3.7
	- Outbound N_2O_4/MMH Module B		~1 kg/kg	20.0	1.64	12.20	408	100	0.245	3.0
4	Alternative to Item 1* 200 lb_f N_2O_4/N_2H_4 engine	ΔI_{sp} = 15 sec								
	- Outbound Module A	+ Weight saving 9 kg	(1.86 kg/sec, 1 kg/kg)	36.9	2.3	12.14	408	100	0.245	2.5
	- Outbound Module B	+ Weight saving 13 kg	(2.81 kg/sec, 1 kg/kg)	55.2	2.3	18.35	680	100	0.147	2.7
5	Alternative to Item 2* 800 lb_f N_2O_4/N_2H_4 engine	ΔI_{sp} = 25 sec								
	- Inbound Module A	+ Weight saving 9 kg	(2.42 kg/sec, 1 kg/kg)	69.5	2.3	30.21	340	100	0.294	8.9
	- Inbound Module B	Weight saving 13 kg	(3.53 kg/sec, 1 kg/kg)	101.3	2.3	44.05	550	100	0.182	8.0

*I_{sp} goal 310 sec

All of the technology increments listed produce payload increases at less than the average cost of payload delivered.

Values obtained in Table 9-4 show that all new technology items considered are highly cost-effective. As shown in the last column the cost-benefit ratio is highest for Items 2 and 5. Future studies and technology work should also consider N_2O_4/N_2H_4 as a propellant combination.

10. CONCLUSIONS AND RECOMMENDATIONS

10.1 DEVELOPMENT OF MULTI-MISSION PROPULSION MODULES FOR PLANETARY ORBITERS

The following principal conclusions regarding the advisability of development of multi-mission propulsion modules are drawn from results of this study:

- Development of a multi-mission propulsion module even for only two of the specified missions rather than custom-designed stages involves lower overall costs.
- Performance advantages of multi-mission space-storable systems over corresponding earth-storable systems are significant and include not only spacecraft gross weight savings, but shorter trip times to distant targets, greater mission flexibility and scientific yield, and lower launch-vehicle capability requirements.
- With larger, more sophisticated payloads (Mariner spacecraft) space-storable propellants are essential if all the missions in the specified set are to be performed. Some of the missions (Uranus orbiter) cannot be achieved within practical time limits with the use of earth-storable propellants.
- With a lower payload weight (Pioneer spacecraft) all missions could be performed with earth-storable propellants, although less satisfactorily than with space-storable propellants.
- Cost-benefit advantages overwhelmingly favor space-storable over earth-storable propellants for multi-mission propulsion modules.
- The estimated development cost of a space-storable multi-mission module exceeds that of earth-storable modules by less than $10M.

These conclusions are based to a large extent on including the three high energetic planetary orbit missions, namely, Mercury, Saturn, and Uranus in the mission set postulated for multi-mission application. Should the Uranus orbiter be given a lower priority, or be eliminated, the strength of the argument for space-storable propellants would be diminished to some extent.

Seven comet missions in the late 1900's and early 1990's were included, but only as secondary objectives. Most of these comet missions

can be performed if space-storable propellants are available, but some only by using two propulsion modules in tandem, as in the case of the Mariner orbiter. Making the multi-mission module as small as possible, consistent with reduced flight times to the outer planets and efficient orbit insertion, limits the propellant capacity. Thus, in the tradeoff between planetary orbiter performance and comet-rendezvous mission feasibility, the former was favored in the design approach.

10.2 ACCOMMODATION BY AND INTERFACES WITH PAYLOAD VEHICLES

The overall systems viewpoint requires that the multi-mission module concept be implemented without imposing difficult and/or costly interface and accommodation requirements on the payload. The cost benefits achievable by the multi-mission module would be partially defeated if major redesign of the existing Pioneer and Mariner spacecraft were necessary. These constraints were taken into account, but not all tradeoffs for a cost-effective overall systems approach were possible within the framework of this study.

Future work should consider detailed structure and performance aspects of Pioneer and Mariner spacecraft, expecially the problem of structural reinforcement against high thrust accelerations. It is to be noted that even with a custom-designed propulsion module configuration some payload vehicle modifications are inevitable, e.g., reinforcement of the solar panels and the change in sun shield location to accommodate the orbit injection pointing requirements in the case of the Mariner Mercury orbiter. Therefore, only part of the added cost and weight penalties associated with such payload vehicle changes are chargeable to the multi-mission propulsion module concept when comparing its effectiveness with that of the custom-designed propulsion module.

10.3 ACCOMMODATION BY AND INTERFACES WITH THE SHUTTLE AND UPPER STAGES

The selected multi-mission stage design concepts satisfy size, weight, and structural constraints imposed by Shuttle launch. Safety requirements involving the use of fluorinated propellants were reflected in the design approach. Other handling, operational, and interface aspects were adapted from concurrent JPL studies.

10.4 TECHNICAL INNOVATIONS

Innovations identified and investigated in the course of the study include:

- The use of double-walled propellant tanks for greater safety and added micrometeoroid protection
- Use of a spin-deployed sun shade for Pioneer Mercury orbiters. Sun shade stowage, deployment, and dynamic properties were investigated but still require further study
- Use of a spin-actuated heat pipe for LF_2 tank thermal control in the Pioneer Mercury orbiter. This heat pipe concept would reduce size and complexity of the deployed sun shade. A fixed sun shade may, in fact, be adequate with this thermal control approach. This concept also is recommended for further study.

10.5 PROPULSION SYSTEM TECHNOLOGY AREAS RECOMMENDED FOR FURTHER STUDY

In addition to the novel concepts listed above, the following propulsion technology areas are recommended for further study and research, particularly in relation to reliability improvement:

1) Propulsion-system design for optimum redundancy. Methods for achieving at least partial mission success in the event of component failures.

2) Propellant corrosion (stress corrosion) of materials used in tanks and valves, including test and verification approaches.

3) Development of very high-reliability ACS thruster valves.

4) All aspects of system safety engineering, especially for LF_2/N_2H_4 (with emphasis on Shuttle launch requirements).

5) Design and utilization of double-wall tanks as related to system reliability aspects and safety during transport by the Shuttle orbiter.

6) LF_2/N_2H_4 engine technology, especially problems of non-equilibrium gas flow, combustion, pressure distribution, and cooling.

7) Design and applicability of N_2O_4/N_2H_4 engine.

REFERENCES

1. T. W. Price and D. L. Young, "Space Storable Propellants Demonstration Module," AIAA paper 73-1288, 1973.

2. R. L. Chase, et al., "Planetary Mission Applications for Space-Storable Propulsion," presented at the AIAA/SAE 10th Propulsion Conference, San Diego, California, October 21-23, 1974.

3. L. D. Stimpson and E. Y. Chow, "Thermal Control and Structures Approach for Fluorinated Propulsion," presented at 8th Thermophysics AIAA Conference, Palm Springs, California, 16-18 July 1973.

4. R. E. Deland, O. O. Haroldsen, and R. N. Porter, "Space Storable Propellant Module Thermal Control Technology. Summary Report, Volume II, F_2/N_2H_4 Propulsion Module," Report No. 14051-6009-RO-00, NAS 7-750, 15 March 1971.

5. "Mariner Jupiter Orbiter Study, Space Shuttle Final Review," Presentation to NASA Headquarters, Codes SL and MK, Jet Propulsion Laboratory Report 760-107, 26 June 1974.

6. "Pioneer Outer Planets Orbiter," NASA Ames Research Center, Moffett Field, California, 10 December 1974.

7. "Pioneer Jupiter Orbiter with Entry Probe PJOp," 27059-6001-RU-00, TRW Systems Group, Redondo Beach, California, 31 March 1975.

8. "Study of Safety Implications for Shuttle Launched Spacecraft Using Fluorinated Oxidizers," TRW Systems Group, Redondo Beach, California, (preliminary draft), 9 May 1975.

9. D. W. Dugan, "Performance Study of Multi-Mission Stages for Planetary Orbiters," NASA Ames Research Center, in preparation.

10. W. S. Cook, G. R. Hollenbeck, P. S. Lewis, D. G. Roos, and D. E. Wainwright, "Study of Ballistic Mode Mercury Orbiter Missions," Volume II, Technical, Martin Marietta Corporation, NASA CR-114618, NAS2-7268, July 1973.

11. "Ballistic Mode Mercury Orbiter Mission Opportunity Handbook Extension," Martin Marietta Corporation for NASA Ames Research Center under Contract NAS2-7268, November 1973, and also Summary Report, July 1973.

12. "Study of a Comet Rendezvous Mission," Volume I, Technical Report, TRW 20513-6006-R0-00, prepared for Jet Propulsion Laboratory under Contract 953247, 12 May 1972.

13. R. R. Teeter, et al., "Report Number BMI-NLVP-TM-73-4 on Space Shuttle Expendable Upper Stages," Battelle Columbus Laboratories, Columbus, Ohio, December 28, 1973.

14. "Summary of Space Tug Program," NASA George C. Marshall Space Flight Center, June 1974.

15. "Baseline Space Tug Configuration Definition," NASA George C. Marshall Space Flight Center, MFSC 68M00039-2, July 15, 1974.

16. Richard D. Cannova, et al., "Development and Testing of the Propulsion Subsystem for the Mariner Mars 1971 Spacecraft, Technical Memorandum 33-552, Jet Propulsion Laboratory, 1 August 1972.

17. "Comparison Study of Fluorine/Hydrazine Engine Concepts," Report No. 2094-FR-1, Aerojet Liquid Rocket Company, Sacramento, California, 1975.

18. "Compatibility Testing of Spacecraft Materials and Space-Storable Liquid Propellants," Report No. 23162-6020-RU-00, TRW Systems Group, Redondo Beach, California, 1974.

19. "Study of Alternate Retro-Propulsion Stage Configurations for the Pioneer Outer Planet Orbiter," 22303-6003-RU-00, TRW Systems Group, Redondo Beach, California, November 30, 1973.

20. L. B. Holcomb and R. L. French, "Study of Orbit Insertion Propulsion for Spinning Spacecraft," Final Report, Jet Propulsion Laboratories, 18 October 1973.

21. "Space Shuttle System Payload Accommodations," and Change No. 10, Johnson Space Center, 4 June 1975.

22. "A Feasibility Study of Developing Toroidal Tanks for a Spinning Spacecraft, MCR-73-223, Martin Marietta Corporation, September 1973.

23. "A Feasibility Study of Developing Toroidal Tanks for a Spinning Spacecraft," MCR-74-372, Martin Marietta Corporation, October 1974.

24. "Pioneer Spacecraft Operation at Low and High Spin Rates," 22303-6002-RU-00, TRW Systems Group, Redondo Beach, California, October 5, 1973.

25. "Saturn/Uranus Atmospheric Entry Probe Mission Spacecraft System Definition Study, Final Report," 23267-6001-RU-00, TRW Systems Group, Redondo Beach, California, 15 July 1973.

REFERENCES (Continued)

26. "Meteoroid Environment Model - 1970 (Interplanetary and Planetary," NASA SP-8038, National Aeronautics and Space Administration, October 1970.

27. "The Planet Saturn (1970)," NASA SP-8091, National Aeronautics and Space Administration, June 1972.

28. "Extended Life Outer Planets Pioneer Spacecraft," Ames Research Center, Moffett Field, California, 5 March 1974.

29. "Demonstrated Orbital Reliability of TRW Spacecraft," 74-2286.142, TRW Systems Group, Redondo Beach, California, December 1974.

30. P. H. Roberts, "Study of Saturn Orbiter Mission with Gravity Assist from Titan," Jet Propulsion Laboratory, in preparation.

31. "KSC Ground Processing of Space Shuttle Payloads Using Fluorine Stages," NAS10-8553, Task 22, TRW Systems Group, Florida Operations, Cape Canaveral, Florida, July 1975.

32. "Final Report STS Planetary Mission Operations Concepts Study," 760-122, Jet Propulsion Laboratory, Pasadena, California, April 15, 1975.

33. "Evaluation of Fine-Mesh Screen Device in Liquid Fluorine," by D. F. Fisher and P. E. Bingham, Report No. R-70-48631-010, Martin Marietta Corp., Denver Division, June 1970.

34. "Space Science Board Summer Study 1974, Planetary Mission Summary: Mariner Mercury Orbiter 1978," SP 43-10, Vol. 7, Jet Propulsion Laboratory, Pasadena, California, August 1974.

35. "Five-Pound Bipropellant Thruster Program," Final Report, AFRPL-TR-54-51, Aerojet Liquid Rocket Co., Sacramento, California, 1974.